Schriftenreihe der Reiner Lemoine-Stiftung

Philip Sterchele

Analysis of Technology Options to Balance Power Generation from Variable Renewable Energy

Case Study for the German Energy System with the Sector Coupling Model REMod

A thesis accepted by the Department of Sustainable Systems Engineering
of the Albert-Ludwigs-Universität Freiburg in partial fulfillment of
the requirements for the degree of Doctor of Engineering Sciences (Dr.-Ing.)

Analysis of Technology Options to Balance Power Generation from Variable Renewable Energy

Case Study for the German Energy System with the Sector Coupling Model REMod

by
Philip Sterchele
born in Sterzing, Italy

First examiner:	Prof. Dr. Hans-Martin Henning
Second examiner:	Prof. Dr. Anke Weidlich
Date of defence:	19 June 2019

Schriftenreihe der Reiner Lemoine-Stiftung

Philip Sterchele

Analysis of Technology Options to Balance Power Generation from Variable Renewable Energy

Case Study for the German Energy System
with the Sector Coupling Model REMod

Shaker Verlag
Düren 2019

Bibliographic information published by the Deutsche Nationalbibliothek
The Deutsche Nationalbibliothek lists this publication in the Deutsche Nationalbibliografie; detailed bibliographic data are available in the Internet at http://dnb.d-nb.de.

Zugl.: Freiburg, Univ., Diss., 2019

Printed in Germany.

ISBN 978-3-8440-6946-4
ISSN 2193-7575

Shaker Verlag GmbH • Am Langen Graben 15a • 52353 Düren
Phone: 0049/2421/99011-0 • Telefax: 0049/2421/99011-9
Internet: www.shaker.de • e-mail: info@shaker.de

Abstract

The German Federal Government committed to drastically reduce its greenhouse gas emissions as part of its climate change mitigation strategy. This will lead to an increasing deployment of variable renewable energy sources (VRE). However, the expansion of VRE is only reasonable if their intermittent electricity generation can be effectively integrated into not only the power sector but also the transport sector and into the supply of space and process heat. To achieve this, the energy system needs to become more flexible while also being able to cope with changing weather influences. In this work, load balancing options for the German energy system are analysed based on an enhancement of the Renewable Energy Model REMod. The model is designed to determine a cost-optimal configuration of the energy system under consideration of an exogenously set limit of energy-related CO_2 emissions. In an integrative approach it depicts interdependencies between all implemented technologies and sectors of the energy system in hourly resolution. Special attention is given to power plant ramping behaviour, the variation of up to five different weather data sets, the implementation of driving profiles and charging strategies for electric vehicles as well as to the heat-controlled or power-controlled operation of heat generators in combination with thermal energy storage.

According to the results, highly flexible gas turbine power plants are becoming increasingly important as the expansion of VRE proceeds. Power plants that require several hours of start-up time exhibit yearly efficiency losses of up to 6 % of their nominal efficiency increasing their emissions and making them less profitable over time. Furthermore plant operation and configuration of the energy system are substantially affected by underlying weather data. It is found that calculations based on one specific data set exhibit variations in costs and system configuration of up to 15 %. Random data distribution over the observation period favours the refurbishment of buildings, the installation of more efficient technologies as well as the deployment of hydrogen-based technologies. An analysis of the motorised private transport shows that battery electric vehicles are a promising option to achieve the set emissions reduction targets, especially when they are charged in a controlled way. As for the supply of space heat and domestic hot water, heat grids and electric heat pumps represent key technologies to achieve the emission reduction targets. The controlled charging of electric vehicles and the power-controlled operation of heat generators with thermal energy storage by demand-side management (DSM) is found to be increasingly beneficial to the energy system as the set CO_2 reduction targets become more ambitious. It is shown that part of thermal power plant generation capacity, stationary power storage systems and Power-to-Gas plants can be substituted by DSM. Power curtailments as well as imports of electricity or synthetic fuels from abroad would be decreasing. In addition to lowering the total system costs, it is found that DSM efficiently integrates power generation from VRE, reducing Germany's energy dependence on other countries.

Zusammenfassung

In seiner Strategie zum Klimaschutz hat sich die Bundesregierung dazu verpflichtet seine Treibhausgasemissionen drastisch zu reduzieren. Damit verbunden ist ein fortschreitender Ausbau fluktuierender erneuerbarer Energien. Dies ist nur dann sinnvoll, wenn die dargebotsabhängige Stromerzeugung durch fEE sowohl im Stromsektor als auch im Verkehrssektor und für die Bereitstellung von Raum- und Prozesswärme genutzt wird. Um dies für verschiedene meteorologischen Bedinungen zu gewährleisten muss das Energiesystem flexibler werden. In dieser Arbeit werden Flexibilitätsoptionen im Deutschen Energiesystem System basierend auf eine Erweiterung des Regenerative Energien Modells REMod untersucht. Das Modell ist konzipiert um eine kostenoptimale Zusammensetzung des Energiesystems unter Einhaltung vorgegebener Höchstwerte an energiebedingten CO_2-Emissionen zu identifizieren. Dabei werden Wechselwirkungen zwischen allen implementierten Technologien und Sektoren des Energiesystems in stündlicher Auflösung erfasst. Im Fokus der Analyse stehen insbesondere das Anfahrverhalten von Kraftwerken, die Variation von fünf verschiedenen Wetterdatensätzen, die Implementierung von Ladestrategien elektrischer Antriebskonzepte sowie der wärme- oder stromgeführte Betrieb von Wärmeerzeugern kombiniert mit thermischen Speichern.

Die Ergebnisse zeigen, dass durch den Ausbau an fEE hochflexible Gasturbinen an Bedeutung gewinnen. Kraftwerke mit mehrstündigen Anfahrprozessen weisen – bezogen auf ihre maximale Wandlungseffizienz – eine durchschnittliche Reduktion von bis zu 6 % auf. Dadurch erhöht sich deren spezifischer CO_2-Ausstoß und ihre Wirtschaftlichkeit nimmt ab. Der Einsatz der Kraftwerke sowie die Zusammensetzung des Energiesystems sind von den berücksichtigten Wetterdaten beeinflusst. So weisen Berechnungen welche auf nur einen Datensatz basieren untereinander Variationen in Gesamtkosten sowie Technologieanzahlen von bis zu 15 % auf. Eine zufällige Streuung verschiedener Wetterdatensätze über den Betrachtungszeitraum erhöht den Anteil energetisch sanierter Gebäude sowie die Installation von effizienteren und wasserstoffbasierten Technologien. Des Weiteren wird gezeigt, dass batterieelektrische Fahrzeuge eine Schlüsseltechnologie zur Erreichung der Klimaschutzziele darstellen, insbesondere dann wenn diese kontrolliert geladen werden. Bei der Bereitstellung von Raumwärme und Trinkwarmwasser spielen hingegen Wärmenetze und elektrische Wärmepumpen eine zentrale Rolle. Das kontrollierte Laden elektrischer Fahrzeuge und der stromgeführte Betrieb von Wärmeerzeugern mit thermischen Speichern gewinnen insbesondere bei ambitionierten Emissionsminderungszielen zunehmend an Bedeutung für das Energiesystem. So kann durch Lastmanagement ein Teil der ansonsten erforderlichen Kraftwerke, stationäre Batterien, Power-to-Gas Anlagen oder der anfallenden Energieimporte reduziert werden. Damit trägt Lastmanagement nicht nur zu einer Reduktion der Gesamtsystemkosten und einer effizienteren Integration von Strom aus fEE im Energiesystem bei sondern auch zu einer geringeren Energieabhängigkeit Deutschlands von anderen Ländern.

Contents

List of Figures

List of Tables

List of Symbols

Symbols utilised for the calculation of the electricity base load (Chapter 3.2.5).

Symbol	Unit	Definition
E_{BL}	kWh_{el}	Yearly electricity base load demand
E_L	kWh_{el}	Yearly electricity base load demand
E_{ICT}	kWh_{el}	Yearly power demand for information and communication
E_C	kWh_{el}	Yearly power demand for cooling
E_M	kWh_{el}	Yearly power demand for mechanical energy
$E_{E,n,adj}$	–	Normalised, adjusted profile of the electricity profile
f_{BL}	%	Factor for increase or decrease of the electricity base load

Symbols used for the description of the objective function (Chapter 3.3.2).

Symbol	Unit	Definition
A_k	€	Annuity of capital-related costs
A_b	€	Annuity of operation-related costs
A_v	€	Annuity of demand-related costs
A_n	€	Cash value for a procured replacement
A_0	€	Investment amount of considered technology
i_{inf}	–	Inflation rate
i_{int}	–	Interest rate
i_d	–	Discounting rate
i_P	–	Price changing rate
a	–	Annuity factor
b	–	Price dynamic cash value factor
q	–	Interest factor
f_{OM}	%	Factor for servicing, inspection and repair
r_{OM}	–	Price change rate of operation-related costs
T_N	–	Service time of considered component

Continued on next page

Symbols used for the description of the objective function (Chapter 3.3.2).

Symbol	Unit	Definition
n	$-$	Technology or component replacement number
P	€	Sum of penalty functions
P_{CO_2}	€	Penalty term accounting for energy-related CO_2 emissions
P_{EB}	€	Penalty term accounting for energy balance
ΔCO_2	t_{CO_2}	Difference between resulting CO_2 emissions and set value
ΔE_{EB}	kWh	Mismatch between supplied and utilised energy
m_{CO_2}	t_{CO_2}	Total quantity of energy-related CO_2 emissions
Q_c	kWh	Imported and on site produced quantity per energy carrier
p_c	€/$_{kWh}$	Price per energy carrier
p_{CO_2}	€/$_{t_{CO_2}}$	Price per CO_2 emissions

Symbols used for the description of the optimisation algorithm (Chapter 3.3.2).

Symbol	Approach	Definition
$\vec{x}$	PSO	Particle describing a possible solution
$\vec{p}_{best}$	PSO	Local best best solution
$\vec{g}_{best}$	PSO	Global best best solution
$\vec{v}$	PSO	Particle velocity
n_G	PSO	Number of generations
n_P	PSO	Number of particles
w	PSO	Particle inertia factor
c_1	PSO	Acceleration coefficients for individual solution
c_2	PSO	Acceleration coefficients for global solution
r_1	PSO	Weighting factor for cognitive particle behaviour
r_2	PSO	Weighting factor for social particle behaviour
λ	CMA-ES	Population size
n	CMA-ES	Number of optimisation variables

Symbols used for the description of the operation principle (Chapter 3.4).
CHP: combined heat and power.

Symbol	Unit	Definition
P_{Res}	kWh_{el}/h	Residual load
$P_{el,Load}$	kWh_{el}/h	Total electric load
$P_{el,Prod}$	kWh_{el}/h	Total non-dispatchable power generation
P_{BL}	kWh_{el}/h	Electricity base load
P_{HP}	kWh_{el}/h	Power load of heat pumps for space heat
P_{DG}	kWh_{el}/h	Power load of deep geothermics for space heat
$P_{EV,must}$	kWh_{el}/h	Power load for vehicle charging
$P_{EC,must}$	kWh_{el}/h	Power load for electrolysis plants
P_{PH}	kWh_{el}/h	Power load for the supply of process heat
P_{ICP}	kWh_{el}/h	Power generation from industrial plants (internal consumption)
P_{Hydro}	kWh_{el}/h	Power generation from run-of-river power stations
P_{NP}	kWh_{el}/h	Power generation from nuclear power plants
$P_{LC,must}$	kWh_{el}/h	Non-dispatchable power generation from lignite power plants
$P_{HC,must}$	kWh_{el}/h	Non-dispatchable power generation from hard coal power plants
$P_{Wind,off}$	kWh_{el}/h	Power generation from offshore wind power stations
$P_{Wind,on}$	kWh_{el}/h	Power generation from onshore wind power stations
P_{PV}	kWh_{el}/h	Power generation from photovoltaic power stations
$P_{I,must}$	kWh_{el}/h	Mandatory import of electricity
P_{CHP}	kWh_{el}/h	Power generation from micro-CHP units for space heat
P_{FC}	kWh_{el}/h	Power generation from fuel cells for space heat
η_G	kWh_{el}/h	Average grid efficiency for consideration of losses

Symbols used for the description of system components (Chapter 3.5).
VRE: variable renewable energy, TES: thermal energy storage.

Symbol	Unit	Definition
$P_{el,VRE}$	kWh_{el}/h	Power generation from considered VRE-technology
$P_{nom,VRE}$	kW_{el}	Installed capacity of considered VRE-technology
$P_{norm,VRE}$	$-$	Normed feed-in profile of considered VRE-technology
$f_{VLH,VRE}$	$-$	Yearly adjustable factor for technological improvement
$P_{el,Coal}$	kWh_{el}/h	Power generation from coal power plant
$P_{el,nom,Coal}$	kW_{el}	Installed capacity of coal power plant
$f_{mustRun,Coal}$	%	Share of must run capacity of nominal load

Continued on next page

Symbols used for the description of system components (Chapter 3.5).
VRE: variable renewable energy, TES: thermal energy storage.

Symbol	Unit	Definition
$P_{flex,Coal}$	kWh_{el}/h	Flexible power generation from coal power plant
Q_{STH}	Wh_{th}/h	Yield of solar thermal systems
$Q_{Loss,HWS}$	Wh_{th}/h	Thermal energy storage losses
A_{coll}	m^2	Collector surface
G	W/m^2	Global radiation
c_0	%	Collectors efficiency
c_1	W/m^2K	Collector heat loss coefficient
c_p	J/kgK	Specific thermal capacity of water
T_{Coll}	°C	Temperature of the solar collector
T_A	°C	Ambient temperature
C_{HWS}	J/K	Thermal capacity of the TES
V_{HWS}	m^3	Endogenously determined storage volume
U_{HWS}	W/m^2K	Thermal transmission coefficient of thermal energy storage
ρ	kg/m^3	Density of water at standard conditions
τ_{HWS}	–	Time constant of the TES
P_{In}	kwh/h	Fuel or power demand of heat generator
P_{el}	kwh_{el}/h	Power generation of heat generator
$\dot{Q}_{Use}$	kWh_{th}	Useful process heat demand
η_{th}	%	Thermal generator efficiency
η_{el}	%	Electric generator efficiency
Δt	–	Considered time step length in hours

Symbols used for the description of the load forecast (excursus) (Chapter 4.1).

Symbol	Unit	Definition
$P_{exp,Res}$	kWh_{el}/h	Expected residual load value
$P_{exp,l,SH}$	kWh_{el}/h	Expected power demand for space heat and hot water
$P_{exp,l,PH}$	kWh_{el}/h	Expected power demand for the supply of process heat
$P_{exp,l,RT}$	kWh_{el}/h	Expected power demand for road transport
$P_{exp,elyse}$	kWh_{el}/h	Expected power demand of electrolysis plants
$P_{exp,BL}$	kWh_{el}/h	Expected power demand of electricity base load
$P_{exp,ndg}$	kWh_{el}/h	Total expected power non-dispatchable power generation
$P_{exp,el}$	kWh_{el}/h	Total expected power demand
$P_{exp,el}$	kWh_{el}/h	Total expected power demand
f_{SL}	–	Load safety factor in

Symbols used for the description of ramping behaviour (Chapter 4.2).

Symbol	Unit	Definition
P	kWh_{el}/h	Hourly energy output of plant
P_{Nom}	kW_{el}	Nominal capacity of plant
P_{Min}	kW_{el}	Minimum load capacity of plant
p_{min}	$\%_{P_{Nom}}$	Minimum load of plant related to its maximum capacity
P_{exp}	kWh_{el}/h	Expected plant production capacity in upcoming time steps
P_H	kWh/h	Energy demand for heat-up of the plant
E_S	kWh/kW	Energy demand for heat-up per installed plant capacity
S_{AP}	%	Available share of the maximum plant capacity
S_{PL}	%	Partial load related to maximum efficiency
R_{RR}	%	Ramp rate of plant
η	%	Conversion efficiency of plant
η_{Nom}	%	Maximum efficiency of plant
h_{PL}	h	Partial load time of plant
h_{DCOp}	h	Time spent in design condition operation
h_{PLOp}	h	Time spent in partial load operation
h_{HS}	h	Hot start-up time of plant
h_{CS}	h	Cold start-up time of plant
h_{PL}	h	Partial load time of plant
D_{HS}	h	Duration of a hot start-up per definition
D_{CS}	h	Duration of a cold start-up per definition
c	h	Ramping counter
c_S	h	Counter for consecutive hours downtime hours
c_H	h	Entity of the heat-up process
c_{CD}	h	Entity of the cool down process

Symbols used for the description of electric vehicle charging (Chapter 4.3).

Symbol	Unit	Definition
P_T	$kW_{el}/vehicle$	Traction power of one average vehicle
P_E	kWh_{el}/h	Final power demand of vehicles of a specific power train technology
P_{mustCh}	kWh_{el}/h	Mandatory vehicle charging
P_{red}	kWh_{el}/h	Reduction of discharged power
P_{V2G}	kWh_{el}/h	Discharged power for feedback into the grid

Continued on next page

Symbols used for the description of electric vehicle charging (Chapter 4.3).

Symbol	Unit	Definition
$P_{V2G,Max}$	kWh_{el}/h	Maximum discharge capacity
P_{G2V}	kWh_{el}/h	Charged power
$P_{V2G,avg}$	$kW_{el}/vehicle$	Average discharge capacity per vehicle
E_{veh}	kWh_{el}	Annual final energy demand of vehicle fleet
$E(t)$	kWh_{el}	Vehicle charge level
E_{inter}	kWh_{el}	Interim charge level
E_{MinAbs}	kWh_{el}	Threshold value for minimum charge level
$E_{avg,pkt}$	kWh_{el}/km_{trav}	Average final energy consumption per kilometre travelled
E_{Max}	kWh_{el}	Maximum available battery capacity
$E_{V2G,Min}$	kWh_{el}	Threshold value for power feedback into the grid
$E_{G2V,Max}$	kWh_{el}	Maximum charge of electricity
$E_{ch,UCSt}$	kWh_{el}	Charging of arriving vehicles
$E_{ch,CCSt}$	kWh_{el}	Charging in case of power deficiency period
E_{exp}	kWh_{el}	Expected charge level in x time steps
SoC	kWh_{el}	State of charge
$C_{avg,bat}$	$kWh_{el}/vehicle$	Average battery capacity per vehicle
S_A	%	Hourly share of arriving vehicles
S_L	%	Hourly share of leaving vehicles
S_P	%	Hourly share of vehicles plugged into a charging facility
S_{MinAbs}	%	Share of battery capacity for minimum charge level
S_{UCSt}	%	User share following an uncontrolled charging strategy
S_{CCSt}	%	User share following an controlled charging strategy
η_{avg}	%	Annual average efficiency of vehicle fleet
f_{V2G}	%	Factor for Vehicle-to-Grid operation
D_{EN}	–	Normalised power demand profile
km_{trav}	–	Kilometres travelled per year
N_{veh}	–	Total number of vehicles
t_{FC}	–	Future time step for forecast
t_{FP}	–	Forecast period
Δt	–	Time step length
x	–	Number of upcoming time steps for forecast

Symbols used for the description of cross-border electricity exchange (Chapter 4.5).

Symbol	Unit	Definition
$P_{Nom,VRE}$	kW_{el}	Installed capacity of VRE technology
P_{IC}	kW_{el}	Assumed interconnector capacity
P_{OI}	kWh_{el}	Available optional import capacity
P_{MI}	kWh_{el}	Mandatory import
p_{MI}	$kWh_{el}/kW_{P_{IC}}$	Specific mandatory import
$P_{norm,VRE}$	–	Normalised power supply profile of bordering countries
w_N	–	Weighting factor for VRE share for neighbouring countries
w_{VRE}	–	Weighting factor for each VRE technology within one country
$f_{C,VRE}$	–	Hourly capacity factors for each VRE technology
N_{NC}	–	Number of neighbouring countries
N_{VRE}	–	Number of considered VRE technologies
l_o	–	Threshold value for optional import
l_m	–	Threshold value for mandatory import

Symbols used for the description of power storages and Power-to-Gas plants (Chapter 4.6).

Symbol	Unit	Definition
$P_{ch,max}$	kW_{el}	Maximum charging (or discharging) capacity
$P_{SR,nom}$	kW_{CH_4}	Nominal capacity of steam reformation plants
E_{bat}	kWh_{el}	Battery storage capacity
$E_{SOC,bat}$	kWh_{el}	Battery level of charge
$E_{ch,bat}$	kWh_{el}	Power charged in battery
$E_{dis,bat}$	kWh_{el}	Power discharged from battery
$E_{H_2,d}$	kWh_{H_2}	Hourly hydrogen demand
$E_{H_2,RT}$	kWh_{H_2}	Hourly hydrogen demand of the motorised road transport
$E_{H_2,SH}$	kWh_{H_2}	Hourly hydrogen demand for space heat and hot water
$E_{H_2,PH}$	kWh_{H_2}	Hourly hydrogen demand for the supply of process heat
$E_{H_2,ex}$	kWh_{H_2}	Exogenously set hydrogen demand
$E_{H_2,SR,min}$	kWh_{H_2}	Must-run hydrogen production from steam reformation plants
η_{bat}	%	Charging efficiency of battery systems
η_{SR}	%	Conversion efficiency of steam reformation plants
$S_{min,SR}$	%	Must-run capacity share of steam reformation plants
C	h^{-1}	Capacity factor of stationary battery
Δt	h	Time step length

Symbols used for the calculation of the average conversion efficiency (Chapter 5.2).

Symbol	Unit	Definition
η_{avg}	%	Average conversion efficiency of technology stock
η_N	%	Average conversion efficiency of newly deployed units
n	–	Number of units
n_N	–	Number of newly deployed units

Symbols used for the calculation of differences in sector composition (Chapter 6.1.1).

Symbol	Unit	Definition
Δ_{2050}	%	Indicator for differences in the final sector composition
Δ_{Path}	%	Indicator for differences over the entire observation period
T	–	Considered end-use sector
n	–	Number of different technologies per end-use sector

Symbols used for the calculation of heat production costs (Chapter 6.3.2).

Symbol	Unit	Definition
E_{CH_4}	$kWhCH_4$	Methane gas consumption
$\dot{Q}_{th,boiler}$	kWh_{th}	Generated heat from hybrid heat pump
$\dot{Q}_{th,elHP}$	kWh_{th}	Generated heat from electric air heat pump
P_{th}	kW_{th}	Building heat load
P_{PP}	kW_{el}	Electric load of thermal power plant
m_{CO_2}	t_{CO_2}	Total quantity of caused energy-related CO_2 emissions
f_{CH_4}	$\frac{kg_{CO_2}}{kWh_{CH_4}}$	Emission factor of methane gas
η_{PP}	%	Electrical efficiency of thermal power plant
η_{boiler}	%	Thermal efficiency of gas unit (hybrid heat pump)
COP	–	Coefficient of performance
p_{hybHP}	€/kW_th	Specific purchase price of hybrid heat pump
p_{elHP}	€/kW_th	Specific purchase price of electric heat pump
p_{PP}	€/kW_{el}	Specific purchase price of thermal power plant
C_{hybHP}	€	Hybrid heat pump costs
C_{elHP}	€	Electric air heat pump and the thermal power plant costs
$c_{HPC,hyb}$	€/kWh_th	Heat production costs of the hybrid heat pump

Continued on next page

Symbols used for the calculation of heat production costs (Chapter 6.3.2).

Symbol	**Unit**	**Definition**
$c_{HPC,elHP}$	€/kWh_th	Heat production costs of electric heat pump and power plant
d_{HPC}	%	Heat production costs related to hybrid heat pump

Symbols used for the calculation of the CO_2 abatement costs (Chapter 6.4.3).

Symbol	**Unit**	**Definition**
$c_{CO_2,A}$	€/t_{CO_2}	CO_2 abatement costs
m_{CO_2}	t_{CO_2}	Total quantity of caused energy-related CO_2 emissions
C	*euros*	Total system costs
BAU	–	Business-as-usual case (today's system configuration)

List of Acronyms

BAU	Business-As-Usual
BEV	Battery Electric Vehicle
CCGT	Combined Cycle Gas Turbine
CCSt	Controlled Charging Strategy
CHP	Combined Heat and Power
CMA-ES	Covariance Matrix Adaptation - Evolution Strategies
CNG	Compressed Natural Gas
CO_2	Carbon Dioxide
COP	Conference of Parties
DHW	Domestic Hot Water
DSM	Demand-Side Management
DWD	Deutscher Wetterdienst
EU	European Union
EV	Electric Vehicle
FCEV	Fuel Cell Electric Vehicle
FSP	Fixed Sequence Parametrisation
G2V	Grid-to-Vehicle
GHG	Greenhouse Gas
GT	Gas Turbine
HCSt	Heat-Controlled Strategy
HP	Heat Pump
HT	High Temperature
ICE	Internal Combustion Engine
LMT	Low to Medium Temperature
PCST	Power-Controlled Strategy
PH	Panel Heating
PHEV	Plug-in Hybrid Electric Vehicle

PSO	Particle Swarm Optimisation
PtG	Power-to-Gas
PtL	Power-to-Liquid
PTT	Power Train Technology
REMod	Renewable Energy Model
RH	Radiator heating
RSP	Random Sequence Parametrisation
SoC	State of Charge
TES	Thermal Energy Storage
UCSt	Uncontrolled Charging Strategy
UNFCC	United Nations Framework Convention
UP	Uniform Parametrisation
V2G	Vehicle-to-Grid
VDI	Association of German Engineers
VRE	Variable Renewable Energy

Danksagung

Die vorliegende Arbeit entstand während meiner Zeit als als Doktorand und wissenschaftlicher Mitarbeiter in der Abteilung Energiesystemanalse am Fraunhofer Insitut für Solare Energiesysteme. Sie wurde finanziell durch ein Promotionsstipendium der Reiner Lemoine Stiftung unterstützt. Dafür und für die Möglichkeit, mich im Rahmen der Stipendiatentage mit weiteren Stipendiaten zu vernetzen, möchte ich mich bei der Stiftung herzlichst bedanken.

Ein besonderer Dank gilt meinem Doktorvater Herr Prof. Dr. Hans-Martin Henning für seine wissenschaftliche und methodische Unterstützung während der gesamten Bearbeitungsphase meiner Dissertation. Für die Übernahme des Koreferats sowie für die vielen hilfreichen Anmerkungen zu meiner Arbeit möchte ich mich bei Frau Prof. Dr. Anke Weidlich bedanken.

Herrn Dr. Andreas Palzer danke ich für die zahlreichen und unermüdlichen fachliche Gespräche, Ratschläge und Anmerkungen, die mich auf dem Weg zur fertigen Arbeit immer wieder neue Aspekte und Ansätze entdecken ließen. Auch die vielen nicht immer wissenschaftlichen aber durchaus unterhaltsamen und motivierenden Gespräche haben meine Arbeit unterstützt.

Des Weiteren möchte ich mich bei allen studentischen Hilfskräften, Markus Bender, Lucas Brucker, Reinhild Möllers, Khaled Al-Dhabbas, Julian Brandes, Judith Heilig, Daniel Wrede, Lisa Bongartz und Anne Joost für Ihre Unterstützung bedanken. Allen weiteren Arbeitskollegen am Insititut danke ich für die spannenden Gespräche zwischendurch und die allzeit angenehme Arbeitsatmosphäre.

Besonders möchte ich an dieser Stelle auch meiner Familie Christine, Enzo und Michele, für die unermüdliche Stärkung und Motivation danken. Ein letzter Dank geht an Sara für ihr Verständnis und ihre stetige Unterstützung.

Freiburg, im Juni 2019

1 Introduction

For the mitigation of climate change, the international community has agreed to limit global warming to maximal 2° C compared to pre-industrial times [1]. In terms of CO_2 emission reduction targets this should lead to a GHG-neutral world economy between 2050 and 2100 [2]. To contribute to the GHG emission reduction, the Federal Government presented its energy concept for a clean, reliable and affordable energy supply in 2010 [3] which was confirmed and further detailed in the Climate Protection Plan 2050, released in 2016 [4]. The Climate Protection Plan 2050 contains specific goals for the individual sectors electricity, buildings, transportation, industry and agriculture. Further, the total GHG emissions shall be reduced by 40 % by 2020, 55 % by 2030, 70 % by 2040 and 80 % by 2050 compared to 1990 values. However, according to current studies, including the climate report of the Federal Government itself, the GHG reduction target set for 2020 will most likely be missed[1] by roughly 8 % [10]. There are two main reasons for that. First, the energy demand in almost all energy-related sectors is increasing. For instance, in the building sector this is due to a trend towards more households, larger living spaces and less members per household or in the transport sector, where technical improvements are compensated by traffic growth [11]. Second, the greater part of the energy utilised in these sectors is based on fossil fuels, such as natural gas, oil, and coal [12]. This is shown in figure 1.1, illustrating the development of final energy consumption in Germany over the last ten years, divided into four sectors: (a) space heat and domestic hot water (b) process heat (c) transport, i.e. road traffic, shipping, aviation and rail traffic and (d) electricity, where all electricity applications are included. The pie chart shows the distribution of the energy-related CO_2 emissions in 2017. With 85 % to 90 % the energy-related emissions account for the large majority of the total GHG emissions [12].

[1] In 2014, the *national action plan 2020* and the *national action plan energy efficiency (NAPE)* were released with the aim to achieve the climate protection targets set for 2020 [5,6]. While the stipulated measures lead to a higher reduction of the resulting emissions (32 % instead of 29 %), it is presumed that they are not sufficient to ensure the set emission reduction target of 40 % compared to 1990 values. This is why the Federal Government is already working on a new climate protection law, which should legally ensure the set climate protection targets for 2030. The law draft should be presented in spring of 2019 [7–9].

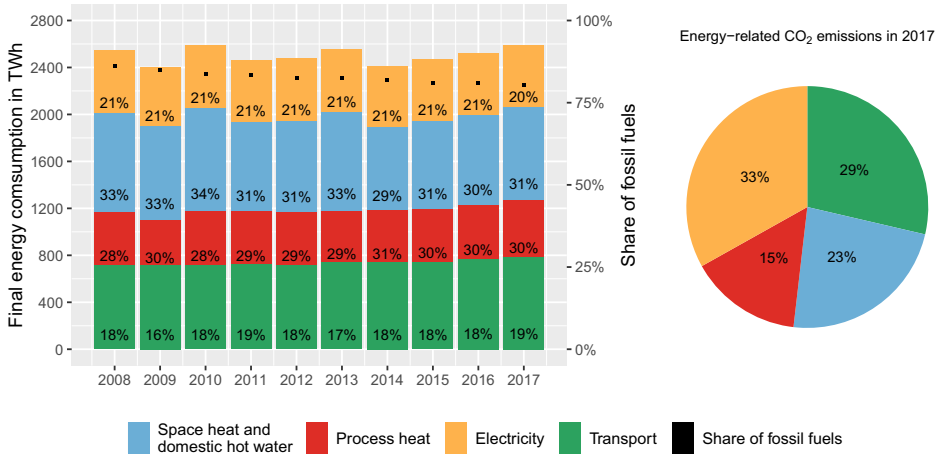

Figure 1.1: Development of energy consumption in Germany and share of fossil fuels over the last ten years, subdivided by end-use sector. Other fuel types include firewood, sewage sludge, mine gas and waste heat. The pie chart describes the distribution of energy-related CO_2 emissions in 2017, subdiveded per end-use sector. The sectoral division is based on the REMod model. Own illustration based on [12–14].

As shown, over the last ten years the trend in energy consumption, as well as the ratio between fossil and other fuels, have remained mostly constant. This also applies to the distribution between the depicted sectors, ranging between approximately 20 % (electricity and process heat) and 30 % (transport and space heat and domestic hot water). As for the energy-related CO_2 emissions, it is revealed that the electricity sector accounts for 33 %, while the transport sector, the supply of space heat and domestic hot water and the supply of process heat amount to 29 %, 23 % and 15 %, respectively. This underlines that in order to achieve the planned emissions reduction targets set by the Federal Government of at least 80 %, and wherever possible 95 %, below 1990 levels, all energy-realted sectors need to be included in the analysis. This is why over the last years the focus of studies analysing the transformation of the German energy system has increasingly shifted from sole consideration of the electricity supply to the integration of all sectors [15–20]. All these publications suggest a progressive electrification of all sectors, for example by introducing electric vehicles in road transport or electric heat pumps for the supply of heat, in order to achieve the climate protection targets. However, this is only reasonable if renewable energy sources provide a substantial contribution to the total generation of power. The Federal Government aims to increase the renewable share of gross electricity generation to at least 80 % by 2050 [3]. The current development shows that their share is constantly growing and amounted to approximately 38 % in 2018 [21, 22]. To increase it even further, in January 2019, the coal commission suggested a withdrawal from coal power between 2035 and 2038 [23].

Various analyses of the electricity generation costs of variable renewable energy (VRE) showed that substantial reductions were achieved over the last years. These reductions are expected to continue, mainly due to technological improvements, competitive procurements and the rise in experience of project developers [24–27]. According to [24], most renewable power generation projects commissioned in 2017 already exhibit electricity generation costs which are at the same level as fossil-based power generation. Recent research [15, 17, 19, 20, 28, 29], considering a CO_2 reduction of at least 80 % and up to 100 % compared to 1990 values, propose an installed capacity ranging between 160 GW_{el} and 610 GW_{el}, corresponding to 1.6[2] to 6 times of today's installed capacity [22].

However, the shift to power generation primarily based on VRE is only meaningful if a large share is integrated effectively and efficiently in the energy system. As a consequence of their intermittent generation of power, one key challenge will be to increase the systems flexibility on the demand and the supply side. According to [31], this means improving the systems ability to respond to the variability and uncertainty of the residual power load[3] within the limits of the electrical grid. The introduction of controllable system components is necessary to produce or absorb power at different rates, over various time scales and power system conditions [34]. In Germany, as of today, differences in power supply and demand are mostly balanced by pumped-storage power plants [35]. This alone will not be sufficient when considering an ongoing expansion of VRE [36]. Additional load balancing options need to be taken into consideration. In [37] load balancing options for the German energy system are identified and classified into eight categories[4]. On the power supply side this concerns flexible power plants (including cogeneration of heat and power) and flexible biomass. On the power load side it includes Power-to-Gas and Power-to-Heat technologies. Another option is the curtailment of VRE, which however, due to the legally determined priority feed-in for renewable energy remains as the last option [38]. Finally, short-term power storages, such as pumped-storage power plants or stationary batteries, and demand-side management the industry and in private households can contribute to the balancing of the electric load in either case. While the mentioned load balancing options are for the most part well researched individually, the question remains what role they may play as part of the energy system. The contribution of this work is to assess load balancing options under consideration of their interactions of other technologies as well as all energy-related sectors of the German energy system.

[2] The expansion of renewable energy sources in this case is considered on a european level. This means that especially photovoltaic systems are deployed regions with higher irradiation conditions, such as in Southern Europe, which restricts their deployment in Germany [30].

[3] Within this work the residual load is defined as the electric load minus the non-dispatchable generation of power, according to [32] and [33] (cf. section 3.4).

[4] Load balancing options to provide grid stabilisation or frequency control, including magnetic energy storages, capacitors or flywheels, with storage periods ranging from less than one second to a few minutes, are not considered in this work [35].

2 Related Work and Research Questions

Over the last years, various research on the flexibility of energy systems has been published. For the assessment of flexibility different metrics and frameworks have been developed, exhibiting different levels of detail and cases of application [39]. A review of research results and applied methodologies for the categorisation of flexibility is presented in [40]. Further, [41] provides a literature review regarding flexibility requirements in power systems, while [42] compares the flexibility demand in Germany resulting from the coupling of the power, heat and transport sectors.

A rather simple and intuitive way for the assesssment of flexiblity is provided by the flexibility charts, introduced in [43]. They compare the installed capacities of different load balancing options to the maximum occurring electric load, including dispatchable plants, pumped-hydro storages and interconnections. While this method highlights potential flexibility sources, it is not suitable for reflecting the accessible flexibility, as other important factors like market design and system operation are not accounted for. Conversely, the flexibility index [44] and the operational flexibility [45] account for the ramping capability, the required start-up times and the maximum load increase of a specific technology. Thus, the available flexibility may vary significantly over time and should be considered as an estimation of technical flexibility.

The ramping characteristics of technologies are usually given special attention in studies analysing the demand and operation of thermal power plants. Due to priority dispatch of VRE in Germany [38], these thermal power plants are expected to undergo substantial changes in the future. According to [12], the operative hours of thermal power plants are already being reduced and additionally the frequency of start-up proceedings increased, making them less profitable. This trend is confirmed by [46], which, based on a numerical optimization model for the German power sector, investigates the ramping behaviour of thermal power plants, concluding that by 2030 the overall number of start-ups will be increased by 81 % as well as the related costs (+ 119 %). A simulation model for the German electricity market is presented in [47]. It shows that negative market prices often derive from lacking flexibility of the thermal power plant park and underlines the importance of depicting flexibility realistically. The provision costs of flexible system components, including thermal power plants, are further analysed in [48], again with regard to the German power system. The study considers the dismantling of coal power

plants and shows that the addition of gas turbine power plants is a key element in increasing the necessary flexibility of the system. An overview of research assessing the future demand of conventional power generation capacity in Germany is provided by [49]. The meta-analysis shows that the 25 considered studies exhibit significant divergences in their suggested conventional generation capacity for 2050, for instance roughly 0 GW_{el} in [50] and to 70 GW_{el} in [51]. The observed differences are traced back to the varying assumptions concerning the pursued climate protection target, the utilisation of biomass in the power sector, the development of electricity demand or the installed capacity of VRE. Further, the individual studies are performed either based on statistical data, considering only specific parts of the energy system, or on model calculations only for the power sector. Other sectors, i.e. the transport sector, the supply of space heat and domestic hot water or the supply of process heat, are accounted for only in part through scenario assumptions. This shows that an integrated approach that considers the interdependencies of all energy-related sectors is missing. Accordingly, the contribution of load management in other sectors is only considered in part of the studies, leading to higher differences in the determined power plant capacity. According to [52], load management is normally utilised by companies to avoid or at least reduce expensive load peaks. Another option often analysed with regard to flexibility, used to benefit the power supply system, is the shift of flexible loads. This is referred to as demand-side management (DSM).

An often discussed application field for DSM is represented by the industrial sector. In [53], a meta-analysis of DSM processes with particular regard to energy intensive industries is presented. This is due to the fact that energy intensive industries exhibit higher power loads and thus an overall greater flexibility potential. For instance, [54] and [55] determine a cost-effective flexibility potential in Germany of up to 3 GW_{el} and 1.3 TWhel of shiftable loads per year. However, [56] underlines that many industrial companies show low interest in DSM, as they mainly buy their electricity for a long-term fixed price. Another meta-study on this topic reveals that the identified DSM potentials in the industrial sector present major differences between each other [57]. This is confirmed by another comprehensive analysis of the available flexibility potential in the German industrial sector [58]. From the evaluation of 45 studies the analysis concludes that although the individual methodological approaches show some similarities, the identified potentials exhibit wide discrepancies. The study also highlights that interrelationships of resources and processes in the production system are hardly taken into account, usually leading to an overestimation of the determined potentials. For the German industrial sector, a DSM potential of roughly 3 GW_{el} is estimated by [59]. The study also indicates that the DSM potential in this sector is not necessarily easy to exploit, due to the high utilisation of industrial plants, costumer requirements as well as the lack of incentives. Overall, it is shown that while DSM might be utilised in the industrial sector, at the

present stage this option still exhibits many uncertainties regarding its potential and its accessibility. For this reason DSM in the industrial sector will not be considered in this work. This simplification is further supported by [59], which reveals that the overall DSM potential in Germany is predominantly provided by electric and thermal storages (including EVs) in private households, instead of industrial processes.

A technical representation of flexibility, including cogeneration power plants in heat grids, is presented in [60]. It shows that they are mostly operated at a specific must-run capacity as they need to ensure constant heat supply. Thus, a way to increase their flexibility is by coupling them to thermal energy storage (TES). This statement also applies to most buildings in Germany, which today according to [61], consume electricity in times of low to average availability. This suggests that most heat generators in Germany are operated in a heat-controlled way. Moreover, based on a comprehensive building model, the study reveals that an optimal operation of heat pumps in combination with TES, could significantly contribute to the balancing of the residual load. Similarly, [62] concludes that by using a heat pump and the building mass as TES, a relevant amount of energy can be shifted by DSM, especially during average winter days. In [63] an office building in Sweden combined with a battery, a heat pump, an electrical heater and a hot water tank is analysed based on a mixed integer linear programming problem. It is revealed that by taking advantage of flexible energy prices, the overall operation costs in the building are reduced. However, like the other analysis on power-controlled heat generation, this study is also focused on a specific building, making generalisation of the results rather difficult.

A review of the interaction of electric vehicles (EVs) with the power grid and utility interfaces is presented in [64]. In [65] an optimisation model is proposed that, based on the modelling of four residential buildings, shows the possibility to fully provide charging of EVs based on renewable energy sources and thus increase their integration into the energy system. An approach to integrating VRE generation into a manufacturing system through EV battery storage is presented in [66]. A simulation reveals that DSM along with Vehicle-to-Grid (V2G) can effectively integrate decentralised VRE while flattening the resulting load curve. Both studies are performed for specific buildings or facilities and can thus not be applied to the whole energy system. A different approach is utilised in [67], which, based on available electricity market information, shows that optimisation of vehicle charging leads to significant financial savings for costumers and grid operators. While the introduced studies all present a qualitative and quantitative assessment of load balancing options, focusing on the generation of heat or the controlled charging of EVs, the introduction of these load balancing options into the energy system is either missing or described in a rather simplified way.

A detailed model-based analysis of power-controlled CHP units under consideration of the German power system is performed by [48], which identifies them as a cost-efficient option for the provision of flexibility. The study focus is on the methodological quantification of the resulting provision costs. Interdependencies between the heating sector and other sectors are not investigated and for example, the expansion of controllable components is exogenously set. A study on load balancing options by demand response and TES considering all energy-related sectors of the German energy system, is presented in [68]. The analysis is based on an enhancement of the REMix model [68–71], which was detailed with regard to its consideration of the heat demand and supply, while predetermined scenarios were used for the transport sector, thus excluding the analysis of feedback effects on the technology deployment. The study reveals that a power-controlled heat supply effectively increases the integration of VRE, therefore reducing the overall curtailments and ultimately benefiting the energy system. Further, it concludes that load shifting proves to reduce the necessary generation capacity in general, when the highest contribution derives from controlled electric vehicle charging.

The importance of considering the transport sector as part of the whole energy system is underlined by [72], pointing out that significant contributions to GHG emissions and associated costs also arise from energy supply, provision and conversion in other sectors. It further presents a comprehensive analysis of alternative fuels and vehicle technologies for the transport sector of Gauteng (South Africa), concluding that EVs play a minor role. However, due to substantial differences in factors, such as infrastructure, demographics and other factors this insight is not transferable to the German transport sector. In [73, 74] the transport sector is analysed as part of the whole energy system, with particular regard to the future role of alternative fuels and power train technologies. However, both studies do not consider neither V2G nor Grid-to-Vehicle (G2V). This is accounted for in [75], which proposes a model for the evaluation of future market shares in Germany. In order to depict interactions between road transport and the energy industry, the model is coupled to the SCOPE model [76–78]. The study reveals that the controlled charging of electric vehicles and the production of alternative electricity-based fuels provide additional and valuable flexibility for the future energy system. However, the utilised approach excludes the analysis of feedback effects occurring between the transport sector and other technologies of the energy system. This is also the case for [79], which, based on extensions of the MARKAL model (EHM and GMM), assesses the role of alternative power train technologies as part of the German energy system. It shows that biofuels play only a major role in the transport sector when moderate climate protection targets are considered, while being used in other consumption sectors otherwise. The study further underlines that hydrogen might become a competitive source of energy.

A model-based analysis of an alkaline electrolysis plant and hydrogen storage in a microgrid is presented in [80]. Within the considered field of study, it is revealed that flexibility rather than the long-term storage capability of hydrogen systems represent their main advantage. On this topic, [81] confirms that the flexibility of Power-to-Gas (PtG) can improve security of supply. It further underlines the value of high density fuels in large parts of aviation, shipping or specific industrial or chemical processes, as the generation of synthetic liquid fuels in addition to biofuels provide the only technically feasible solution to achieve ambitious CO_2 reduction targets. Their significance in achieving the pursued climate protection targets is also highlighted in [82], again underlining the relevance of considering all sectors of the energy system. A different conclusion is reached in [83] and [84], showing that while DSM applied to heat generators and EVs leads to a high integration of VRE, PtG technologies are not cost-efficient. Both analyises are based on calculations performed with the Pan-European TIMES model [85], which accounts for interdependencies between all sectors of the energy system, under consideration of 224 time segments per year[1]. In [59] it is assumed that PtG plants are operated only in case of excess electricity production from VRE. The study shows that this alone is not sufficient to guarantee an economic operation, making power curtailment the preferred option. It also concludes that long-term storage of energy, in a time range of one to four weeks, is only necessary if particularly ambitious climate protection targets and prolonged periods with low feed-in from VRE are considered. This analysis was performed based on only one specific weather data, which suggests that a variation of weather data or the investigation of extreme weather influences could affect the respective outcome. This aspect, for instance, will be addressed as part of the project „long-term scenarios and strategies for the expansion of renewable energy sources in Germany“ [88]. While most calculations will be performed based on the weather data of 2010, in the ninth module of [88], a consideration of extreme weather influences, including prolonged periods of low feed-in from VRE, is planned.

The presented literature review shows that over the last years different approaches were used for the analysis of load balancing options in Germany and beyond. Multiple studies assessed the flexibility potential of single system components or specifically of the power sector, by considering high spatial and temporal resolutions as well as market mechanisms. Various studies analysed the German energy system under consideration of all sectors. However, these studies are often performed based on scenario calculations, assumptions or independent model runs and further consider only one specific weather data set, such as in [16–18, 75, 89–95]. As a consequence, the feed-back effects occurring

[1]The TIMES model generator was developed within the Energy Technology Systems Analysis Programme (ETSAP) and provides a generic series of equations, offering a certain degree of flexibility regarding the spatial and temporal resolution as well as the investigated period [86], [87]. The intertemporal resolution within one year is represented by specific time segments, which may consist of typical weeks, days and hours.

between different sectors and technologies of the energy system can only be considered to a certain degree. On this regard, [59], [96] and [97] suggest to complement such analyses by following a cross-sectoral modelling approach. This is for instance presented in [98], which, based on the TIMES-D-DSM model, analyses the DSM potential in Germany. In order to perform this analysis the temporal resolution of the model is increased to 672 time segments. Other examples utilising the TIMES-D-DSM model for the assessment of DSM in energy systems with a high penetration of VRE, such as [99] and [100], consider temporal resolutions of less than 300 time segments per year. Especially for studies related to energy systems based on a high penetration of VRE this may represent a relevant issue. An energy system model which considers all sectors and depicts the interdependencies occurring between them while considering an hourly resolution, is the Renewable Energy Model (REMod) [15, 101–103]. Thus, it presents a good basis to fill the identified gap and therefore is utilised within this work (cf. section 3). However, the model lacks some features, relevant for the assessment of flexibility. For instance, thermal power plants are able to provide their full generation capacity whenever necessary, i.e. without consideration of start-up times, ramp rates, partial load operation or other restrictions. As for the supply of heat, all generators are a priori operated in a power-controlled way, preventing a qualitative or quantitative assessment of a heat-controlled or power-controlled operation. Further, the charging of EVs is modelled as a constant load, thus neglecting the effects deriving from a more realistic consideration of driving behaviour and thus a possible simultaneous charging. These examples show that a detailed analysis of load balancing options based on REMod was yet not performed. Accordingly, the model needs to be further developed. On that basis, the following research questions are investigated:

1. How are the model results influenced by the consideration of ramping behaviour?
2. How does the availability of demand-side management influence the value of electric vehicles and heat generators for the energy system?
3. What value does demand-side management represent for the entire energy system and how sensitive are results to the underlying weather data?

Structure of this Work

This work begins with a presentation of the utilised energy system model and a introduction of load balancing options. After this, the underlying input data is described and a calibration of the model for the year 2015 performed. Lastly, all relevant model runs for the assessment of load balancing options are presented and an outlook for future research given. Figure 2.1 illustrates the structure of this work.

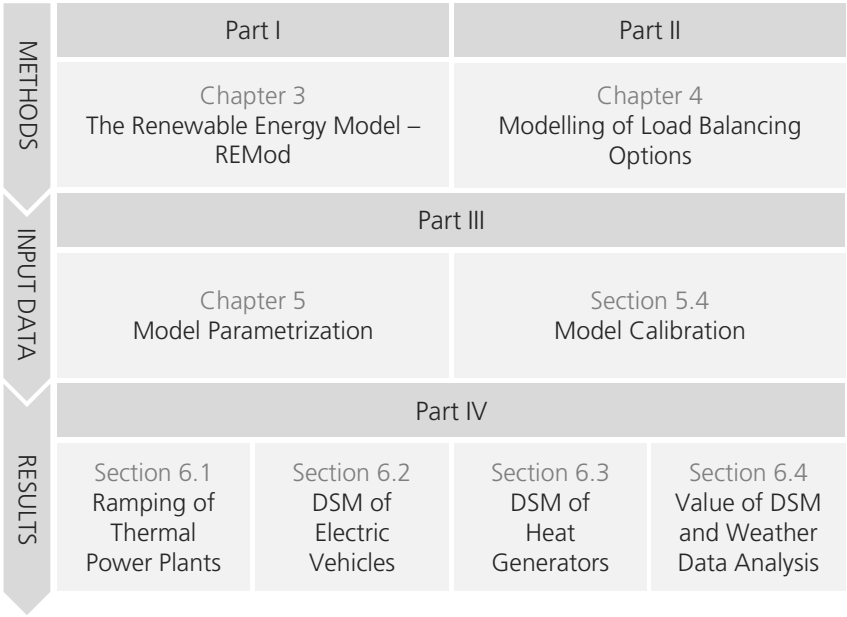

Figure 2.1: Structure of this work.

Part I - The Renewable Energy Model - REMod

This work opens with an introduction of the utilised energy system model REMod. First, an overview of the model history, including the most relevant publications is presented. After this, the model's structure, its objective function, its design and the utilised optimisation algorithm are described. The chapter closes with the most relevant system components and their implementation in the model.

Part II - Modelling of Load Balancing Options

This part delivers a detailed presentation of the major model extensions developed in this work, necessary for the assessment of load balancing options in REMod. This includes the consideration of ramping behaviour, DSM of EVs and of heat generators. Further, the modelling of electricity cross-border exchange and load balancing by power storage systems and PtG plants is described.

Part III - Model Parametrisation

In this part, the structure of the necessary input data is presented. While the parametrisation of system components is adjusted on a yearly basis, time series consider an hourly resolution. After this, the model is calibrated for the year 2015 and the differences between the results and real data discussed. This serves as starting point for the following result evaluation.

Part V - Results

The result chapter is divided into four sections and includes all optimisation and simulation runs performed to answer the identified research questions. The first section presents an assessment of thermal power plants. The second and the third parts provide an isolated analysis of DSM for EVs and for heat generators, respectively. The last section analyses the value of DSM based on uncertainties in technology deployment and weather influences and provides a cost assessment of DSM. The thesis concludes with a summary of key results and provides an outlook for future research.

Parts of the research have been published in articles, presented at conferences [104–110] or research projects [18, 111–113]. The master theses [114–118] were supervised by the author.

3 The Renewable Energy Model - REMod

The Renewable Energy Model (REMod) was developed as part of an internal research project at the Fraunhofer Institute. The main idea of REMod is to provide a deeper understanding for national energy systems with particular regard to interdependencies occurring between different sectors and energy carriers. In this chapter, the model's main development steps, its structure and functioning principle are presented.

3.1 Model History

Since REMod was launched it has been utilised within various projects and studies. Through regular collaboration with stakeholders from industry, politics and non-governmental organisations the model is constantly improved in order to address current issues. Previously to this work, three main stages of development can be identified.

In its first stage, in 2012, REMod provided a tool for the simulation and optimisation of a potential future German energy system entirely based on VRE [119–121]. Its aim was the detailed description of interdependencies occurring between the heat and electricity sector. This was in particular represented by electric heat pumps and combined heat and power units. At this stage the fuel-based energy consumption of the transport sector and those for the supply of process heat were not included. As a calculation result, all considered system components were dimensioned in a way to achieve minimum annual costs. At this time the model calculations were performed based on a „green field optimisation approach“, meaning that the current system configuration was not accounted for. For this purpose a modified, multi-dimensional regula falsi approach was utilised.

In 2013, after diverse improvements a new model state was presented [101, 102]. While the focus remained the linking of the electricity and heat sector, the study area was extended. The transport sector and the supply of process heat were considered as constant loads, however not being subject to the optimisation process. This means that the technology distribution in those sectors had to be specified beforehand. Similarly, the power generation was no longer limited to VRE but included thermal power stations, such as nuclear, hard coal, lignite and oil plants. Their respective installed capacities were also

predetermined. Compared to the previous version, the building sector was considered in greater detail. This includes the addition of new heat generation systems, the distinction of different energetic retrofitting measures as well as a more detailed calculation of the hourly heat load. Besides structural improvements, it was now possible to determine a threshold value for the energy-related CO_2 emissions. This boundary condition enabled to assess the compliance of the endogenously determined energy system with specific climate protection targets. As a consequence of the implemented model extensions, the former optimisation algorithm proved to be inefficient and was substituted by a better performing Particle Swarm Optimisation approach.

In 2015 the model took another step forward [15, 103]. While the fuel-based energy consumption of aviation, shipping and rail travel was considered as yearly balance, the motorised road transport sector was modelled in greater detail. In total seven distinctive power train technologies for the private as well as the freight transport were introduced and their respective shares optimised. Further, the model observation period was extended, ranging from 2015 to 2050. Thus, the transition process of the energy system, rather than its final state, could be assessed. The time line shown in figure 3.1 summarises the main features and development steps of REMod up to 2016.

	2012	2013	2015
Considered end-use sector			
Space heat and domestic hot water	X	X	X
Electricity	X	X	X
Transport sector		X	X
Process heat demand		X	X
Investigated time horizon	One year	One year	2015 to 2050
Optimisation characterisitcs			
Optimisation Approach	Modified regula falsi	Particle Swarm Optimisation	Particle Swarm Optimisation
Optimisation objective	Annual system costs	Annual system costs	System transformation costs
Main boundary condition	100 % VRE	Limitation of CO_2 emissions	Limitation of CO_2 emissions

Figure 3.1: Timeline describing the main development steps of REMod. VRE: variable renewable energy.

Over the last years the model has further been extended. In the next section, a description of the current model structure and its operating principle is provided. The focus hereby is on information considered necessary for the understanding of the model as well as contents describing developments following the model state of [103].

3.2 Model Structure

In this section the structure of REMod is introduced. First, two databases containing all relevant input data and assumptions are presented. Then, all end-use sectors considered in the model are explained one by one. This includes the transport sector, the generation of process heat, the supply of space heat and domestic hot water as well as the electric base load. Figure 3.2 provides an overview of the model, including key input and output parameters as well as the main considered energy conversion technologies and end-use sectors.

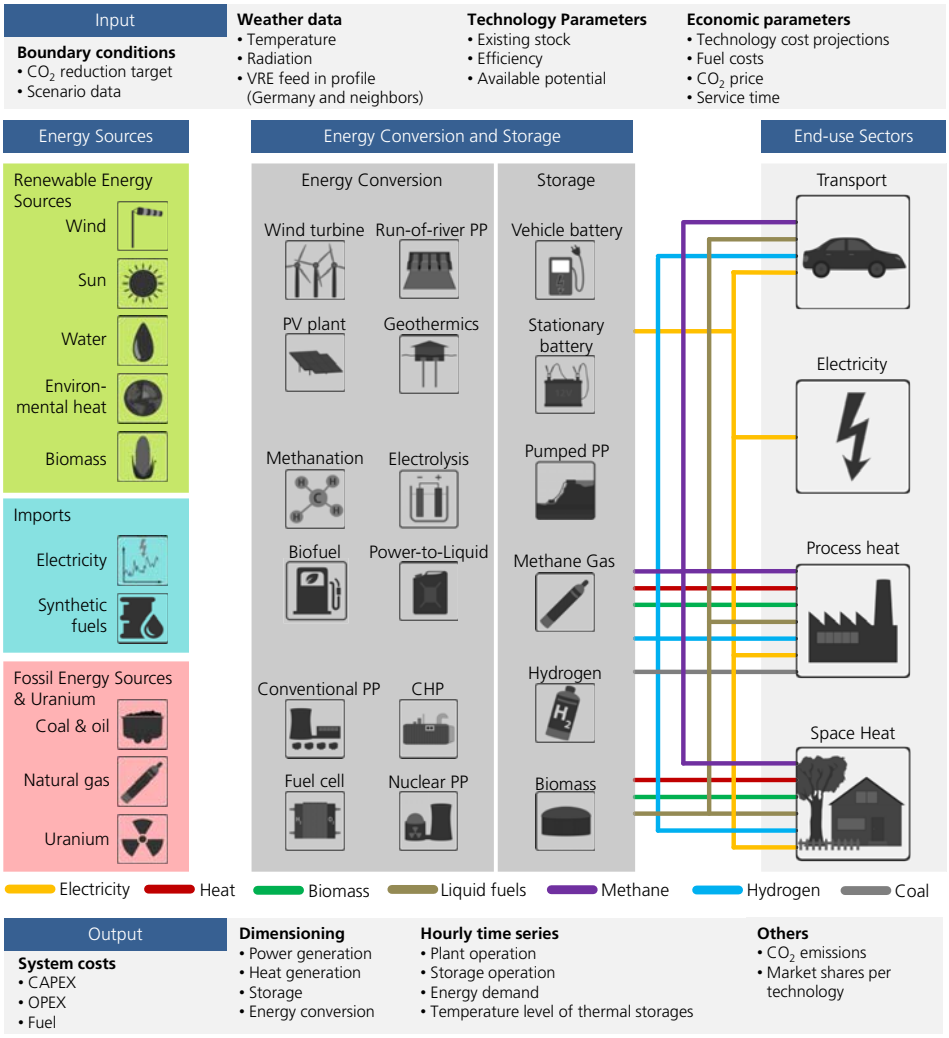

Figure 3.2: Scematic overview of REMod, including key input and output parameters as well as main energy conversion technologies and end-use sectors. Technologies belonging to specific end-use sectors are not included in this illustration.

3.2.1 Required Input Data

The model calculations are based on two comprehensive databases, which can be distinguished according to their temporal resolution. The first contains information regarding hourly time series for the time period of 2011 to 2015. This for example includes the driving behaviour in the motorised transport sector or energy demand profiles, like the process heat demand or the supply of hot water. It also contains weather dependent data, such as the ambient temperature and radiation values for North and South Germany, provided by the German Meteorological Service (DWD). Further, feed-in profiles from onshore and offshore wind as well as photovoltaic and hydroelectric power stations are documented.

The second database deals with technology and economic parameters as well as boundary conditions on a yearly resolution from 1990 to 2050. This database is subdivided into two parts. The first contains technical parameters of all relevant components of the energy systems from 1990 to 2018. This for example includes efficiencies and installed capacities of power plants and other conversion technologies, storage facilities and heat generators in buildings, information concerning the building stock as well as its physical characteristics, the number of vehicles subdivided by power train technology and other modes of transport. The second part, ranging from 2019 to 2050, mainly deals with assumptions regarding cost or performance projections of each technology, their service time, the pricing of imported energy carriers and CO_2 emissions as well as other technical restrictions which will be introduced in section 5.

Here, a distinction between two sector structures needs to be introduced, namely system components with a Non-Predetermined or with a predetermined total amount. The penetration of technologies of systems with a non-predetermined total amount may be increased or decreased as long as it does not violate the exogenously set capacity limit. For example, an assumed technical potential of offshore wind turbines of $85\,GW_{el}$ would lead to an average yearly expansion limit of roughly $2.4\,GW_{el}$ per year starting from 2015. Here it is possible to consider restrictions linked to production or installation capacities by starting from lower capacity limits and increasing them over time. Likewise, the optimisation results could also suggest not to install any offshore wind turbine, such that through shut-downs, the total amount of offshore wind power decreases over the years. While the installed capacity of each technology within systems with a non-predetermined total amount can increase or decrease within the set boundary, in systems with a predetermined total amount the technologies are further limited by other constraints. For example, the cumulative deployment of technologies for space heat and domestic hot water supply is determined by the total number of buildings in Germany per year. The assumption made is that every building is supplied by one heating system. Whenever it reaches the end of its expected service life, either a heat generator of the same type is

installed or a different option is chosen. This means that the share of each technology available within the system with a predetermined total amount is endogenously determined. Conversely, the total number of heating systems is exogenously set according to the expected development of the building stock in Germany up to 2050.

Whether a technology is belongs to a systems with a non-predetermined or with a predetermined total amount mainly depends on the considered end-use sector. As mentioned, heating systems for the supply of space heat and hot water are subject to systems with a predetermined total amount as they are limited by the total number of buildings assumed each year[1]. This also applies to the energetic refurbishment of buildings, which can also not exceed their number in the first place. Similarly, this concerns the deployment of technologies utilised for the supply of process heat. Here the limitation is represented by the energy demand at a given temperature level (cf. section 3.2.3). Another sector with a predetermined number of overall components is the motorised transport sector, where the expected development of private vehicles and trucks or buses defines the total number of vehicles. Technologies used for the generation of power, such as VRE and thermal power plants or for the production of synthetic fuels as well as storage facilities are not linked to a specific end-use sector and thus represent systems with a non-predetermined total amount. Subsequently, a description of the four end-use sectors considered in REMod as well as the technology options related to them is presented in detail.

3.2.2 Transport Sector

The transport sector in REMod can be divided into two categories, namely the motorised road transport and other means of transport. Other means of transport include aviation, shipping and the fuel-based railway traffic[2]. All three are described by a yearly energy demand, i.e. without considering a temporal resolution and can be met exclusively by liquid fuels. As a consequence, the CO_2 emissions resulting from this category can only be reduced by varying the fuel composition. Here, different options exist, such as the conversion of electricity into synthetic liquid fuels (Power-to-Liquid), the production of biodiesel out of rapeseed, the gasification of biomass and conversion into liquid fuels or finally, the import of synthetic fuels.

The motorised transport sector is considered by passenger cars and trucks (including buses). Both are mapped in detail concerning temporal resolution and seven distinctive power train technologies each. This includes internal combustion engines (ICE) fuelled

[1] Solar thermal systems represent an exception, as they are part of an system with a non-predetermined total amount. The reason why is that they are not modelled in a way to meet the entire heat demand, but rather to complement the installed heat generator (for instance an oil boiler).

[2] The demand profile of the electrical rail transport is considered as part of the electric base load, which is presented in the next section 3.2.5

with methane gas[3] or liquid fuels (gasoline, diesel), hydrogen fuel cells, purely battery powered or plug-in hybrid drive systems. The latter consist of an ICE or a fuel cell combined with a battery utilised for driving.

Depending on the distribution of power train technologies, a corresponding expansion of the charging infrastructure is considered. Each charging facility is characterised by yearly adjustable parameters. This includes their costs of investment, maintenance and operation, their technical service time as well as their individual coverage rate. The coverage rate describes how many vehicles can be supplied by one facility of a specific type. For instance, a coverage ratio for CNG filling stations of 0.001 and one million CNG-vehicles would yield to a number of required filling stations of one thousand. If over the following year the number of CNG-vehicles decreases, the existing CNG filling stations will remain for as long as intended by their technical service time. Conversely, whenever an additional CNG-vehicle is introduced, the number of filling stations is only increased if necessary. In total, eight different charging facilities are considered, divided by passenger cars and trucks, respectively:

- Slow charging station (wallbox) for electric vehicles.
- Fast charging facilities for electric vehicles.
- CNG filling stations for CNG-vehicles (including plug-in hybrids)
- Hydrogen filling stations for fuel cell powered vehicles (including plug-in hybrids)

The final energy demand of aviation, shipping and fuel-based railway traffic is exogenously set for each year and modelled without consideration of a timely resolution. As for the motorised transport sector a higher level of detail is introduced. The modelling approach and the respective equations are presented in detail in section 4.3. Figure 3.3 summarises the main components belonging to the transport sector.

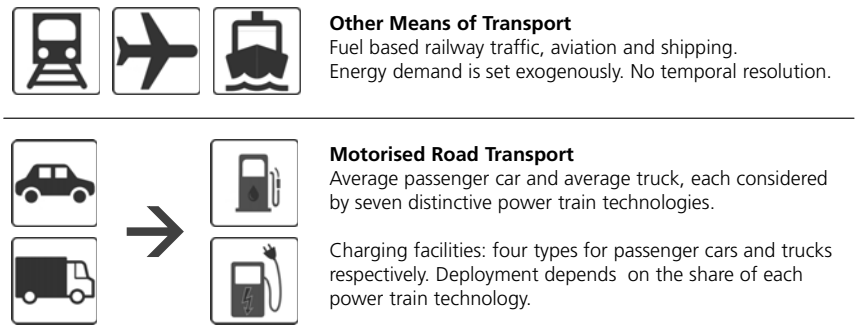

Figure 3.3: Overview of technologies belonging to the transport sectors, subdivided into motorised road transport and other means of transport.

[3]The methane slip of CNG-vehicles is considered according to [122] with $500\,{}^{mg_{CH_4}}/_{m^3}$.

3.2.3 Process Heat Supply

As shown in figure 3.4 the final process heat consumption in Germany remained relatively stable over the last few years. According to [123], from 2010 to 2016, it amounted on average to 535 TWh_{th} with variations of $\pm$ 2 %. Together, the households and the tertiary sector account for roughly 10 % of this demand, while the remaining 90 % are used for industrial applications.

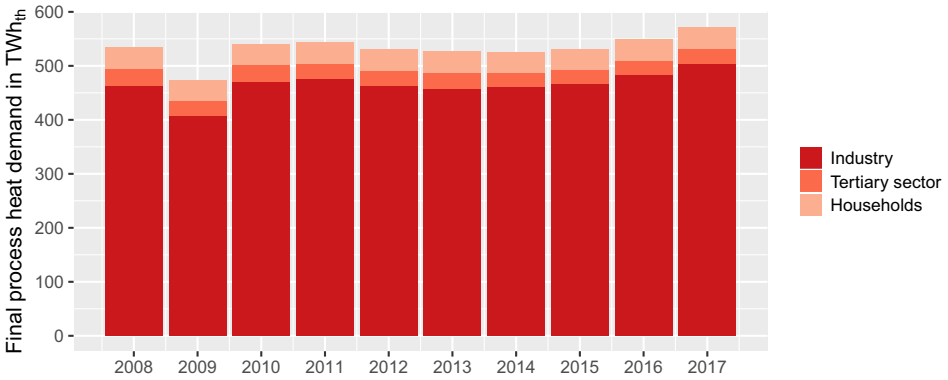

Figure 3.4: Development of process heat consumption in Germany based on [123]

Based on [124], the process heat demand is grouped into two different temperature ranges. The first includes all processes requiring low to medium temperature levels, i.e. below 500 °C. For example, bleaching and drying in the pulp and paper industry or distilling and pressing in the chemical industry [124, 125]. Processes requiring higher temperatures, such as the production of various metals, are summarized in the high temperature range. Table 3.1 provides an overview of the process heat demand in Germany in 2008, categorised by end-use sector and supply temperature level.

While the data displayed in table 3.1 is representative for the year 2008, the stable energy consumption over the last years in this sector (figure 3.4) suggests that the supply temperature requirements did not change significantly either. Concretely, the total process heat demand in 2008 year differs from the mean value between 2010 and 2016 by only 0.05 %, being almost identical [123]. Therefore, the information concerning the temperature distribution provided by table 3.1 will be utilised as approximation for years following 2008. This means that for each year the energy demand shares below or above 480 °C will be assumed equal to 35.6 % and 64.4 % respectively[4]. Conversely, the yearly process heat demand may be adjusted in the model parametrisation, offering the possibility to consider various possibilities of its development.

[4] According to available data summarised in table 3.1, the distinction between high and low temperature process heat in the model is defined at 480 °C rather than 500 °C.

Table 3.1: Process heat demand in Germany in 2008 subdivided by end-use sector and supply temperature level. Based on [125, 126] and own assumptions.

Temperature level in °C	Textile, printing and polymer processing	Wood and paper	Vehicle construction	Chemical	Metal production and processing	Food	Glass and ceramics	Sum	Share
0 - 60	4.78	16.92	8.46	0.68	1.47	3.51	0.19	36.01	7.6 %
60 - 100	0.63	37.12	0.22	0.83	1.00	9.23	0.00	49.03	10.3%
100 - 120	1.26	0.19	0.01	0.00	0.00	23.51	4.99	29.96	6.3 %
120 - 180	1.10	0.42	0.00	0.43	0.00	0.07	0.00	2.02	0.4 %
180 - 240	1.12	0.60	0.61	1.60	0.00	2.12	0.33	6.38	1.3 %
240 - 300	5.03	0.00	0.00	0.81	0.00	0.00	0.00	5.84	1.2 %
300 - 360	0.04	0.00	0.00	10.67	0.00	0.00	0.00	10.71	2.3 %
360 - 420	0.00	0.00	0.00	3.95	0.00	0.01	0.00	3.96	0.8 %
420 - 480	3.28	0.00	0.00	21.40	0.00	0.00	0.69	25.37	5.3 %
480 - 540	0.00	0.00	0.00	1.47	0.00	0.01	1.31	2.79	0.6 %
540 - 600	0.00	0.00	0.00	0.00	0.00	0.12	2.25	2.37	0.5 %
600 - 700	0.00	0.00	0.00	0.00	0.00	0.00	3.75	3.75	0.8 %
700 - 800	0.00	0.00	0.51	0.32	0.33	0.00	4.50	5.66	1.2 %
800 - 900	0.00	0.00	0.00	61.71	0.00	0.00	1.88	63.59	13.4%
900 - 1000	0.00	0.00	0.53	0.00	8.12	0.00	1.12	9.77	2.1 %
1000 - 1100	0.00	0.00	0.00	0.00	1.91	0.00	7.84	9.75	2.1 %
1100 - 1200	0.00	0.00	0.00	0.00	17.08	0.00	0.00	17.08	3.6 %
1200 - 1300	0.00	0.00	0.00	2.58	11.26	0.00	0.00	13.84	2.9 %
1300 - 1400	0.00	0.00	0.00	0.00	0.00	0.00	10.09	10.09	2.1 %
1400 - 1500	0.00	0.00	0.00	0.00	115.00	1.43	38.02	154.45	32.5%
> 1500	0.00	0.00	0.68	0.00	10.07	0.00	1.66	12.41	2.6 %
Sum	17.24	55.25	11.02	106.5	166.24	40.01	78.62	474.83	
Share	3.6%	11.6%	2.3%	22.4%	35.0%	8.4%	16.6%		

The distinction between low to medium and high supply temperature is further utilised to determine the progression of the process heat demand profile within each temperature range. Plants supplying heat at high temperatures aim to run at highest possible utilisation to limit thermal losses and energy intensive heat-up procedures. In this case, a constant energy demand is assumed. Conversely, the demand profile of low to medium temperature processes is based on the progression of the electric base load (cf. section 3.2.5), therefore exhibiting a temporal dependency.

In total nine different technology options for the supply of process heat are implemented in REMod. The maximum demand share each generator can meet, is determined based on process-related restrictions as well as its application range. This range depends on the maximum supply tempearture of the considered technology and the process temperature distribution shown in table 3.1. For instance, [124, 127] show that combined cycle plants and biomass boilers are used for the supply of process heat up to 500 °C. According to [124, 125], solar thermal systems can provide supply temperatures until 300 °C. Further, by considering restrictions like the available waste heat potential, efficiency enhancements, limited installation area and the solar coverage ratio in Germany, approximately 12 % of this potential can be exploited, yielding an upper technical limit of 14.4 TWh_{th} per year [125]. Another restriction regards the application range of heat pumps. Their standard use concernes supply temperatures below 100 °C, i.e. for industrial processes like washing, drying or pasteurizing. However, [128–130] show that further variants under development are able to reach significantly higher supply temperatures up to 160 °C and should be available in the near future.

Process-related restrictions regard, for example, the steel industry and more precisely the production of iron. The chemical equation 3.1 describes the reduction of iron ore, where coal (and coke) is used as reducing agent. In 2015 and 2016, 14.3 million tons of coke coal were imported in Germany and used for the production of steel, leading to a final energy demand of 105 TWh [123, 131]. The emissions originating from this process are classified as energy-related emissions as the coal besides being used for the reduction of iron ore also provides the necessary process heat. One promising option to reduce this coal demand is its substitution by hydrogen (ratio: 1/2 [112]) as described in eq. 3.2 [132]. While this process is well known as laboratory experiment, it is not yet sufficiently mature for economic large scale operation [133]. As a consequence, the process heat demand for the production of iron in the model is by default met by hard coal. An optional shift to hydrogen is implemented and can be investigated by adjusting the substitution share in each individual year.

$$Fe_2O_3 + 2\,C \longrightarrow 2\,Fe + CO + CO_2 \tag{3.1}$$

$$Fe_2O_3 + 3\,H_2 \longrightarrow 2\,Fe + 3\,H_2O \tag{3.2}$$

Table 3.2 provides an overview of the implemented technology options for the supply of process heat as well as their ranges of application and specifications.

Table 3.2: Overview of technologies considered in REMod for the supply of process heat. LMT: low to medium temperature (up to 480 °C), HT: high temperature (more than 480 °C).

Technology	Temperature	Specifications and restrictions
Coal-fired boiler	LMT/HT	Mandatory utilisation for iron production if not substituted by hydrogen [112, 131, 133]
Oil-fired boiler	LMT/HT	
Methane Gas boiler	LMT/HT	
Electrode boiler	LMT/HT	
Hydrogen-fired boiler	LMT/HT	Mandatory utilisation for iron production if coal is substituted
Biomass boiler	LMT	Only for processes $< 480\,^{\circ}\mathrm{C}$ [124] Up to 35.6 % of total demand
CCGT	LMT	Only for processes $< 480\,^{\circ}\mathrm{C}$ [127] Up to 35.6 % of total demand
Solar thermal heat	LMT	Only for processes $< 300\,^{\circ}\mathrm{C}$ [124, 125] Up to 3.0 % of total demand
Heat pumps	LMT	Only for processes $< 120\,^{\circ}\mathrm{C}$ [128–130] Up to 24.2 % of total demand

While the specifications in table 3.2 describe the maximum theoretical potential of each technology per application area, the starting deployment in 2015 is based on the present state. On this basis a conversion factor for final to useful energy is calculated. The useful energy demand represents the starting point for the determination of the final energy consumption and depends on the occurring technology distribution, i.e. the thermal efficiency of the utilised heat generators. The parametrisation and market shares of all technologies considered for the supply of process heat are discussed in section 5.

3.2.4 Space Heat and Domestic Hot Water Supply

This sector accounts for the energy demand required for space heat and the supply of domestic hot water in Germany. As described in [103], the German building stock is subdivided into residential and non-residential buildings, which are depicted by nine and ten reference buildings, respectively. Each one represents the average characteristics for a specific usage type and age class. This for example includes its physical properties, such as the thermal transmission coefficients, the total surface and volume, the orientation of the building components, the level of water consumption or the night setback parameters. On this basis, the useful energy demand for space heat of Germany's building stock is calculated according to the DIN EN 13790. In order to consider different climates, the reference buildings are equally distributed over two locations, namely Braunschweig and Würzburg, for North and South Germany, respectively. Different user behaviours are considered by distributing the resulting demand profile with a Gaussian function. This

ensures, to avoid exact simultaneity and therefore unrealistic peak demands[5]. Further, it is considered that users living in older buildings tend to be more energy efficient, for instance by ventilating less. The opposite trend is observed for refurbished buildings, where the energy consumption exceeds the calculated energy demand [103,104]. For this purpose, the resulting heat demand is adjusted by converting it into energy consumption values. The useful energy demand for domestic hot water supply is assumed as a constant load and added to the demand profile for space heat, yielding to the total heat load profile.

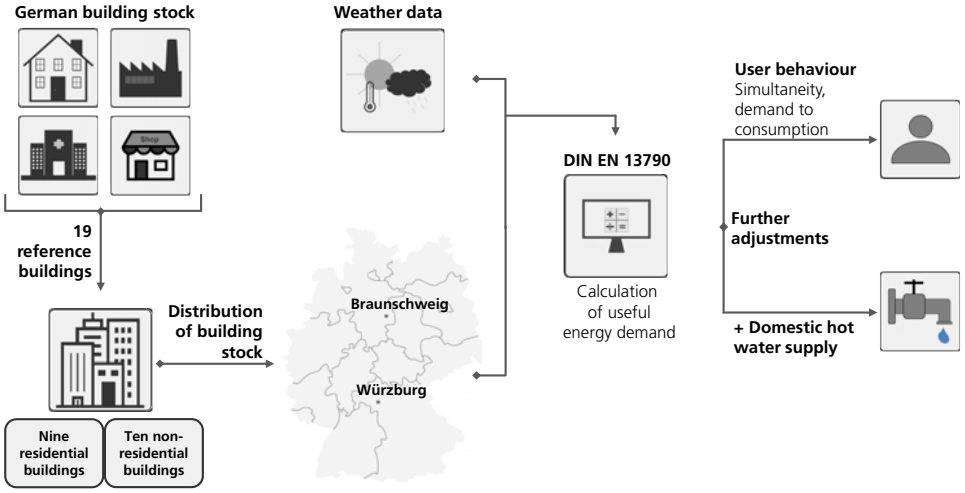

Figure 3.5: Schematic representation of the heat demand calculation (space heat and domestic hot water).

The heat load profile can be influenced by different mechanisms. The first concerns the exogenously set number of buildings, which is yearly adjustable. This parameters allows to indirectly consider demographic changes as well as the increase or decrease of the assumed living area per person. The second option is provided by endogenously determined energetic refurbishment of buildings. Here, three different levels are defined. The first level describes the building in its unrenovated state. The second level is based on the EnEV guideline [134], considering lower transmission coefficients for windows, walls, doors and the roof (fully refurbished). These parameters are further reduced by 25 % in the third refurbishment level (highly efficient). Table 3.3 describes provides an overview of the building physics requirements linked to the refurbishment levels considered in the model and the relative reduction of the heat load in relation to the unrenovated state.

[5] An accurate representation of the heat load calculation is described in [103]

Table 3.3: Refurbishment levels considered in REMod and respective heat transmission coefficients. Based on [103, 134].

Characteristics	Unit	Fully refurbished	Highly efficient
Coefficient Window	W/m^2K	1.365	0.7
Coefficient Wall	W/m^2K	0.294	0.1
Coefficient floor	W/m^2K	0.367	0.1
Coefficient Roof	W/m^2K	0.210	0.2
Heat demand referred to unrenovated	%	50.3	35.7

In order to meet the determined useful heat demand 12 different technologies are implemented. Thereof, ten decentralised systems are further distinguished depending on their heating transfer system, i.e. radiator or panel heating. The transfer system determines the required supply temperature and may influence the performance of the considered heat generator and therefore the final energy demand.

Subsequently, all considered technologies for the supply of space heat and domestic hot water supply are listed. Each technology can be complemented by a solar thermal system as well as a hot water storage equipped with a heating rod.

- Boilers (in single buildings): oil, gas or biomass boilers.
- Micro-CHP units (in single buildings): run with methane gas.
- Fuel Cells (in single buildings): run with methane gas or hydrogen.
- Heat pumps (in single buildings): represented by electric air-to-water or brine-to-water heat pumps, as well as methane gas-based air-to-water heat pumps. Further a hybrid heat pump is considered, which consists of a methane gas-fired boiler combined with an electric air-to-water heat pump.
- District heat (in heat grids): combination of methane gas-CCGT, large scale electric air-to-water heat pump, methane gas-boiler and deep geothermics (only for heat generation).

Each building can be supplied by one heating system or one connection to the heat grid, respectively. Thus, the number of heat generators is determined by the exogenously set number of buildings, which is referred to as system with a predetermined total amount. The share of each technology is endogenously determined within the set expansion limits.

3.2.5 Electricity Base Load

The electricity base load accounts for those fields of the power system, which in REMod are not subject of the optimisation. They can be subdivided into four main categories of power demand. The first two contain lighting technologies as well as information and communication devices. The third, describes room air-conditioning and process-cooling applications, which exhibit a substantially higher share. The last category accounts for mechanical energy based on the supply of power. In order to account for weather-dependency, the profile of the electricity base load is derived from real data provided by the European Network of Transmission System Operators for Electricity (ENTSO-E). This time series need to be adjusted, as they also contain application fields, which are endogenously determined by the model. For instance, the deployment of electricity-based heat generators is determined by the optimisation process. A possible transition towards electric heat pumps would therefore lead to a corresponding increase of the cumulative electric load. Conversely, it would also be possible that electricity-based heat generators are replaced by other options. This shows why their power demand needs to be excluded from the electricity base load. The same holds for electricity-based technologies, utilised for the supply of process heat. As for the road transport sector, no adaptation is required, since at the present day, electric vehicles in Germany still play a minor role. Table 3.4 summarises the total electricity demand for the years from 2011 to 2015 according to [123].

Table 3.4: Overview of the power demand in Germany in TWh_{el} from 2011 to 2015. Based on [123]. DHW: domestic hot water.

Application	2011	2012	2013	2014	2015
Lighting technologies	86.0	88.9	78.9	75.6	77.1
Information and communication	58.8	59.7	59.3	57.6	57.9
Cooling applications	52.1	53.0	56.3	54.9	55.7
Mechanical Energy	204.1	200.4	208.5	209.7	207.2
Electricity base load demand	401.0	402.0	402.9	397.8	397.9
Space heat and DHW	40.7	40.8	41.7	36.6	37.4
Process heat	84.3	85.3	83.6	83.4	84.4

The power demand for space heat and domestic hot water supply for each of the five weather data sets is listed in table 3.4. In order to detract it from the electricity base load it is distributed over the year according to the outside temperature. For this purpose a heating threshold temperature of 15 °C is assumed[6]. This approach is exemplarily shown in figure 3.6, where the distributed power demand for the supply of heat is illustrated for Northern and Southern Germany in case of the weather data of 2011.

[6]The approach is documented in detail in [103]

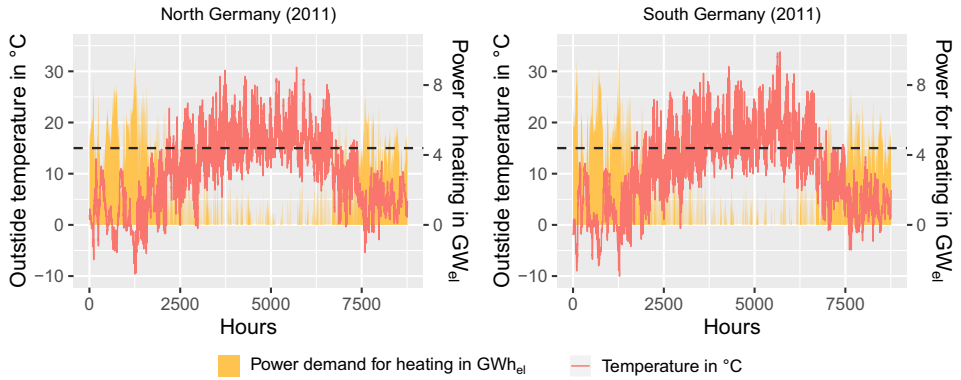

Figure 3.6: Power demand for the supply of heat in Northern and Southern Germany for 2011, distributed according to the outside temperature. The dashed line represents the assumed heating threshold value, which is set to 15 °C [103].

The main axis of figure 3.6 shows the outside temperature in °C. The secondary axis represents the hourly distributed power demand of electricity-based heat generators. In total, according to table 3.4, it amounts to 40.7 TWh_{el} for 2011.

As previously mentioned, the power demand for the supply of process heat needs also to be excluded from the electricity base load. In this case, a distribution of the power demand according to the outside temperature does not seem appropriate. Instead, two different electricity demand profiles are assumed, depending on the considered temperature supply level. One is distributed according to the normalised electricity demand profile from ENTSO-E, which was previously adjusted by the power load of technologies for the supply of space heat. This profile is utilised for process heat supply temperatures below 480 °C. As a consequence of the increased utilisation of heat generators in the high-temperature range, the hereby resulting power demand is assumed constant (cf. section 3.2.3). Relating to table 3.4 the total power demand for the supply of process heat in 2011 amounts to roughly 84 TWh_{el}. The electricity base load demand E_{BL} for a particular year i is calculated as described in eq. 3.3.

$$E_{BL,i}(t) = (E_{L,i} + E_{ICT,i} + E_{C,i} + E_{M,i}) \cdot E_{E,n,adj,i}(t) \cdot f_{BL,i} \tag{3.3}$$

where:

E_{BL} = Yearly electricity base load demand in kWh_{el}
E_L = Yearly power demand for lighting in kWh_{el}
E_{ICT} = Yearly power demand for information and communication in kWh_{el}
E_C = Yearly power demand for cooling in kWh_{el}
E_M = Yearly power demand for mechanical energy in kWh_{el}

$E_{E,n,adj}$ = Normalised, adjusted profile of the electricity profile in [−]
f_{BL} = Factor for increase or decrease of the electricity base load in %
i = Considered weather data (2011 to 2015)

The yearly power demand for lighting, information and communication, cooling and mechanical energy are denoted by E_L, E_{ICT}, E_C and E_M, respectively. $E_{E,n,adj}$ represents the normalised demand profile, derived from real data provided by the ENTSO-E, which is adjusted by the power demand for the supply of space heat and the process heat. A yearly adjustable factor f_{BL} is further used to consider a possible increase or decrease of the electricity base load demand. This could for instance be achieved by a transition to more energy-efficient systems or conversely, by a higher penetration of electrical devices (such as cooling systems or computers) in the building sector. Figure 3.7 shows four exemplarily days of the normed electricity base load profile in 2011.

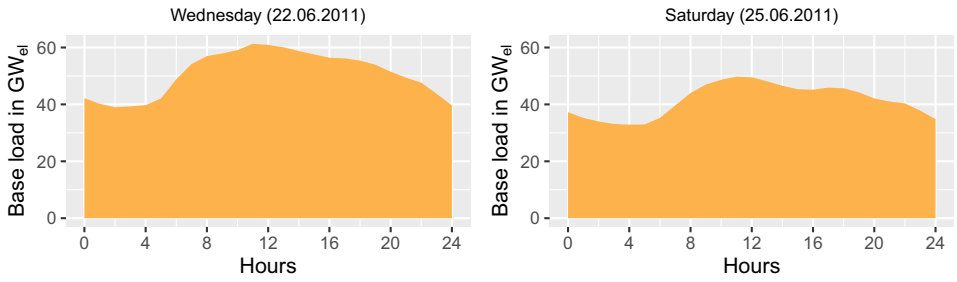

Figure 3.7: Normalised profile of the electricity base load in Germany for two exemplarily days in June 2011.

3.3 Objective Function and Model Design

This section starts with an overview of all system components considered for the calculation of the objective function in REMod. After this, the model design and its solving approach are introduced. This includes the applied optimisation algorithm as well as the solver foresight.

3.3.1 Objective Function

The aim of the optimisation is the minimisation of the discounted, cumulative system costs for the time period from 2015 to 2050 [103]. The objective function is introduced in eq. 3.4. Capital, operation and demand-related costs are calculated based on the annuity method described in the guideline no. 2067 of the Association of German Engineers

(VDI) [135]. In order to assess future investments, all amounts can be discounted by specifying a discounting rate. Further, the objective function considers penalty functions, which are applied whenever the set value of energy-related CO_2 emissions or any other boundary condition are violated. Subsequently, all relevant equations of the objective function are introduced.

$$C = \sum_{t=2015}^{2050} \sum_{i=1}^{I} (A_{k,i,t} + A_{b,i,t} + A_{v,t}) \cdot (\frac{1 + i_{inf}}{1 + i_{d,n}})^{t-2015} + P_t \tag{3.4}$$

where:

t = Considered year, ranging from 2015 to 2050
i = Considered system component
I = Total number of system components
A_k = Annuity of capital-related costs in €
A_b = Annuity of operation-related costs in €
A_v = Annuity of demand-related costs in €
i_{inf} = Inflation rate [−]
$i_{d,n}$ = Discounting rate [−]
P = Sum of penalty functions in €

Capital-Related Costs

The capital-related costs include the investments required for the purchase of a technology or a building component. Their annuity $A_{k,i}$, for a system component i, is calculated according to eq. 3.5. Here, A_0 describes the purchase price and A_n the cash value for a procured replacement, where n denotes the number of replacements (cf. eq. 3.6). The price changing rate and the interest rate are denoted by $i_{P,i}$ and $i_{int,i}$. In the model calculations they are for comparability reasons, set to 1.7 % and 7 % respectively for each technology. The price change factor r_P and the interest factor q are calculated according to eq. 3.7 and 3.8. They are both adjusted for inflation i_{inf}, which is assumed equal to 1.7 % according to the calculated and expected inflation rate of 2017 and 2018 of 1,77 % and 1,65 %, respectively [136]. The interest factor q is utilised to discount a cash value to the beginning of the set observation period, i.e. 2015. T_N denotes the technology service time and can be parametrised individually parametrised for each system component. The present values of future cash flows are determined by the annuity factor a, which is calculated according to eq. 3.9.

$$A_{k,i} = (A_{0,i} + A_{1,i} + A_{2,i}...A_{n,i}) \cdot a_i \tag{3.5}$$

$$A_{n,i} = A_{0,i} \cdot \frac{r_{P,i}^{n \cdot T_N}}{q_i^{n \cdot T_N}} \tag{3.6}$$

$$r_{P,i} = \frac{1 + i_{P,i}}{1 + i_{inf}} \tag{3.7}$$

$$q_i = \frac{1 + i_{int,i}}{1 + i_{inf}} \tag{3.8}$$

$$a_i = \frac{q_i^{T_N}(q_i - 1)}{q_i^{T_N} - 1} \tag{3.9}$$

where:

A_k = Annuity of capital-related costs in €
A_n = Cash value for a procured replacement in €
a_i = Annuity factor [−]
i_P = Price changing rate [−]
r_P = Price change factor [−]
i_{int} = Interest rate [−]
i_{inf} = Inflation rate [−]
T_N = Service time of considered component [−]
q = Interest factor [−]
i = Considered system component [−]
n = Replacement number [−]

The annuity of the capital-related costs A_k represents a substantial part of the objective function described in eq. 3.4. Figure 3.8 provides an overview of all system components considered in this context. It is important to note that for technologies belonging to a system with a predetermined total amount, only the differential costs, i.e. the extra costs compared to a reference technology, are taken into account. These are represented by methane gas boilers in the case of heat generators and by internal combustion engines (ICE) based on liquid fuels (gasoline or diesel) in the motorised transport sector.

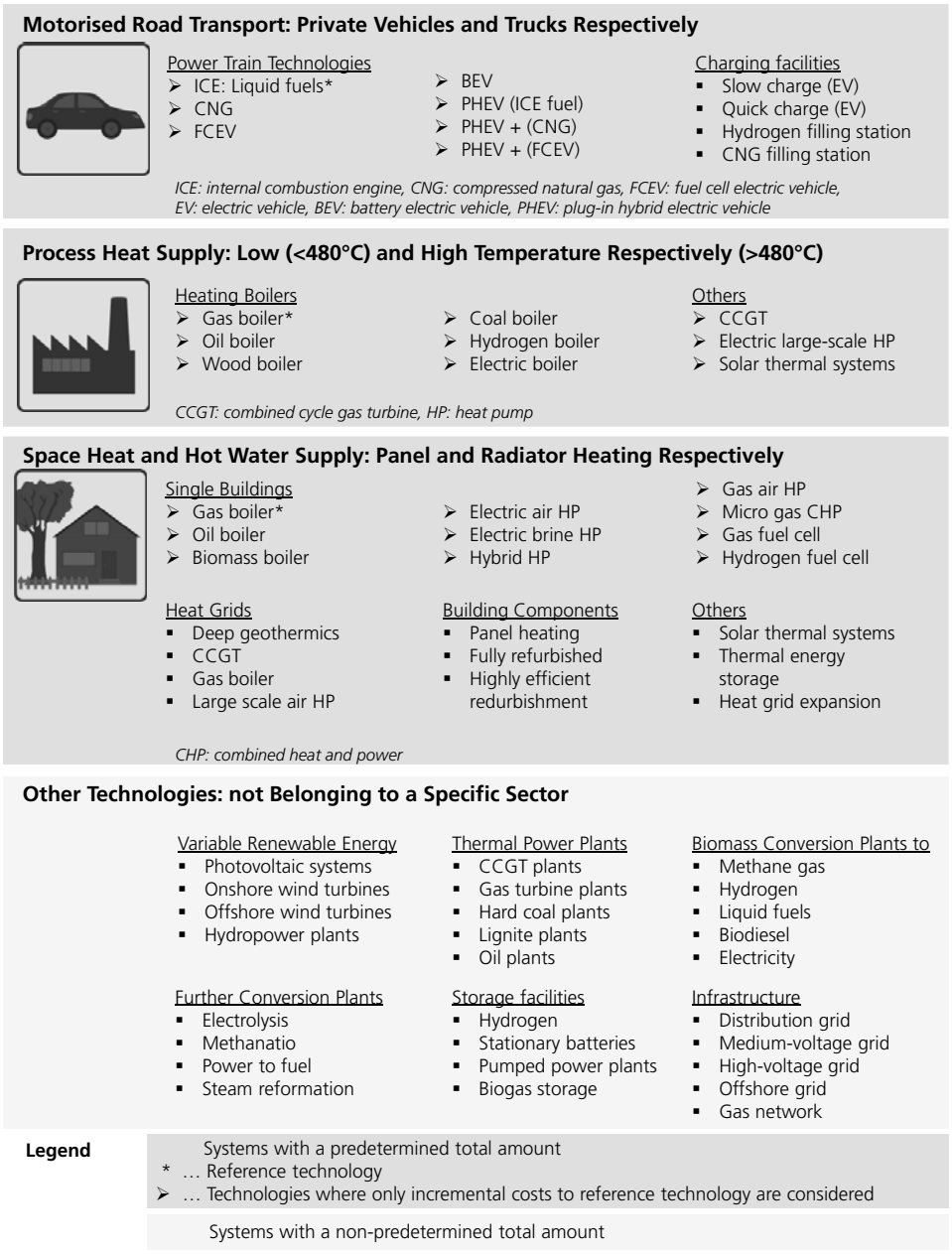

Figure 3.8: Considered system components for the calculation of capital and operation-related costs according to guideline no. 2067 of the Association of German Engineers (VDI) [135].

Operation-Related Costs

The operation-related costs contain expenses for maintenance and operation such as inspection and repair of the considered technology or component. In the objective function they are considered for the same system components as for the capital-related costs, i.e. those shown in figure 3.8. The annuity of operation-related costs is calculated according to eq. 3.10, where $A_{0,i}$ represents the investment amount of a specific technology or component i and $f_{OM,i}$ the assumed factor for maintenance and operation. The costs for maintenance and operation are derived as share of the total investment amount. Price changes can be taken into account by the price dynamic cash value factor b_i which is calculated according to eq. 3.11. Here, a price change rate r_{OM} equal to 1.7 % is considered for all system components.

$$A_{b,i} = A_{0,i} \cdot f_{OM,i} \cdot a_i \cdot b_i \tag{3.10}$$

$$b_i = \frac{1 - (\frac{r_{OM,i}}{q_i})^{T_N}}{q_i - r_{OM,i}} \tag{3.11}$$

where:

$A_{b,i}$ = Annuity of operation-related costs in €
$A_{0,i}$ = Investment amount of considered technology in €
f_{OM} = Factor for servicing, inspection and repair in %
r_{OM} = Price change rate of operation-related costs [−]
T_N = Service time of considered component [−]
b = Price dynamic cash value factor [−]
a = Annuity factor [−]
q = Interest factor [−]

Demand-Related Costs

This category includes all costs for imported and on site produced fuels or energy as well as those for emitted CO_2 emissions. Its annuity A_v is calculated as described in eq. 3.12, where Q_c is the imported and on site produced quantity of each considered energy carrier c and p_c its respective price. The total number of energy carriers considered in the model is denoted by C. The total total quantity of energy-related CO_2 emissions is described by m_{CO_2} and its specific costs by p_{CO_2}. Price changes can be considered through the price dynamic cash factor b, while a represents the annuity factor described by eq. 3.9. Figure 3.9 represents all quantities considered in the objective function for the calculation of demand-related costs.

$$A_v = \sum_{c}^{C} Q_c \cdot p_c \cdot a_c \cdot b_c + m_{CO_2} \cdot p_{CO_2} \cdot a_{CO_2} \cdot b_{CO_2} \tag{3.12}$$

where:

A_v = Annuity of demand-related costs in €
Q_c = Imported and on site produced quantity per energy carrier in kWh
m_{CO_2} = Total total quantity of energy-related CO_2 emissions in t_{CO_2}
p_c = Price per energy carrier in $€/kWh$
p_{CO_2} = Price per CO_2 emissions in $€/t_{CO_2}$
C = Total number of considered energy carriers

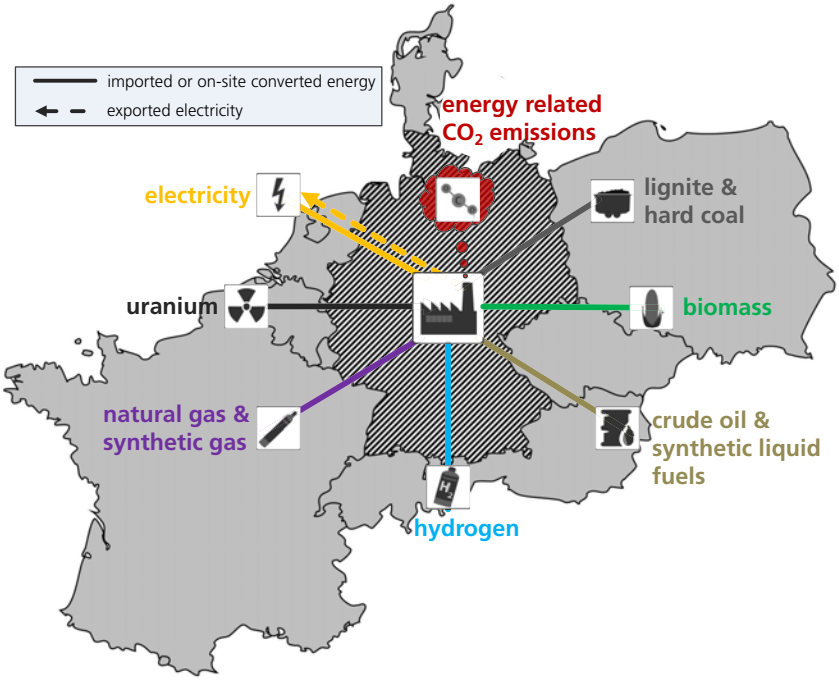

Figure 3.9: Overview of considered domestic production and import of energy carriers and emissions for the calculation of demand-related costs according to guideline no. 2067 of the Association of German Engineers (VDI) [135].

Penalty Functions

Penalty functions are not part of any specific cost category described in the VDI guideline no. 2067 as they do not represent a cost value of the energy system. They represent a common method for the handling of contraints [137,138]. All penalty terms in REMod

are calculated according to a potential function, where the power coefficient varies depending on the violated condition. For instance, an excessive amount of energy-related CO_2 emissions of 30 million tons would increase the system costs by $30^4 = 810.000$ billion Euro[7]. This approach ensures a significant increase of the cumulative system costs, yielding to a corresponding reaction of the optimisation. While the penalty terms are part of the objective function, they should always be equal to zero in the final optimisation result. Whenever this is not the case, it means that with the current parametrisation settings, no valid configuration of the energy system could be identified. Subsequently, a brief overview of all boundary conditions considered in the model is presented, which if violated will lead to a corresponding penalty term P_{CO_2} or P_{EB} (eq. 3.13 - 3.15).

- **CO_2 emissions**: Energy-related CO_2 emissions exceed the set threshold value in any of the simulated years (P_{CO_2}).
- **Energy balance**: The quantity of energy utilised per year is not equal to the supply. The energy imports, the domestic production and the available energy in storage systems[8] must be equal or higher than the respective energy consumption (including losses, such as storage losses). This condition is verified for all energy carriers and storage types considered in the model (P_{EB}).

$$P = P_{CO_2} + P_{EB} \tag{3.13}$$

$$P_{CO_2} = \Delta CO_2{}^4 \tag{3.14}$$

$$P_{EB} = \sum_{t=1}^{8760} \sum_{c=1}^{C} \Delta E_{EB,c}(t)^2 \tag{3.15}$$

where:

P_{CO_2} = Penalty term accounting for energy-related CO_2 emissions in €
P_{EB} = Penalty term accounting for energy balance in €
ΔCO_2 = Difference between emitted CO_2 emissions and the set threshold value in t_{CO_2}
ΔE_{EB} = Mismatch between supplied and utilised energy in kWh

[7] According to [138], trial-and-error is the only method for the definition of penalty functions. A too low penalty value leads to an accordingly low convergence performance of the optimisation algorithm. Conversely, if too high penalty values are considered, the optimisation is more likely to be trapped in local minimum solutions.

[8] The charge levels of all energy storage systems are transferred from one year to the next, meaning that their charge levels might be > 0 at the beginning of a year.

3.3.2 Problem Design and Optimisation Algorithm

This chapter starts with a description of frequently used formulations of energy system models. In this context, the model design of REMod and the applied optimisation algorithm are introduced. Lastly, a description of solver foresight types is presented, highlighting their advantages and drawbacks.

Problem Design and Optimisation Approach

The approach chosen for the optimisation of a problem may significantly influence its design and vice versa. Classic approaches, like the simplex method, are used to solve linear problems with continuous variables. Branch-and-bound or branch-and-cut-techniques as well as the CPLEX solver represent frequently used optimisation approaches in the field of Mixed Integer Linear Programming (MILP). Generally, the mentioned options provide a simple implementation while being able to identify the optimal global solution. In the field of energy system modelling these approaches are used in various models or model generators, such as shown in [83, 139–143]. According to [144], one drawback is that the modelling of complex processes occurring in reality can be particularly difficult. Thus, a high intuition of the developer is required.

An alternative to classic optimisation approaches is represented by modern heuristics. One difference consists in the fact that with heuristic approaches finding the global optimum is - from a mathematical point of view - not guaranteed or rather unlikely. Thus, the problem solving in general proves to be much more demanding. However, at the same time the model development becomes simpler, posing less limitations and allowing a closer representation of real processes [144]. For REMod a heuristic optimisation approach was chosen, allowing its design in form of a simulation-based optimisation model. Besides enabling an effective debugging, whenever necessary for the detailed representation of real processes, it is possible to include non-linear relationships. Further, plant operation management can be depicted similarly to real processes, i.e. in a signal-controlled way. These discontinuities are modelled by introducing various decision variables. Conversely to a linear programming design, they can be implemented without substantially increasing the computational time required for the solving of the optimisation problem. For instance, the operation mode of most system components in REMod can be adjusted multiple times within each time step, depending on the residual load or on other signals (cf. section 4). This allows to consider interactions occurring between different technologies and sectors in an intuitive way and as close to reality as possible.

Optimisation Algorithm

As introduced in section 3.1, since 2013 the optimisation problem formulated in REMod is solved via a particle swarm optimisation algorithm (PSO). The main idea behind this approach is based on the imitation of the social behaviour of bird flocking in search for food. The swarm of birds is hereby represented by a swarm of particles exploring the solution space, where each particle $\vec{x}$ describes a possible solution. Applied to REMod this means that each particle contains all optimisation variables for the time period ranging from 2015 to 2050. This for example includes the installed capacities of all energy conversion technologies, the refurbishment level of buildings or the distribution of power train technologies in the road transport sector. At the beginning of the optimisation process, the first generation of particles is randomly distributed within the solution space. Their position is adjusted in each subsequent generation until the set number of generations n_G is reached. Whenever the position of a particle is changed, a new solution is identified. If this solution is better than all of its previous solutions, it is documented as new local best $\vec{p}_{best}$. On top of that, all particles of the swarm n_P exchange information concerning their best solution. Thus, the global best solution $\vec{g}_{best}$ in each generation is noted as well. The local and global best solutions are utilised to influence the particles velocity $\vec{v}$ (eq. 3.16) which serves to determine the particles position in the upcoming generation as described in eq. 3.17.

$$\vec{v}_{i,k+1} = w_k \cdot \vec{v}_{i,k} + c_{1,k} r_1 (\vec{p}_{best,i} - \vec{v}_{i,k}) + c_{2,k} r_2 (\vec{g}_{best,i} - \vec{v}_{i,k}) \tag{3.16}$$

$$\vec{x}_{i,k+1} = \vec{x}_{i,k} + \vec{v}_{i,k+1} \tag{3.17}$$

PSO variants, where information is shared across all particles of the swarm, are referred to as *global neighbourhood* types. As for *local neighbourhood* types, information is exchanged only with a specific number of neighbouring particles. According to [145] PSO variants with global information exchange, like the one utilised in [103], generally converge fast, however, they risk being trapped in local minimum solutions. This can partially be prevented by adjusting the inertia factor of the particles w, which is used to avoid sharp changes of their velocity. c_1 and c_2 are the acceleration coefficients. They are utilised to weight the influence of the individual or global best solution ($\vec{p}_{best}$ and $\vec{g}_{best}$). This is why they are also referred to as cognitive or social coefficients. The starting and ending values for the inertia factor and the acceleration factors are exogenously set. Conversely, $r1$ and $r2$ represent random numbers between zero and one, generated within each iteration step.

According to [145–147] the convergence velocity of the PSO as well as its general performance highly depend on its parametrisation. Thus, [103] presented an optimal parameter

set for the solution of the optimisation problem formulated in REMod. However, since 2016 the model was further extended, which is why the optimisation parameters need to further be adjusted. For this purpose multiple optimisation runs are performed and evaluated.

First, the number of particles n_P and generations n_G are gradually increased. A higher number of particles allows a more throughout investigation of the solution space. At the same time, by raising the number of generations the information exchange within the swarm occurs more frequently, providing a higher number of attempts to approach the optimum solution. It is noted that the computational time is proportional to the product between the total particle and generation number. Taking this and the relative performance enhancement of the algorithm into account, the best solutions in statistical terms were identified for a number of particles and generations equal to 200 and 4,000, respectively.

Compared to [103], the inertia factor w was barely changed to 0.9 in the start and 0.5 at the end. According to section 3.3.2 this parameter contributes to overcome local minima, which happens to be a major issue for PSO with global neighbourhood. It can be assumed that, while the solution space and the number of local minima compared to [103] increased, their characteristics did not vary significantly.

Conversely, the relation between the acceleration factors c_1 and c_2, used for the weighting of the local and global best solution, is changed noticeably. The results show that a higher starting value of r_1 statistically leads to better solutions. This suggests that the cognitive particle behaviour should prevail over the social behaviour in the start. As a consequence of this setting the first generations investigate a larger area of the solution space, being influenced mainly by their own findings. This relation is reversed towards the final part of the optimisation, where the social behaviour described by r_2 is two thirds higher than c_1. Thus, the velocity adaptation of the particles gives gradually more weight to the information exchanged with the entire swarm. As a consequence, the area enclosing the optimal solution is explored extensively by particles belonging to the last generations of each optimisation.

Table 3.5 summarises the final parameter set for the PSO algorithm. With these settings, the processing time per iteration on a computing server with 3 GHz and 88 cores, amounts to 75 milliseconds. For a total of 800.000 iterations, this yields to roughly 17 hours per optimisation run.

Despite the adjustment of the PSO parameters, the obtained model results exhibit a non negligible inaccuracy. Due to the model extensions following [103], the applied PSO algorithm does not seem longer suited for the solution of REMod. As an alternative, the optimisation based on a covariance matrix adaptation - evolution strategy (CMA-ES) algorithm [148] is tested. Like the PSO the CMA-ES belongs to evolutionary algorithms.

Table 3.5: Overview of the utilised optimisation parameters. The number of generations and particles is denoted by n_G and n_P. w, c_1 and c_2 describe the inertia and acceleration factors, respectively.

	n_G	n_P	w	c_1	c_2
Value	200	4000	/	/	/
Starting value	/	/	0.9	10.0	1.5
Final value	/	/	0.5	1.5	2.5

For the identification of the optimum solution first particles are initialised within the search space, which are then translated to solutions based on the objective function. The parents of the new generation are selected according to the fitness value of the best identified solutions. One special feature of the CMA-ES is that it calculates a covariance matrix which describes if optimisation parameters affect each other in a proportional or inversely proportional way or do not affect each other at all. Further, the matrix contains information about whether optimisation parameters exhibit a negligible or substantial effect on the objective function value. Based on the determined covariance matrix and the mean of all best solutions within a generation, a new generation is produced. The particles in this generation will presumably identify a better solution than those of previous generations. This mechanism allows the CMA-ES to adapt its parametrisation during the optimisation process and thus increase or reduce the search space depending on whether the optimal solution is far away or relatively close. Instead, the PSO algorithm produces the new generation based on velocity and position update equations (cf. eq. 3.16 and eq. 3.17), which also depend on exogenously set parameters (cf. table 3.5) [149].

The CMA-ES is applied in [150], where the configuration of a European energy system is identified. Here, the performance of the CMA-ES was compared to a genetic algorithm as well as to a simplex algorithm. As a result, the CMA-ES proved to perform better than the genetic algorithm by reaching a significantly lower objective function value, close to the result of the linear optimization approach. The developer of the CMA-ES in [151] provides a set of default values for its parametrisation. He does not recommend to change them, as they represent a robust setting, applicable to a wide range of functions to be optimised. One exception is the set population size. By increasing it, the overall global search capability of the CMA-ES is increased. Figure 3.10 represents the convergence of the PSO algorithm and the CMA-ES for the exact same parameter setting in REMod. In one case, the population size of the CMA-ES was increased from the default value of 28 to 88, equating the core size of the utilised processor.

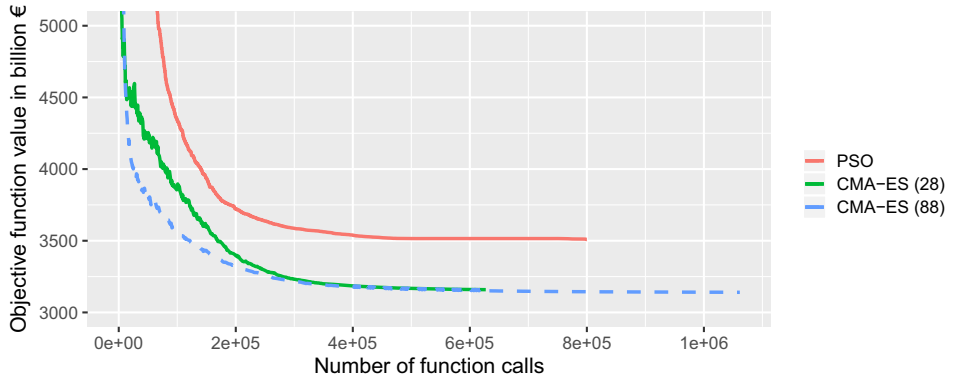

Figure 3.10: Comparison of the convergence behaviour of the Particle Swarm Optimisation algorithm (PSO) and the covariance matrix adaptation - evolution strategy (CMA-ES) algorithm over number of function calls. The default population size λ is set to 28 according to [151], with n = 3331. The stricter abort criterion in for the CMA-ES in case of $\lambda = 28$ leads to a higher computational time compared to $\lambda = 88$.

According to figure 3.10 CMA-ES performs significantly better than the PSO algorithm, which in the illustrated example reaches a final value of 3509 billion € (+ 369 billion €). The difference between both CMA-ES variants is relatively small, amounting to less than 20 billion € in favour of the higher population size. While these numbers may vary from calculation to calculation, the outlined trend was confirmed over several optimisation runs. Overall, the results obtained with the CMA-ES revealed to be very consistent to each other. This does still not guarantee the identification of the global optimal solution. However, the analysis of systems with similar costs and differing system configurations can be profitable to identify robust or uncertain technology developments. A condition for this is that the identified optimisation solutions exhibit a high quality or, in other words, that they do not vary substantially regarding their objective function values. The CMA-ES proved to be able to fulfil this requirement.

Solver Foresight

When solving an optimisation problem two types of solver foresights can be distinguished, namely the myopic and the perfect-foresight approach. As shown in figure 3.11 the length of one optimisation step equals the total observation period when a perfect-foresight is considered. This means that within this optimisation step all the input data is known and that the entire system can be solved optimally. On the contrary, in the myopic approach the optimisation problem is divided into a series of sub-problems with a specific extension. Each one of those problems is optimised individually. Hereby, only data concerning the current sub-problem is known, neglecting parameter developments or other

data related to following sub-problems. Thus, within each sub-problem perfect foresight exists, however, this is not the case if the entire observation period is considered. Myopic optimisation approaches can further be distinguished in two categories, depending on whether the sub-problems are related to strictly divided periods or present an overlap. These differentiation within myopic approaches is also referred to as time-step and moving window foresight. Figure 3.11 provides a schematic overview of the mentioned solver foresight approaches.

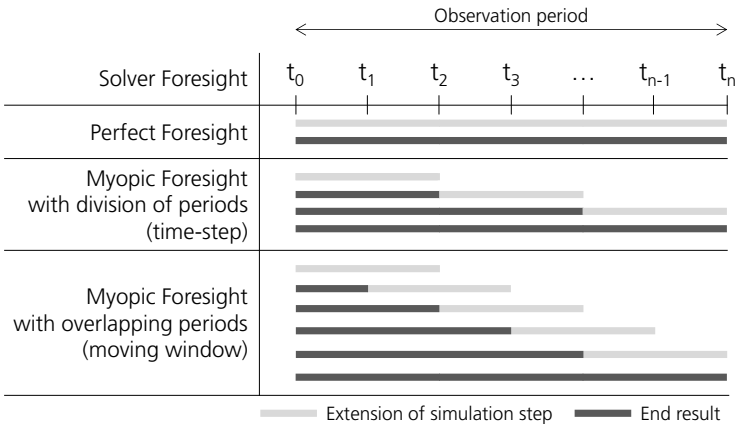

Figure 3.11: Graphical representation of three solver foresight approaches.

As shown in figure 3.11 the extension of each sub-problem in the myopic foresight approach was set to two time steps, respectively. In the case of strict divided periods, the optimisation results determined for the period $t_0 \rightarrow t_2$ are set as end result. They provide the basis for the optimisation of the subsequent sub-problem ranging from t_2 to t_4. This procedure is repeated until all sub-problems of the total observation period are solved, leading to the final solution. On the contrary, when overlapping periods are considered the optimisation results of each sub-problem are set as end results only in part. The overlapped period may be adjusted, as it is also part of the following sub-problem. Thus, a specific time period may be solved multiple times, depending on the extension of the simulation steps and the corresponding overlap. With regard to figure 3.11 the first and second sub-problem range from t_0 to t_2 and t_1 to t_3, exhibiting an overlap of one time step ($t_1 \rightarrow t_2$). Thus, after the solution of the first sub-problem, only $t_0 \rightarrow t_1$ is set as end result. The results related to $t_1 \rightarrow t_2$ may be reconsidered and are set as end results after the solution of the second sub-problem and so on.

The myopic and perfect foresight approach have been analysed in a series of studies, highlighting their assets and drawbacks [18,141,143,152–154]. For instance, in [141] they were both applied to the PERSEUS-NET model and assessed with particular regard to their computing time and result spread. This model is designed as linear problem in

GAMS (General Algebraic Modelling System) and solved by a CPLEX solver. It is shown that the myopic approach is suitable for stable input parameters, identifying a similar solution to the perfect foresight approach. Compared to the perfect foresight approach, the optimisation time of the myopic approach amounts to less than one tenth. A similar study was performed by [143] on the DISTRICT energy system model, which is also designed in GAMS as MILP. This study confirms the findings of [141]. Depending on the investigated scenario the optimisation run time with the perfect foresight approach is at least five times and up to 31 times higher compared to the myopic approach. Both studies conclude that the problem complexity can be substantially decreased when the myopic approach is used. Here the optimisation problem is divided into smaller sub-problems, decreasing the number of variables and thus the extension of the solution space.

Another characteristic of the myopic approach concerns its depiction of real investment decisions. These decisions are based on knowledge limited to a specific time horizon and may prove more or less profitable depending on the future development of determinate parameters. This makes them better suited when disruptive elements should be assessed [18, 153, 154]. This, for instance, includes the sudden increase of energy prices, the introduction of a new policy or the sudden decline of power generation capacity. Such disruptions can not be properly analysed when a perfect-foresight approach is used, as they are considered in the problem solution right on from the start. Conversely, this means that the perfect-foresight approach is able to make the best investment decisions, rather than basing them on a limited time period. For instance, a myopic approach might favour a power generation technology which is economical in the current simulation step. However, this plant might not be optimal with regard to the total observation period. Conversely, technology options which are not beneficial at the current time step might be excluded, even though they would be beneficial over the total observation period. This mechanism is also referred to as lost opportunities and can be represented by the gap between the optimisation results obtained by both approaches. This gap is evaluated in [143, 152], showing that the obtained solutions are similar on a macroscopic scale. However, their composition may vary as a consequence of lock-in/out effects, describing the exclusion of a technology due a previous investment in an alternative, less beneficial option. The expected differences between both approaches generally decrease if (1) a continuous temporal development of input parameters is chosen, (2) the input parameters don't vary substantially, as this may lead to non-optimal decisions in the case of the myopic approach and (3) the technical service time of system components is relatively short compared to the total observation period. This ensures that non optimal investments can be replaced.

Overall, myopic approaches are better suited to depict real investment behaviour. Conversely, perfect-foresight approaches should be applied when the optimal solving of the problem is of interest. In case of REMod, a perfect-foresight approach is chosen. Despite the extensive usage of decision variables for the description of system operation the model design and the optimisation algorithm allow its application without expecting a substantial increase of the solution space. Further, the perfect-foresight approach is better suited for the aim of the model, which is the description of interactions occurring between different energy carriers and sectors of the energy system, rather than the depiction of business management decisions.

3.4 Operating Principle

One of the major features of REMod is its technical representation of interactions between various technologies and sectors of the energy system, while providing a high temporal resolution. All calculations are carried out on an hourly basis for every year, starting from 2015 until 2050. However, at the same time its spatial resolution is considered by one node. This implies that generators, storage facilities or passenger cars are aggregated and therefore represented as one average system component. For instance, lignite power plants are described by one virtual plant. Its efficiency corresponds to the average value of all plants located in the investigated area. Efficiency enhancements or other variation of performance can be adjusted for each year from 2015 to 2050. The consideration of a single node further implies that the supply and usage of energy virtually occurs in the same spot. Thus, while costs for the expansion of the electrical grid (distribution, medium and high-voltage), the heat grid, the gas network and the charging infrastructure for the transport sector are considered, no technical restrictions are imposed. As for the electrical grid, distribution losses are considered in general terms by a parametrisable factor (cf. eq. 3.20).

The Residual Load

Another simplification concerns the operational sequence of technologies within the power sector. This sequence follows a predefined pattern which is determined depending on the carbon footprint of each technology as well as on the value of the respective energy carrier. Depending on the residual load value, a variety of load balancing options can be operated. Throughout literature various definitions for the residual load exist. For instance, [155–160] define it as difference between the power load and the electricity production from renewable sources. In other cases the power generation refers only to

variable renewable energy sources (VRE), therefore excluding biomass generated electricity [161, 162]. In REMod the residual load P_{Res} is defined based on [32, 33]. Thus, it refers to the electric load in the power grid $P_{el,Load}$ (eq. 3.19) minus the occurring non-dispatchable power generation $P_{el,Prod}$ (eq. 3.20). It is calculated according to eq. 3.18.

$$P_{Res}(t) = P_{el,Load}(t) - P_{el,Prod}(t) \tag{3.18}$$

$$P_{el,Load}(t) = P_{BL}(t) + P_{HP} + P_{DG} + P_{EV,must} + P_{EC,must} + P_{PH} + P_{ICP} \tag{3.19}$$

$$\begin{aligned} P_{el,Prod}(t) = (&P_{Hydro}(t) + P_{NP}(t) + P_{LC,must}(t) + P_{HC,must}(t) + P_{Wind,off}(t) \\ &+P_{Wind,on}(t) + P_{PV}(t) + P_{I,must}(t)) \cdot \eta_G + P_{CHP}(t) + P_{FC}(t) \end{aligned} \tag{3.20}$$

where:

P_{Res}	=	Residual load in $^{kWh_{el}}/_{h}$
$P_{el,Load}$	=	Electric load in $^{kWh_{el}}/_{h}$
$P_{el,Prod}$	=	Non-dispatchable power generation in $^{kWh_{el}}/_{h}$
P_{BL}	=	Electricity base load in $^{kWh_{el}}/_{h}$
P_{HP}	=	Power load of heat pumps for space heat in $^{kWh_{el}}/_{h}$
P_{DG}	=	Power load of deep geothermics for space heat in $^{kWh_{el}}/_{h}$
$P_{EV,must}$	=	Power load for vehicle charging in $^{kWh_{el}}/_{h}$
$P_{EC,must}$	=	Power load for electrolysis plants in $^{kWh_{el}}/_{h}$
P_{PH}	=	Power load for the supply of process heat in $^{kWh_{el}}/_{h}$
P_{ICP}	=	Power generation from industrial plants (internal consumption) in $^{kWh_{el}}/_{h}$
P_{Hydro}	=	Power generation from run-of-river power stations in $^{kWh_{el}}/_{h}$
P_{NP}	=	Power generation from nuclear power plants in $^{kWh_{el}}/_{h}$
$P_{LC,must}$	=	Non-dispatchable power generation from lignite power plants in $^{kWh_{el}}/_{h}$
$P_{HC,must}$	=	Non-dispatchable power generation from hard coal power plants in $^{kWh_{el}}/_{h}$
$P_{Wind,off}$	=	Power generation from offshore wind power stations in $^{kWh_{el}}/_{h}$
$P_{Wind,on}$	=	Power generation from onshore wind power stations in $^{kWh_{el}}/_{h}$
P_{PV}	=	Power generation from photovoltaic power stations in $^{kWh_{el}}/_{h}$
$P_{I,must}$	=	Mandatory import of electricity in $^{kWh_{el}}/_{h}$
P_{CHP}	=	Power generation from micro-CHP units for space heat in $^{kWh_{el}}/_{h}$
P_{FC}	=	Power generation from fuel cells for space heat in $^{kWh_{el}}/_{h}$
η_G	=	Average grid efficiency for consideration of losses in %

As introduced in section 3.2.5, the electricity base load is derived from real data and adjusted according to the power demand for the supply of space and process heat. The power demand of heat pumps, described by P_{HP}, includes single buildings as well as large-scale heat pumps in heat grids. Deep geothermal plants are considered by P_{DG}. They are implemented as option for the supply of heat, instead for power production. The electricity demand for the supply of process heat by large-scale heat pumps or electrode boilers is summarised by P_{PH}. Further, the internal consumption provided by industrial plants, which is not detected by data provided by ENTSO-E, is denoted by P_{ICP}. The terms, $P_{EV,must}$ and $P_{EC,must}$ describe a possibly occurring electric load due to charging of electric vehicles or required operation of electrolysis plants. Both, are generally equal to zero and depend on the charge level of vehicle batteries and hydrogen storage facilities. If the storage operation is not sufficient, an according unavoidable electric load ensures that vehicles can be charged or the hourly hydrogen demand is met. This concept is explained in detail in section 4.3.

The non-dispatchable power generation consists of ten terms in total. The feed-in from run-of-river power stations P_{Hydro} and nuclear plants P_{NP} are both exogenously set, i.e. their installed capacities are not optimised. For lignite and hard coal power plants a minimum load requirement can be considered. This means that an exogenously fixed share of their installed capacity is operated during every hour. This quantity is denoted by $P_{LC,must}$ and $P_{HC,must}$, respectively (cf. section 3.5). $P_{I,must}$ represents a mandatory import of electricity from neighbouring countries, which depends on their respective feed-in from VRE (cf. section 4.5). Distribution losses can be accounted for by η_G. This value is exogenously set, according to literature values (cf. appendix,A). The power generation occurring from CHP units and fuel cells is denoted by P_{CHP} and P_{FC}. This includes micro-CHP units as well as CCGT-plants in heat grids for the supply of space heat or process heat.

Load Balancing

The balancing of the residual load can be distinguished in two cases. The First is indicated by a positive value of the residual load, meaning that power deficiency occurs. The second applies in case of power surplus, i.e. when the power from non-dispatchable sources exceeds the electric load (eq. 3.18). In either case, the operational sequence of technologies in the power sector is predetermined according to figure 3.12.

Once the cumulative electric load and the non-dispatchable power generation are determined, the residual load value is calculated according to eq. 3.18. The operation of electric heat pumps may be adjusted, depending on whether the residual load value is positive or negative. If power deficiency occurs, the electricity demand of electric heat

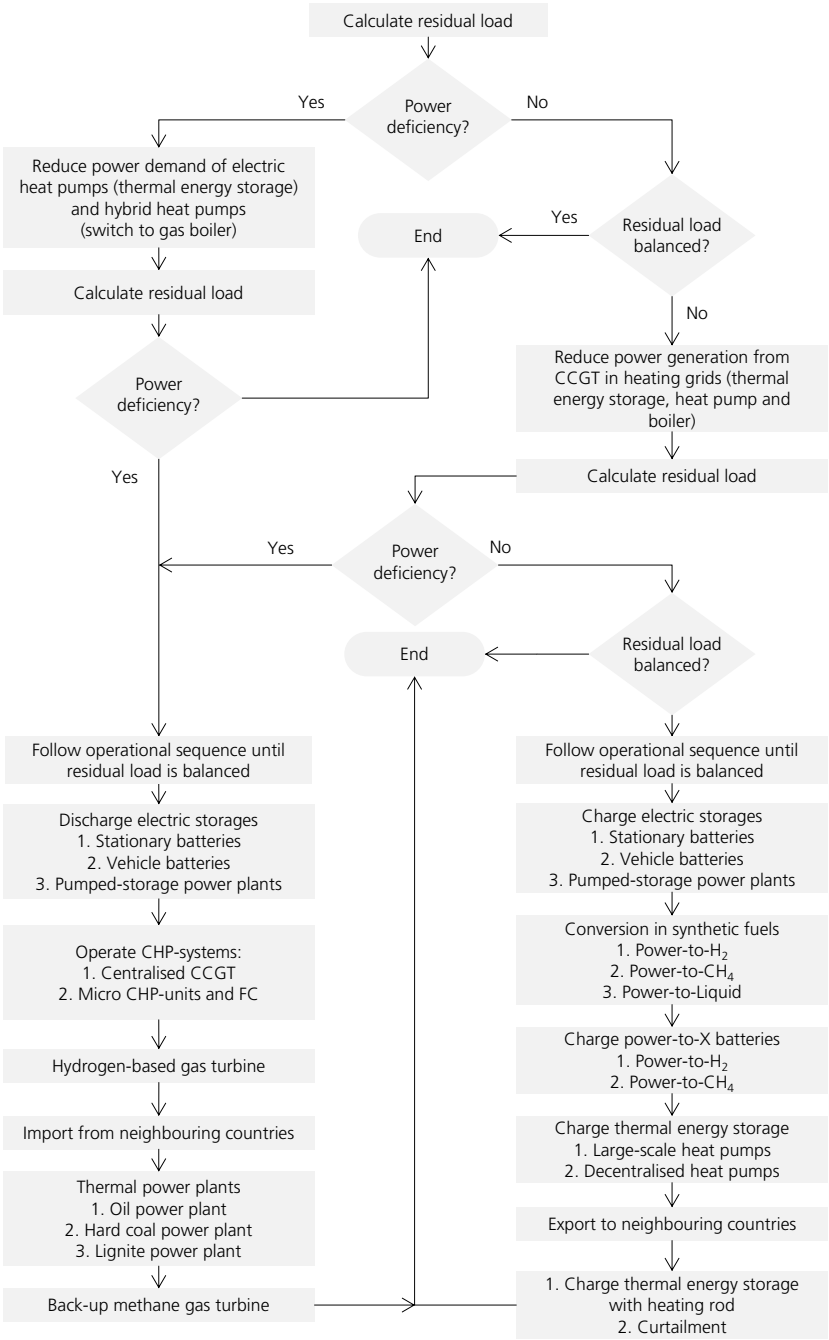

Figure 3.12: Flowchart describing the operational sequence to balance the residual load in case of power surplus or deficiency. CCGT: combined cycle gas turbine, CHP: combined heat and power, FC: fuel cell.

pumps is reduced (and vice versa). Thus, the heat load is covered for as much as possible by discharging the thermal energy storages. On top of that, hybrid heat pumps may switch from electrical to a methane gas based operation. Similarly, if power surplus occurs, the heat supply from CCGT-plants in heat grids may be reduced. For this purpose, the optimal heat supply share between the CCGT-plant and the large-scale heat pump is calculated, reducing the residual load as much as possible.

At this point a series of technology options is operated in a fixed sequence to balance the residual load. In the case of power power deficiency the sequence is arranged based on the driving key boundary condition of the optimisation process, which is the CO_2 emissions. Thus, for each technology option, the quantity of CO_2 emissions per kWh_{el} of supplied power is calculated. For instance, a lignite power plant with an emission factor of $0.403\,g_{CO_2}/kWh_{lignite}$ and an average efficiency of 34 % leads to a assessment factor of $1.18\,g_{CO_2}/kWh_{el}$. Whereas for a hard coal power plant, with an efficiency of 38 % and an emission factor of $0.337\,g_{CO_2}/kWh_{hardcoal}$ it amounts to $0.886\,g_{CO_2}/kWh_{el}$. Thus, the hard coal plant is operated first, as it exhibits a lower carbon footprint.

In case of power surplus, i.e. for a negative value of the residual load, technologies are used first according to their efficiency and the value of the converted or stored energy. For instance, as shown in figure 3.12, power is first stored into electric batteries, while being converted into synthetic fuels afterwards, mainly because of higher losses. For the same reason, power is converted into hydrogen first and into methane gas and liquid fuels afterwards. In the next step, batteries linked to Power-to-Gas (PtG) plants are charged. This process is designed to increase the full load hours of PtG plants and thus it is valued as less relevant in the operational sequence. It is noted that this sequence is in part changed at every hour according to an implemented load forecast algorithm. For instance, thermal power plants are operated depending on the expected duration of power deficiency. As a consequence, a back-up methane gas turbine, rather than a coal power plant, will be utilised in case of particularly short periods of power deficiency (cf. figure 3.12). This concept is described in further detail in section 4.

For a correct interpretation of the illustrated operational sequence of technologies in the power sector, it is necessary to understand how the individual model components are considered in the model. A description of all main model components, is provided in the next section 3.5.

3.5 System Components

The following section provides a brief description of the main system components deemed necessary for the interpretation of the model results (cf. section 6). Other technologies are described in [103] or are presented in in the next chapter, introducing the operation of load balancing options in REMod.

Power Generation from Variable Renewable Energy

The feed-in from VRE is derived from the renewables.ninja platform [163], which provides simulated profiles for each European country for the time period from 1990 to 2016 [164]. This includes onshore and offshore wind turbines and photovoltaic power stations. The normed feed-in profiles are distributed between north and south Germany for the years from 2011 to 2015 by two factors and take into account the full load hours of each technology measured in Germany's federal states [165–168]. The distribution factors for north and south Germany amount to 0.9673 and 1.0546 for photovoltaic plants and to 1.0721 and 0.8798 for onshore wind turbines, respectively. Feed-in values of higher than one are corrected. An overview of the resulting full load hours is provided in table 3.6.

Table 3.6: Full load hours of VRE for each weather data set (2011-2015), for north and south Germany.

	Photovoltaics			Wind Onshore			Wind Offshore
	South	North	Average	South	North	Average	
2011	1137	1043	1090	1658	2021	1840	4003
2012	1072	983	1028	1580	1925	1753	3918
2013	990	908	949	1475	1798	1636	3643
2014	1100	1009	1055	1504	1833	1669	3897
2015	1133	1039	1086	1712	2085	1899	4074

The hourly power generation of VRE is obtained according to eq. 3.21. Here, $P_{nom,VRE,i}$ describes the installed capacity of the considered VRE-technology i. The corresponding normed feed-in profile is denoted by $P_{norm,j,VRE,i}$, where j is one of the considered weather data sets, i.e. 2011, 2012, 2013, 2014 or 2015. Lastly, the full load hours resulting in table 3.6 can be scaled by the parametrisation of a yearly adjustable factor ($f_{VLH,VRE}$). Thus, it is possible to consider technological improvements on one side, or - on the other side - the exploitation of less favourable locations. Figure 3.13 shows the utilised feed-in profiles of the main VRE sources for 2011 to 2015.

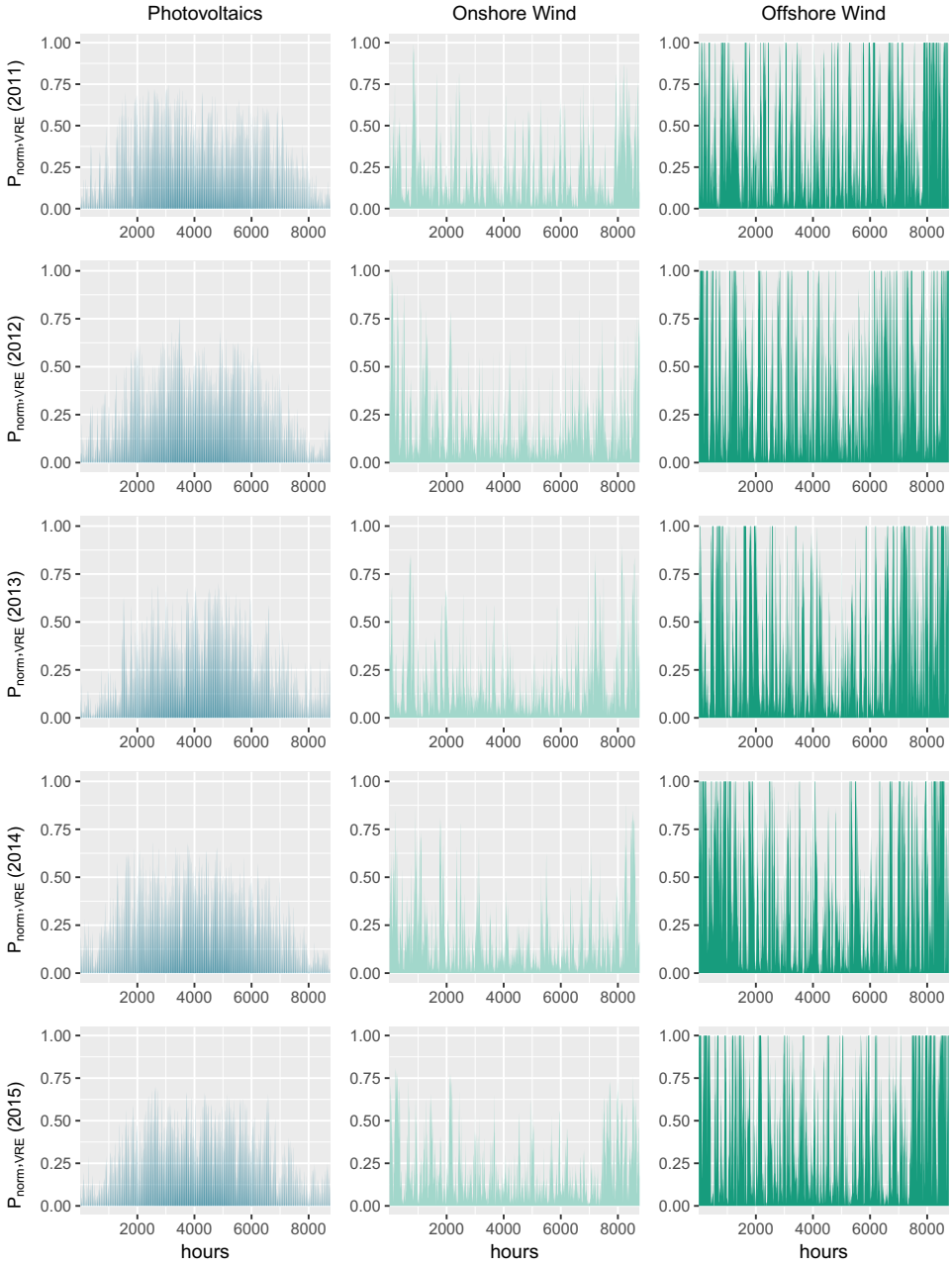

Figure 3.13: Normalised feed-in profiles from wind onshore, wind offshore and photovoltaic stations, for the five weather data sets: 2011 to 2015.

$$P_{el,VRE,i}(t) = P_{nom,VRE,i} \cdot P_{norm,j,VRE,i} \cdot f_{VLH,VRE,i} \tag{3.21}$$

where:

$P_{el,VRE}$ = Power generation from considered VRE-technology $^{kWh_{el}}/_{h}$
$P_{nom,VRE}$ = Installed capacity of considered VRE-technology in kW_{el}
$P_{norm,VRE}$ = Normed feed-in profile of considered VRE-technology in [−]
$f_{VLH,VRE}$ = Yearly adjustable factor for technological improvement in [−]

Power Generation from Thermal Power Plants

The power generation of thermal power plants includes hard coal and lignite power plants, gas turbines, CCGT, biogas plants as well as oil and nuclear power plants. Their installed capacity is determined by the optimisation, except for oil and nuclear power plants. The reason why is that oil power plants in Germany do play a tangential role and an increase of their installed capacity is not foreseeable [169]. As for nuclear power plants it is due to the planned the withdrawal from nuclear energy by 2022, decided by the German Federal Government. This means that the installed capacity of both plants is exogenously set for each year from 2015 to 2050. In the case of lignite and hard coal power plants, a minimum load operation can be considered by a yearly parametrisable factor $f_{mustRun,Coal,i}$. This generation is accounted for as non-dispatchable generation and therefore influences the residual load. Moreover, coal power plants may increase their contribution by a flexible generation term $P_{flex,Coal,i}$ to balance the electric load (eq. 3.22 and 3.23).

$$P_{el,Coal}(t) = \sum_{i=1}^{CP} P_{el,nom,Coal,i} \cdot f_{mustRun,Coal,i} + P_{flex,Coal,i} \tag{3.22}$$

$$P_{flex,Coal,i} = P_{el,nom,Coal,i} \cdot (1 - f_{mustRun,Coal,i}) \tag{3.23}$$

where:

CP = Type of coal power plant (lignite or hard coal)
$P_{el,Coal}$ = Power generation from coal power plant in $^{kWh_{el}}/_{h}$
$P_{flex,Coal}$ = Flexible power generation from coal power plant in $^{kWh_{el}}/_{h}$
$P_{el,nom,Coal}$ = Installed capacity of coal power plant in kW_{el}
$f_{mustRun,Coal}$ = Share of must run capacity of nominal load in %

The feed-in of other thermal power plant is influenced by the value of the residual load as it is restricted to times when a power deficiency occurs. Their individual contribution is influenced by the predetermined operational sequence introduced in section 3.4, as well as by their ramping characteristics and current operating status. This concept is introduced in detail in section 4.2. Further, the model considers a spare capacity of 20 %, which means that back-up methane gas turbine plants are accordingly dimensioned.

Systems for the Supply of Space Heat and Domestic Hot Water

As described in [103], heating systems for the supply of space heat and domestic hot water are considered as a combination of different components. For decentralised systems this includes a thermal energy store (TES) equipped with a heating rod, solar thermal systems and a main heat generator. The heat generator can for instance be represented by a heat pump, a boiler, a CHP unit or a fuel cell. The general configuration of a heating system of single buildings within REMod is depicted in figure 3.14.

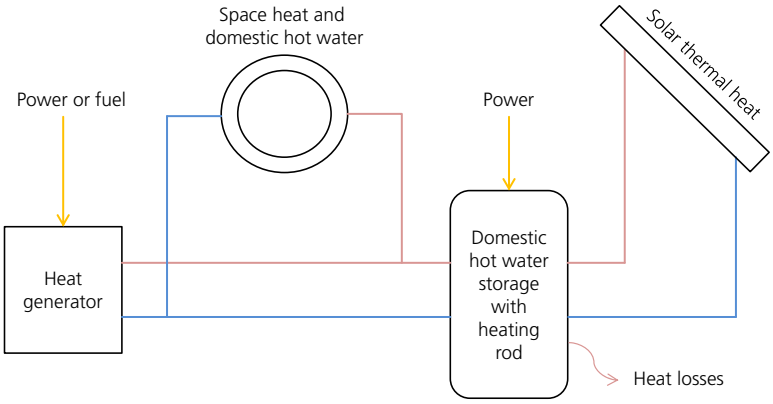

Figure 3.14: General configuration of system for the supply of space heat and domestic hot water for a single building in REMod.

The yield of solar thermal systems Q_{STH} is calculated according to [103] (eq. 3.24). Here, A_{coll} denotes the collector surface oriented in a specific direction i, with an inclination of 45°. It is assumed that 40 % of the collectors are directed to the south, while 30 % to southeast and southwest, respectively. The global radiation is described by G and is exogenously set as timeline for each of the five considered years from 2011 to 2015. Further, the collectors efficiency and its heat loss coefficient are represented by c_0 and c_1, respectively. The difference between the temperature of the solar collector and the ambient is represented by $(T_{Coll} - T_A)$.

As represented in figure 3.14 the yield from the solar thermal system is utilised to increase the temperature level of the TES. The storage exhibits a simple cylindrical geometry with a diameter to hight ratio of 1:1.5 according to [103]. Storage losses ($Q_{Loss,HWS}$) are calculated at the beginning of each time step as described by eq. 3.25. The thermal capacity and the time constant of the TES are denoted by C_{HWS} and τ_{HWS}, respectively. Their ratio is used to describe the thermal transmission proprieties of the TES. Both parameters are obtained according to equations 3.26 and 3.27. The storage losses are mainly influenced by the difference between the ambient temperature T_A and the storage temperature T_{HWS}. For simplification purposes, a homogeneous mixing within the TES is assumed, yielding to one average temperature level.

$$Q_{STH}(t) = \sum A_{coll,i} \cdot G_i(t) \cdot (c_0 - c_1 \cdot \frac{(T_{Coll}(t) - T_A(t))}{G_i}) \tag{3.24}$$

$$Q_{Loss,HWS}(t) = \frac{C_{HWS}}{\tau_{HWS}} \cdot (T_{HWS}(t) - T_A(t)) \tag{3.25}$$

$$C_{HWS} = c_p \cdot \rho \cdot V_{HWS} \tag{3.26}$$

$$\tau_{HWS} = \frac{3}{8}(\frac{1}{3\pi} \cdot V_{HWS})^{1/3} \cdot \frac{\rho \cdot c_p}{U_{HWS}} \tag{3.27}$$

where:

Q_{STH}	= Yield of solar thermal systems in $\frac{Wh_{th}}{h}$
$Q_{Loss,HWS}$	= Storage losses in $\frac{Wh_{th}}{h}$
A_{coll}	= Collector surface in m^2
G	= Global radiation in $^{W}/_{m^2}$
c_0	= Collectors efficiency in %
c_1	= Collector heat loss coefficient in $^{W}/_{m^2K}$
c_p	= Specific thermal capacity of water in $^{J}/_{kgK}$
T_{Coll}	= Temperature of the solar collector in °C
T_A	= Ambient temperature in °C
C_{HWS}	= Thermal capacity of the TES in $^{J}/_{K}$
V_{HWS}	= Endogenously determined storage volume in m^3
U_{HWS}	= Thermal transmission coefficient of thermal energy storage in $^{W}/_{m^2K}$
ρ	= Density of water at standard conditions in $^{kg}/_{m^3}$
τ_{HWS}	= Time constant of the TES in [−]

The conversion of power or fuel into heat is modelled by assuming a technology specific thermal efficiency, which is exogenously set. This efficiency can be distinguished depending on the assumed distribution system, i.e. radiator or panel heating. Thus, this parameter represents both, generation as well as distribution losses. One exception are electric heat pumps. Their coefficient of performance is not constant over the year, but modelled as a function of the difference between the source and the sink temperature [103]. The source temperature for air-to-water heat pumps depends on the outside ambient temperature. For brine heat pumps a constant ground temperature of 10 °C is considered [170]. Further details on the modelling of heat pumps and their contribution in a future German energy system have been studied in [106].

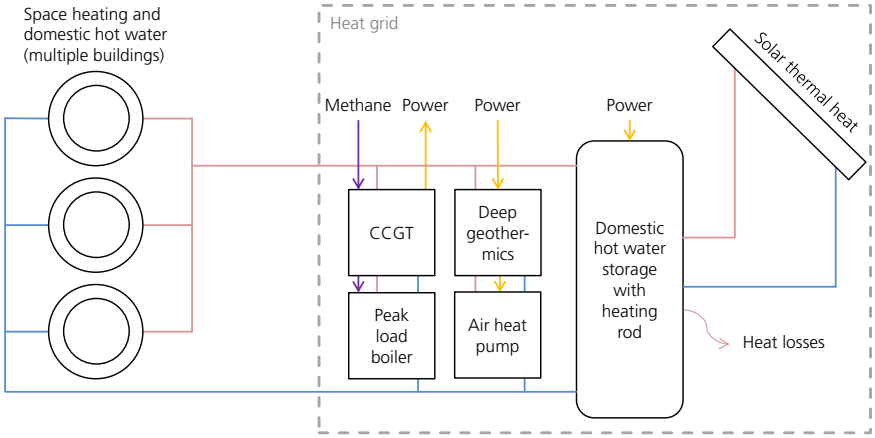

Figure 3.15: General configuration of a heat grid for the supply of space heat and domestic hot water in REMod.

As shown in figure 3.15, district heating systems are represented by a combination of up to five components. The heat generators are connected in parallel and include a CCGT, a peak load boiler as well as an electric air-to-water heat pump. Further, a TES equipped with a heating rod and a solar thermal system are considered. The dimensioning of these two components, as well as the share of the heat load supplied by heat grids, is endogenously determined. While the general mode of operation does not vary from those described for decentralised systems, heat grids can adjust their operation to balance the residual load in cases of power surplus or deficiency. This flexible behaviour is explained in more detail in section 4.4.

Systems for the Supply of Process Heat

Generators for the supply of process heat are not operated according to grid conditions. As a consequence, they directly meet their endogenously determined share of process heat demand. This simplification is based on the assumption that the required plant utilisation, the daily production capacity of a facility or the manufacturing requirements of a product could pose several limitations to a flexible plant operation. The necessary amount of fuel or power P_{In} to meet the useful process heat demand $\dot{Q}_{Use}$ by a determined heat generator i at the supply temperature level j is calculated according to eq. 3.28. The thermal efficiency of the generator is denoted by η_{th}. In case of combined heat and power generation plants, the according power production is obtained by considering the electric efficiency η_{el} eq. 3.29.

$$P_{In}(t) = \frac{\dot{Q}_{Use,i,j}(t)}{\eta_{th,i,j} \cdot \Delta t} \tag{3.28}$$

$$P_{el}(t) = \frac{\dot{Q}_{Use,i,j}(t)}{\eta_{th,i,j} \cdot \Delta t} \cdot \eta_{el,i,j} \tag{3.29}$$

where:

P_{In} = Fuel or power demand of heat generator in $^{kwh}/_{h}$
P_{el} = Power generation of heat generator in $^{kwh_{el}}/_{h}$
$\dot{Q}_{Use}$ = Useful process heat demand in kWh_{th}
η_{th} = Thermal generator efficiency in %
η_{el} = Electric generator efficiency in %
Δt = Considered time step length [−]

A list of all implemented technologies for the supply of process heat as well as other information regarding the modelling of this sector is provided in section 3.2.3.

Utilisation of Biomass

Based on [103], multiple options for the utilisation of biomass are considered in REMod. The yearly available biomass potential is subdivided into three different categories, namely woody biomass, biomass cultivation and organic waste. Their potential is specified exogenously for each year ranging from 2015 to 2050. An overview of the possible biomass conversion paths is shown in figure 3.16.

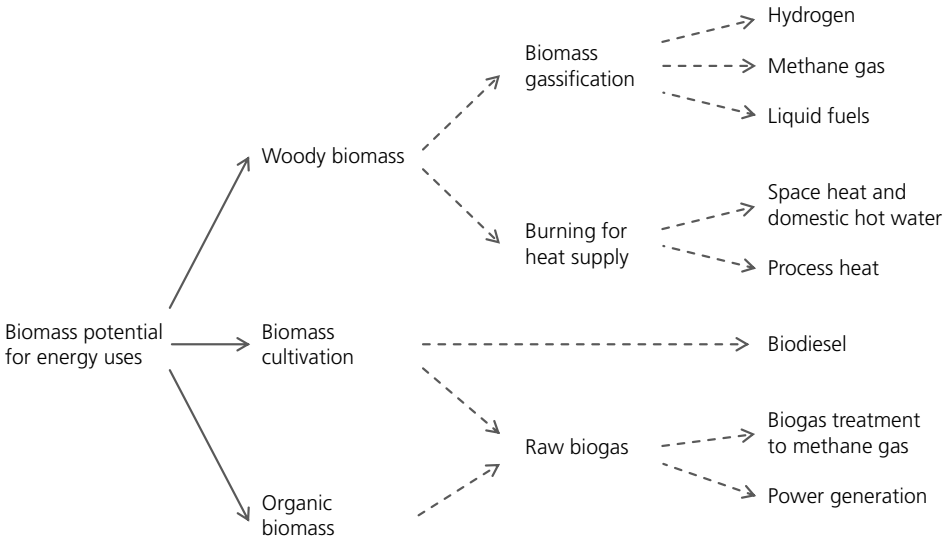

Figure 3.16: Considered conversion path of biomass for energy uses in REMod. Dotted lines indicate that the share of each path is endogenously determined, while continued lines indicate exogenously set amounts.

Woody biomass can either be gasified to produce hydrogen, methane gas or second-generation biofuels. Besides its gasification, it can also be burned to supply heat in the building sector or process heat. The share of each option is endogenously determined. This is represented by dotted lines in figure 3.16.

The next category includes the cultivation of energy crops such as rapeseed or maize. They can be utilised for the production of oil and subsequent conversion into biodiesel. Similarly to the utilisation of woody biomass, the share of cultivation biomass converted into biodiesel is endogenously determined while the production capacity is set constant throughout the year. Energy crops from cultivation biomass (maize) can alternatively be used for the production of biogas. This amount is summed up with the set potential of organic biomass. The produced raw biogas can either be upgraded to pipeline-quality standards and then stored or used for power generation in times of power deficiency.

Import of Synthetic Fuels

Depending on the model parametrisation, it is possible to consider the import option of electricity-based, CO_2-neutral fuels from abroad. This includes synthetic hydrogen, methane as well as liquid fuels. While their yearly limit is specified exogenously, the utilised quantity represents an endogenous result. Further, their import prices need to be specified as well, as their usage substantially depends from the resulting CO_2 abatement costs.

Imported hydrogen from abroad is directly loaded into the hydrogen storage. To avoid a sudden increase of its charge level, the import capacity is evenly distributed over the year. The hydrogen storage may be discharged to meet the hydrogen demand over all sectors. This process is explained in section 4.6. Conversely to hydrogen, methane gas and liquid fuels are considered on a yearly, instead of an hourly, resolution. Accordingly, the import of synthetic methane gas and synthetic liquid fuels may both utilised to fulfil the yearly balance.

4 Modelling of Load Balancing Options

This chapter introduces the modelling approaches of the main load balancing options considered in REMod. The aim of the chapter is to provide the necessary understanding for facilitating the interpretation of the model results in section 6. First, an algorithm for the description of ramping behaviour is introduced. This issue is of growing importance, as the operation of energy conversion plants will increasingly depend on the fluctuating feed-in of VRE. Second, the flexible operation of electric vehicles is depicted. Their batteries could provide the energy system with additional flexibility, if a controlled charging strategy is assumed. Similarly, heat generators combined with thermal energy stores (TES) could be operated in a grid-supportive way and contribute to the balancing of the residual load. Another flexibility option is provided by cross-border exchange of electricity. A simplified approach for consideration of Germany's neighbouring countries is introduced and the available import capacity is modelled on an hourly resolution. Lastly, the modelling approach to short and long-term storage options is described. This includes the operation of power storages as well as the conversion of surplus electricity into synthetic fuels. The first section of this chapter is an excursus introducing a load forecast algorithm. This module is utilised to optimise the operation of multiple flexibility options within the model.

4.1 Excursus: Load Forecast

The load forecast is designed in a way to determine the expected value of the residual load in a future time step t_{FC}. This becomes of increasing importance for an energy system with an expanding share of VRE. For instance, the forecast can be utilised to identify upcoming prolonged periods of power deficiency. For this purpose a counter is introduced. It is increased by one, if at the current time step a positive residual load in an future time step is forecasted. Otherwise, the counter is set to zero. Once it reaches an exogenously specified threshold value, the future time period is classified as period of power deficiency. When this period is reached, the operation of specific system components can be adjusted accordingly. A simplified flow chart of the program sequence, is depicted in Figure 4.1.

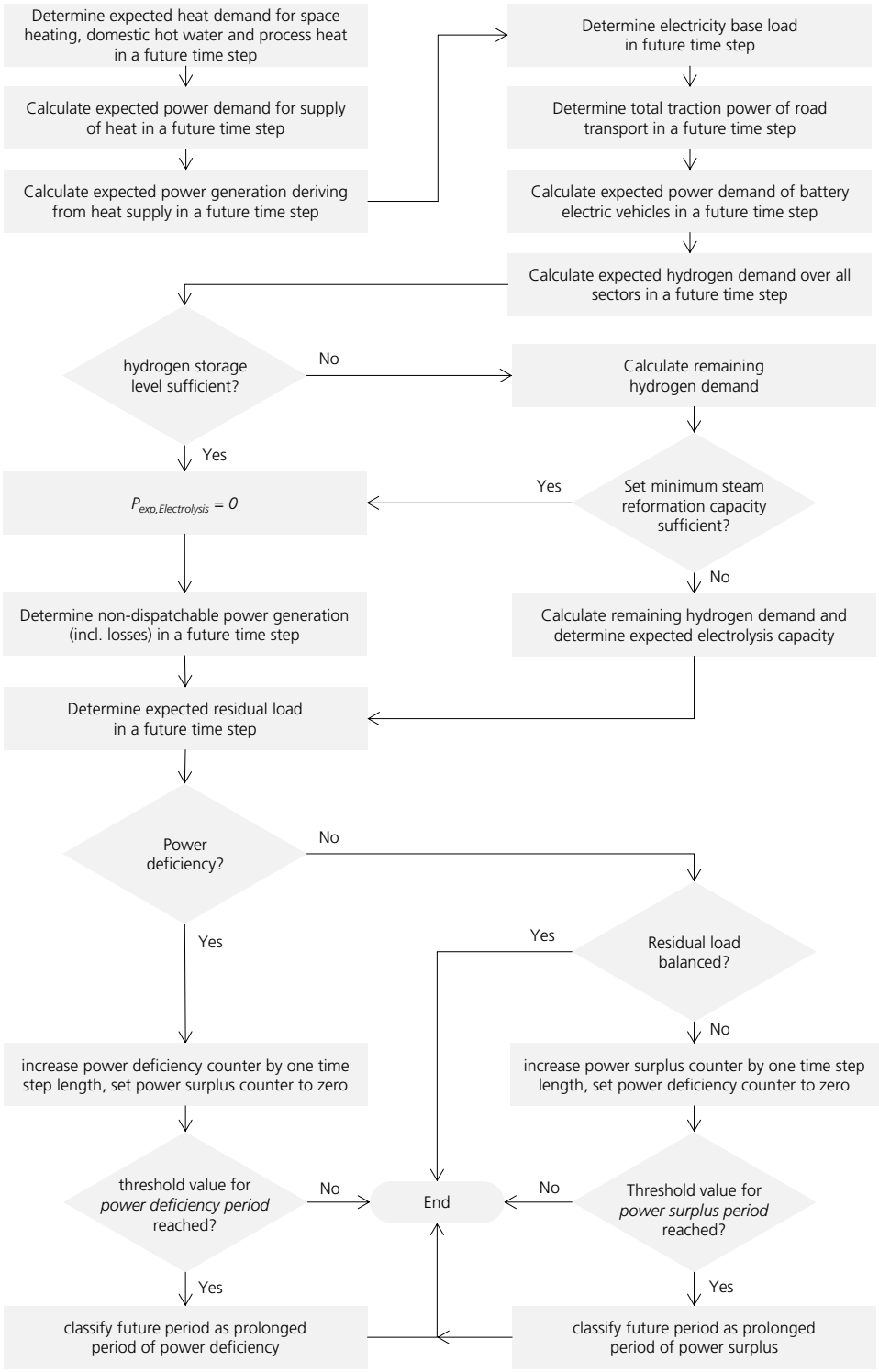

Figure 4.1: Flowchart describing the modelling approach for the calculation of the expected residual load value and the identification of prolonged power surplus or power deficiency periods.

The implemented load forecast is mainly utilised to optimise the operation of various flexible technologies (for instance, cf. sections 4.2 and 4.3). Thus, depending on the considered application case, the forecast time horizon (or period) t_{FP} can be set accordingly. The forecast time t_{FC} is obtained as shown in eq. 4.1. Here, t denotes the current time step.

$$t_{FC} = t + t_{FP} \tag{4.1}$$

When forecasting, it is important to distinguish between variables, which are determined based on exogenous or endogenous quantities. Quantities based on exogenously set parameters, such as weather data, feed-in profiles or load profiles, can be predicted with a negligible computational effort. This is not the case for variables, which instead depend on the operation of other system components, such as thermal, chemical or other power storage options. For instance, the prediction (and adjustment) of the TES temperature would be influenced through continuous feedback effects on the system. As a consequence, an accurate forecast would require an iterative approach . The associated computing effort would increase considerably, which is why, instead, several assumptions are introduced.

The energy demand for space heat and domestic hot water in a future time step t_{FC} can exactly be predicted, as its value depends on exogenously set data (such as physical properties of buildings and weather data). Based on this information, the expected power demand $P_{exp,l,SH,i}$ and power generation $P_{exp,g,SH,i}$ of all heat generators I can be calculated. It is assumed that TES do not contribute to the coverage of the heat demand, as their discharge would lead to several feedback effects, which are not easily predicted. This also implies that the coefficient of performance of electrical heat pumps, which per definition depends on the storage temperature, is not forecasted. Instead, for each considered heat pump technology it is set accordingly to its annual mean performance factor. While this approach represents a loss of accuracy, it is necessary to keep the computational time as low as possible. This uncertainty primarily occurs when heat generators are operated according to the residual load, as in this case, the storage temperature is increased more frequently and overall, reaches higher values (cf. section 6.3).

The electricity base load (cf. section 3.2.5) as well as the heat demand for the supply of process heat in a future time step t_{FC} can be determined based on the exogenously provided data (cf. section 3.2.3). Thus, the expected power demand $P_{exp,l,PH,j}$ and generation $P_{exp,g,PH,j}$ of all heat generators considered for the supply of process heat J can be calculated. Further, the power demand $P_{exp,l,RT,k}$ of electric vehicles, can be determined based on the underlying driving profiles and their share within all power train technologies K. In this case, similarly to the operation of TES, an inflexible operation of vehicle batteries is assumed. Thus, it is neglected that the calculated value of the

expected electric load might possibly be lower, due to the charging of surplus power into the vehicles batteries.

As shown in figure 4.1 the algorithm also accounts for the expected power demand of electrolysis plants. An expected hydrogen demand P_{exp,l,H_2} for the supply of space heat, domestic hot water and process heat as well as for the motorised road transport sector is calculated. If the resulting demand can be sustained over the whole forecast period by the hydrogen storage, then the expected electrolysis power demand $P_{exp,elyse}$ is set to zero. Otherwise, the remaining hydrogen demand may be met by a set minimum capacity of steam reformation plants (cf. section 4.6). Should this option not be sufficient to guarantee a coverage of the expected hydrogen demand, than an expected electricity demand for an according operation of electrolysis plants $P_{exp,elyse}$ is calculated. The total expected power demand in the time future time step t_{FC} is determined as shown in eq. 4.2.

The expected non-dispatchable generation $P_{exp,ndg}$ is calculated according to section 3.4. It includes photovoltaic stations, wind turbines (onshore and offshore), hydro power plants, nuclear power plants, the must-run capacity of lignite and hard coal power plants, the mandatory import of electricity as well as the non-dispatchable power generation resulting from all heat generators (and the respective grid losses). Finally, the expected residual load is calculated according to eq. 4.3. It is possible to apply a load safety factor f_{SL} to account for the above described forecast uncertainties. They include TES (and coefficient of performance of heat pumps), hydrogen storages as well as power storages (including those of electric vehicles).

$$P_{exp,el} = \sum_{i=1}^{I} P_{exp,l,SH,i} + \sum_{j=1}^{J} P_{exp,l,PH,i} + \sum_{k=1}^{K} P_{exp,l,RT,j} + P_{exp,elyse} + P_{exp,BL} \quad (4.2)$$

$$P_{exp,Res} = P_{exp,ndg} - P_{exp,el} \cdot f_{SL} \quad (4.3)$$

where:

$P_{exp,Res}$ = Expected residual load value in $^{kWh_{el}}/_{h}$
$P_{exp,ndg}$ = Total expected power non-dispatchable power generation in $^{kWh_{el}}/_{h}$
$P_{exp,el}$ = Total expected power demand in $^{kWh_{el}}/_{h}$
$P_{exp,el}$ = Total expected power demand in $^{kWh_{el}}/_{h}$
$P_{exp,l,SH}$ = Expected power demand for space heat and hot water in $^{kWh_{el}}/_{h}$
$P_{exp,l,PH}$ = Expected power demand for the supply of process heat in $^{kWh_{el}}/_{h}$
$P_{exp,l,RT}$ = Expected power demand for road transport in $^{kWh_{el}}/_{h}$
$P_{exp,elyse}$ = Expected power demand of electrolysis plants in $^{kWh_{el}}/_{h}$

$P_{exp,BL}$ = Expected power demand of electricity base load in $^{kWh_{el}}/_{h}$
f_{SL} = Load safety factor in [−]
I = Number of heat generators for space heat and domestic hot water
J = Number of heat generators for the supply of process heat
K = Number of power train technologies in the road transport

For the flexible operation of vehicle batteries (cf. section 4.3), the forecast is utilised to identify prolonged time periods of power deficiency. During such time periods, a gradual, mandatory charging of electric vehicles is started. This is necessary to avoid a complete discharge of vehicle batteries[1].

As for thermal power plants the load forecast does not stop at the expected residual load value $P_{exp,Res}$ as shown in figure 4.1. It also takes into account competing power generation options. For instance, the load forecast of a coal power plant also considers the available power generation capacity of CCGT, gas turbine or oil power plants as well as the option of importing electricity from neighbouring countries. Further, all thermal power plants are characterised by an exogenously set minimum operation time (cf. section 5.3). Thus, the forecast also accounts for consecutive hours of expected power demand. This concept is further described in the next section, where the modelling approach for the consideration of ramping behaviour of energy conversion plants is presented.

4.2 Ramping Behaviour of Energy Conversion Technologies

Historically, to secure a stable grid operation, power generation technologies were run according to load predictions. For this purpose power plants were divided into base load and peaking load plants. Nuclear, lignite and hard coal power plants are, for instance, usually used as base load plants due to their high power generation capacity and thermal inertia. On the contrary, peaking plants, like gas turbines, exhibit a higher capability of adjusting their power level. Thus, they are operated mainly for a couple of hours when maximum power demand occurs. In 2016, Germany‘s installed capacity of nuclear and coal-fired power plants amounted to 11 GW_{el} and 48 GW_{el}, respectively [22]. According to [171], coal power plants were responsible for roughly 350 billion tons of CO_2 emissions, accounting for more than a third of Germany‘s GHG-emissions. In 2000, with the German Renewable Energy Sources Act (EEG) [172] priority dispatch from VRE was determined, contributing to a progressive capacity increase of photovoltaic and wind power stations. As a consequence of their fluctuating power supply, more and

[1] This effect is studied in detail in [105]

more baseload power plants need to undertake specific retrofit measures to achieve a more flexible operation. Various examples of different retrofitting measures are presented in [60, 173–175]. Further, [175] points out that those measures usually represent the by far more economical choice over a new construction. Today, various examples of plant retrofitting exist [60].

As the share of VRE rises, the consideration of ramping behaviour of power plants will become of increasing importance. Besides for conventional power plants, this might also be the case for technologies operated in times of power surplus, i.e. when the feed-in from VRE is comparably high. For this reason, a generic methodological approach was developed and implemented in REMod.

4.2.1 Term Definitions and Methodological Approach

According to the definition of Agora-Energiewende „*The flexibility of a power plant can be described as its ability to adjust the net power fed into the grid, its overall bandwidth of operation and the time required to attain stable operation when starting up from a standstill*“ [60]. Thus, to implement the flexible behaviour of a generic energy conversion plant in REMod, various parameters need to be introduced. For instance, the available capacity $P_i(t)$ of a plant at the time t as well as its conversion efficiency $\eta_i(t)$. Both parameters may be restricted depending on the current operation state of the plant. Figure 4.2 portraits the simplified ramp-up behaviour of a generic plant, marking three different operation states and their respective limitations.

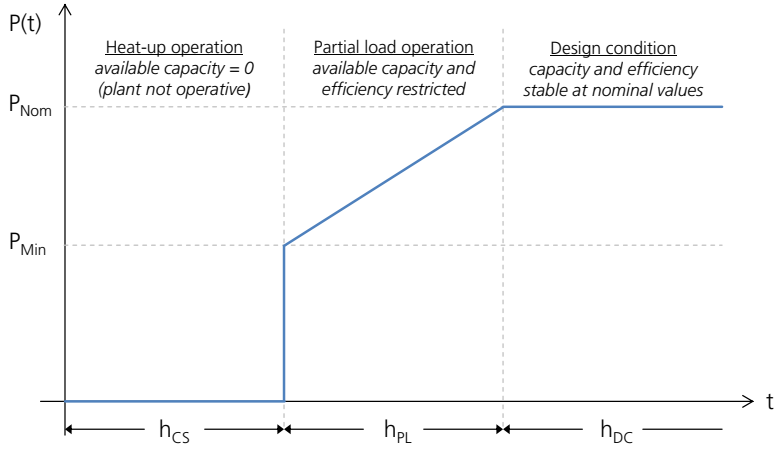

Figure 4.2: Simplified operative states of energy conversion plants considered in REMod. P_{Nom}: nominal capacity, P_{Min}: minimum load capacity, h_{CS}: cold start-up time, h_{PL}: time spent in partial load operation, h_{DC}: time spent in design condition operation. Own illustration based on [60]

The minimum load p_{Min} describes the minimum plant capacity - related to the maximum load - under which a stable operation is possible. Thus, to provide a useful energy output, a plant operated either for the first time or after a downtime of at least two days is heated up for a duration equal to its cold start-up time h_{CS}. In figure 4.2 this operation is referred to as *heat-up operation*. Depending on the considered plant type i, fuel or electric power may be required. While in this phase, the available conversion capacity of the plant is set to zero. The cold start-up time duration heavily depends on the plant design, i.e. on its ramping characteristics. Generally, the lower the minimum load, the lower the corresponding start-up time and the faster the plant is able to adjust its operation when power deficiency occurs.

After the heat-up phase the plant can run at stable operating conditions in partial load. In this area the plant efficiency is reduced according to its characteristics. As shown in figure 4.2, its lower boundary is represented by the minimum load P_{Min} while its upper limit is denoted by the nominal plant capacity P_{Nom}. The time spent in partial load operation h_{PL} is described by eq. 4.4 and heavily depends on the ramp rate R_{RR}. The latter reveals the load increase per minute while in partial load operation. The higher the ramp rate, the shorter the operation in partial load and the faster the plant can reach its nominal conversion capacity. Further, as described in eq. 4.5, it is considered that while in partial load operation, only a given share S_{AP} of the maximum plant capacity is available. Accordingly, the efficiency of the plant $\eta_i(t)$ is reduced as shown in eq. 4.6. The conversion efficiency of the plant in partial load related to its maximum efficiency is denoted by S_{PL}.

The third part in figure 4.2 denotes the operation at design conditions. Neither the capacity nor the efficiency are limited, meaning that the plant operates at its maximum efficiency η_{Nom} for the duration $h_{DC}(t)$.

$$h_{PL,i}(t) = \frac{100 - p_{Min,i}}{R_{RR,i} \cdot 60} \tag{4.4}$$

$$P_i(t) = P_{Nom,i} \cdot S_{AP,i}(t) \tag{4.5}$$

$$\eta_i(t) = \eta_{Nom,i} \cdot \left(h_{DCOp,i}(t) + h_{PLOp,i}(t) \cdot S_{PL,i} \right) \tag{4.6}$$

where:

p_{Min} = Minimum load of plant related to its maximum capacity [$\%_{P_{Nom}}$]
P_{Nom} = Nominal capacity of plant in kW_{el}
P = Hourly energy output of plant in $^{kWh_{el}}/_{h}$
R_{RR} = Ramp rate of plant in $\%/_{min}$

h_{PL} = Partial load time of plant $[h]$
h_{DCOp} = Time spent in design condition operation $[h]$
h_{PLOp} = Time spent in partial load operation $[h]$
S_{AP} = Available share of the maximum plant capacity in %
S_{PL} = Conversion efficiency in partial load related to maximum efficiency in %
η = Conversion efficiency of plant in %
η_{Nom} = Maximum efficiency of plant in %

Based on the underlying ramping characteristics (cf. appendix A, table A.2) a plant operation curve, analogous to figure 4.2, is obtained for each plant type considered in REMod. This curve substantially describes a linear function interpolating the minimum load and the nominal load while taking into account the respective time intervals defined by the cold start-up and partial load. In order to determine the operating condition of the plant during each time step t, a ramping counter $c_i(t)$ is introduced. This counter can take values between zero and the sum of the cold start-up and partial load time, as shown in eq. 4.7. The curve and the counter combined are used to identify the operation mode of the plant at the considered time step. For instance, a ramping counter lower than the cold start-up h_{CS} time would result in heat-up operation and therefore limit the available plant capacity. On the contrary, its maximum value would imply that the plant can be run at design conditions.

$$c(t) \in [0; h_{CS} + h_{PL}] \tag{4.7}$$

The ramping counter must take into account that the operation of an energy conversion plant, instead of progressing from heat-up to partial load to design condition operation, may be discontinuous. For instance, depending on the duration of the standstill time a plant might resume its operation in partial load or even heat-up state. Thus, the ramping counter must consider a heat-up or a cool down of the plant, which are linked to its consecutive operating or standstill hours, respectively. Figure 4.3 shows the program sequence for identification of the operating mode and the associated adjustment of the ramping counter.

In case of required plant operation, the starting (t) and ending $(t+1)$ operation points on the operation curve are determined according to eq. 4.8 and 4.9. These two points provide insight about whether the plant is ready for operation as well as about its available capacity share. Further, they indicate if, at the current time step, the plant is restricted to one or more operation modes. This is exemplarily shown in figure 4.4, where depending on the ramping characteristics and the value of the ramping counter, different operation states result.

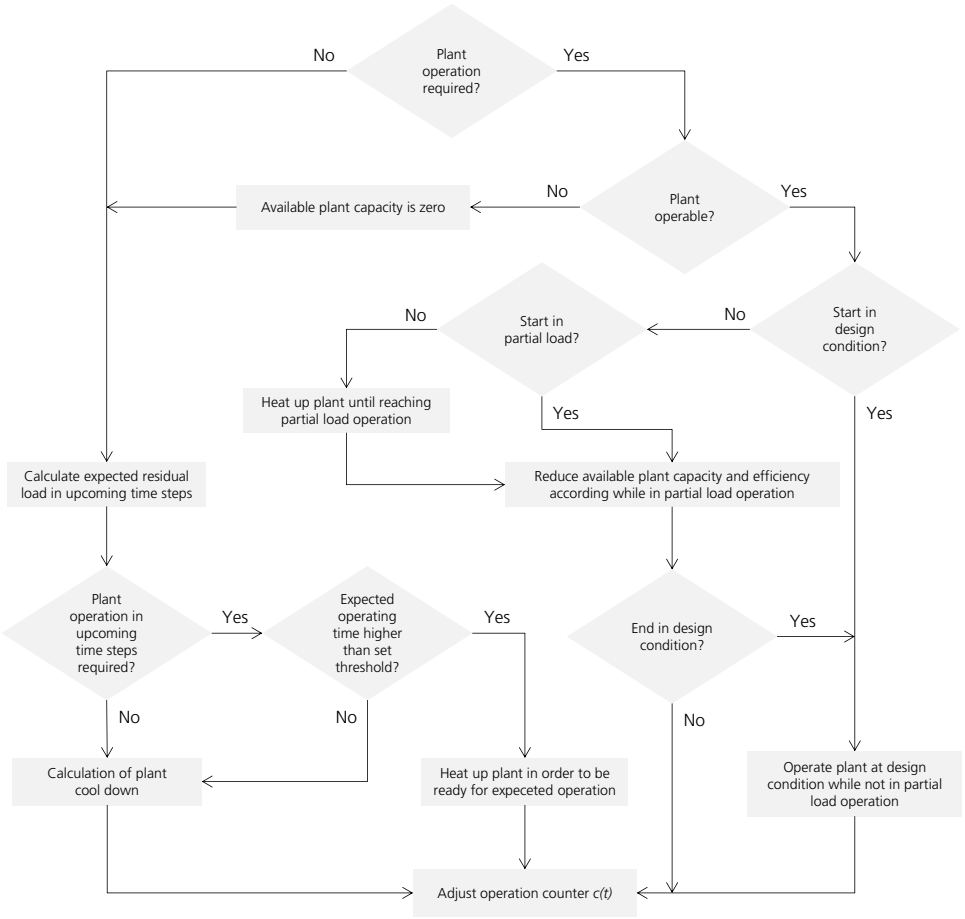

Figure 4.3: Flowchart of modelling approach for the identification of plant operating mode and ramping counter.

$$S_{AP,i}(c_i(t)) = \frac{100 - p_{Min,i}}{h_{PL,i}(t)} \cdot \Big(c_i(t) - h_{CS}\Big) + p_{Min,i} \qquad \forall c \in [h_{CS}; h_{CS} + h_{PL}] \quad (4.8)$$

$$S_{AP,i}(c_i) = 0 \qquad \forall c \in [0; h_{CS}[\quad (4.9)$$

where:

c = Ramping counter $[h]$

h_{CS} = Cold start-up time of plant $[h]$

h_{PL} = Partial load time of plant $[h]$

p_{Min} = Minimum load of plant related to its maximum capacity [$\%_{P_{Nom}}$]
S_{AP} = Available share of the maximum plant capacity in %

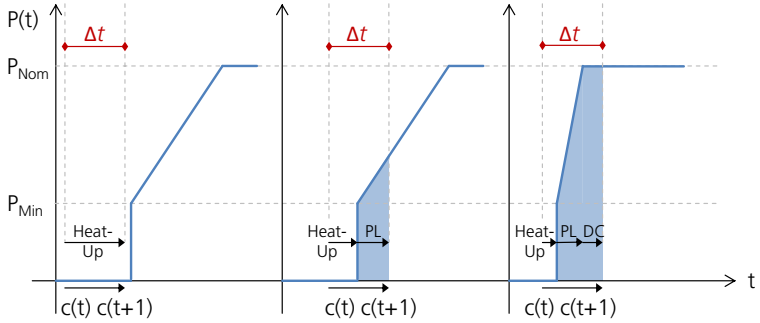

Figure 4.4: Example for plant operation through one, two or three operation modes within one time step. The individual starting positions and operation curves are varied. PL and DC denote the plant operation in partial load mode and design conditions, respectively. P_{Nom}: nominal capacity, P_{Min}: minimum load capacity. Δt: time step length.

In figure 4.4 three examples concerning the determination of the operation mode and the available plant capacity are illustrated. In the first case the beginning and ending value of the ramping counter is lower than the cold start-up time. This means that the plant may be heated up without providing any energy output. Also in the second example, the plant starts its operation in heat-up mode. In this case, the counter ends in the partial load area ($c(t+1)$), i.e. its value exceeds the cold start-up time. The available capacity share of the plant for this time interval is equal to the integral of the operation curve (eq. 4.10), represented by the blue area in figure 4.4. In the third example, different ramping characteristics are assumed, leading to a steeper operation curve and a shorter partial load time. In this particular case the plant operation goes through all three operation modes, i.e. from heat-up to partial load to full load operation. This behaviour is not unusual for technologies with particularly low cold start-up times and high ramp rates, such as gas turbines or polymer electrolyte membrane electrolysis plants.

$$S_{AP} = \int_{c_{Min}[t;t+1]}^{c_{Max}[t;t+1]} \frac{1-p_{Min}}{h_{PL}} \cdot (t - h_{CS}) + p_{Min} \qquad \forall c \in [h_{CS}; h_{CS} + h_{PL}[\tag{4.10}$$

As shown in figure 4.3, the ramping counter is adjusted at the end of each time step (eq. 4.12). If the plant was heated up or utilised for the conversion of energy at the current time step, the counter is increased by one time step length t. In the opposite case, it means that the plant operation either was not required or that no conversion

capacity was available, for instance due to a low value of the ramping counter (eq. 4.9). In this case, the plant may still be heated up at time step, if two conditions are met: first, the plant operation is expected to be necessary in upcoming time steps and needs to be heated up to get ready for operation. Second, the plant is expected to run for at least an exogenously set amount of time, which corresponds to the minimum duration for an cost-efficient operation (cf. section 5.3). If so, the necessary energy demand $P_{H,i}$ for the heat-up of the plant i is calculated according to eq. 4.11. Here, E_S describes the energy demand per installed capacity in $^{kWh}/_{kW}$ which is based on literature values (cf. appendix A.2). The required production capacity of the plant in an upcoming time step $P_{exp,i}$ is identified by a forecast. This forecast calculates the expected residual load (cf. section 3.4, eq. 3.18) in upcoming time steps, taking into account the estimated generation capacity of other competing power generation technologies. The forecast also includes the estimated power demand of all end-use sectors as well as those of electrolysis plants and other storage technologies. The implementation of the load forecast is presented in detail in section 4.1.

$$P_{H,i}(t) = E_S \cdot \frac{P_{exp,i}(t)}{P_{Nom,i}} \tag{4.11}$$

where:

P_H = Energy demand for heat-up of the plant in $^{kWh}/_{h}$
E_S = Energy demand for heat-up per installed plant capacity $^{kWh}/_{kW}$
P_{exp} = Expected production capacity of plant in upcoming time steps in $^{kWh_{el}}/_{h}$
P_{Nom} = Nominal capacity of plant in kW_{el}

Finally, as shown in figure 4.3, if the plant is not heated up, it is cooled down as a consequence of the standstill. Depending on the duration of the downtime it is necessary to differentiate in cold and hot start-up time. While a cold start-up happens for a standstill duration of at least two days, a hot start-up is defined by a standstill duration of less than eight hours. Between these two durations a warm start-up occurs. The entity of the cool down process $c_{CD,i}(t)$ depends on the current temperature level of the plant, meaning that it occurs faster for higher temperature levels and slower afterwards (eq. 4.13 and 4.14). For this purpose a downtime counter $c_S(t)$ is introduced, monitoring the succesive hours of downtime of each plant. This counter is increased by one time step for each consecutive hour of downtime and set to zero otherwise. This means that a plant running at design conditions is cooled down faster during the first eight hours and slower afterwards. This behaviour is illustrated in figure 4.5. Here, according to literature, the duration for a cold start-up D_{CS} and a hot start-up D_{HS} is set to 48 and 8 hours, respectively [60].

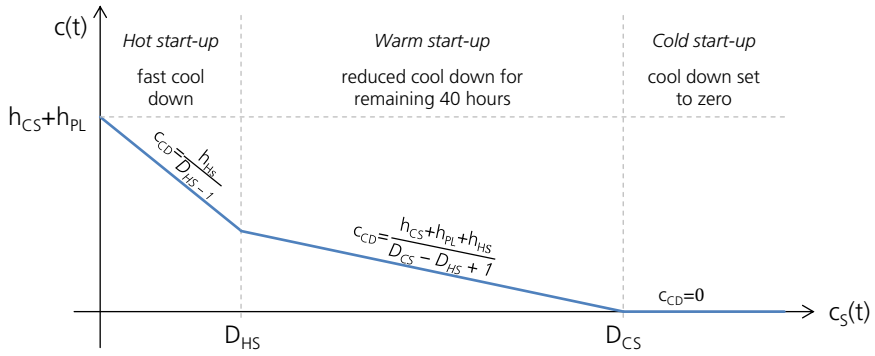

Figure 4.5: Adjustment of cool down counter depending of consecutive hours of downtime. D_{HS}: duration of a hot start-up (48 h), D_{CS}: duration of a cold start-up (8 h), h_{CS}: cold start-up time of plant, h_{PL}: partial load time of plant.

$$c_i(t) = c_i(t-1) + c_{H,i}(t-1) - c_{CD,i}(t-1) \tag{4.12}$$

$$c_{CD,i}(t) = \frac{h_{HS,i}(t)}{D_{HS} - 1} \qquad \forall c_{S,i}(t) < D_{HS} \tag{4.13}$$

$$c_{CD,i}(t) = \frac{\left(h_{CS,i}(t) + h_{PL,i}(t) - h_{HS,i}(t)\right)}{D_{CS} - D_{HS} + 1} \qquad \forall c_{S,i}(t) \geq D_{HS} \tag{4.14}$$

where:

c = Ramping counter $[h]$
c_S = Counter for consecutive hours downtime hours $[h]$
c_H = Entity of the heat-up process $[h]$
c_{CD} = Entity of the cool down process $[h]$
h_{HS} = Hot start-up time of plant $[h]$
h_{CS} = Cold start-up time of plant $[h]$
h_{PL} = Partial load time of plant $[h]$
D_{HS} = Duration of a hot start-up per definition $[h]$
D_{CS} = Duration of a cold start-up per definition $[h]$

4.2.2 Discussion of the Model Extension

The flexibility of energy conversion plants will become of increasing importance for energy systems characterised by a substantial share (and priority dispatch) of VRE. For its representation a generic modelling approach was developed and implemented in REMod.

The introduced methodology distinguishes between three operation modes for a generic energy conversion plant, namely heat-up, partial load and design condition operation. These options are described by an operation curve which is derived from the ramping characteristics of the power plant. These characteristics may be individually adjusted for each year from 2015 until 2050, thus reflecting technological enhancements. The curve is modelled as linear function, thus representing a simplification of reality. The same holds for the cool down behaviour. For the identification of the plant's operative state within each time step two distinctive counters are utilised, monitoring the successive operative hours as well as the downtime. Thus, when resuming operation after a standstill, it is possible to distinguish between cold start-up, warm start-up or hot start-up condition. The plant efficiency in partial load operation is reduced according to a factor, which is determined as the integral of the efficiency curve of a given plant and thus representing an average value (cf. section 5.3, table 5.5). Further, a forecast is implemented (cf. section 4.1), determining the expected duration of operation in upcoming time steps. For instance, a thermal power plant may be heated up to be ready for operation in a future time step when power deficiency occurs. Due to this mechanism the exogenously set operational sequence of energy conversion plants (cf. section 3.4) is no longer the only determining factor. Instead, besides the conversion efficiency and the carbon footprint of each plant, also its flexibility characteristics may influence the operational sequence, adding a greater level of detail compared to a fixed order. While the forecast is based on a perfect foresight approach, it contains some uncertainties, in particular regarding the operation of energy storage facilities. Thus, it may be that even though a plant operation of a given duration is expected, the real operation might result slightly lower or higher. Finally, it is noted that the focus of the presented methodology is on the technical operation of power plants. Costs arising from retrofitting measures are therefore not taken into account. They can, however, be considered when parametrising the model.

Another technology option, which might significantly influence the flexibility of the energy system, is the introduction of battery electric vehicles. Their background and methodology are presented in the next section.

4.3 Battery Electric Drive Concepts

Eventhough electric vehicles (EVs) yet represent a small fraction compared to the global car stock (0.2 %), their numbers are expected to increase over the next years [176]. In Germany, in the beginning of 2018, their share accounted for roughly 0.1 % of all motorised private vehicles [177]. In order to increase their numbers, the German Federal Government introduced buying incentives as well as funds for the expansion of the charging infrastructure [178]. Germany aims to bring one million EVs on the road by 2020, which corresponds to approximately 1.75 % of the total vehicle fleet. To give an idea of the theoretically associated battery capacity, a rough calculation is made. Assuming an average battery capacity per vehicle of 60 kWh_{el} [179], this yields to a cumulative battery capacity of 60 GWh_{el}. Accordingly, a complete shift of today's private road transport sector to electric vehicles, would lead to a cumulative battery capacity of roughly 3 TWh_{el} [180]. Operating a small share of this potential according to the residual load value could improve flexibility of the energy system. However, potential power load peaks originating from simultaneous charging should be accounted for as well. In order to assess opportunities and challenges linked to the integration of EVs into the energy system, model based calculations can be performed. In [105] a comprehensive analysis of flexible electric vehicle charging based on REMod is presented. The study introduces an approach for the generation of driving profiles and further compares two modelling approaches for the depiction of the electrified road transport sector. Based on the acquired insights, an extension of this work is subsequently presented.

In the first part of this section, a general modelling approach for the depiction of the road transport sector in REMod is introduced. Afterwards, the focus is on the modelling of battery electric vehicles (BEVs) and their (optional) flexible operation. The chapter closes with a summary and discussion of the implemented modelling approach.

4.3.1 Modelling Approach

Due to the single node approach utilised in REMod, all vehicles belonging to the same power train technology (PTT) are aggregated (cf. section 3.2.2), resulting in one energy demand profile each[2]. This profile describes the mechanical energy needed for the traction of one average vehicle $P_T(t)$ at each considered time step t. Starting from the annual final energy demand of the vehicle fleet E_{veh}, its average efficiency η_{avg} and the total number of vehicles N_{veh}, an hourly value for the traction power per vehicle can be calculated according to eq. 4.15. Alternatively, as shwon in eq. 4.16, the hourly traction power per vehicle can also be determined based on the kilometres travelled per year km_{trav}

[2] A distinction for vehicles of the private road transport sector and the freight transport sector is made (cf. section 3.2.2)

and the average energy consumption per kilometre travelled $E_{avg,pkt}$. The indicated parameters for the calculation of the hourly traction power per vehicle are documented in [181] (for Germany). It is noted that the traction power obtained in eq. 4.15 or 4.16 describes a constant energy demand profile [103].

$$P_T(t) = \sum_{i=1}^{N_{PTT}} \frac{E_{veh,i} \cdot \eta_{avg,i}}{(N_{veh,i} \cdot t)_{t=8760}} \tag{4.15}$$

$$P_T(t) = \sum_{i=1}^{N_{PTT}} \frac{km_{trav,i} \cdot E_{avg,pkt,i}}{(N_{veh,i} \cdot t)_{t=8760}} \tag{4.16}$$

$$P_{E,i}(t) = \frac{P_T(t) \cdot N_{veh,i}}{\eta_{avg,i}} \tag{4.17}$$

where:

P_T = Traction power of one average vehicle in $^{kW_{el}}/_{vehicle}$
P_E = Final power demand of vehicles of a specific power train technology in $^{kWh_{el}}/_{h}$
N_{PTT} = Number of considered power train technologies [−]
E_{veh} = Annual final energy demand of vehicle fleet in kWh_{el}
$E_{avg,pkt}$ = Average final energy consumption per kilometre travelled in $^{kWh_{el}}/_{km_{trav}}$
km_{trav} = Kilometres travelled per year [−]
η_{avg} = Annual average efficiency of vehicle fleet in %
N_{veh} = Total number of vehicles [−]
i = Considered power train technology [−]

For each individual power train technology i the final power demand of the vehicles $P_E(t)$ is calculated according to eq. 4.17. This approach represents a simplified solution for the calculation of the final power demand of different power train technologies, while at the same time being able to consider efficiency enhancements of both conventional and new drive systems. For the modelling of BEVs and plug-in-hybrid vehicles (PHEVs), additional time dependent variables and restrictions need to be considered. For instance, to consider simultaneous vehicle charging, which might lead to power load peaks. Or to model the availability of BEVs as battery storages.

Modelling of Electric Vehicles: Flow Chart and Model Equations

BEVs and PHEVs of a specific power train technology are represented as one distinctive battery storage each. All parameters regarding this storage relate only to those vehicles which are currently plugged into a charging facility and therefore connected to the electrical grid. This means that parameters used to describe the vehicle battery, such as its maximum capacity $E_{Max}(t)$, may vary according to the underlying driving profiles, i.e. the time dependent share of vehicles currently plugged into a charging facility (cf. figure 4.7). This approach implies that the battery charge level $E(t)$ does not indicate the exact charge level of each individual vehicle, but rather describes the average charge level of all vehicles plugged into a charging facility of a specific power train technology (PTT).

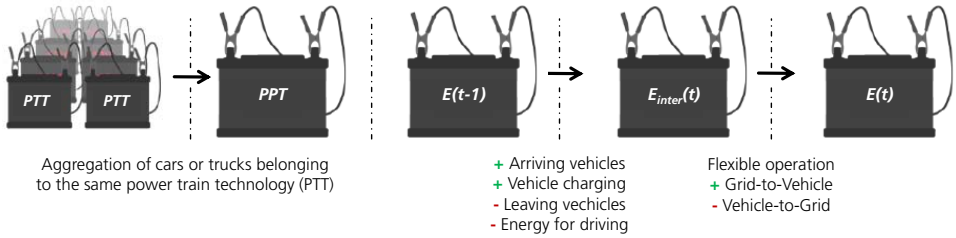

Figure 4.6: Schematic overview of the main steps undertaken for the modelling of electric vehicles. E: battery charge level, E_{inter}: interim charge level.

Figure 4.6 depicts the main steps for the calculation of the charge level $E(t)$. Starting from the previous charge level $E(t-1)$, an interim charge level $E_{inter}(t)$ is first determined. This value accounts for the drop or increase in charge level due to vehicles leaving from or arriving at the charging facility. The interim charge level may, in a second step, be adjusted due to flexible operation of the vehicle batteries, resulting in the final charge level for the current time step $E(t)$. This approach is further explained in two consecutive parts. The first part provides an overview of required input data and illustrates the calculation of the interim charge level (figure 4.8). In the second part, the charging or discharging of the vehicle batteries due to power surplus or deficiency is presented (cf. figure 4.9).

The required model inputs can be divided into hourly time series and constant parameters. The hourly time series are directly linked to the underlying driving profiles. For each time step, they account for the share of vehicles leaving from or arriving at a charging facility ($S_L(t)$, $S_A(t)$). In case of power deficiency, a factor describing the allowed depth of discharge ($f_{V2G}(t)$) of the aggregated vehicle battery is used to limit the feed-in into the electrical grid. Further, the state of charge $SoC(t)$ is used to consider a relative weighting of the vehicles energy demand during each time step t, depending on their arrival time or season. For example, it could be assumed that trips that end later in

the evening or happen in summer instead of winter are, on average, longer and therefore require more electricity, leading to a lower state of charge of the battery. The constant parameters on the other hand, mainly represent average values for the description of the considered power train technology, whether it is their total number (N_{veh}), the resulting traction power for each vehicle (eq. 4.15), their efficiency (η_{avg}), battery size ($C_{avg,bat}$) or the assumed charging/discharging capacity ($P_{G2V,avg}$, $P_{V2G,avg}$). The power demand of each vehicle $P_E(t)$ is calculated starting from the hourly traction power per vehicle $P_T(t)$ (cf. eq. 4.15 and 4.16), the average efficiency η_{avg} and the total number of vehicles N_{veh} of the power train technology i. For BEVs and PHEVs, the power demand $P_E(t)$ is distributed over the hours of the year according to the normalised profile $D_{EN}(t)$. This profile depends on the time series of arriving vehicles $S_A(t)$ as well as the state of charge $SoC(t)$ as shown in eq. 4.18 and 4.19.

$$D_{EN,i}(t) = \frac{S_{A,i}(t) \cdot (1 - SoC_i(t))}{max(S_{A,i}(t) \cdot (1 - SoC_i(t))} \tag{4.18}$$

$$P_{E,i}(t) = D_{EN,i}(t) \cdot \frac{\sum_{t=1}^{8760} P_T(t) \cdot N_{veh,i}}{\sum_{t=1}^{8760} D_{EN,i}(t) \cdot \eta_{avg,i}} \tag{4.19}$$

where:

D_{EN} = Normalised power demand profile [−]
S_A = Hourly share of arriving vehicles in %
SoC = State of charge in kWh_{el}
P_T = Traction power of one average vehicle in $^{kW_{el}}/_{vehicle}$
P_E = Final power demand of vehicles of a specific power train technology in kW_{el}
η_{avg} = Average vehicle efficiency in %
N_{veh} = Total number of vehicles [−]
i = Considered power train technology [−]

For the modelling of the battery storage and the restrictions posed on its charge level $E(t)$, a series of threshold values is utilised. The upper limit for the charge level is described by the maximum available battery capacity $E_{Max}(t)$. As shown in figure 4.7, this value may increase or decrease according to the share of electric vehicles connected to the electrical grid at each considered time step (eq. 4.20, 4.21). Similarly, $E_{V2G,Min}(t)$ is used to restrict the discharging of the battery storage in case of power deficiency (Vehicle-to-Grid). This means that the vehicle battery can only be discharged to supply power to the electrical grid, if the charge level of the battery $E(t)$ is higher than the assumed threshold value. Relating to figure 4.7, this is only true for a charge level equal to a. Further, the charge level can not be lower than the imposed absolute lower

limit $E_{MinAbs}(t)$. Relating to figure 4.7, d represents the lowest possible value for the charge level at the time t_0. Eq. 4.20, 4.22, 4.23, 4.24 describe the mentioned physical restrictions.

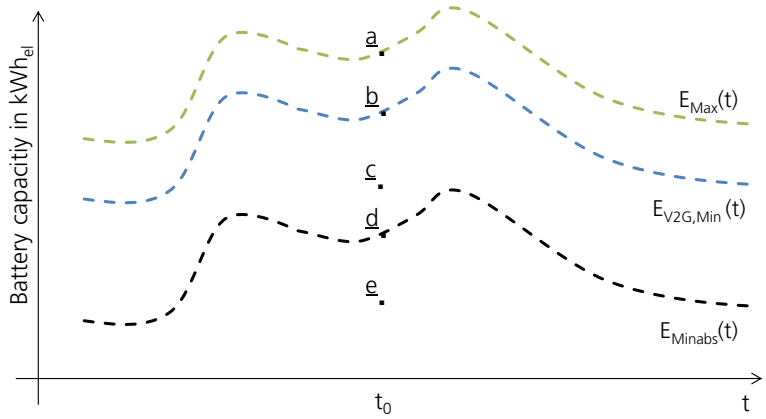

Figure 4.7: Exemplarily illustration of the functional battery storage: restrictions and charge levels. E_{Max}: maximum available battery capacity, $E_{V2G,Min}$: threshold value for power feedback into the grid, E_{MinAbs}: threshold value for minimum charge level.

$$E_{Max}(t) = S_P(t) \cdot C_{avg,bat} \tag{4.20}$$

$$S_P(t) = S_P(t-1) + S_A(t) - S_L(t) \tag{4.21}$$

$$E_{V2G,Min}(t) = E_{Max}(t) \cdot f_{V2G}(t) \tag{4.22}$$

$$E_{MinAbs}(t) = E_{Max}(t) \cdot S_{MinAbs} \tag{4.23}$$

$$E_{Max}(t) \geq E(t) \geq E_{MinAbs} \tag{4.24}$$

where:

E_{Max} = Maximum available battery capacity in kWh_{el}
$E_{V2G,Min}$ = Threshold value for power feedback into the grid in kWh_{el}
E_{MinAbs} = Threshold value for minimum charge level in kWh_{el}
$E(t)$ = Charge level in kWh_{el}
S_P = Hourly share of vehicles plugged into a charging facility in %

S_L = Hourly share of leaving vehicles in %
S_A = Hourly share of arriving vehicles in %
S_{MinAbs} = share of battery capacity for minimum charge level in %
$C_{avg,bat}$ = average battery capacity per vehicle in $^{kWh_{el}}/_{vehicle}$
f_{V2G} = factor for Vehicle-to-Grid operation in %

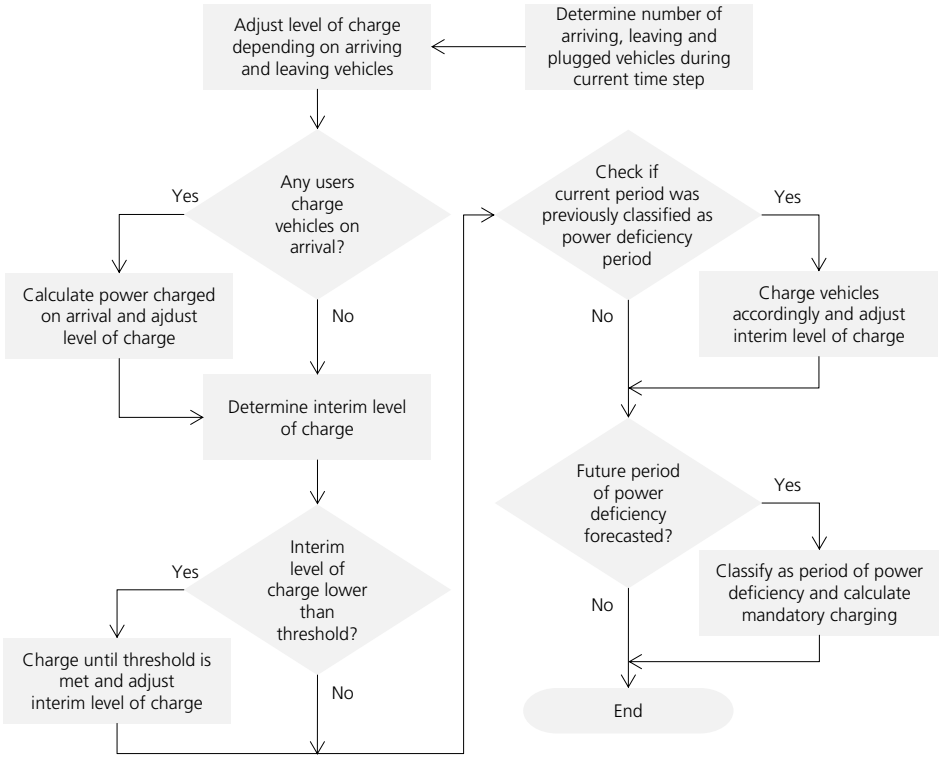

Figure 4.8: Flowchart describing the calculation of the interim charge level.

Figure 4.8 illustrates the simplified approach for the calculation of the interim charge level $E_{inter}(t)$. This charge level is calculated starting from the previous charge level $E(t-1)$ according to eq. 4.28. The interim charge level increases if arriving vehicles are plugged into a charging facility and decreases if they are disconnected (leaving vehicles). At the same time, the charge level is reduced by the term $P_E(t)$, which takes into account that the battery of arriving vehicles is less charged than it was at the beginning of their trip. Further, it is considered that a given share of vehicles gets charged as they return to the charging facility. This behaviour will be referred to as Uncontrolled Charging Strategy (UCSt). The charging of vehicles on arrival $E_{G2V,UCSt}$ is calculated according to eq. 4.25,

where the exogenously specified share of users following an UCSt is denoted by S_{UCSt}. The charging behaviour in the Controlled Charging Strategy (CCSt) is influenced by the occurring residual load. The share of users following a CCSt, S_{CCSt}, is obtained according to eq. 4.26. In this case, vehicle users try to charge their vehicles exclusively when the feed-in from non dispatchable sources exceeds the electric load, i.e. when electricity surplus occurs. Likewise, their vehicle batteries may be discharged in case of power deficiency. The underlying idea is that users try to minimize their operation costs while maximising their revenues, charging their vehicles when the electricity price is low (power surplus due to large share of VRE) and feeding power into the grid when it is comparably high (power deficiency). During prolonged periods of low feed-in from VRE, this charging behaviour may lead to a progressive decrease of the batteries charge level. Should the interim charge level $E_{inter}(t)$ be lower than the threshold value $E_{MinAbs}(t)$, then the vehicle batteries are charged to meet this threshold value. In this case, according to eq. 4.29, an additional electric load, $P_{MustCh}(t)$, is applied to the system. Relating to figure 4.7, for a resulting interim charge level equal to e, the electric load would be increased by the difference between d and e, leading to a final interim charge level of d. However, if $E_{inter}(t)$ does not violate the boundary condition set by $E_{MinAbs}(t)$, than $P_{MustCh}(t)$ is zero and the energy demand at considered time step t to power the vehicle engines is entirely met by discharging the vehicle batteries.

To avoid charging peaks during prolonged periods of power deficiency, a forecast mechanism is implemented (cf. section 4.1). This forecast calculates the expected residual load in a future time step t_{FC}, for an exogenously specified forecast period t_{FP} (cf. eq. 4.1). For each consecutive hour of predicted power deficiency, a counter is increased by one time step length Δt and set to zero otherwise. If the counter reaches an exogenously defined threshold value, then the upcoming period is classified as *period of power deficiency* (PDP). In this case, once that period begins, users following a CCSt are required to charge their vehicles on arrival. This mandatory charge $E_{ch,CCSt}$ (eq. 4.27) prevents the batteries charge level to drop when power deficiency occurs over prolonged time periods. A detailed representation of the implemented load forecast in provided in section 4.1.

$$E_{ch,UCSt}(t) = P_E(t) \cdot \Delta t \cdot S_{UCSt} \tag{4.25}$$

$$S_{CCSt} = 1 - S_{UCSt} \tag{4.26}$$

$$E_{ch,CCSt}(t) = \frac{\sum_{t=t_{FC}}^{t_{FC}+t_{FP}} P_E(t)}{t_{FP}} \cdot S_{UCSt} \qquad \forall t \in PDP \tag{4.27}$$

$$E_{inter,i}(t) = E_i(t-1) + \big(S_{A,i}(t) - S_{L,i}(t)\big) \cdot C_{avg,bat,i} + \big(P_{mustCh,i}(t)) - P_{E,i}(t)\big) \cdot \Delta t + E_{ch,UCSt,i} + E_{ch,CCSt,i} \tag{4.28}$$

$$P_{mustCh,i}(t) = \frac{E_{inter,i}(t) - E_{MinAbs,i}(t)}{\Delta t} \qquad \forall E_{inter,i}(t) < E_{MinAbs,i}(t) \tag{4.29}$$

where:

S_{UCSt} = User share following an uncontrolled charging strategy in %
S_{CCSt} = User share following a controlled charging strategy in %
S_A = Hourly share of arriving vehicles in %
S_L = Hourly share of leaving vehicles in %
PDP = Classified period of power deficiency
$E_{ch,UCSt}$ = Charging of arriving vehicles in kWh_{el}
$E_{ch,CCSt}$ = Charging in case of PDP in kWh_{el}
E_{inter} = Interim charge level in kWh_{el}
E_{MinAbs} = Threshold value for minimum charge level in kWh_{el}
P_{mustCh} = Mandatory charging in $^{kWh_{el}}/_{h}$
P_E = Final power demand of vehicles of a specific power train technology in kW_{el}
t_{FC} = Future time step for forecast [−]
t_{FP} = Forecast period [−]
$C_{avg,bat}$ = Average battery capacity per vehicle in $^{kWh_{el}}/_{vehicle}$
Δt = Time step length in [−]
i = Considered power train technology [−]

Starting from the interim charge level $E_{inter}(t)$ the vehicle battery may be operated flexibly, i.e. be charged ($P_{G2V}(t)$) or discharged ($P_{V2G}(t)$) depending on the residual load value (cf. section 3.4). Figure 4.9 illustrates the methodological approach for either case.

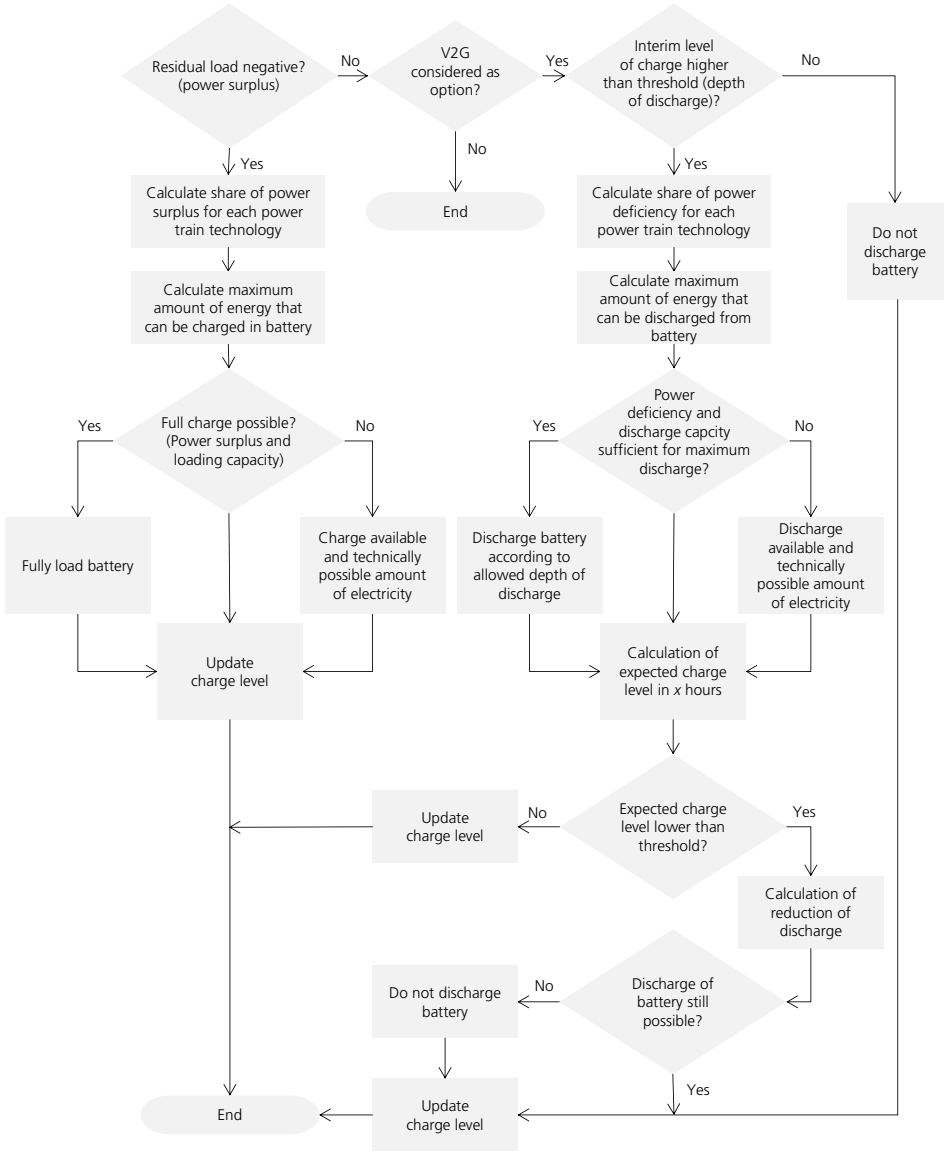

Figure 4.9: Flowchart describing the flexible operation of vehicle batteries. V2G: Vehicle-to-Grid.

Flexible Battery Charging: Grid-to-Vehicle (Power Surplus)

If at any time step the residual load happens to be negative, i.e. the feed-in from non-dispatchable sources is higher than the electric load, the batteries of the considered power train technologies may be charged. Figure 4.7 illustrates the modelled battery storage with its respective levels of charge indicated by the letters a to d. As described in eq. 4.20, the charge level of the battery can not be higher than the maximum available battery capacity $E_{Max}(t)$. Therefore, an interim charge level equal to a means that the battery is already fully charged while for all other charge levels b, c or d electricity surplus may be used to increase the occurring interim charge level. The maximum amount of electric energy that can be charged into the battery $E_{G2V,Max}(t)$ is described by eq. 4.30. This amount is further limited by the maximum charging capacity $P_{G2V,Max}(t)$, which accounts for the assumed deployment of charging facilities (as well as their type: fast or slow charging) and the total share of vehicles plugged into a charging facility (eq. 4.31). Further, η_{G2V} is utilised to account for losses related to the charging process of the vehicle battery.

$$E_{G2V,Max}(t) = E_{Max}(t) - E_{inter}(t) \tag{4.30}$$

$$P_{G2V,Max}(t) = S_P(t) \cdot P_{G2V,avg}(t) \cdot N_{veh} \tag{4.31}$$

$$P_{G2V}(t) \leq min\Big(\frac{E_{G2V,Max}}{\Delta t \cdot \eta_{G2V}}, P_{G2V,Max}(t)\Big) \tag{4.32}$$

where:

$E_{G2V,Max}$ = Maximum charge of electricity in kWh_{el}
E_{Max} = Maximum available battery capacity in kWh_{el}
E_{inter} = Interim charge level in kWh_{el}
$P_{G2V,Max}$ = Maximum charging capacity in kWh_{el}
$P_{G2V,avg}$ = Average charging capacity per vehicle in $^{kW_{el}}/_{vehicle}$
P_{G2V} = Charged power in $^{kWh_{el}}/_{h}$
S_P = Hourly share of vehicles plugged into a charging facility in %
N_{veh} = Total number of vehicles [–]
η_{avg} = Average vehicle efficiency in %
Δt = Time step length [–]

Flexible Battery Discharging: Vehicle-to-Grid (Power Deficiency)

In case of power deficiency, i.e. when the feed-in from non-dispatchable sources is lower than the electric load, the vehicle batteries may be discharged to supply power to the electrical grid. This operation mode is only possible if the interim charge level $E_{inter}(t)$ is higher than the set threshold value $E_{V2G,Min}(t)$ (eq. 4.22). This means that the power flow from the grid to vehicles (G2V) can be modelled either separately, or be considered as a combined option to the feed-in from electric vehicles into the grid (G2V and V2G).

Referring to figure 4.7, a discharge would be only possible starting from an interim charge level equal to a, while c and d are below the threshold value. As a consequence, the maximum amount of electric power which may be discharged during each time step is described by eq. 4.34. Analogous to the restrictions posed on the charging capacity, also the discharge of the battery can be restricted by the current capacity limits $P_{V2G,Max}(t)$ according to eq. 4.33 - 4.35.

Before the final charge level $E(t)$ is calculated, the algorithm provides the possibility to decrease the currently discharged electricity to reduce a possible additional electric load in upcoming time steps. Thus, the expected charge level $E_{Exp}(t+x)$ is determined according to eq. 4.36. This value accounts for the expected drop or increase of the battery charge level due to arriving or leaving vehicles in the upcoming x time steps (eq. 4.18, 4.19 and 4.28).

$$E_{V2G,Max}(t) = E_{inter}(t) - E_{V2G,Min}(t) \qquad \forall E_{inter}(t) > E_{V2G,Min}(t) \tag{4.33}$$

$$P_{V2G,Max}(t) = S_P(t) \cdot P_{V2G,avg}(t) \cdot N_{veh} \tag{4.34}$$

$$P_{V2G}(t) \leq min(\frac{E_{V2G,Max}}{\Delta t}(t), P_{V2G,Max}(t)) \tag{4.35}$$

$$E_{exp}(t+x) = E_{inter}(t) - P_{V2G}(t) \cdot \Delta t - \sum_{t}^{t+x}(S_L(t) - S_A(t)) \cdot C_{avg,bat} - \sum_{t}^{t+x} P_E(t) \cdot \Delta t \tag{4.36}$$

where:

$E_{G2V,Max}$ = Maximum discharge of electricity for feedback into the grid in kWh_{el}
$E_{V2G,Min}(t)$ = Minimum charge level for Vehicle-to-Grid operation in kWh_{el}
E_{inter} = Interim charge level in kWh_{el}
E_{exp} = Expected charge level in x hours in kWh_{el}

$P_{V2G,Max}$ = Maximum discharge capacity in $^{kWh_{el}}/_{h}$
$P_{V2G,avg}$ = Average discharge capacity per vehicle in $^{kW_{el}}/_{vehicle}$
P_{V2G} = Discharged power for feedback into the grid in $^{kWh_{el}}/_{h}$
P_E = Final power demand of vehicles of a specific power train
S_A = Hourly share of arriving vehicles in %
S_L = Hourly share of leaving vehicles in %
S_P = Hourly share of vehicles plugged into a charging facility in %
N_{veh} = Total number of vehicles [−]
$C_{avg,bat}$ = Average battery capacity per vehicle in $^{kWh_{el}}/_{vehicle}$
Δt = Time step length [−]
x = Number of upcoming time steps for forecast [−]

If the expected charge level in upcoming time steps $E_{Exp}(t+x)$ is lower than the absolute minimum charge level $E_{MinAbs}(t+x)$, the amount of discharged energy in the current time step $P_{V2G}(t)$ is reduced by $P_{Red}(t)$ according to eq. 4.37. As a consequence, the battery will be discharged less to avoid a possible additional electric load $P_{MustCh}(t)$ in an upcoming time step (eq. 4.29). For example, relating to figure 4.10, after the discharge of the battery from a to b in t_0, an expected charge level equal to c is determined in t_{0+x}. In this particular case, the discharge of the battery in t_0 is reduced by the difference between d and c, leading to a charge level equal to e instead of b. Should the determined reduction in battery discharge be higher than possible discharge itself, the battery charge level will remain unchanged. Finally, the charge level of the vehicle battery $E(t)$ is calculated according to eq. 4.38.

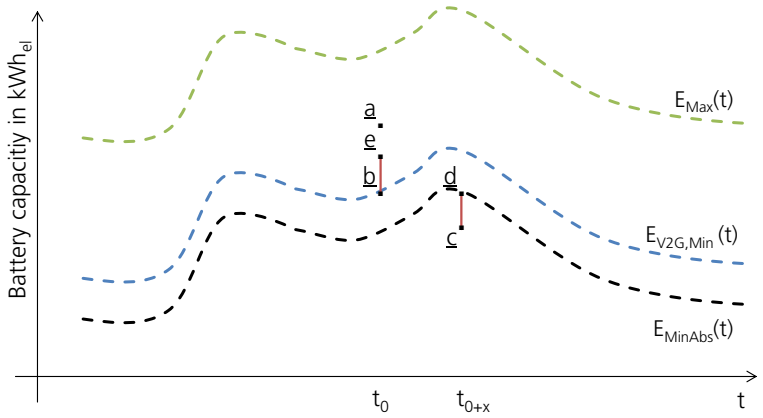

Figure 4.10: Exemplarily illustration of the functional battery storage: restrictions and charge levels for discharge of vehicle battery. E_{Max}: maximum available battery capacity, $E_{V2G,Min}$: threshold value for power feedback into the grid, E_{MinAbs}: threshold value for minimum charge level.

$$P_{red}(t) = \frac{E_{MinAbs}(t+x) - E_{exp}(t+x)}{\Delta t} \tag{4.37}$$

$$E(t) = E_{inter}(t) + (P_{G2V}(t) - P_{V2G}(t) + P_{red}(t)) \cdot \Delta t \tag{4.38}$$

where:

E_{exp}	= Expected charge level in x hours in kWh_{el}
E_{inter}	= Interim charge level in kWh_{el}
E_{MinAbs}	= Threshold value for minimum charge level in kWh_{el}
P_{red}	= Reduction of discharged power in $^{kWh_{el}}/_{h}$
P_{V2G}	= Discharged power for feedback into the grid in $^{kWh_{el}}/_{h}$
P_{G2V}	= Charged power in $^{kWh_{el}}/_{h}$
Δt	= Time step length [−]
x	= Number of upcoming time steps for forecast [−]

4.3.2 Discussion of the Model Extension

In this section, a novel approach for the modelling of BEVs and PHEVs in REMod was presented. The methodology accounts for different driving profiles and charging strategies, as well as the option to operate vehicle batteries flexibly.

Vehicle users are classified according to whether they follow a Controlled or an Uncontrolled Charging Strategy (CCSt and UCSt). The UCSt implies that the vehicles are charged at their return to a charging facility. Conversely, in the CCSt the charging preferably takes place in times of power surplus, i.e. when the feed-in from non-dispatchable sources is higher than the electric load. Further, in times of power deficiency, the vehicle batteries may be discharged, depending on an exogenously set depth of discharge. This parameter can be specified on an hourly basis, thus providing more room for the design of the CCSt. Further, a forecast is utilised to predict prolonged time periods of power deficiency. During such periods, a mandatory vehicle charging for users following a CCSt is implemented. Thus, a substantial drop of the vehicle batteries charge level and a possibly resulting load peak can be avoided.

While the introduced modelling approach accounts for physical restrictions of vehicle batteries, it does not consider further costs for their flexible operation. This additional option is included within the purchase price of the electric vehicle itself. Thus, the deterioration of the vehicle batteries due to increased charging cycles or associated transaction

costs are neglected. In order to address this concern, additional costs should be considered at the model parametrisation[3].

Besides the motorised road transport sector, also technologies for the supply of space heat and domestic hot water could contribute to the balancing of the residual load. Through their combination with TES, the individual operation modes can be adjusted and excess heat be stored accordingly. This provides the conditions for a Heat-Controlled or Power-Controlled Strategy of heat generators. The modelling approach for its consideration in REMod is presented in detail in the next section.

4.4 Grid-Supportive Heat Generation

The introduction of digitisation represents one major objective of the German Government's Energy Research Programme to meet climate protection targets [182]. As a consequence, the rollout of smart meters is being gradually enforced, primarily for users with a higher power consumption and thus a higher flexibility potential. For instance, since 2017, bulk consumers with an annual power consumption above 10 MWh_{el} are obligated by law to install a smart meter. From 2020 on, this also applies for private costumers with an annual consumption of above 6 MWh_{el} [183]. Through intelligent infrastructure and real-time communication, the operation of heat generators, such as electric heat pumps (HP) or micro-CHP units and fuel cells, can be adjusted. As a consequence, consumers progressively become prosumers and therefore actors within the energy market. However, to achieve this, various obstacles have to be addressed, such as educational work, data security, freedom of choice, fair cost distribution, social innovation as well as the lacking economic efficiency [37, 184].

In order to assess the technical potential or rather the effects resulting from a flexible or non flexible operation of heat generators with REMod, an according methodology is developed. A flexible operation presumes an according smart meter rollout. Thus, whenever possible, heating systems are operated according to the residual load (Power-Controlled Strategy, PCSt). Conversely, in the non flexible operation, a purely heat-controlled operation is implemented. The chapter closes with a discussion of the presented model extension.

4.4.1 Operating Principle and Grouping of Heat Generators

As described in section 3.2.4, in total twelve distinctive heating systems for the supply of space heat and domestic hot water are considered in REMod. Each system consists of one or multiple heat generators, which may be supplemented by a solar thermal system

[3] An according sensitivity analysis is presented in chapter 6.2.2.

and TES. The storage unit includes a heating rod, which in case of power surplus may convert electric power into heat, increasing the storage temperature. Similarly, electric heat pumps may adjust their current heat generation capacity and therefore contribute to the balancing of the electric load. Conversely, the operation of combined heat and power systems may be increased when power deficiency occurs and thus raise the overall supply of electricity. In this case too, the additionally generated heat is stored in TES and may be used in a future time step to meet the occurring heat demand. The described flexible operation of heat generators assumes a Power-Controlled Strategy (PCSt). This means that, whenever possible, heat generators are utilised depending on the hourly residual load value. It is also possible to consider a Heat-Controlled Strategy (HCSt), where the operation of heat generators is based on the sole supply of the occurring heat demand. Overall, this strategy better reflects the present-day standards.

Whether a heating system should follow a PCSt or HCSt, i.e. a flexible or inflexible operation, can be specified exogenously. This condition may be adjusted for each year from 2015 until 2050 as the model is parametrised. Further, instead of specifying the flexible behaviour for each individual technology, they are grouped into nine categories. These categories, together with the associated technologies and their respective case of application, are summarised in table 4.1.

Table 4.1: Grouping of heat generators for the supply of space heat and domestic hot water demand. In group 8, micro CHP and fuel cells are excluded. CHP: combined heat and power, HG: heat generators (oil, gas and wood boiler as well as gas heat pump)

Nr	Heating System	Affected Technology	Increases
1	Decentralised electric HP	Brine and air HP	Load
2		Heating rod	Load
3	Decentralised CHP	Micro-CHP and fuel cell	Supply
4		Heating rod	Load
5	Heat grid	CCGT	Supply
6		Large scale air heat pump (HP)	Load
7		Heating rod	Load
8	Decentralised fuel-based HG	Heating rod	Load
9	Decentralised hybrid HP	Heating rod	Load

As introduced in section 3.2.4, each heating system in REMod needs to provide for a specific part of the hourly heat demand. The respective share depends on the endogenously determined technology deployment. How each heat generator is operated may, in turn, vary within each time step, depending on if a HCSt or a PCSt is considered. An overview of the possible operation modes is illustrated in figure 4.11.

In case of a HCSt, all heating systems are operated in the same way: first, solar thermal systems can be provided to charge the TES, which is in turn utilised to meet the hourly

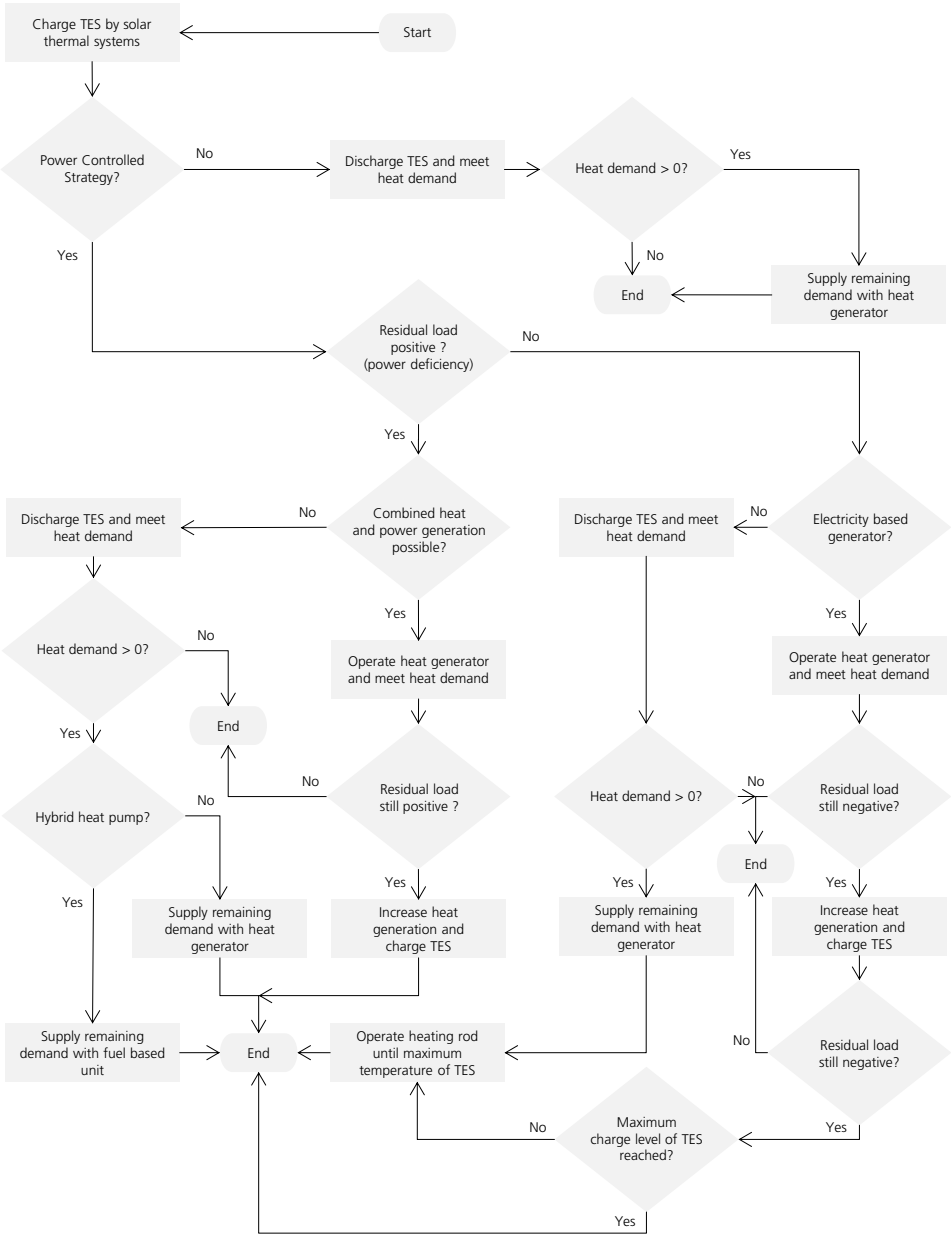

Figure 4.11: Flowchart describing the operation for each heat generator considered in REMod for the supply of space heat and domestic hot water. In case of a Power-Controlled Strategy the operation is adjusted according to the residual load value.

heat demand. A possibly remaining demand is supplied by the electricity or fuel-based heat generator. This can for instance be represented by an electric heat pump or a gas boiler. The operation becomes more complex, if a PCSt is considered instead, as it further depends from the residual load value. In case of power deficiency, all technologies with combined production of heat and power, are operated until their respective share of heat demand is met. At this point, if the residual load is still positive, their generation capacity is increased until either their nominal capacity or the maximum TES temperature of 95 °C is reached. In case of CCGT in heat grids, an additional operation mode is considered, in which the plants are actively cooled and excess heat is wasted. For all other heat generators, where no CHP operation is possible, the TES is first discharged. This mechanism leads to a reduction of the hourly heat demand and thus, in case of electricity-based generators, to a smaller increase of the electric load. Further, when power deficiency occurs, hybrid heat pumps may be switched from an electricity-based to a fuel-based operation.

In case of power surplus, all non electricity-based heat generators first discharge the TES to reduce their hourly heat demand as much as possible. This mechanism ensures that the power generation from CHP units is limited and thus does not lead to a further increase of the already occurring power surplus. Conversely, all electricity-based heat generators, such as electric heat pumps, are operated to meet their share of heat demand. If the residual load is still negative, their generation capacity is further increased and the excess heat stored in the TES. This process can either be restricted by the nominal generator capacity or its maximum supply temperature. If this temperature is not reached and the residual load is still negative, then heating rods may be utilised as further load balancing option. The conversion of power into heat by heating rods is available for all heating systems, if they are equipped with TES. Compared to the operation of heat pumps, heating rods exhibit a lower conversion efficiency, but also allow to increase the TES temperature until 95 °C. While this leads to higher losses due to the increased temperature level, it also provides an additional load balancing capacity.

4.4.2 Discussion of the Model Extension

As of today, technologies for the supply of space heat and hot water demand are mostly operated in a heat-controlled way (HCSt). However, an increasing share of VRE and thus more frequent fluctuations of the residual load could lead to a switch in favour of a PCSt. The introduced approach allows the consideration of a HCSt and a PCSt by specifying the desired mode for each year from 2015 to 2050. Thus, it is possible to analyse the effects coming from an early or delayed adaptation of a PCSt or a business-as-usual case, for which a HCSt is considered. However, due to the utilised perfect foresight approach, a delayed adaptation of a PCSt might have a rather small influence

on the results. Hypothetically, the deployment of flexible heat generators might start early on, in the knowledge that their operation mode will be changed to a PCSt in the upcoming years. This, presuming that a PCSt is beneficial for the entire energy system (cf. section 6.3).

It is noted that within each simulated year either a PCSt or HCSt must be specified. Thus, a simultaneous consideration of both options where one part of the heat generators follows a PCSt and the other a HCSt is not possible. However, this only applies within each one of the specified groups. For instance, decentralised heat pumps may follow a HCSt, while large scale heat pumps, in heat grids, may be set on a PCSt. The developed methodology allows to change between these two strategies for nine designated technology groups, instead of for each individual heat generator. While this leaves out some combinations, the implemented grouping provides a wide variety of analysis options.

Another possibility to balance the residual load is represented by the exchange of electricity with countries bordering Germany. Subsequently, a simplified approach for its consideration in REMod is introduced.

4.5 Cross-border exchange of electricity

In 2018, the electricity imports from neighbouring countries to Germany amounted to roughly 9 TWh_{el}, while its exports totalled approximately 68 TWh_{el} [22]. While the exchange of electricity between countries represents a further option to balance the residual load, its characteristics substantially differ from other flexible technologies. First of all, the availability of electricity exchange varies over time, depending on the power load and generation capacity in neighbouring countries. Second, the limit for the exchange of power is determined by the interconnector capacity and therefore by the expansion of the electrical grid. These points are accounted for in a simplified approach. First, the utilised data base and its processing for the calculation of a power supply curve, representing Germany's bordering countries, is described. In the second part, two import options are introduced. The optional import of electricity accounts for restrictions of the available exchange capacity, if the current power supply in neighbouring countries is relatively low. Conversely, if it is particularly high, a mandatory power flow to Germany is considered. Finally, strengths and weaknesses of the implemented methodology are highlighted and discussed.

4.5.1 Data Processing and Power Supply Curve

The consideration of electricity imports in REMod is based on the feed-in from solar and wind power stations of countries bordering Germany. They include Denmark, Poland, Czech Republic, Austria, Switzerland, France, Luxembourg, Belgium and Netherlands. The assumption made is that each of those countries, to reduce their GHG emissions, will further expand their share of VRE. Thus, whenever their feed-in from VRE is low, the available import capacity share in Germany is reduced. Conversely, it is increased when a high feed-in from VRE in neighbouring countries occurs. For the determination of the power supplied by VRE over all neighbouring countries at a particular time step t, an aggregated feed-in profile is constructed. For this purpose, the installed capacities of VRE and their hourly capacity factors of each neighbouring country are considered. Figure 4.12 illustrates the countries bordering Germany as well as the installed capacity of VRE from 2010 to 2015.

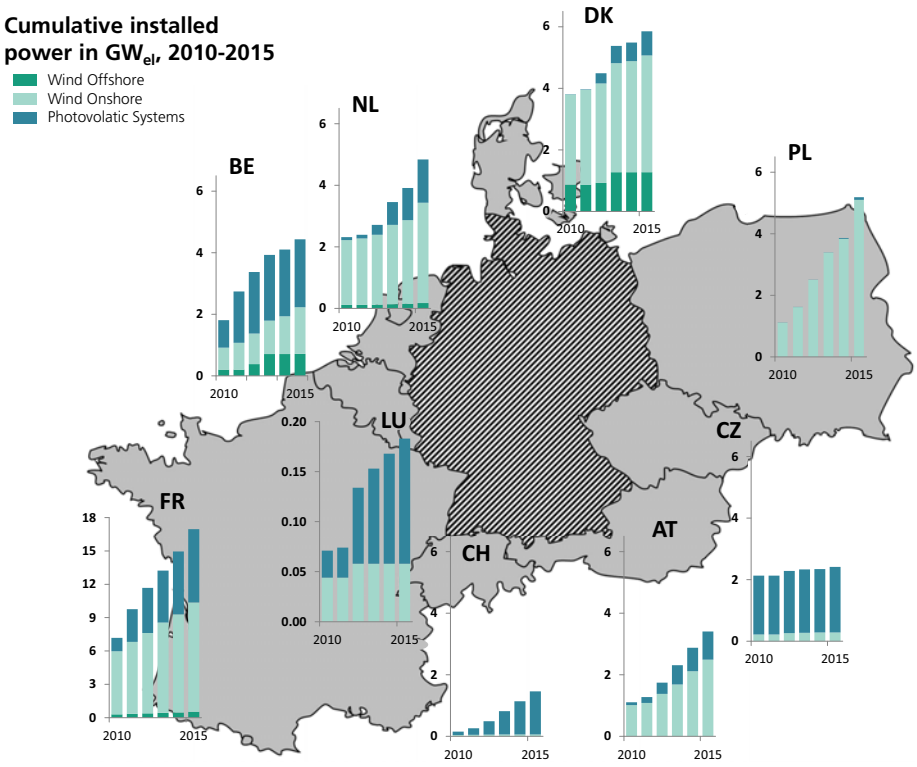

Figure 4.12: Installed capacity of main VRE sources of countries bordering Germany from 2010 to 2015. For the countries France and Luxembourg a different scaling of the y-axis is used. Own illustration based on [185–200].

The capacity factors of wind and photovoltaic power stations are derived from the renewables.ninja platform, which provides simulated values, taking into account 30 years of validated hourly reanalysis and satellite data [163]. The database includes all countries in the EU-28 plus Norway and Switzerland for the years 1985 until 2016 [164, 201]. The capacity factors $f_{C,VRE}$ are weighted according to the proportion of VRE installed in all neighbouring countries (w_N, eq. 4.39) as well as by the share of each VRE technology within one country (w_{VRE}, eq. 4.40). Here, c represents the countries bordering Germany, while i describes the considered VRE technology, i.e. photovoltaic power stations, onshore or offshore wind turbines. The observed weather data set is denoted by j and may be based on one of the years from 2011 to 2015 (cf. section 5). The result described in eq. 4.41 is an aggregated, normalised power supply profile $P_{norm,VRE}$ representing the nine countries bordering Germany.

$$w_{N,c,i,j} = \frac{P_{Nom,VRE,c,i,j}}{\sum_{c=1}^{N_{NC}} P_{Nom,VRE,c,i,j}} \tag{4.39}$$

$$w_{VRE,i,j} = \frac{\sum_{c=1}^{N_{NC}} P_{Nom,VRE,c,i,j}}{\sum_{i=1}^{N_{VRE}} \sum_{c=1}^{N_{NC}} P_{Nom,VRE,c,i,j}} \tag{4.40}$$

$$P_{norm,VRE,j}(t) = \sum_{i=1}^{N_{VRE}} \sum_{c=1}^{N_{NC}} f_{C,VRE,c,i,j}(t) \cdot w_{N,c,i,j} \cdot w_{VRE,i,j} \tag{4.41}$$

where:

$P_{Nom,VRE}$ = Installed capacity of VRE technology in kW_{el}
$P_{norm,VRE}$ = Aggregated, normalised power supply profile over neighbouring countries [−]
w_N = Weighting factor for VRE share over all neighbouring countries [−]
w_{VRE} = Weighting factor for each VRE technology within one country [−]
$f_{C,VRE}$ = Hourly capacity factors for each VRE technology [−]
N_{NC} = Number of neighbouring countries [−]
N_{VRE} = Number of considered VRE technologies [−]
j = Considered weather data set (2011 to 2015) [−]
c = Country bordering Germany [−]

Figure 4.13 shows the obtained power supply profiles for each of the five considered years (2011 to 2015). These curves describe weighted averaged quantities over all nine countries bordering Germany. This means that at a particular time step t, the feed-in from VRE in a specific country c might be higher than the value of $P_{norm,VRE}(t)$, while being lower in others.

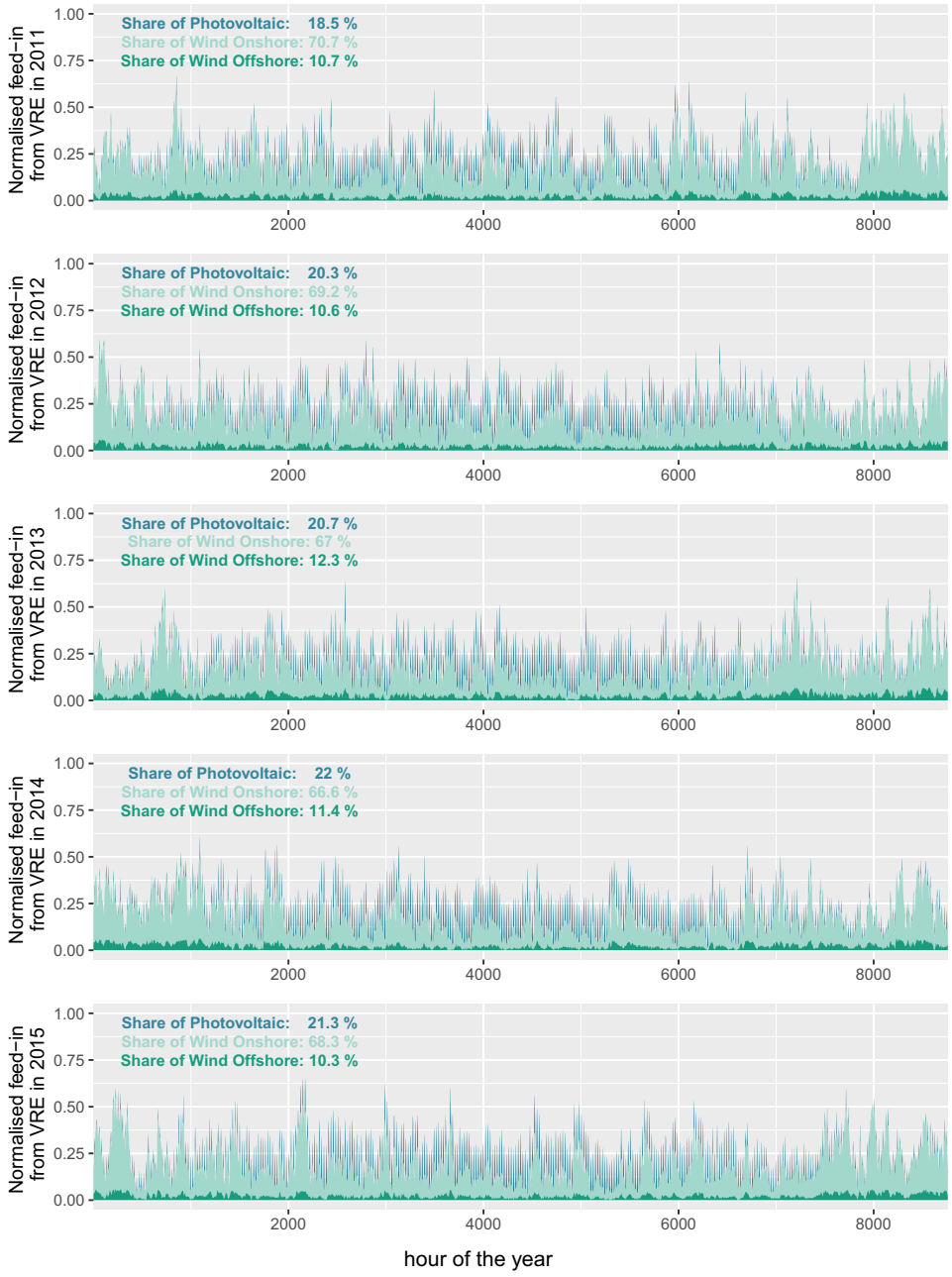

Figure 4.13: Normalised power supply profiles for photovoltaic systems, onshore and offshore wind power stations for Germany's neighbouring countries and five weather data sets for the years 2011 to 2015.

The curves shown in figure 4.13 provide insight about the power supplied by VRE during each time step over all neighbouring countries. For instance, a value of $P_{norm,VRE}$ equal to 0.3 would suggest that the current feed-in amounts to 30 % of the cumulative installed capacity. This share, combined with the assumed interconnector capacity, is used to define the available amount of electricity that can be imported in Germany during a given time step t. Thus, by increasing the yearly interconnector capacity between Germany and its bordering countries, a proportional expansion of VRE in these countries can be considered. In 2015, the interconnector capacity P_{IC}, amounted to approximately 20 GW_{el} [202].

4.5.2 Mandatory and Optional Import of Electricity

The methodical approach for the determination of the available import capacity is illustrated in Figure 4.14. The graph shows an exemplarily progression of the previously determined power supply curve $P_{norm,VRE,j}$, with its value on the primary axis. The secondary axis describes the available interconnector capacity share in percent of P_{IC}, which may be used for the import of electricity. Two threshold values, l_m and l_o, delimit the graph in three sections, grouped into mandatory and optional import.

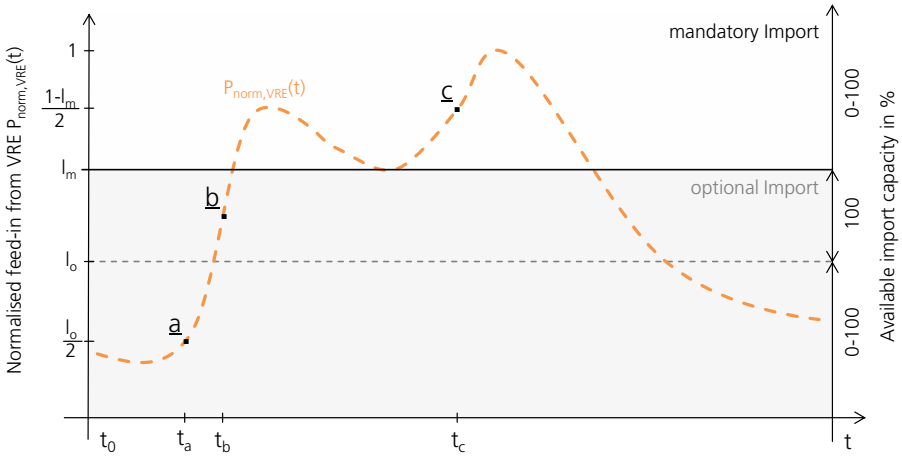

Figure 4.14: Methodological approach for the consideration of cross-border electricity exchange with Germany's neighbouring countries. l_m: threshold value for mandatory import, l_o: threshold value for optional import.

The optional import condition area in figure 4.14 ranges from a value of $P_{norm,VRE,j}$ of zero until the limit for mandatory import l_m. As long as the aggregated power supply curve lies within this area, electricity can be imported from neighbouring countries to

balance the occurring positive residual load. If $P_{norm,VRE}(t)$ is equal or superior than the threshold value for optional import l_o, then the maximum available quantity of electricity import is equal to the assumed interconnector capacity P_{IC}. In the case that $P_{norm,VRE,}(t)$ happens to be lower than l_o, the available import capacity is reduced in a linear ratio between $P_{norm,VRE,}(t)$ and l_o as described in eq. 4.42. For instance, with regard to figure 4.14, at the time t_a (a), the available interconnector capacity is halved, while it is fully available in b ($P_{norm,VRE}(t_b)$). The mandatory import condition area ranges from values of $P_{norm,VRE}(t)$ equal to the threshold value for mandatory import l_m until one. Whenever the aggregated feed-in profile from VRE lies within this area, a specific amount of electricity is imported. This allows to consider that particularly high power generation from VRE in neighbouring countries might lead to a likelier exchange of electricity. In the case of mandatory import, electricity can not be exported from Germany to its neighbouring countries.

The mandatory import of electricity provides an option to balance the residual load if power deficiency occurs. If power surplus occurs, the imported electricity could be used to charge TES, power storage systems or to be converted into synthetic fuels via Power-to-Gas technologies. Conversely, the optional import serves exclusively to balance the residual load in times of power deficiency. The amount of the mandatory import $P_{MI}(t)$ is obtained according to eq. 4.43 and eq. 4.44 and mainly depends on the set threshold value l_m as well as on the aggregated power supply profile $P_{norm,VRE}(t)$. Referring to figure 4.14 at the time t_c (c), the mandatory import yields to half of the assumed interconnector capacity P_{IC}.

$$P_{OI,j}(t) = \frac{l_o - P_{norm,VRE,j}(t)}{l_o} \cdot P_{IC} \qquad \forall\, P_{norm,VRE,j}(t) \in [0; l_o[\tag{4.42}$$

$$p_{MI,j}(t) = \frac{(P_{norm,VRE,j}(t) - l_m)}{1 - l_m} \qquad \forall\, P_{norm,VRE,j}(t) \in]l_m; 1] \tag{4.43}$$

$$p_{MI,j}(t) = {}^{P_{MI,j}(t)}/_{P_{IC}} \tag{4.44}$$

where:

P_{IC} = Assumed interconnector capacity in kW_{el}
P_{OI} = Available optional import capacity in kWh_{el}
p_{MI} = Specific mandatory import in ${}^{kWh_{el}}/_{kW_{P_{IC}}}$
P_{MI} = Mandatory import in kWh_{el}
l_o = Threshold value for optional import [−]
l_m = Threshold value for mandatory import [−]

Figure 4.15 shows the correlation between the mandatory import P_{MI}, the interconnector capacity P_{IC} and the threshold value for mandatory import l_m.

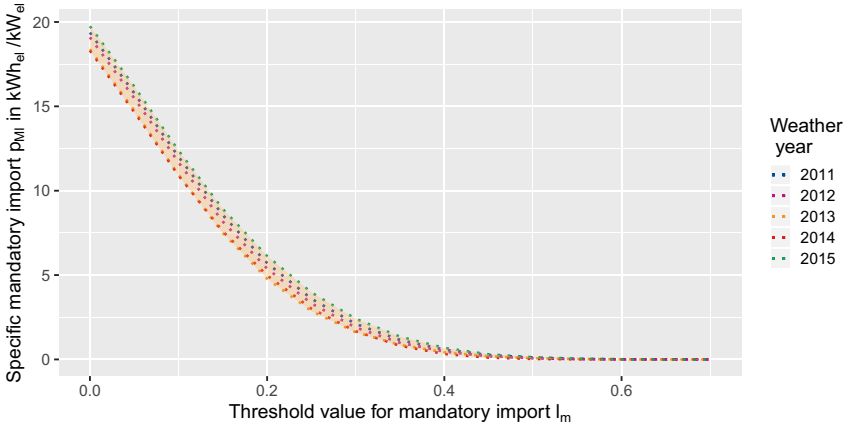

Figure 4.15: Specific mandatory import of electricity p_{MI} depending on the threshold value for mandatory import l_m and the considered weather data (2011 to 2050).

According to eq. 4.44, the forced yearly amount of electricity imported in Germany is obtained by multiplying the set interconnector capacity P_{IC} and the specific mandatory import value p_{MI}. For example, a threshold value l_m equal to 0.2 would lead to a yearly mandatory electricity import of approximately five times the assumed interconnector capacity P_{IC}. Figure 4.15 shows that the values of p_{MI} vary slightly depending on the considered weather data. On average, they are highest for the year 2015 and lowest for 2013 and 2014. While the values of p_{MI} for a mandatory threshold value lower than 0.3 are within a range of approximately ± 1.5, the differences get progressively reduced afterwards. The higher the set threshold value, the less hours meet the requirement of mandatory import and the greater the similarity between the five years. Table 4.2 summarises during how many hours per year the respective aggregated VRE power supply profile is higher than the set mandatory import threshold value l_m.

Table 4.2: Hours of mandatory import depending on the considered weather data and on the threshold value for mandatory import l_m.

	Weather data of year				
l_m	2011	2012	2013	2014	2015
0	8760	8760	8760	8760	8760
0.05	8717	8713	8699	8656	8744
0.10	7823	7949	7843	7602	7977
0.15	6223	6253	5992	5749	6239
0.20	4542	4345	4158	4157	4527
0.25	3053	3003	2626	2765	3196
0.30	1886	1779	1529	1698	2029
0.35	1075	1018	817	927	1226
0.40	576	492	442	436	679
0.45	261	225	200	159	310
0.50	120	81	72	39	133
0.55	46	30	32	11	52
0.60	13	0	12	2	18
0.65	3	0	2	0	0
0.70	0	0	0	0	0

4.5.3 Discussion of the Model Extension

The exchange of electricity with neighbouring countries represents one option to balance the residual load. For its consideration in REMod a novel approach was developed. It is based on the assumption that, to meet the climate protection targets, all countries bordering Germany will further increase their installed capacities of VRE. For simplification purposes it is further assumed that the hourly available import capacity in Germany correlates with the residual load profile of its bordering countries, which in turn depends on the respective power generation from VRE. Thus, whenever the feed-in from VRE in Germany's bordering countries is low, the available import capacity share is reduced and increased otherwise.

While the residual load and the power supply from VRE correlate, their isolated consideration is not sufficient for the determination of the available import capacity. It would be more accurate to model each country bordering Germany as well as the transformation of its energy system. This would require a comprehensive database of each sector and country as well as the extension of REMod from a single to a multi node model. These adjustments would substantially increase the complexity of the problem as well as the necessary computational time of each model run. In contrast, the introduced modelling approach represents an approximate solution which considers a time dependent variation of the available import capacity (depending on the utilised weather data) without requiring the modelling of each single country. Further, this approach enables the adjustment of the interconnector capacity in every simulated year until 2050. Thus,

it is possible to indirectly account for the expansion of VRE in Germany's bordering countries. Additionally, the threshold values for optional and mandatory import allow the assessment of different study cases. For example, a conservative scenario could assume an unvaried interconnector capacity as well as particularly high threshold values. Further, the mandatory import case opens new pathways for the usage of power. For instance, instead of balancing a positive residual load, the mandatory import might also be used in times of power surplus and be stored into batteries or converted into synthetic fuels. The modelling of power storage systems and Power-to-Gas/Power-to-Liquid plants is presented in the next section.

4.6 Power Storages and Production of Synthetic Fuels

Today, in Germany and Europe, the large-scale storage of power is almost exclusively performed by pumped-storage plants. As a consequence of relatively long payback times as well as reasons of public acceptance, their expansion potential seems rather limited [203, 204]. This is one reason why the research for alternative storage options is being promoted [182]. For instance, batteries provide a viable solution for the short- to mid-term storing of power. Alternatively, by converting surplus electricity from VRE into synthetic fuels, it may be possible to cover the energy demand over extended time periods. Synthetic methane gas could be stored in tanks or be added to the gas network. This, to a certain degree, also applies to synthetic hydrogen, which otherwise can be stored into underground cavern storage facilities [205]. Similarly, tailor made fuels via Power-to-Liquid technologies (PtL) can be generated based on electricity, utilising the already existing infrastructure for storage. The generated synthetic fuels might contribute to the emission reduction of those sectors of the energy system, where a complete technological reorientation may be hard to achieve under today's economic and political structures. This, for instance, applies to aviation, where liquid fuels with a high energy density are utilised. Another example concerns the usage of hydrogen in the industrial sector, which in Germany amounts to roughly 50 TWh per year [206, 207]. Typical applications are the production of fertilisers (ammonia synthesis) [208] or refinery processes (hydrocracking) [206]. The basis for the generation of synthetic fuels is provided by electrolysis plants. Due to the high ramping rates and short response times of electrolysis plants (cf. section 5), they can provide a major contribution to load balancing. In the following section, first the modelling approach of power storages and then of PtG and PtL technologies is presented.

4.6.1 Modelling Approach

Power Storage Systems

In REMod, three distinctive types of power storages are considered, namely stationary batteries, pumped-storage power plants as well as batteries in electric vehicles. The latter are presented in section 4.3 and may be used either only in case of power surplus (G2V, Grid-to-Vehicle) or also when power deficiency occurs (V2G and G2V). Pumped-storage plants can be operated in both cases. Their deployment, however, is not endogenously determined, which means that their storage capacity, input and output capability are set exogenously for each year from 2015 to 2050. Conversely, the storage capacity of stationary batteries is determined as a result of the optimisation [103]. Its charging and discharging capacity is calculated according to eq. 4.47, where C denotes the assumed capacity factor. Further, for each battery type, individual charging losses can be determined by an exogenously set efficiency (eq. 4.45). Its value may vary over the total observation period and thus consider technology improvements.

$$E_{SOC,bat}(t) = \left(E_{SOC,bat}(t-1) + E_{ch,bat}(t) \cdot \eta_{bat} - E_{dis,bat}(t)\right) / \Delta t \tag{4.45}$$

$$E_{ch,bat}(t) / \Delta t \leq P_{ch,max} \tag{4.46}$$

$$P_{ch,max} = C \cdot E_{bat} \tag{4.47}$$

where:

$P_{ch,max}$	=	Maximum charging (or discharging) capacity in kW_{el}
E_{bat}	=	Battery storage capacity in kWh_{el}
$E_{SOC,bat}$	=	Battery level of charge in kWh_{el}
$E_{ch,bat}$	=	Power charged in battery in kWh_{el}
$E_{dis,bat}$	=	Power discharged from battery in kWh_{el}
η_{bat}	=	Charging efficiency in %
C	=	Capacity factor of stationary battery in h^{-1}
Δt	=	Time step length in h

Electrolysis Plants

The operation of electrolysis plants in REMod can be distinguished in two cases. The first case describes the coverage of the hourly hydrogen demand, while the second case is based on the value of the residual load. Both operation modes are illustrated in figure 4.16.

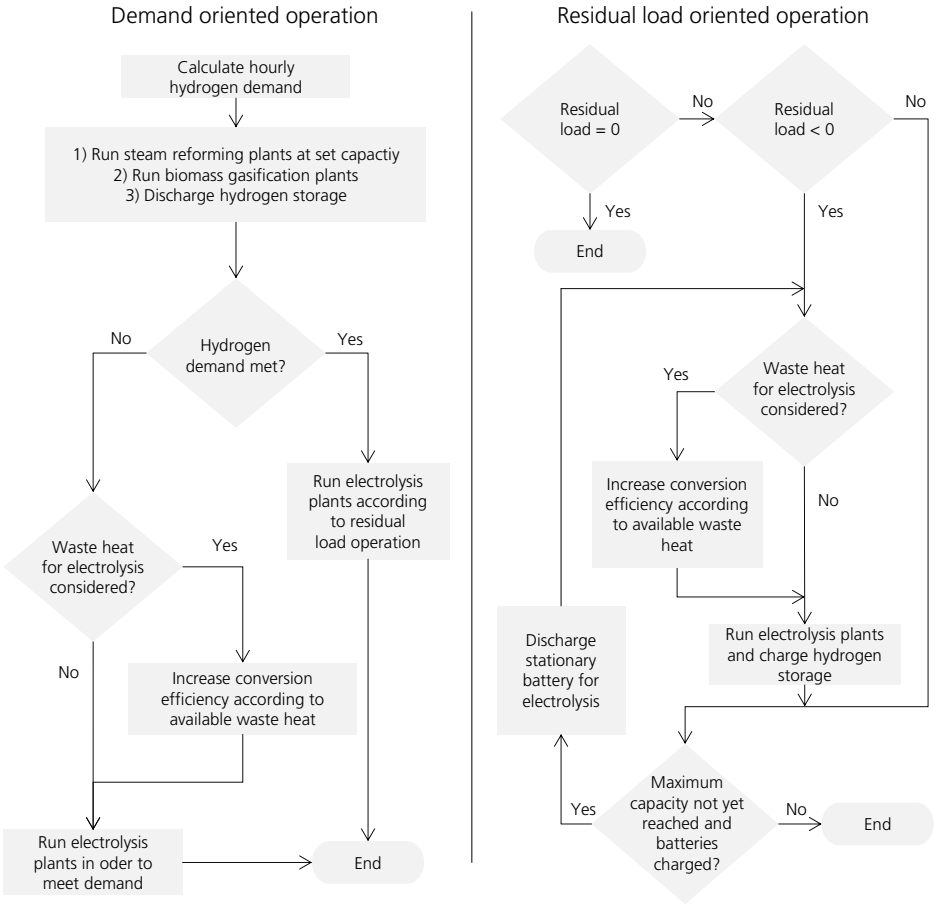

Figure 4.16: Flowchart describing the considered operating modes of electrolysis plants in REMod: demand and residual load oriented operation.

The demand oriented operation is designed in a way to ensure that the hydrogen demand $E_{H_2,d}$ is met at every hour. It is calculated according to eq. 4.48, as a result of the hydrogen demand resulting from the motorised road transport sector $E_{H_2,RT}$, the supply of space heat and domestic hot water $E_{H_2,SH}$ and the supply of process heat $E_{H_2,PH}$. Further, an additional quantity ($E_{H_2,ex}$) can be specified exogenously. This term can be used to account for a non energy-related demand of hydrogen, such as for the production

of fertilizers or for refinery processes in the industrial sector. To meet the calculated hydrogen demand, steam reformation plants are continuously operated according to a set must-run capacity. The respective hydrogen production $E_{H_2,SR,min}$ is obtained as shown in eq. 4.49, where $P_{SR,nom}$ denotes their nominal capacity, η_{SR} the plants efficiency and $S_{min,SR}$ the minimum utilisation share.

$$E_{H_2,d}(t) = E_{H_2,RT}(t) + E_{H_2,SH}(t) + E_{H_2,PH}(t) + E_{H_2,ex}(t) \tag{4.48}$$

$$E_{H_2,SR,min} = \left(P_{SR,nom} \cdot \eta_{SR} \cdot S_{min,SR}\right) \cdot \Delta t \tag{4.49}$$

where:

$E_{H_2,d}$	= Hourly hydrogen demand in kWh_{H_2}
$E_{H_2,RT}$	= Hourly hydrogen demand of the motorised road transport in kWh_{H_2}
$E_{H_2,SH}$	= Hourly hydrogen demand for space heat and hot water in kWh_{H_2}
$E_{H_2,PH}$	= Hourly hydrogen demand for the supply of process heat in kWh_{H_2}
$E_{H_2,ex}$	= Exogenously set hydrogen demand in kWh_{H_2}
$E_{H_2,SR,min}$	= Must-run hydrogen production from steam reformation plants in kWh_{H_2}
$P_{SR,nom}$	= Nominal capacity of steam reformation plants in kW_{CH_4}
η_{SR}	= Conversion efficiency of steam reformation plants in %
$S_{min,SR}$	= Must-run capacity share of steam reformation plants %
Δt	= Time step length in h

The remaining hydrogen demand is then met by a discharge of hydrogen storage. The storage can be charged by three different options. The first option is provided by a gasification of biomass and subsequent conversion into hydrogen (cf. section 3.4). The second option is the import of synthetic fuels (section 3.5) and the third option is the residual load oriented operation of electrolysis plants (cf. figure 4.16). If the hydrogen supply from the storage system is not sufficient to meet the occurring demand, electrolysis plants are operated. In this case, they are run independently from the residual load value. Thus, if power deficiency occurs, the electric load is further increased and must possibly be covered by thermal power plants.

The second operation mode of electrolysis plants is based on the residual load value. Whenever the residual load is negative, electrolysis plants might be run to balance the occurring surplus of electricity (cf. section 3.4). If the maximum production capacity of the plant is not reached, a dedicated stationary battery can be discharged to increase the hydrogen output. This operation mode may also occur when the residual load is positive. The hydrogen produced according to a residual load oriented operation is, as

previously mentioned, directly charged into the hydrogen storage system. The hydrogen discharged from the storage may either be used to cover the hourly hydrogen demand or to be reconverted into electricity by gas turbine power plants.

The conversion efficiency of the electrolysis plant can be increased if the utilisation of waste heat from the industrial sector is considered [112]. This is only possible for high-temperature steam electrolysis plants. If considered, the characteristics of these plants as well as the usable waste heat potential have to be specified exogenously at the model parametrisation[4].

Besides the hydrogen production through electrolysis plants, two further options for the production of synthetic fuels are implemented. Methanation plants are modelled similarly to electrolysis plants. In this case, a demand oriented operation is not considered, as an occurring methane gas demand can be covered by the import of natural gas. Hydrogen reacts with carbon dioxide to produce methane gas in a process known as Sabatier reaction (eq. 4.50). Another difference concerns the concurrent generation of waste heat (exothermic reaction), which is utilised for the supply of low temperature process heat.

$$CO_2 + 4\,H_2 \longrightarrow CH_4 + 2\,H_2O \tag{4.50}$$

The second option is represented by PtL plants. Here, similarly to the methanation process, carbon monoxide and hydrogen are converted into liquid hydrocarbons according to the Fischer-Tropsch process. The necessary carbon for both processes is extracted from ambient air. The conversion efficiencies of PtG and PtL plants are exogenously set for each year from 2015 to 2050. These technologies may be subjected to ramping behaviour[5] as explained in detail in section 4.2.

4.6.2 Discussion of the Model Extension

Power storage systems in REMod are operated according to the residual load, i.e. they are charged whenever power surplus occurs and vice versa. Similarly to home storage solutions, they do not take the duration of the surplus or deficiency period into account. Thus, an additional battery could be introduced and its operation linked to the developed load forecast proceeding (cf. section 4.1). This would lead to a more uniform charging or discharging behaviour and therefore complement the currently implemented battery

[4] A study concerning the synergies of high-temperature electrolysis plants and waste heat from the industrial sector based on REMod calculations is presented in [112]

[5] The effect of ramping behaviour is negligible for polymer electrolyte membrane electrolysis plants and more substantial if high-temperature steam electrolysis plants are considered instead.

system. The same applies to PtG and PtL technologies which are mainly operated when power surplus occurs.

The carbon dioxide required for the methanation process is provided by an additional air separation plant. However, it is more likely that the carbon dioxide is first obtained from biogas plants, the chemical industry (bioethanol production) or coal power plants with carbon capture and storage. The consideration of this sector coupling effects may lead to new insights regarding the benefits of the mentioned technologies. Further, the conversion of surplus electricity into synthetic fuels might, to a certain degree, reduce the otherwise necessary expansion of the electrical grid. However, due to the single-node approach of the model, on this regard only qualitative statements can be made.

This chapter presented the methodological approaches for the consideration of load balancing options in REMod. In the next chapter the main assumptions and parameter setting are introduced. Thereafter, based on a series of model calculations, the flexibility of various technologies within the energy system is assessed.

5 Model Parametrisation

This chapter describes the main input parameters utilised in REMod. It is divided into four sections. The first section introduces the characteristics of systems with a non-predetermined total amount through the example of photovoltaic power stations. In this context a distinction between different technology potentials is presented. For the introduction of systems with a predetermined total amount, in the second section, electrical air heat pumps are chosen as an example. Further, the calculation of their hourly coefficient of performance is outlined. The third section first addresses hourly resolved time series through the example of the driving behaviour in the motorised private road transport, followed by other main input parameters, such as the availability of energy carriers and their prices, the ramping behaviour of energy conversion plants as well as the parametrisation of meteorological data. Based on the input data, the model is calibrated for the year 2015. The evaluation is dependent on the supply of process heat, generation of power and energy-related CO_2 emissions. Lastly, the obtained results compared to literature values and any discrepancies are discussed.

5.1 Systems with Non-Predetermined Total Amount

As introduced in section 3.2, the components and technologies considered in the model are distinguished between systems with a non-predetermined or with a predetermined total amount. Technologies belonging to systems with a non-predetermined total amount, such as VRE, thermal power plants, PtG plants or energy storages do not belong to a specific sector of the energy system. Their maximum deployment is restricted by an exogenously set expansion potential. This potential is distributed over the time period from 2015 to 2050, in order to account for limitations in manufacturing capacities, the number of available craftsmen or the diffusion of a new component [209]. Thus, a gradual expansion of each technology, rather than a complete exploitation of the set expansion potential within one year is ensured. A distinction between different technology potentials is subsequently outlined.

As shown in figure 5.1, the maximum available potential of a technology is defined by its theoretically available potential [210–212]. In case of VRE, this would result from meteorological and geographic circumstances. A subset thereof is the technical potential

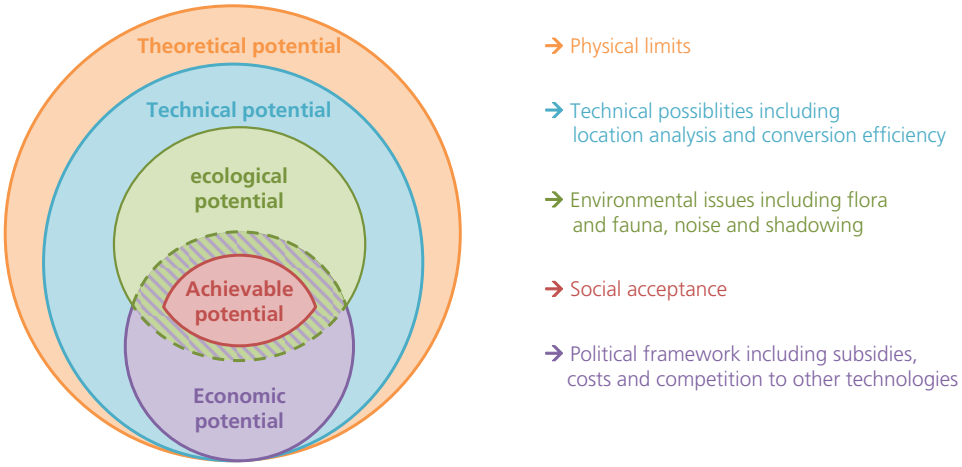

Figure 5.1: Disambiguation of technology potentials. For the model parametrisation the ecological potential is considered unless otherwise specified. Own illustration based on [210–212].

which represents its technically usable share and accounts for technical factors, like the conversion efficiency or the analysis for suitable locations. Environmental limitations, deriving from proximity to nature reserves, conservation of nature and environment are considered by the ecological potential. The economic potential accounts for energy-political conditions, which for instance include subsidies, taxes or CO_2 prices as well as other parameters such as competing alternative options, the amortisation period or the equity share. Finally, the achievable potential results as a subset from the overlap between the ecological and the economic potential. Thus, it accounts for technical, ecological and economic limitations as well as other inhibiting factors, such as the social acceptance of a technology. If not otherwise specified, the technology expansion limit in REMod is based on the definition of the ecological potential. Other potentials may be considered depending on the study focus. For instance, to account for limitations in the market share of a specific technology due to social acceptance or political guidelines. Table 5.1 shows the assumed input parameters for photovoltaic stations. The first two rows describe their minimum and maximum expansion potentials.

Besides the discussed potential limits, each technology is characterised by its purchase price, the technical service life, its costs for maintenance and operation, the imputed interest, the rate for purchase as well as for maintenance and operation. Each of these parameters is yearly adjustable for the whole time period from 2015 to 2050, which means that the learning curve of each technology is not linked to its deployment. The full load hours of photovoltaic power stations are not included in table 5.1, as they indirectly result from the hourly weather conditions described in section 5.3. However,

Table 5.1: Input parameters for photovoltaic power stations from 2015 to 2050 in steps of five years. M & O: maintenance and operation in % from purchase price. f_{VLH}: factor for adjustment of full load hours. Data based on [22,113,213,214] and own assumptions.

Photovoltaic stations		2015	2020	2030	2040	2050	total
min potential	GW_{el}	1.32	0	0	0	0	5.1
max potential	GW_{el}	1.32	10	15.75	15.75	15.75	530.0
purchase price	€/kWh_{el}	1166	976	718	597	571	/
service life	years	25.1	25.6	26.6	27.6	28.7	/
imputed interest	%	7.0	7.0	7.0	7.0	7.0	/
M & O	%	2.0	2.0	2.0	2.0	2.0	/
r_Invest	%	1.7	1.7	1.7	1.7	1.7	/
r_Invest	%	1.7	1.7	1.7	1.7	1.7	/
f_{VLH}	-	0.9	1.0	1.0	1.0	1.0	/

they may be increased or decreased in each year to consider technology improvements or the exploitation of less favourable locations otherwise.

5.2 Systems with Predetermined Total Amount

Conversely to systems with a non-predetermined total amount, technologies belonging to systems with a predetermined total amount are limited by sector-specific boundaries. As introduced in section 3.2, they are represented by (i) the number of buildings for heat generators utilised to supply space heat and domestic hot water, (ii) by the number of vehicles in the motorised road transport sector and (iii) by the maximum process heat load for heat generators providing process heat demand. The number of buildings in Germany is set to approximately 25 millions in 2015 and increases to almost 27 millions by 2050 [215–217]. The development of the motorised road transport is based on [218–220], which was commissioned by the Federal Ministry of Transport, Innovation and Technology. Lastly the maximum heat load for the supply of process heat is calculated according to [123, 124, 131]. While the useful energy process heat demand can be adjusted on a yearly basis, it is set constant over the whole time period[1]. This is due to the assumption that efficiency enhancements are counterbalanced by a growth of the industrial sector.

Within each system with a predetermined total amount, the deployment of a specific component may vary between zero and 100 %, except if technological restrictions need to be considered. This, for instance, applies to electric heat pumps for the supply of process heat demand, which due to their supply temperatures can cover the resulting process heat demand only up to a certain degree or supply temperature level (cf. section 3.2.3). Further, the market share of each technology may be limited depending on the intended

[1] Further values are included in appendix A.

study focus. Thus, it is possible to account for limitations deriving from a low social acceptance, political guidelines or other inhibiting factors. Table 5.2 provides an overview of the main input parameters for an electrical heat pump.

Table 5.2: Exemplarily input parameters for an electric air heat pump system from 2015 to 2050 in steps of five years. The maximum market share is exemplarily set to 50 %. PH: Panel heating as heat transfer system. Data based on [103, 113, 221–223].

Electric air heat pump (PH)		2015	2020	2030	2040	2050
min potential	%	0	0	0	0	0
max potential	%	50	50	50	50	50
Purchase price	€/kWh_{th}	975	900	815	725	640
service life	years	20	20	20	20	20
imputed interest	%	7.0	7.0	7.0	7.0	7.0
M & O	%	1.0	1.0	1.0	1.0	1.0
r_Invest	%	1.7	1.7	1.7	1.7	1.7
r_Wartung	%	1.7	1.7	1.7	1.7	1.7
a_{COP}	-	6.14	6.14	6.14	6.14	6.14
b_{COP}	10^{-2}	-9.73	-9.7	-9.7	-9.7	-9.7
c_{COP}	10^{-4}	5.30	5.30	5.30	5.30	5.30

Based on [103], the coefficient of performance of electric heat pumps is described by characteristic performance curves. This means that the relation between the heat delivery and the necessary operating power is represented as a function of the difference between the source and the sink temperature. The source temperature for air heat pumps depends on the outside ambient temperature, where for brine heat pumps the ground temperature is assumed to be constant at 10°C [170]. Figure 5.2 shows the coefficient of performance as a function of the temperature difference between the source and sink for the described systems. [106]

The sink temperature depends from the respective time step. The hourly inlet temperature is calculated from the weighted average space heat and hot water demand. The curve for electrical air heat pumps illustrated in figure 5.2 is obtained from measurement campaigns, conducted at Fraunhofer ISE ([221–223]). Gas driven heat pumps are still considered to be at the research stage. Thus, the available data was complemented by an expert survey and an approximated curve for the coefficient of performance drawn [103]. [106]

While the conversion efficiency of air heat pumps is defined as a potential function, for most other technologies it is described by a specific value (cf. appendix A.5). As shown in eq. 5.1, the efficiency of a technology is calculated for each year as weighted average over the already existing stock and the new deployments. For example, if the number of BEVs in a particular year amounts to 1.2 million units with an average efficiency of 60 % and in the following year 200 thousand of these vehicles reach their service life,

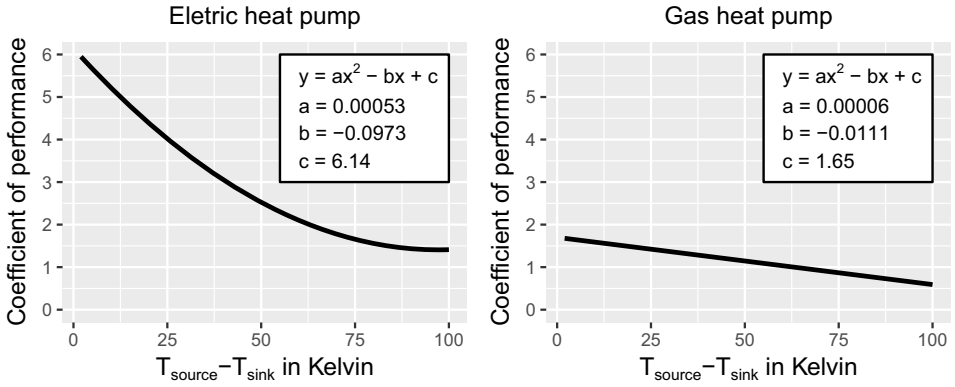

Figure 5.2: Function of the coefficient of performance for electrically driven and gas driven heat pumps depending on the difference between the source and the sink temperature. Illustration based on [103].

this results in one million BEVs with a fleet efficiency of 60 %. If at the same time one million new BEVs are deployed, with an efficiency of 70 %, this would lead to an overall fleet efficiency of 65 %.

$$\eta_{avg,i}(a) = \frac{(n_i(a) - n_{N,i}(a)) \cdot \eta_{avg,i}(a-1) + n_{N,i}(a) \cdot \eta_{N,i}(a)}{n_i(a)} \tag{5.1}$$

where:

η_{avg} = Average conversion efficiency of technology stock in %
n = Number of units
n_N = Number of newly deployed units
η_N = Average conversion efficiency of newly deployed units in %
a = Considered year
i = Considered technology

All parameters presented so far are utilised for the characterisation of model components on a yearly basis. The next section introduces the structure of time series, which serve for the description of interannual effects.

5.3 Time Series and Further Parameters

Hourly resolved input parameters mainly describe data linked to meteorological conditions, such as the outside temperature, the solar radiation or the feed-in profiles from VRE. Accordingly, all entries are defined for all five weather years considered in the model

(2011 to 2015). Further, they include the demand profiles of the electricity baseload, the low temperature supply of process heat, the supply of domestic hot water as well as power generation profiles of nuclear power plants. Another time series concerns the description of the motorised road transport sector, which contains driving profiles as well as hourly resolved constraints for the modelling of the vehicle battery (cf. section 4.3).

As an example, figure 5.3 shows a weekday and weekend day during winter, describing the driving behaviour of private electric vehicles. This also includes the average state of charge of vehicle batteries after each trip, as well as the allowed discharge depth in case of a power feedback into the electrical grid (Vehicle-to-Grid operation).

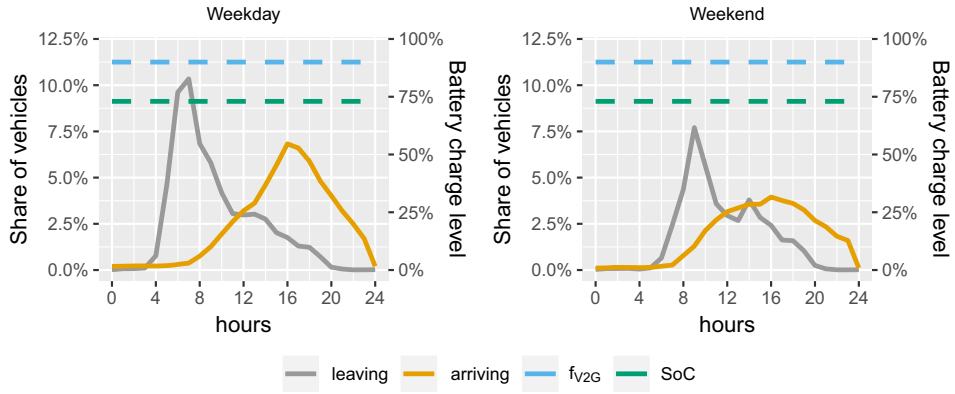

Figure 5.3: Driving profiles for the motorised private road transport for an exemplarily weekday and weekend day. The primary axis describes the hourly share of vehicles arriving at or leaving from the charging facility. The secondary axis (dashed lines) accounts for the State of Charge (SoC) and the factor for Vehicle-to-Grid operation (f_{V2G}) relative to the battery charge level. Both are assumed as constant values within the depicted time period.

The illustrated driving profiles result from an assessment of real driving patterns of today's passenger vehicles based on [224]. Assuming an average battery size of 50 kWh_{el}, allows a driving range of roughly 330 km. This distance is per day reached by less than 1 % of all vehicles in Germany. As a simplification it is assumed that the effect of charging at public fast chargers or high power charging stations is rather low. Thus, the utilised vehicle profiles account for vehicle charging taking place at home. The methodological approach for the derivation of the utilised driving profiles is described in detail in [105]. As for the driving behaviour of the freight traffic, it is based on traffic counts performed by the Federal Highway Research Institute [225, 226]. In the following paragraphs an overview of relevant model input parameters is provided. Further data is included in appendix A.

Availability of Energy Carriers and Prices

The main boundary condition for the identification of the model solution is represented by the CO_2 reduction target. An upper threshold value can be specified for each year from 2015 to 2050. It describes the available quantity of energy-related CO_2 emissions, which may at maximum be emitted during each year. This approach ensures that the set climate protection goal is not only met in 2050, but also over the entire time period. The maximum emission levels per year are calculated by linear interpolation between the CO_2 emission level today and the set reduction target in 2050.

Similarly, fossil fuel prices may be set for each year. However, they are assumed as constant values over the entire observation period according to [109]. For the import of synthetic energy carriers a cost degression due to technological progress according to [113] is considered. The calculation considers all expenses resulting from the production of power and its conversion into synthetic fuels via PtG and PtL plants in North African regions as well as their transport by tankers to Germany. An overview of the price development of different energy carriers is presented in table 5.3.

Table 5.3: Development of energy carrier prices from 2015 to 2050 in time steps of five years. Values in €/MWh based on [109, 113]. PP: power plant.

in €/MWh	2015	2020	2025	2030	2035	2040	2045	2050
Natural gas	23.0	23.0	23.0	23.0	23.0	23.0	23.0	23.0
Fossil liquid fuels	51.0	51.0	51.0	51.0	51.0	51.0	51.0	51.0
Hard coal	13.1	13.1	13.1	13.1	13.1	13.1	13.1	13.1
Lignite	1.5	1.5	1.5	1.5	1.5	1.5	1.5	1.5
Power from nuclear PP	30.0	30.0	30.0	30.0	30.0	30.0	30.0	30.0
Solar process heat	96.7	88.9	81.7	75.1	69.0	63.4	58.3	53.6
Import of hydrogen	312.5	274.8	241.7	212.6	186.9	164.4	144.6	127.1
Import of methane	480.8	423.3	372.6	328.0	288.8	254.2	223.8	197.0
Import of liquid fuels	562.9	498.3	441.1	390.4	345.6	305.9	270.8	239.7

The yearly maximum availability of energy carriers from 2015 to 2050 is summarised in table 5.4. For imported synthetic fuels it is set according to [113]. As for biomass a fixed maximum quantity is considered, based on [12].

Ramping Behaviour of Thermal Power Plants and PtG Plants

The input parameters for the description of ramping behaviour of thermal power plants are based on [60, 173, 174, 227–232]. Within the identified literature the definition of specific parameters may vary. For instance, the indicated cold start-up time refer to a plant stand still of at least 48 hours in [60], while to 24 hours in [228]. Thus, only values corresponding to the specifications made in section 4.2 are considered (for instance, a cold

Table 5.4: Availability of biomass, divided in woody biomass, cultivation biomass and organic biomass, as well as of imported synthetic fuels (hydrogen, methane and liquid fuels) from 2015 to 2050 in time steps of five years. Values in $^{TWh}/_{year}$ based on [12, 113] and own assumptions.

in TWh	2015	2020	2025	2030	2035	2040	2045	2050
Woody biomass	42	42	42	42	42	42	42	42
Biomass cultivaiton	131	131	131	131	131	131	131	131
Organic biomass	120	120	120	120	120	120	120	120
Import of hydrogen	150	350	550	700	850	1000	1000	1000
Import of methane	150	350	550	700	850	1000	1000	1000
Import of liquid fuels	150	350	550	700	850	1000	1000	1000

start is defined as a plant stand still of at least 48 hours). The data basis concerning PtG and PtL plants is based on [112,227]. Due to the short start-up times, the high ramp rates and the small amount of available data, for polymer electrolyte or alkaline electrolysis plants the efficiency decrease resulting from partial load operation is neglected[2]. For high temperature electrolysis plants, the methodology is slightly different, as the hourly efficiency is calculated depending on the operating mode and the possible utilisation of industrial waste heat. The approach is documented in detail in [112]. Table 5.5 exemplarily shows the standard dataset utilised in the model for the consideration of ramping behaviour of four selected thermal power plants. The parameters of other technologies are included in appendix A.2.

Table 5.5: Ramping input parameters of thermal power plants and Power-to-Gas (PtG) or Power-to-Liquid (PtL) plants based on [60, 173, 174, 227–232]. h_{CS}: cold start time, h_{HS}: hot start time, P_{Min}: minimum load capacity, S_{PL}: conversion efficiency in partial load related to maximum efficiency, E_S: energy demand for heat-up per installed plant capacity, R_{RR}: ramp rate.

	Year [-]	h_{CS} [h]	h_{HS} [h]	h_{PL} [h]	P_{Min} [$\%_{PNom}$]	S_{PL} [$\%_{\eta Nom}$]	E_S [kWh_{th}/kW]	R_{RR} [$\%/min$]
HardCoal PP	2017	7.88	2.44	0.36	33.50	97	2.70	3.05
	2030	7.13	2.18	0.32	30.75	97	2.70	3.58
	2050	6.38	1.92	0.29	28.00	97	2.70	4.10
Lignite PP	2017	9.00	5.00	0.50	55.00	97	2.70	1.50
	2030	7.81	3.75	0.32	47.60	97	2.70	2.70
	2050	6.88	3.00	0.30	42.20	97	2.70	3.20
CCGT	2017	3.50	1.25	0.31	45.00	93	2.80	3.00
	2030	3.00	0.91	0.21	44.11	93	2.80	4.38
	2050	2.50	0.73	0.17	43.21	93	2.80	5.50
Gas turbine	2017	0.18	0.18	0.09	45.00	83	0.10	10.00
	2030	0.14	0.11	0.08	36.07	83	0.10	12.55
	2050	0.13	0.10	0.08	33.93	83	0.10	13.40

[2]The available capacity and the electricity demand for the start-up process are considered in both cases.

Based on [233], minimum operating times for a cost-efficient plant operation are considered. They amount to four hours for CCGT and hard coal plants and to six hours for lignite power plants. These threshold values are utilised in the forecast routine introduced in section 4.1, to determine if the expected duration of consecutive plant operation is sufficiently long. If it is, the plant may be heated up in advance and thus be operative once necessary (cf. section 4.2). As will be shown in section 6.1.3 this mainly depends on the consecutive hours of power deficiency, which in turn are heavily influenced by the underlying weather year. In the next paragraph different approaches for their consideration are presented.

Parametrisation of Meteorological Data

By performing model calculation with multiple weather years instead of one, REMod identifies an energy system which can cope with differing weather influences. This means that the resulting system configuration is more robust to changes resulting from meteorological conditions, such as variations in the outside temperature, the solar radiation on more generally, the feed-in profiles from VRE.

For each year (2015-2050) calculated in REMod, a specific weather year is utilised. Which one of the five weather years depends on the respective parametrisation. In this work three approaches are utilised. The first considers a fixed sequence of weather years from 2015 to 2050 as shown in figure 5.4. This sequence was determined randomly and is maintained unchanged for most of the model calculations presented in section 6. The reason why is to ensure a comparability between different model calculations. Thus, whenever the model results for a specific year of two or more model calculations are compared with each other, the underlying weather conditions will be identical. For instance, with regard to figure 5.4, in 2050 the utilised weather year would be based on real weather data of 2014.

The second approach describes a manual adjustment of the weather vector. This method can be utilised to test the robustness of the model results against differing weather years, or simply to verify operational variations resulting from different weather conditions. This approach is applied in section 6.1.3, where the operation mode of thermal power plants is assessed.

In the third method a randomised weather vector is generated within each function call[3]. This means that the optimisation will be performed against continuously changing weather conditions. One major advantage of this approach is that the identified energy system is insensitive to variations of the meteorological conditions, at least within the

[3] Each optimisation run performs approximately one million function calls. The exact number may however vary depending on the individual convergence pattern (cd. section 3.3.2).

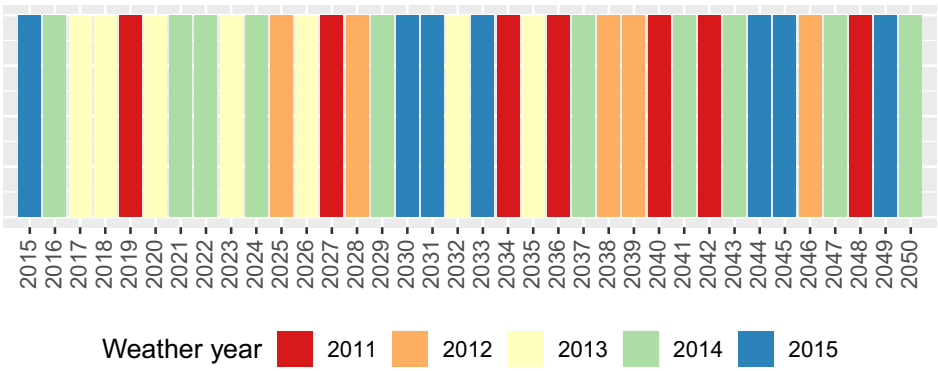

Figure 5.4: Randomly generated weather vector describing which weather year is utilised at what year of the observation period.

five considered weather years. A calculation based on this approach is presented in section 6.4.2. Regardless of which one of the three introduced methods is chosen, the model calculations in 2015 are always based on the related weather year. Since it represents the most recent year in the model for which real weather data is implemented, it is utilised to calibrate the model.

5.4 Model Calibration

Model results can not exactly represent reality, as they entail uncertainty resulting from multiple assumptions and simplifications. For energy system models, one option to assess their accuracy is the comparison of their output with a reliable database. For Germany, such data is provided by the Federal Ministry of Economics and the Federeal Environment Agency, documenting energy flows, energy consumption, CO_2 emissions and further quantities [123, 234].

In order to keep deviations between the model results and this data as low as possible, REMod is calibrated after each major extension. For this purpose three areas are analysed in detail. First, the supply of process heat, as it was changed within this work. Second, the emission factor for electricity, which indirectly provides insight about the dimensioning and operation of all electricity supplying and demanding technologies. Third, the overall energy-related CO_2 emissions. They are of particular interest since their reduction represents the main boundary condition for the transformation of the German energy system.

Calibration of the Process heat supply

The parametrisation of this sector presumes that each heat generator is attributed its share of demand within the low and high temperature range. In order to make the data from [123] comparable to REMod results, their structure needs to be adjusted accordingly. Further, since the technologies and energy carriers considered in REMod represent only a part of the options available in reality, simplifying assumptions have to be made. This for example concerns the utilisation of lignite and hard coal boilers for the supply of heat, which in the model are not distinguished. Instead, they are grouped into hard coal fired boilers as they occur more frequently in Germany [123]. Another example is the usage of firewood, fuel peat, sewage sludge, waste and waste heat summarised as „others“ in the BMWi database [123]. This category in the model is best represented by biomass boilers which the largest part of it (90 %) is assigned to. Further the maximum heat supply temperature of each technology have to be taken into account (cf. section 3.2.3). Biomass for example, is supposed to be used only in the low temperature range, i.e. below 500 °C. This means that 4.5 % of the overall process heat demand (coal for iron production excluded) have to be shifted to the low temperature area, yielding to roughly 10 %. Another example concerns the deployment of oil based heat generators which in the model are considered by boilers, neglecting industrial oil fired CHP plants. At the present state, they are mainly operated by gas or coal and only to a small degree (less than 4 % [123]) by oil, suggesting a rather small error. Nonetheless, their fuel demand is added to those of oil boilers, slightly increasing their share and yielding to a total consumption of 18.7 TWh in 2015. Lastly, the largest part of the category „renewables“ is allocated to electricity, while solar thermal systems is attributed a share of 5 %.

As a result of the mentioned assumptions, the literature values are made compatible with the result structure of REMod. Thus, the technology distribution for the low and high temperature segment in 2015 is determined. If the conversion efficiency of each technology is taken into account, this leads to conversion factor of final to useful energy equal to 83.6 % (cf. section 3.2.3). Table 5.6 shows the final energy consumption for the supply of process heat in Germany in 2015, categorised by energy carriers considered in REMod. This includes the values based on literature data as well as those resulting from the simulation within the REMod model after the model calibration.

Despite the fact that compared to reality the number of technologies considered in the model is significantly reduced, a good compliance between the literature data and the model results is achieved. The total energy demand in both cases is equal, while individual differences on average amount to 4 %. The only exception is solar thermal heat. However, with less than 0.2 % of the total energy demand it plays a minor role in 2015.

Table 5.6: Final energy consumption in TWh for the supply of process heat in 2015. Database is made compatible witch the structure of REMod.

	Database	REMod results		
	[123, 235]	sum	≤ 480 °C	> 480 °C
Mineral oil	18.7	17.1	7.2	9.9
Gas	264.2	280.7	141.9	138.8
Electricity	110.1	98.3	41.5	56.8
Coal	118.3	117.6	5.3	112.3
Biomass	17.2	17.1	17.1	0.0
Solar thermal heat	1.4	1.0	1.0	0.0
Sum	531.7	531.7	214.0	317.7

Calibration of the Power generation

With a contribution to the total energy-related CO_2 emissions of roughly 40 %, the power generation sector plays an important role in the transformation of the German energy system [236]. For its calibration the installed capacity of all power generators as well as the full load hours of photovoltaic and wind power stations are adjusted according to [22, 214]. Table 5.7 shows a comparison between literature values and model results in 2015 for the installed capacities as well as for the power generation categorised by technology or energy source.

Table 5.7: Installed capacity in GW_{el} and power generation in TWh_{el} in 2015 according to literature values and model results, categorised by technology or energy source. Database values derived from [22, 214]

	Capacity in GW_{el}		Energy in TWh_{el}	
	Database	REMod	Database	REMod
Solar Power	39.2	39.2	38.7	38.7
Wind Offshore	3.3	3.3	72.2	72.3
Wind Onshore	41.3	41.3	8.3	8.3
Hydro	5.5	4.7	18.8	17.0
Biomass	7.2	7.2	47.0	17.6
Lignite	21.4	21.1	139.4	138.8
Hard coal	28.7	27.8	106.2	106.5
Oil	4.2	4.2	0.0	0.0
Nuclear	10.8	10.8	86.8	86.8
Gas	28.4	32.9	30.1	68.9

Table 5.7 shows a good concordance with regard to the installed capacities of power generators for the year 2015, differing on average less than 1 %. This also applies for most of the described electricity production. An exception is represented by biomass and gas, exhibiting disparities between the model results and [22] of 30 TWh_{el} and -39 TWh_{el}, respectively. These differences suggest that the definitions utilised in [22] and REMod for the delimitation of biomass might not be uniform. In REMod gas represents a mix

of different sources, including natural gas, synthetic fuels, hydrogen and also biogas. Conversely, it is assumed that in [22] biogas is allocated to biomass. As a consequence more gas and less biomass is used in REMod and vice versa. In fact, [237] shows that in 2015 31.3 TWh_{el} were generated from biogas, explaining the difference displayed in table 5.7.

Based on the power generation and the corresponding fuel consumtion determined by the model results, an emissions factor for electricity equal to 0.521 kg_{CO_2}/kWh_{el} is determined. Compared to the literatur value provided by the Federeal Environment Agency of 0.534 kg_{CO_2}/kWh_{el} ([238]) this yields to a difference of roughly 2 %. Both emissions factors are obtained without consideration of the upstream chain.

Calibration of the Energy-related CO_2 Emissions

The energy-related CO_2 emissions represent the main boundary condition in REMod. According to [236], in 2015 they were reduced by 26 % compared to 1990 values, yielding to 732.6 million t_{CO2}. With 715 million t_{CO2} the model results are slightly lower, suggesting a reduction of 27.8 % compared to 1990 values. The missing amount of roughly 18 million t_{CO2} can for the most part be traced back to missing technology options in the model for the supply of space heat and domestic hot water. In 2015, this end-use sector exhibited energy demand of roughly 16 TWh_{th}, which was met by electricity based technologies [123]. It is assumed that night storage heaters and flow heaters in 2015 represented the largest share of electricity demanding technologies. Both are not considered in REMod. Taking this difference into account and factoring in the emissions factor for electricity of 2015, this yields to 8.54 billion t_{CO2}. Similarly, 11 TWh_{th} of heat demand in this sector were covered by coal, leading to further 4.43 billion t_{CO2} emissions. By counting in these factors 728 billion t_{CO2} are determined, differing from [236] by roughly 0.5 %.

Summary and Conclusion

Due to model simplifications and assumptions the results obtained with REMod for the year 2015 can not exactly reproduce literature values. Still, it is shown that by calibrating the model the occurring differences can significantly be reduced. This is the case for the supply of process heat, were the consumption of all main energy carriers on average diverges from literature values by 4 %. An even better compliance was obtained with regard to the generation of electricity and the energy-related CO_2 emissions, differing from literature values by less than 2 % each. It was shown that the differences mainly

arise due to the lack of coal boilers, night storage and flow heaters. While this leads to an inaccuracy of the energy-related emissions of 1.7 % in 2015, the impact on the transformation of the German energy system, with a time horizon of 2050, is estimated to be low. In an optimised energy system, those technologies would most likely be replaced by less polluting options with higher efficiencies, such as gas boilers or heat pumps. Overall, the calibration process described in this section shows a good correlation between the model results and the values found in literature. This provides a sufficiently accurate starting point for the investigation of years following 2015.

6 Results

The aim of this chapter is twofold: to provide a deeper understanding of the main modelling extensions (cf. section 4) and to provide an assessment of load balancing options in Germany. In section 6.1 model calculations with and without the consideration of ramping behaviour are performed. Additionally, power plant operation under variation of weather data and ramping characteristics is analysed. As a consequence, the impacts resulting from the consideration of ramping behaviour are assessed. In section 6.2.3, the value of DSM in the road transports is analysed. First, the role of alternative power train technologies is presented. Then, BEVs are investigated in more detail, including the effects resulting from an uncontrolled or a controlled vehicle charging. The utilisation of DSM for the generation of heat is investigated in section 6.3. This includes a study of heat generator deployment and their operation in case of a Heat-Controlled or Power-Controlled Strategy. DSM for BEVs and for heat generators is analysed with regard to uncertainties linked to technology deployment and weather data in section 6.4. In the last section, a cost evaluation of DSM for five CO_2 reduction targets and the possibility to import synthetic fuels from abroad is laid out. As a result, a qualitative and quantitative assessment of DSM from various viewpoints is provided.

6.1 Flexibility of Thermal Power Plants

In this section, the role of thermal power plants in an energy system with an increasing share of VRE is analysed. First, a comparison of the optimisation results obtained with and without the consideration of ramping behaviour is presented (cf. section 4.2). Here, differences and similarities in the resulting system configuration are highlighted. Further, based on time series of the supply and demand of electricity, the operation of thermal power plants is analysed. Afterwards, two sensitivity analyses are performed. The first analysis investigates the power plant utilisation and its yearly conversion efficiency under variation of the underlying weather data. The second analysis accounts for uncertainties in the assumed ramping characteristics. The chapter closes with a short summary of the key findings and a critical appraisal of the results.

6.1.1 Impact of Ramping Behaviour on the System Configuration

In this section, the optimisation results obtained with and without considering the ramping behaviour of thermal power plants are compared with each other. The analysis is performed for two distinctive CO_2 reduction targets. Previous studies have shown that this parameter may substantially influence the obtained results [18,107,113]. At first, differences in the configuration of the end-use sectors are assessed. Afterwards, an analysis of other relevant power supply and storage components is presented.

For comparing the end-use sectors of the energy system, two indicators are introduced. The first, denoted by Δ_{2050}, provides insight about differences in the final composition of each sector, i.e. its configuration at the end of the observation period in 2050. It is determined according to eq. 6.1, where n describes the total number of units per technologies T per sector. Conversely, the indicator Δ_{Path} accounts for deviations from 2015 to 2050 (eq. 6.2). Table 6.1 summarises the respective values of Δ_{2050} and Δ_{Path} for a CO_2 reduction target of 85 % and 90 % compared to 1990 levels. The optimisation results concerning the composition of each sector are illustrated in appendix B.

$$\Delta_{2050} = \frac{\sum_{i=1}^{n} |T_{i,1}(2050) - T_{i,2}(2050)|}{n(2050)} \tag{6.1}$$

$$\Delta_{Path} = \frac{\sum_{j=2015}^{2050} \sum_{i=1}^{n} |T_{j,i,1}(2050) - T_{j,i,2}(2050)|}{n(2050) \cdot 35} \tag{6.2}$$

where:

Δ_{2050} = Indicator for differences in the final sector composition in %
Δ_{Path} = Indicator for differences over the entire observation period in %
T = Considered end-use sector [−]
n = Number of different technologies per end-use sector [−]

Table 6.1: Relative differences in sector composition obtained with and without consideration of ramping for two CO_2 reduction targets. DHW: domestic hot water.

	-85 % CO_2		-90 % CO_2	
	Δ_{Path}	Δ_{2050}	Δ_{Path}	Δ_{2050}
Space heat and DHW	0.5 %	0.8 %	0.6 %	0.5 %
Building refurbishment	0.0 %	0.6 %	0.0 %	0.5 %
Motorised private transport	0.8 %	0.7 %	0.0 %	0.0 %
Freight transport	0.0 %	0.1 %	0.1 %	0.2 %
Process heat supply (<480 °C)	1.5 %	1.4 %	1.7 %	1.9 %
Process heat supply (>480 °C)	0.3 %	0.9 %	0.7 %	1.6 %

As shown in table 6.1, both indicators (Δ_{2050} and Δ_{Path}) on average exhibit values below 0.8 %, with a maximum of 1.9 %. This suggests that the consideration of ramping behaviour does not significantly influence the final configuration of the end-use sectors nor their development. This conclusion is further enhanced by the heuristic optimisation approach utilised for the problem solution (cf. section 3.3.2). Thus, two optimisation runs with the exact same input parameters would not necessarily lead to the same results, but possibly exhibit slight variations[1].

While the consideration of ramping behaviour does not restrict the operation mode of any technology belonging to one of the above listed end-use sectors, it does affect the supply of power. Here, the results obtained for both CO_2 reduction targets show that, under consideration of ramping behaviour, a roughly 7 % higher installed capacity of VRE and thermal power plants is obtained. The operational restrictions posed on power generators, especially those with higher start-up times, lead to an according installation of highly flexible power plants. This leads to an increase of the cumulative installed capacity of thermal power plants. Further, by considering their operation in partial load, the respective conversion efficiencies are, on average, reduced. This indirectly causes higher emissions, which leads to a higher demand for CO_2-neutral electricity, translating into a slightly higher share of VRE. Figure 6.1 shows the resulting technology distribution of photovoltaic systems and wind power stations for a CO_2 reduction target of 85 %.

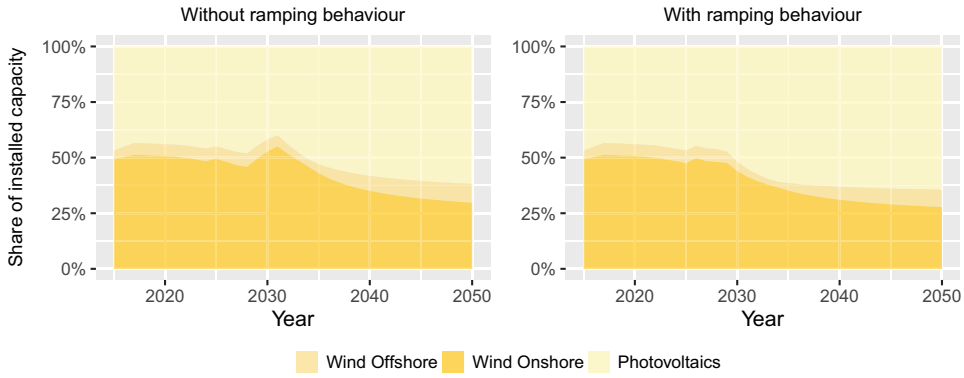

Figure 6.1: Share of installed VRE capacity from 2015 to 2050 for a 85 % CO_2 reduction compared to 1990 values, obtained with and without the consideration of ramping behaviour.

The illustrated technology distribution of VRE, exhibits a slight difference around the year 2030, exhibiting a higher installed capacity of photovoltaic systems in the case when ramping behaviour is considered. This results from the assumption that the must-run operation of coal power plants beginning in 2035 is set to zero. As a consequence of their higher start-up times, coal power plants are only operated as reserve capacity systems

[1] This was verified for several optimisation runs, yielding to variations of 1 % on average.

once ramping is considered (cf. section 6.1.2). This missing power generation capacity is then provided by photovoltaic systems. Besides that, the share of installed VRE capacity is almost identical, with a variation at the end of the observation period of less than 2 %. Analogously to figure 6.1, figure 6.2 presents the distribution of thermal power plants.

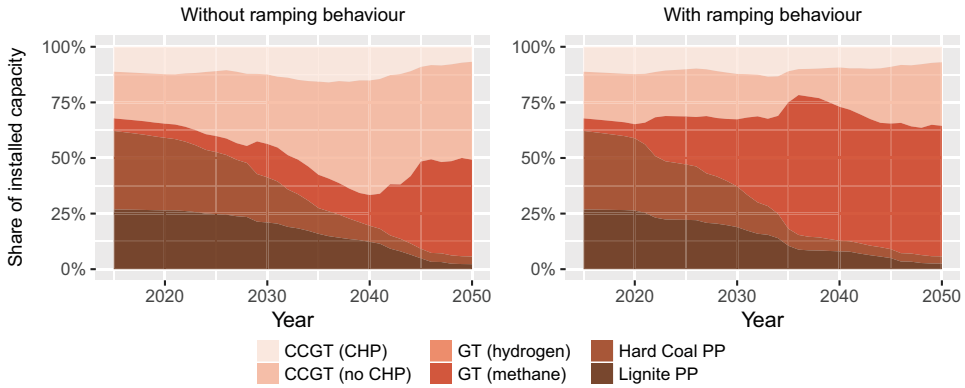

Figure 6.2: Share of installed thermal power plant capacity from 2015 to 2050 for 85 % CO_2 reduction targets obtained with and without the consideration of ramping behaviour. Hydrogen-based gas turbine (GT) power plants (PP) are not installed. CCGT: combined cycle gas turbine.

The resulting technology distribution of thermal power plants depicted in figure 6.2, varies significantly over the entire observation period. This is particularly visible for combined cycle gas turbine (CCGT) power plants and for gas turbine (GT) power plants. The latter are deployed in a larger scale in the case when the ramping behaviour of power plants is considered. This suggests that, despite the higher efficiency of CCGT power plants (cf. appendix A.1), the shorter response time of GT power plants indirectly leads to a reduction of the CO_2 abatement costs. This result highlights the correlation between the increasing deployment of VRE and the necessity for highly flexible power plants. However, even though the consideration of ramping behaviour leads to a substantial decrease of CCGT power plants, their capacity still amounts to roughly 35 % of the total power plant park in 2050. Thus, they make an important contribution to the generation of power.

Table 6.2: Installed capacity of stationary batteries obtained with and without consideration of ramping for an 85 % CO_2 emission reduction related to 1990 values.

Assumption	Unit	2030	2035	2040	2042	2044	2046	2048	2050
Without Ramping	GWh_{el}	0	1	4	4	7	13	39	106
With Ramping	GWh_{el}	0	1	4	47	93	170	205	271

As shown in table 6.2, the operational restrictions of thermal power plants due to ramping behaviour also affect the utilisation of stationary batteries. Their deployment reaches almost three times the capacity in 2050, if ramping behaviour is considered . By increasing the availability of short-term power storage options, the system tries to counterbalance the inertia of thermal power plants, which is of increasing importance as the share of VRE grows. As for coal power plants, their installed capacity is equal in both calculations. They still persist in 2050 due to their extended service life. However, their contribution to power generation is negligible beginning in 2035. This interaction is further explained in the following section. Based on time series analysis for the supply and demand of power, further insights regarding the consideration of ramping behaviour are presented.

6.1.2 Assessment of Power Plant Operation

In this section, the operation of thermal power plants under the consideration of ramping behaviour is assessed. Figure 6.3 depicts the power generation and demand for three days in March 2050. During this time period the feed-in from wind power is particularly low, while the power generation from photovoltaic systems is more pronounced. This leads to regular fluctuations of the residual load.

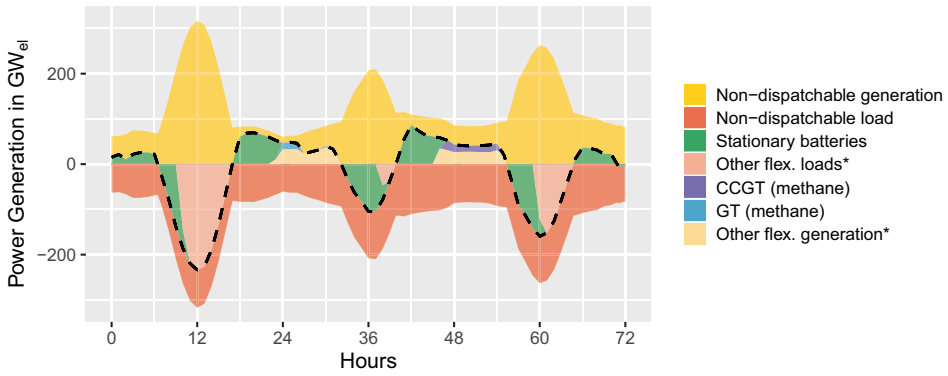

Figure 6.3: Power supply and demand for three days in March 2050. The dashed line represents the residual load. Other flexible loads*: includes vehicles batteries, pumped-storage power plants (PP), Power-to-Gas and Power-to-Fuel, electric heat pumps, heating rods, export of electricity and curtailment. Excluded are stationary batteries. Other flexible generation*: includes vehicles batteries, pumped-storage PP, biomass power generation, heat generators with combined supply of heat and power, oil PP, lignite PP, hard coal PP and electricity imports. Excluded are stationary batteries, gas turbine (GT) PP and combined cycle gas turbine (CCGT) PP. Underlying weather data: 2014.

Figure 6.3 shows two major time periods of power deficiency ranging from hour 17 to 32 and from hour 40 to 55. Even though their duration (from sunset to sunrise) and amplitude is similar, different thermal power plants are operated in either case. This behaviour is of particular interest, as the operational sequence of power plants in REMod is exogenously set according to their CO_2 footprint (cf. section 3.4).

The first period of power deficiency, is mostly covered by short-term stationary batteries and other flexible options, like the combined generation of heat and power or the import of electricity. Due to the substantial contribution of stationary batteries (cf. figure 6.3, green), only a small part of power deficiency remains. Here, methane gas-fired GT power plants are operated for three consecutive hours (cf. figure 6.3, blue). On the following day, after sunset, the residual load becomes positive again for a similar duration. In this case, instead of methane-fired GT power plants, CCGT power plants are operated for eight consecutive hours (cf. figure 6.3, violet). According to the assumed ramping parameters (cf. section 5.3, table 5.5), CCGT power plants are only heated up, if a continuous duration of operation of at least four hours is expected. This explains why, in the first case (figure 6.3, blue) GT are operated. If CCGT power plants would have been operated instead, their average efficiency over the three hour time period would have dropped significantly. Due to their greater ramp-up time it would have decreased by 15 %, from 59 % to 44 %.

If power deficiency occurs for extended durations, CCGT power plants are operated first, as they exhibit higher efficiencies and therefore lead to lower CO_2 abatement costs. This behaviour is shown in figure 6.4, where three days in February with particularly low feed-in from VRE are depicted.

The selected time period shown in figure 6.4 exhibits a prolonged duration of power deficiency. Thus, according to the exogenously set operational sequence CCGT power plants are operated before GT power plants, which meet the remaining demand peaks. However, during the illustrated three day period GT power plants are utilised almost as much, as the electricity supply from CCGT power plants alone is not sufficient to balance the residual load. After sunset of the first day, coal power plants are operated as well. They are utilised for the generation of power starting at 5 pm, for a continuous duration of one and a half days. Compared to other thermal power plants, coal power plants exhibit greater start-up times as well as higher minimum operation times. They are assumed equal to roughly 6 hours and 4 hours for hard coal and to 7 hours and 6 hours for lignite power plants. This is why in systems with a substantial share of VRE, both power plant types mainly function as reserve capacity systems, i.e. they are operated when power deficiency occurs over a prolonged period of time.

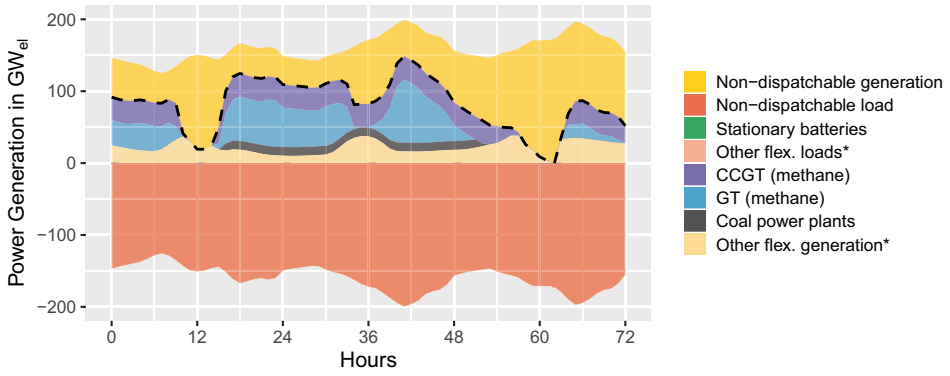

Figure 6.4: Power supply and demand for three days in February 2048. The dashed line represents the residual load. Other flexible loads*: includes vehicles batteries, pumped-storage power plants (PP), Power-to-Gas and Power-to-Fuel, electric heat pumps, heating rods, export of electricity and curtailment. Excluded are stationary batteries. Other flexible generation*: includes vehicles batteries, pumped-storage PP, biomass power generation, heat generators with combined supply of heat and power, oil PP and electricity imports. Excluded are stationary batteries, gas turbine (GT) PP and combined cycle gas turbine (CCGT) PP. Underlying weather data: 2011.

The utilisation of thermal power plants proves to decrease as the expansion of VRE increases. This is shown in figure 6.5. Here, the share of VRE in the gross final energy electricity production (secondary axis) and the power generation of methane-fired GT power plants, CCGT and coal power plants (primary axis) are depicted for the years from 2035 to 2050.

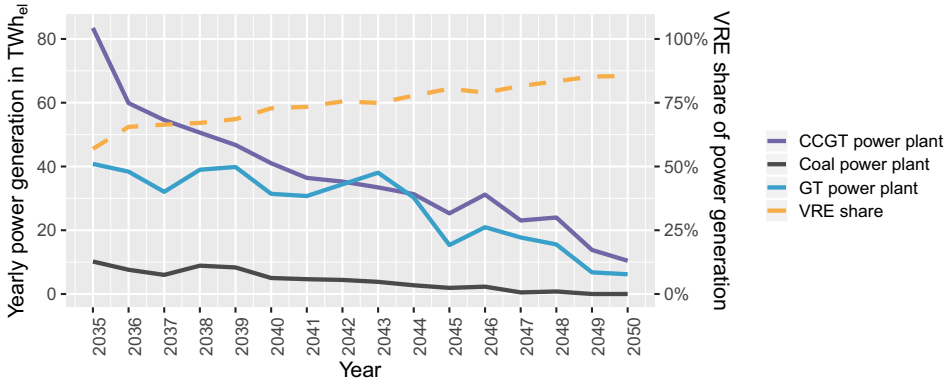

Figure 6.5: Development of the yearly power generation of thermal power plants and respective share of variable renewable energy (VRE) in total power generation for the years 2035 to 2050. Beginning in 2035 coal power plants function as reserve capacity as no must-run capacity is considered. CCGT: combined cycle gas turbine, GT: gas turbine, VRE: variable renewable energy.

With the continuous expansion of VRE the cumulative installed capacity of thermal power plants increases over time. However, their full load hours follow the opposite trend. In 2050, the power generation from CCGT power plants is reduced to roughly 15 % compared to 2030. While GT power plants also lower their operation, the decrease is less pronounced, exhibiting a power generation of 28 % in 2050 compared to 2030. This shows that, relative to other thermal power plants, the higher flexibility potential of GT power plants leads to higher utilisation rates. For instance, they are operated in times when power deficiency occurs for a duration of less than four consecutive hours. This becomes more frequent as the share in power generation from VRE increases. Further, figure 6.5 shows that the yearly power generation from coal power plants is rather small over the selected time period. Thus, coal power plants become more and more unprofitable not only due to their specific CO_2 emissions, but also because of their lower flexibility potential, leading to a progressive reduction of their installed capacity (cf. figure 6.2).

The fluctuations in power generation illustrated in figure 6.5 result from the consideration of different weather data over the whole time period (cf. section 5.3). For instance, in 2046 the power generation share of VRE is slightly lower than in 2045, even though their installed capacity until 2050 constantly increases. This is a consequence of the lower full load hours of wind power stations and photovoltaic systems in 2046, when the weather data of 2012 is assumed (cf. section 3.5). This is also why a slight increase in the thermal power plants utilisation is visible from 2045 to 2046. Thus, the underlying weather data, by influencing the power generation from VRE, indirectly also affects the operation of thermal power plants. Against this background, their utilisation and their annual conversion efficiencies are analysed in the following section.

6.1.3 Variation of Weather Data and Ramping Assumptions

The operation of thermal power plants heavily depends on the frequency and the respective duration at which power deficiency occurs. Both are substantially affected by the power generation from VRE, which itself is determined by the underlying weather conditions. Table 6.3 summarises the resulting numbers of periods with certain numbers of consecutive hours with a positive residual load, for a share of VRE in the gross final energy electricity production equal to roughly 80 %.

According to table 6.3, power deficiency occurs during 4029 hours on average, which corresponds to approximately 46 % of the year. This number decreases to 42 % when real weather data from 2015 is utilised and reaches its maximum value of roughly 52 % if the underlying weather data is set to 2013. The weather data of 2013 exhibits the least times of power deficiency in the short duration range, i.e. up to 12 hours, and the highest, when durations greater than half a day are considered. Thus, it favours a comparatively long-lasting, continuous operation of thermal power plants. In order to

Table 6.3: Numbers of periods with certain numbers of consecutive hours of power deficiency depending on the selected weather data for an 80% share of VRE in power generation.

Duration	2011	2012	2013	2014	2015	average
Yearly	3810	4019	4586	4022	3708	4029
1 - 3 h	54	62	38	52	48	51
4 - 6 h	35	46	29	44	42	39
7 - 12 h	52	58	39	63	61	55
13 - 24 h	154	138	152	146	139	146
25 - 48 h	6	7	14	7	5	8
> 39 h	4	10	10	7	7	8

verify this, five simulation runs are performed, for which the underlying weather data is varied, while the system configuration is kept the same.

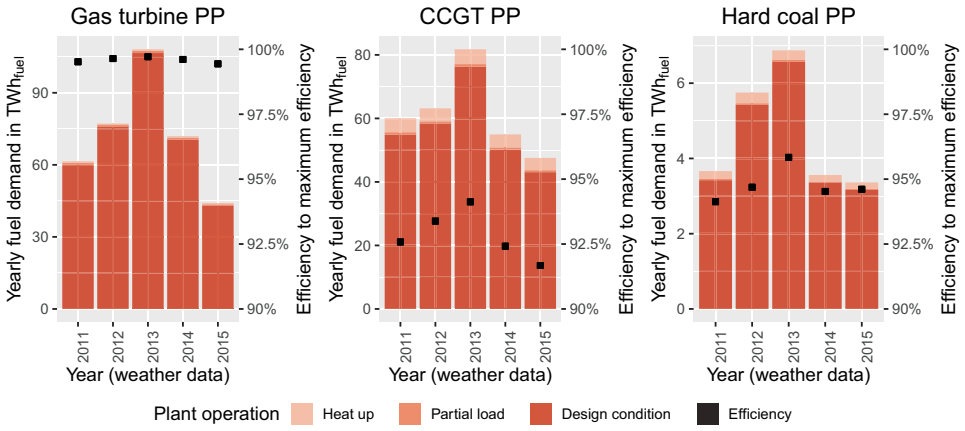

Figure 6.6: Utilisation of three thermal power plants with high, medium and low flexibility potential as well as yearly efficiency for a renewable power generation share of roughly 80 %.

Figure 6.6 shows the power demand of GT, CCGT and hard coal power plants for a power generation share of VRE of roughly 80 %. All three power plants present different ramping characteristics, where GT power plants exhibit the lowest start-up times and hard coal power plants the highest start-up times. Each column is divided according to the yearly fuel demand of each operational state, namely heat-up, partial load and design condition operation (cf. section 4.2). The secondary axis depicts the relation between the yearly plant conversion efficiency and its maximum value, i.e. the plant efficiency when running at design conditions. The results show that depending on the underlying weather data, the yearly fuel demand per plant varies between roughly -30 % to +45 % of their average value. All plants present the highest fuel demand in case of the weather data of 2013. As previously shown in table 6.3, this year exhibits the highest number of

hours in which power deficiency occurs for at least half a day. Conversely, the lowest fuel demand is obtained for the weather data of 2015. This underlines that if a priority feed-in from VRE is implemented, the operation of thermal power plants is influenced by the underlying weather conditions.

The illustrated results reveal that GT power plants are operated almost entirely at design conditions, regardless of the considered weather data. This is due to their cold start-up time, which amounts to less than ten minutes. Conversely, the effect of heat-up and partial load operation becomes more visible if CCGT or coal power plants are considered. The secondary axis of figure 6.6 shows that the conversion efficiency of CCGT power plants varies between 92 % and 94 % of their nominal efficiency. This means that the loss in conversion efficiency amounts to 3 % to 5 %, depending on the plant utilisation, i.e. the selected weather data. Compared to GT and CCGT power plants, the energy demand of coal power plants is significantly reduced. Their fuel demand in heat-up and partial load operation makes up for roughly 6 % of their total energy demand. Accordingly, depending on the underlying weather data, their efficiency is reduced by 4 % to 6 % compared to its nominal value. This corresponds to a yearly efficiency drop of roughly 2 %.

The analysis shown in this chapter is based on one specific data set of ramping characteristics (cf. section 5.3, table 5.5). The uncertainties that lie within these assumptions are subsequently investigated by up or downgrading each plants flexibility by 25 % and 50 %. An upgrade of 50 % means that the cold and warm start-up times as well as the required fuel for the plants start-up phase are cut by half. Further, the ramp rate is increased by 50 % of its reference value. Conversely, a downgrade of the plants flexibility indicates that the ramp rate is reduced, while the start-up times and the start-up fuel are increased.

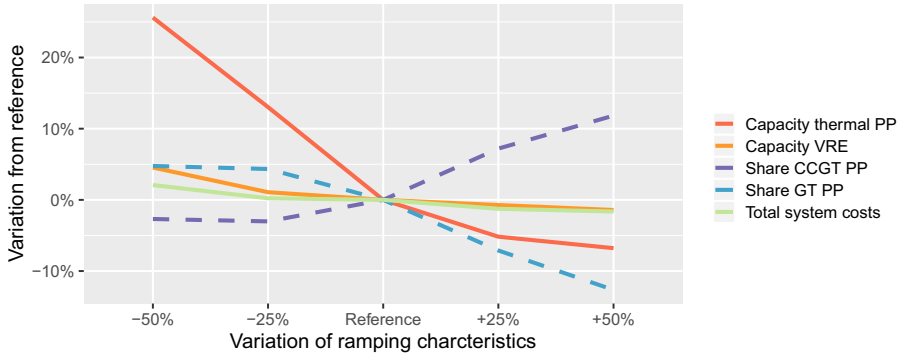

Figure 6.7: Variation of ramping characteristics and influence on selected results for a 85 % CO_2 emission reduction by 2050 compared to 1990 values. PP: power plant, VRE: variable renewable energy, GT: gas turbine, CCGT: combined cycle gas turbine.

Figure 6.7 shows the resulting variations in total system costs, installed capacity of VRE and thermal power plants as well as the share of GT and CCGT power plants related to the reference parametrisation of table 5.5. By downgrading the plants flexibility, the utilisation of CCGT and coal power plants is further reduced, while their time spent in heat-up and partial load operation is increased (cf. figure 6.6). As a consequence, an according deployment of highly flexible GT power plants is required, thus, leading to a greater installed capacity of the German power plant park. For instance, the installed capacity of thermal power plants increases by approximately 13 % for each 25 % downgrade of the assumed flexibility characteristics. According to table 5.5, a downgrade of 50 % would roughly lead to ramping characteristics equal to those of today's power plant park. On one hand this means that until 2050 no repowering measures of the existing power plants would take place. On the other hand, it also implies that newly installed plants would be build with a state of the art lower than today's standards. At the same time, downgrading the flexibility of power plants leads to a reduction of their average conversion efficiency and thus to a higher CO_2 footprint. These effects are counterbalanced by a greater deployment of VRE, which in figure 6.7 increases to 5 %. All these mechanisms combined lead to higher system costs, reaching + 2 % for a downgrade of the plants flexibility equal to 50 %.

The opposing trend is revealed if the flexibility of thermal power plants is improved. Figure 6.7 shows that the share of CCGT power plants increases up to 12 % at the cost of GT power plants. Since GT power plants already exhibit short response times, a further improvement is rather negligible. This is not the case for CCGT power plants, which by combining their higher efficiency with an enhancement of their flexibility, become increasingly attractive. Further, in case of an upgrade, the installed capacities of VRE and thermal power plants and thus the total costs are progressively reduced. While the cost reduction for an improved flexibility behaviour of 50 % amounts to approximately 2 %, the required capacities of VRE and thermal power plants are 1.5 % and 7 % below the reference results. This shows that the power generation is more sensitive to a downgrade of the ramping parameters than vice versa.

6.1.4 Summary and Conclusions

In this section, the developed methodological approach of ramping behaviour was assessed through the analysis of thermal power plants. It was studied, whether a more detailed consideration of thermal power plants has an effect on the energy system. For this purpose, several model calculations under variation of the underlying weather data and ramping characteristics were performed. In the following, the key findings are summarised and discussed.

The obtained results showed that the structure of energy demanding technologies remained almost unchanged, regardless of whether the ramping behaviour of thermal power plants was considered or not. This was verified for each end-use sector by introducing two indicators. These indicators account for variations occurring in the final sector configuration in 2050 and for the entire observation period, ranging from 2015 to 2050. The analysed end-use sectors include the supply of space heat and hot water demand, the motorised road transport as well as the supply of process heat. Significant differences were observed in the power sector, where the cumulative installed capacity of VRE and thermal power plants resulted approximately 7 % higher when ramping behaviour was considered. It was noticed that especially the composition of the thermal power plant park changed once their ramping behaviour was accounted for. Highly flexible GT power plants were deployed to a greater degree at the cost of CCGT power plants. As the share of VRE increased, the residual load exhibited more frequent fluctuations and the system required a higher degree of flexibility.

A further finding concerns the exogenously set operational sequence of thermal power plants (cf. section 3.4). Through the implemented forecast and the consideration of the plants flexibility characteristics (cf. section 4.2), this order is no longer the only decisive factor determining which plant is utilised for the generation of power. For instance, the results showed that for short periods of power deficiency, GT power plants were operated before CCGT power plants, although, according to the exogenously set operational sequence, CCGT power plants should be given priority. Coal power plants were gradually taken off the grid as, compared to other thermal power plants, they exhibited higher start-up times, higher minimum operation requirement times and higher CO_2 emission factors. Beginning in 2035, they functioned as reserve capacity systems. This means that their utilisation was limited to times when power deficiency occurred over a prolonged period. This result is in line with statements of the coal committee which suggests the withdrawal from coal-fired power generation in 2038 or even 2035 [23].

It was further shown that the operation of thermal power plants is increasingly affected by the continuous expansion of VRE. Their full load hours and feed-in profiles are in turn determined by the underlying weather data[2]. For this reason, the operation of thermal power plants was investigated under consideration of five different weather data sets. The analysis was performed for a renewable energy share to the gross electricity generation of 80 %, which corresponds to the target of the Federal Government by 2050 [3]. The results showed that the fuel demand of three different thermal power plant types exhibited a variation ranging from -30 % to +45 % of their average value. The most favourable conditions for the operation of thermal power plants were noticed when the weather data of 2013 was assumed. This year exhibits the highest number of power deficiency

[2] A further analysis based on the variation of weather data is presented in section 6.4.2

periods lasting for at least half a day. Conversely, the weather data of 2015 turned out as the least favourable, as due to the higher feed-in from VRE the yearly power generation from thermal power plants exhibited its lowest value. This led to a reduction of the plants full load hours and required them to ramp-up and ramp-down more frequently and therefore to spent more time in partial load operation. While [60] shows that this behaviour does not have a significant impact on the overall plant efficiency, the obtained results suggest that this is only the case for highly flexible power plants, such as GT power plants. For CCGT and coal-fired power plants, the yearly drop in efficiency amounted up to 5 % and 2 %, respectively. Roughly, this loss in efficiency translates to additional 26 kt_{CO_2} and 64 kt_{CO_2} for each $\mathrm{TWh_{el}}$ generated.

To account for uncertainties in the parametrisation of the ramping characteristics, the flexibility of the power plant park was up and downgraded by 25 % and 50 %. The results showed a rather small influence of the installed capacity of VRE and the total system costs. Substantial differences concern the distribution between highly flexible GT and CCGT power plants. The deployment of GT power plants is favoured in case of a downgrade, while CCGT power plants become increasingly attractive if the flexibility of the power plant park is upgraded. An upgrade has a major impact on CCGT power plants instead of GT power plants, which are already highly flexible and operational within few minutes. Further, it was noticed that the cumulative installed capacity of the power plant park is increased in case of a downgraded flexibility behaviour. A downgrade equal to 50 % would mean, on one hand, that until 2050 no repowering measures of the existing power plants would take place. On the other hand, it also implies that newly installed plants would be build with a state of the art lower than today's standards. Thus, it can be considered as an extreme case. It is noted that increasing the flexibility of a thermal power plant to achieve higher ramp rates and perform multiple start-ups, may put more strain on the components. This may decrease their technical service life and raise their maintenance and operation costs. This factor has to be accounted for in the model parametrisation as currently the maintenance and operation costs are exogenously set and thus are not linked to the plant operation itself.

In summary, while a flexible power plant operation does not directly lead to a reduction of the CO_2 emissions, its consideration is important as it may lead to a higher integration of VRE while maintaining a stable grid operation. The implemented methodological approach proved to be suited for the depiction of ramping behaviour of energy conversion plants in REMod. Thus, besides their carbon footprint and costs, energy conversion plants are also evaluated according to their flexibility characteristics. Another option to increase the flexibility of the energy system is by exploiting DSM in the motorised private transport. A further possibility is to utilise surplus electricity from VRE for the production of hydrogen and increase the deployment of fuel cell electric vehicles (FCEVs). Both configurations are analysed in the next section.

6.2 The Role of Alternative Drive Concepts

With the promotion of fuel cell electric vehicles (FCEVs) and battery electric vehicles (BEVs), the Federal Government signalises that it further intends to increase the number of alternative drive concepts [239]. This section investigates their role in a German energy system based on a large share of VRE. Under consideration of three different CO_2 reduction targets, the production and usage of electricity-based synthetic fuels in the motorised road transport is analysed. It is determined which power train technologies prevail in case of an Uncontrolled Charging Strategy (UCSt), meaning that BEVs are charged as soon as users return to a charging facility. Further, a sensitivity analysis for BEVs is performed, which accounts for uncertainties concerning user acceptance as well as additional costs deriving from greater demands in terms of range. After this, the focus is on the effects resulting from a Controlled Charging Strategy (CCSt) of BEVs. This analysis is performed under variation of the user share following a CCSt and the allowed battery discharge depth in case of a power feedback into the electrical grid (Vehicle-to-Grid). Thus, a better understanding for the developed modelling approach (cf. section 4.3) is provided and DSM in the motorised road transport is evaluated.

6.2.1 Electrification of the Motorised Road Transport

The ongoing expansion of VRE represents a key element for the successful introduction of alternative power train technologies, as this ensures that the utilised electricity is predominantly CO_2-neutral. This is not only the case for BEVs, but also applies to FCEVs and hybrid variants. When power surplus occurs, Power-to-Gas (PtG) or Power-to-Liquid (PtL) plants can be used to produce synthetic fuels and contribute to the balancing of the residual load. These examples lead to a gradual electrification of the energy system. Here, a distinction between direct and indirect electrification is made. Technologies exhibiting an electricity demand, such as BEVs or electric heat pumps, increase the direct degree of electrification. The indirect degree of electrification is represented by technologies based on liquid fuels or gases which, in turn, are produced based on electricity such as from PtG or PtL plants. Thus, the indirect degree of electrification depends from the produced amount of synthetic fuels and the deployment of fuel-based technologies. For instance, if half of the yearly hydrogen supply is provided by electrolysis plants, then 50 % of all fuel cell electric vehicles (FCEVs) count as indirectly electrified. However, if no FCEVs are deployed, than the indirect degree of electrification in the motorised road transport remains equal to zero. The share of synthetic fuels per energy carrier and the total degree of electrification for the year 2050 are summarised in table 6.4. The calculations are performed for three different CO_2 reduction targets, i.e. -85 %, -90 % and -95 % compared to 1990 values.

Table 6.4: Share of synthetic fuel production and total degree of electrification in 2050 in the motorised road transport. The three different CO_2 reduction targets indicate a reduction compared to 1990 values. T.: transport.

CO_2 target	Share of synthetic fuels in %			Total electrification in %	
	Liquid fuels	Methane	Hydrogen	Freight T.	Private T.
85 %	0.7	0.3	87	65	100
90 %	1.2	0.6	90	87	100
95 %	4.2	8.5	100	100	100

While the total degree of electrification in 2050 for the motorised private transport is constant at 100 %, for the motorised freight transport it increases as the considered climate protection target becomes more ambitious. The same trend is observed for the production of synthetic fuels. In order to evaluate the contribution of the direct and indirect electrification in the motorised road transport in more detail, their degrees are determined on a yearly basis. The resulting progression for three distinctive CO_2 reduction targets is depicted in figure 6.8. For completeness, an analogue representation of remaining sectors, i.e. the supply of space heat and domestic hot water and the supply of process heat, is included in appendix C.

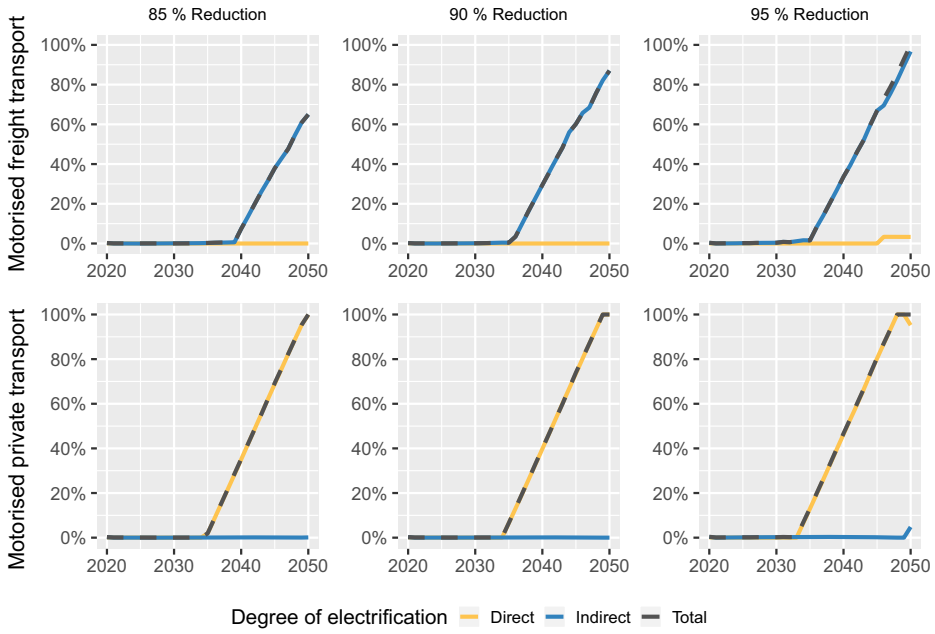

Figure 6.8: Development of the degree of electrification for the motorised private transport and the motorised freight transport. The indirect electrification accounts for synthetic fuels, generated by Power-to-Gas or Power-to-Liquid plants.

As shown in figure 6.8, the degree of electrification of the motorised freight transport and the motorised private transport both gradually increase over the considered time period from 2015 to 2050. The total degree of electrification in the motorised freight transport in 2050 raises from 65 % over 87 % to 100 % as the considered CO_2 reduction target becomes more ambitious. According to the model parametrisation in appendix A.8, only small transporters can entirely rely on purely battery powered systems. Thus, for the ramaining vehicles of this sector, the shift to synthetic fuels represents the only electricity-based alternative[3]. As a consequence, this is the only sector, where the indirect electrification plays a major role.

As for the motorised private road transport, a complete electrification is attained at the end of the observation period, regardless of the investigated CO_2 reduction target (cf. table 6.4). According to figure 6.8, the related progressions of the degree of electrification results almost the same in each case, representing a substantial difference compared to other sectors. This behaviour suggests that the same power train technologies are deployed each time. In order to verify this, the share per milage, divided per power train technology is illustrated in figure 6.9 for a 90 % CO_2 reduction target. The developments for the 85 % and 95 % cases are not included, as they exhibit almost the same behaviour. For completeness they are included in appendix C.

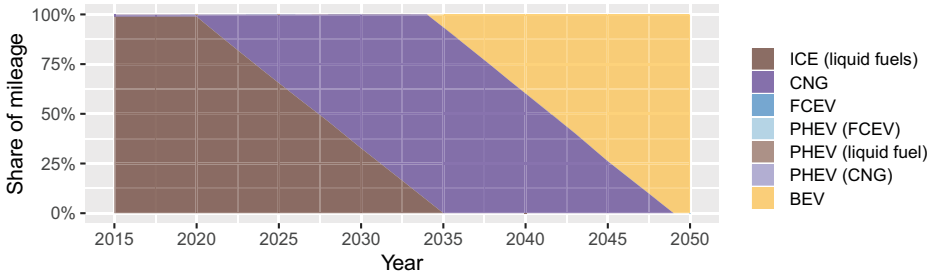

Figure 6.9: Development of the milage share per power train technology in the motorised private transport for a 90 % CO_2 emission reduction by 2050 compared to 1990 values. BEV: battery electric vehicle, CNG: compressed natural gas vehicle, PHEV: plug-in hybrid electric vehicle, FCEV: fuel cell electric vehicle, ICE: internal combustion engine.

According to the optimisation results illustrated in figure 6.9, the transition of the motorised transport sector from conventional to alternative drive concepts happens in two consecutive steps. First, beginning in 2020, a shift from gasoline or diesel based power trains to compressed natural gas (CNG) vehicles takes place. Fifteen years later, they are gradually replaced by BEVs, which in 2050 account for 100 % of the total vehicle fleet of this sector. The shift from liquid fuels to methane to electricity can be traced back

[3] A scenario under consideration overhead wire infrastructure and thus direct electrification of the motorised freight transport sector was assessed in [113].

to the respective CO_2 abatement costs of each power train technology. In 2020, when the first CNG-vehicles are introduced, the vehicle purchase price is assumed to roughly 24,000 € for CNG-vehicles and to 25,000 € for gasoline or diesel based internal combustion engines (ICE). The costs of BEVs still amount to more than 38,000 €. The higher efficiency of BEVs (74 % versus 22 %) is not yet sufficient to counterbalance this price difference. This, combined with the lower emission factor of methane gas compared to oil, is why in 2020 the deployment of CNG-vehicles represents the most cost-effective solution for the reduction of the CO_2 emissions in the private transport[4]. After the existing CNG-vehicles reach their assumed technical service life of 15 years (cf. appendix,A.8), they are replaced by BEVs. In 2035, the cost difference between these two power train technologies is reduced to 6,000 € and to less than 300 € by 2050. Further, as the end of the observation period is approached and the share of renewable power generation increases, BEVs become increasingly CO_2-neutral. Conversely, as previously shown in table 6.4, the share of synthetic methane produced by PtG plants amounts to less than 1 % for a CO_2 reduction target of 85 % and 90 %, while reaching a value of 8.5 % for a 95 % emission reduction in 2050. As a consequence, starting in 2035, BEVs represent the better option in terms of costs, efficiency and emissions, which is why they are deployed to achieve the set climate protection targets. In the following section, the next best alternative power train technology to BEVs is identified and the respective cost gap is assessed.

6.2.2 Cost Sensitivity Analysis of BEVs

The model results in the motorised private transport so far suggest a complete transition from conventional ICE to BEVs by 2050. In reality, this development may be hindered due to technical requirements or a low user acceptance. In [113] an analysis of possible inhibiting factors, such as the charging time or a limited drive range, lead to a maximum deployment of BEVs equal to 50 %. In order to assess the effects resulting from such a restriction, a further calculation is performed. It is assumed that the yearly market share of BEVs is limited to 50 % right on from the start in 2015, while the remaining parametrisation remains unchanged. Figure 6.10 illustrates the resulting development of the motorised road transport sector for a CO_2 reduction target of 90 %.

[4] The calculations consider the expansion of the necessary charging infrastructure as well as the methane slip of CNG-vehicles with 500 $^{mg_{CH_4}}/_{m^3}$ [122].

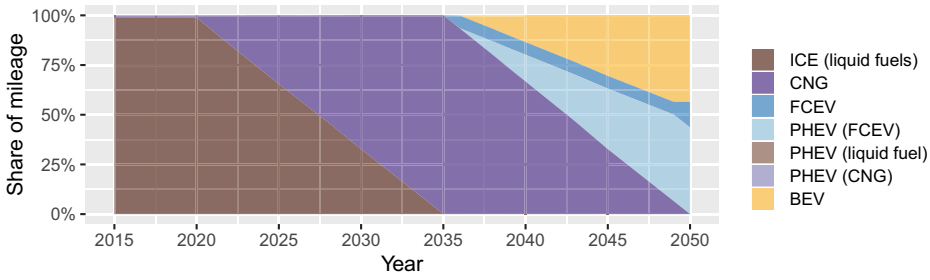

Figure 6.10: Development of the milage share per power train technology in the motorised private transport for a 90 % CO_2 emission reduction by 2050 compared to 1990 values. Yearly market share of BEVs at each year are restricted by 50 %. BEV: battery electric vehicle, CNG: compressed natural gas vehicle, PHEV: plug-in hybrid electric vehicle, FCEV: fuel cell electric vehicle, ICE: internal combustion engine.

As shown in figure 6.10, the shift from conventional power train technologies to CNG-vehicles is confirmed according to previous results. Once the deployed CNG-vehicles gradually reach their technical service life, they need to be replaced by one of the seven implemented power train technologies. The chosen technology will remain part of the energy system for 15 years and thus until the end of the observation period, when the CO_2 emissions are reduced to their minimum. As a consequence, the carbon footprint of the power train technologies becomes increasingly more important than the vehicle price. Accordingly, beginning in 2035, CNG-vehicles are gradually driven out by BEVs and FCEVs, with no share left in 2050. A comparison to the previously obtained results shows that the limited market share of BEVs leads to an earlier deployment of electrolysis plants, hydrogen storage systems and the respective charging facilities. This suggests that the expansion of the hydrogen infrastructure leads to a lock-in effect, where the share of FCEVs reaches a value higher than 50 % in 2050. The results further show that the limitation of BEVs and the associated introduction of FCEVs do not increase the installed capacity of electrolysis plants in 2050. Instead, the utilisation of hydrogen for the supply of process heat is cut by half and substituted by mainly electricity-based heat generators. Similarly, the usage of biomass is in part shifted from the supply of process heat to its conversion into hydrogen. These effects represent typical examples for interdependencies occurring within the sectors of the energy system. Thus, the limitation of BEVs in the motorised transport sector can cause structural differences in the supply of process heat and vice versa.

According to the results illustrated in figure 6.10, FCEVs, including hybrid variants, represent the next best alternatives to BEVs. For this reason, a cost analysis of these three power train technologies is performed for the year 2050. The following factors are taken into consideration:

- Vehicle purchase price
- Proportionate costs for charging facility (cf. section 3.2.2)
- Photovoltaic system for the supply of the resulting power demand[5] (1,000 full load hours per year).
- Electrolysis plant for the supply of the resulting hydrogen demand (1,500 full load hours per year and a conversion efficiency of 66 %)
- Vehicle efficiencies (73 % for BEVs and 48 % for FCEVs. It is assumed that hybrid vehicles perform 40 % of their milage based on their battery and 60 % based on their fuel cell)

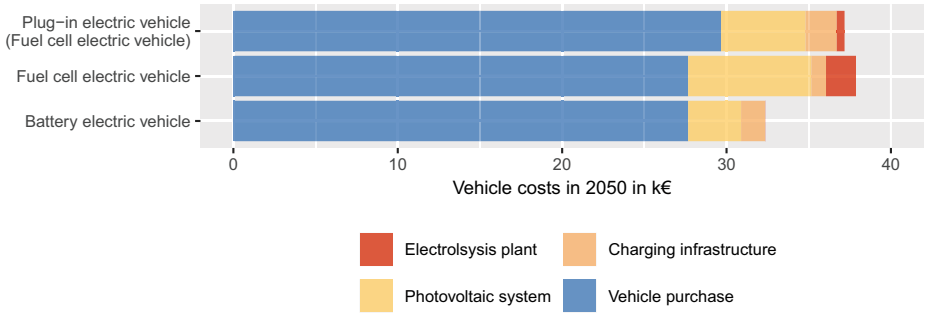

Figure 6.11: Qualitative assessment of private vehicle costs in 2050. Photovoltaic systems and electrolysis power plants are dimensioned assuming 1,000 and 1,500 full load hours, respectively.

As shown in figure 6.11, the associated costs are lowest for BEVs, with roughly 32,500 € per vehicle. Both hydrogen-based power trains exhibit costs of approximately 38,000 €, with a slight edge in favour of hybrid power trains (less than 700 €). The results reveal that the largest part of the cumulative costs is represented by the vehicle purchase price. By increasing the purchase price for BEVs only, the difference of total costs per vehicle to both hydrogen-based power train technologies is progressively reduced. For a 10 % price increase, the cumulative costs are still in favour of BEVs with roughly 2,200 €. They amount to 400 € and 3,100 € in favour of FCEVs, if it is further increased to 20 % and 30 %, respectively. Based on this qualitative cost assessment, three more optimisation runs are performed and the purchase price of BEVs adapted accordingly. In this case, the limitation concerning the yearly market share of BEVs is again lifted. The resulting share of milage per power train technology for a CO_2 reduction target of 90 % is illustrated in figure 6.12.

[5] In this analysis photovoltaic systems are considered as they provide the greatest contribution to power generation option in 2050. The same analysis was also performed based on wind turbines, leading almost to the same outcome.

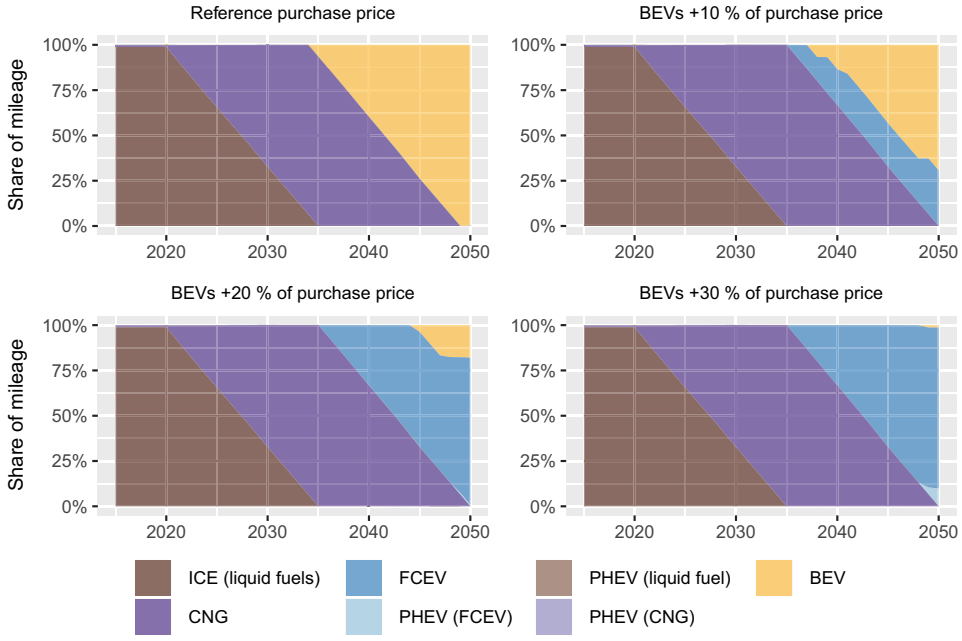

Figure 6.12: Cost sensitivity: Development of the milage share per power train technology in the motorised private transport for a 90 % CO_2 emission reduction by 2050 compared to 1990 values. The purchase price of BEVs is increased by from zero to 30 % in steps of 10 %. BEV: battery electric vehicle, CNG: compressed natural gas vehicle, PHEV: plug-in hybrid electric vehicle, FCEV: fuel cell electric vehicle, ICE: internal combustion engine.

Figure 6.12 shows the development in milage share per power train technology for a respective increase of BEVs purchase price from 0 % to 30 %. The reference parametrisation and the price increase of 30 % lead to two completely different configurations, being dominated by BEVs in one case and by FCEVs in the other case. Starting from a price increase of BEVs of 10 %, the share of FCEVs in 2050 is already increased from zero to 31 %. A further price increase of 10 % raises their share to 81 %, demonstrating that the results are sensitive to the vehicle purchase price. Since the vehicles considered in the model parametrisation represent average requirements, it can be assumed that, in reality, a small share needs to fulfil a more stringent demand in terms of range. This translates to a higher battery capacity and thus increased vehicle costs. According to the results, an increase of the BEVs purchase price by 10 % or 20 %, leads to a mixed composition of BEVs and FCEVs in 2050. As both power train technologies are almost or fully CO_2-neutral towards the end of the observation period, it could be assumed that the consideration of the total costs per vehicle is sufficient to determine which power train technology should be deployed. However, other factors, including interdependencies to other sectors, which can not easily be considered in a qualitative cost assessment, must

be taken into account. This, for instance, concerns the temporally resolved supply and demand profiles of energy, which play a major role for BEVs. As for FCEVs, their demand in the model is evenly distributed throughout the year. Further, especially towards the end of the observation period, hydrogen is almost exclusively produced in times of power surplus (cf. table 6.4). This does not only make FCEVs almost CO_2-neutral, but allows to supply them with hydrogen without necessarily inducing additional electricity load peaks[6].

Conversely, the power demand of BEVs is determined according to exogenously specified driving profiles. The calculations presented so far are based on an UCSt. This means that users charge their vehicles as soon as they return to the charging facility, regardless of the residual load value. Thus, their charging load peak occurs around 5 pm to 6 pm, when most users return home from work and the power generation from photovoltaic plants is relatively low (cf. section 5.3). The increase in power demand may eventually lead to a higher requirement for power storage units or extend the operation of thermal power plants and therefore increase the overall system costs. In the next section, the effects resulting from a CCSt are investigated. Thus, users will be able to charge their vehicles in times of power surplus, increasing the systems flexibility.

6.2.3 Assessment of Controlled Vehicle Charging

By operating vehicle batteries flexibly (CCSt), users may charge their batteries when power surplus occurs and discharge them otherwise. According to previous studies based on REMod [105], a CCSt favours the deployment of BEVs. In order to verify this, all calculations presented in this section are based on a scenario, for which the motorised private road transport in 2050 is dominated by fuel cell powered vehicles. Thus, according to figure 6.12, the purchase price of BEVs is increased by 30 %.

For this analysis two parameters are investigated in greater detail. The first accounts for the user share charging their vehicles preferably when power surplus occurs. The second describes the allowed discharge depth in case of a power feedback into the electrical grid (cf. section 4.3, V2G factor).

[6] If the hydrogen storage is not able to meet the hourly hydrogen demand, the electrolysis plant is operated and thus the electric load is increased (cf. section 3.4). The amount of hydrogen produced by electrolysis plants this way amounts to less than 0.4 %, in case of a 30 % price increase of BEVs (which is when FCEVs exhibit their highest share). This analysis was performed for the years 2035, 2040, 2045 and 2050. A more detailed investigation of electrolysis plants and the hydrogen storage is presented in section 6.4.2.

Variation of the Controlled Charging Strategy Share

The available vehicle battery capacity to balance the residual load heavily depends on the total number of BEVs which represents an optimisation result. The Controlled Charging Strategy share (CCSt share) is specified exogenously. By increasing it a larger part of the electricity demand for the vehicle charging is shifted from times of power deficiency to times where power surplus occurs, contributing to the balancing of the residual load. Figure 6.13 illustrates an exemplarily time series for three days in summer 2050. The CCSt share and the V2G factor are both set to 10 %.

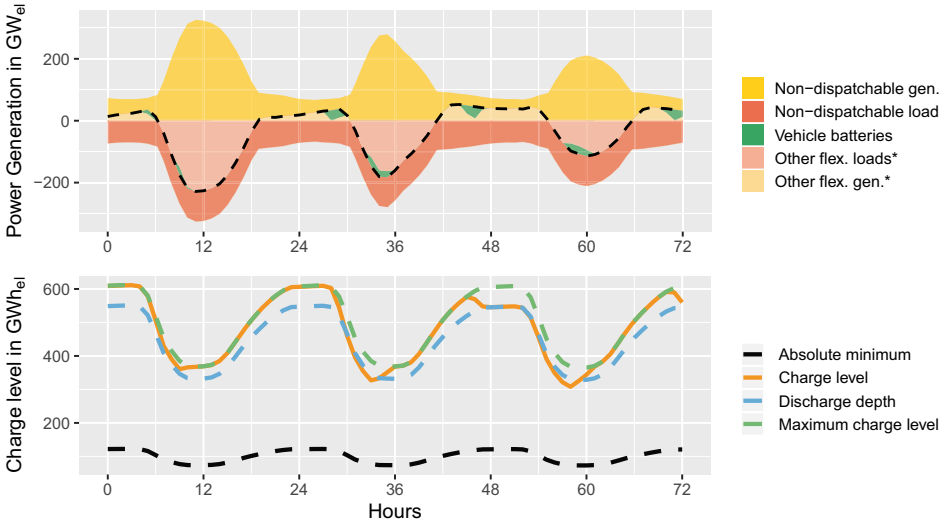

Figure 6.13: Exemplarily time series in summer for flexible operation of battery electric vehicles (BEVs). The black dashed line represents the residual load. Assumptions: 10 % of users follow a Controlled Charging Strategy. The Vehicle-to-Grid factor is set to 10 %. gen: generation. Other flexible loads*: includes stationary batteries, pumped-storage power plants (PP), Power-to-Gas and Power-to-Fuel, electric heat pumps, heating rods, export of electricity and curtailment. Excluded are vehicles batteries. Other flexible generation*: includes stationary batteries, pumped-storage PP, biomass power generation, heat generators with combined generation of heat and power, gas turbine (GT) PP and combined cycle gas turbine (CCGT) PP, oil PP, lignite PP, hard coal PP and electricity imports. Excluded are vehicles batteries.

The top part of figure 6.13 shows the supply and demand of power for three weekdays in summer in 2050. The flexible vehicle battery operation is illustrated in green. In the bottom part of figure 6.13, the charge level of the vehicle batteries as well as their respective limitations are depicted. The green dashed curve represents the maximum battery charge level of all vehicles currently plugged into a charging facility. According to section 4.3, vehicle batteries may only be utilised for a power feedback into the grid, if

their charge level (orange) is higher than the threshold value for a V2G operation (blue). This, for instance, occurs before and after sunrise of the second day, in hours 27 and 45. By increasing the CCSt share, electric vehicles provide a higher contribution to the balancing of the residual load as a larger part of users charge their vehicles in a more grid supportive way. Figure 6.14 shows how the resulting milage share is affected by an increase of the CCSt share in steps of 10 % and 25 %. In either case, the V2G factor is set to 10 %.

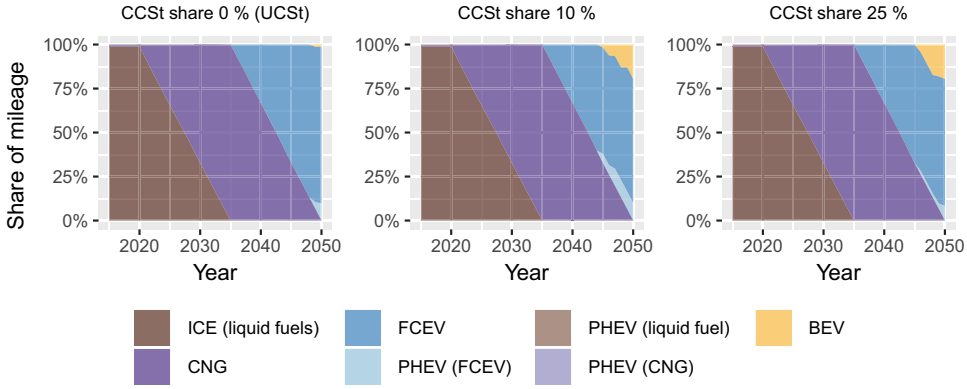

Figure 6.14: Sensitivity of the Controlled Charging Strategy (CCst) share: Development of the milage share per power train technology in the motorised private transport for a 90 % CO_2 emission reduction by 2050 compared to 1990 values. The purchase price of BEVs is increased by 30 % compared to reference parametrisation. The Vehicle-to-Grid (V2G) factor is set to 10 %. BEV: battery electric vehicle, CNG: compressed natural gas vehicle, PHEV: plug-in hybrid electric vehicle, FCEV: fuel cell electric vehicle, ICE: internal combustion engine.

The obtained results confirm that the consideration of a CCSt favours the deployment of BEVs. Their share in 2050 is increased from 1 % to 19 % if 10 % of the vehicle users follow a CCSt. A further increase of the CCSt share to 25 % only slightly increases the penetration of BEVs. The reason why can partially be traced back to the modelled restrictions of a V2G operation. As shown in figure 6.13, each day the vehicle batteries are charged with surplus electricity during the day and discharged after sunrise. However, due to the assumed V2G factor of 10 %, the maximum charge level (bottom part of figure 6.13, green) and the possible discharge depth (blue) are close to each other. This translates in a rather small capacity for a power feedback into the electrical grid. As a consequence, the vehicle batteries can only be discharged to a small degree and thus can not contribute significantly to the supply of electricity in times of power deficiency. This suggests that to exploit more of the flexible potential of BEVs, the V2G factor needs to be increased. In order to verify this, another sensitivity analysis is performed.

Variation of the Vehicle-to-Grid Factor

Figure 6.15 illustrates the resulting milage share for an increase of the V2G factor. All calculations assume a CCSt share equal to 10 %.

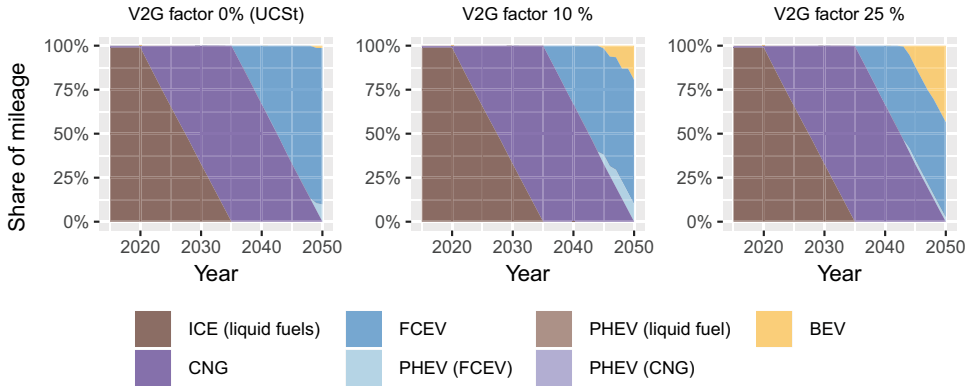

Figure 6.15: Sensitivity of the Vehile-to-Grid factor: Development of the milage share per power train technology in the motorised private transport for a 90 % CO_2 emission reduction by 2050 compared to 1990 values. The purchase price of BEVs is increased by 30 % compared to reference parametrisation. The Controlled Charging Strategy share is set to 10 %. BEV: battery electric vehicle, CNG: compressed natural gas vehicle, PHEV: plug-in hybrid electric vehicle, FCEV: fuel cell electric vehicle, ICE: internal combustion engine.

The illustrated results confirm that the variation of the V2G factor has a major influence on the penetration of BEVs. In 2050, their share is increased from 1 % to 19 % if the V2G factor is raised from 0 % to 10 %. A further increase of the V2G factor to 25 % leads to a share of BEVs of 44 % by 2050. Even though the purchase price of BEVs is assumed 30 % higher compared to the reference parametrisation, they account for almost half of the vehicle fleet. This shows that their higher purchase price is in part offset by cost-savings in other areas suggesting that the flexible operation of BEVs represent an added value for the entire energy system. For instance, if a CCST is considered, stationary batteries are deployed to a smaller degree. This is shown in table 6.5, which summarises the share of BEVs in 2050, as well as the resulting installed capacity of stationary battery storages. Further, the yearly amount of power stored in and discharged from vehicle batteries to balance the residual load are included.

Figure 6.16 shows a time series of power supply and demand for the same three day period introduced in figure 6.13. In this case, a CCSt share of 10 % and a V2G factor of 25 % are assumed.

Table 6.5: Summary of key results in case of a flexible operation of battery electric vehicles (BEVs). Users following a Controlled Charging Strategy (CCSt) and the Vehicle-to-Grid (V2G) factor are varied. UCSt: Uncontrolled Charging Strategy.

Share of CCSt		0 % (UCSt)	10 %	25 %	10 %
V2G factor		0 % (UCSt)	10 %	10 %	25 %
Share of BEVs	%	1	19	20	43
Grid-to-Vehicle	TWh_{el}	0	13	15	60
Vehicle-to-Grid	TWh_{el}	0	11	12	55
Stationary Battery	GWh_{el}	361	188	161	112

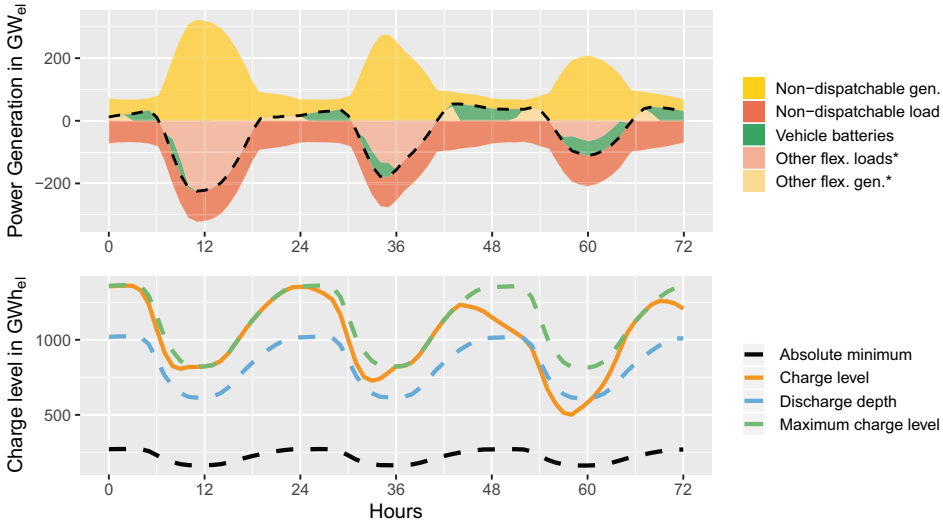

Figure 6.16: Exemplarily time series in summer for flexible operation of battery electric vehicles (BEVs). The black dashed line represents the residual load. Assumptions: 10 % of users follow a Controlled Charging Strategy. The Vehicle-to-Grid (V2G) factor is set to 25 %. gen: generation. Other flexible loads*: includes stationary batteries, pumped-storage power plants (PP), Power-to-Gas and Power-to-Fuel, electric heat pumps, heating rods, export of electricity and curtailment. Excluded are vehicles batteries. Other flexible generation*: includes stationary batteries, pumped-storage PP, biomass power generation, heat generators with combined generation of heat and power, gas turbine (GT) PP and combined cycle gas turbine (CCGT) PP, oil PP, lignite PP, hard coal PP and electricity imports. Excluded are vehicles batteries.

A comparison of figures 6.13 and 6.16 shows that BEVs play a larger role as load balancing option when the V2G factor is increased from 10 % to 25 %. The reason why, is that a higher V2G factor significantly increases the maximum discharge capacity. Therefore, the battery charge level can take lower values meaning that BEVs may provide a larger

contribution in times of power deficiency. Further, once that power surplus occurs again BEVs start from a lower charge level and therefore, a higher amount of electricity can be charged into the vehicle batteries. Thus, while a higher V2G factor increases the discharging capacity, it indirectly also leads to a higher receptivity of surplus electricity.

6.2.4 Summary and Conclusions

This section presented an assessment of alternative driving technologies with particular regard to the private road transport. The first part of the analysis was performed for three different CO_2 emission reduction targets and an UCSt of BEVs. In the second part, the effects of a Controlled Charging Strategy (CCSt) were investigated.

The results showed that the end-use sectors of the energy system were progressively electrified as the set climate protection targets became more ambitious. While this was mainly achieved through a direct electrification, for the motorised freight transport the indirect electrification played a major role. In this case, FCEVs were deployed, as hydrogen towards the end of the observation period was almost completely CO_2-neutral. The contribution of methanation and PtL plants was negligible, particularly because of their higher costs, additional conversion steps and thus lower efficiencies. Even in case of a 95 % CO_2 reduction target, the share of synthetic liquid fuels and synthetic methane gas remained under 5 % and 10 % of the total fuel demand, respectively.

As for the motorised private transport, a transition from gasoline and diesel ICE over CNG-vehicles to BEVs was observed, even though an UCSt was assumed. In 2020, the costs of CNG-vehicles are comparable to those of conventional power train technologies while being significantly lower than those of BEVs. Due to the smaller emission factor of methane gas compared to oil, CNG-vehicles represented a cost-effective option for the reduction of the overall CO_2 emissions (despite the consideration of the methane-slip). Towards the end of the observation period, once the emission targets became more restrictive, the CO_2 abatement costs of BEVs became lower, which is why CNG-vehicles were driven out. While the shift to CNG-vehicles represents a comprehensible model result, the new admissions of private vehicles over the last ten years suggest that a complete transition starting in 2020 is rather unlikely [240,241]. Instead, the German Federal Government is encouraging the introduction of BEVs and aims to increase their numbers to one million by 2020 [3]. However, according to [177], in 2018, BEVs accounted only for 54,000 vehicles, which could be a consequence of their still higher purchase price. Against this background, further calculations are presented in section 6.4.3, for which the deployment of CNG-vehicles is restricted.

In another analysis, the purchase price of BEVs was raised in steps of 10 % and the effects on the sector composition analysed. A price increase of 10 % corresponded to almost

3,000 €/*vehicle* and led to a reduction of BEVs from 100 % to 69 % in 2050, in favour of FCEVs. The share of FCEVs was increased to 81 % and 99 % if the purchase price of BEVs was raised by 20 % and 30 %, respectively. This behaviour revealed that the fleet composition is sensitive to the assumed vehicle prices. Although in case of the reference parameter setting BEVs account for 100 % of the vehicle fleet, it should be kept in mind that the gap to FCEVs is rather small. From this it can be concluded that they might become increasingly attractive especially if higher driving ranges are considered, which otherwise would require higher battery capacities. Another factor, which could favour the deployment of FCEVs is the import of synthetic fuels from abroad. This was shown in [113] and is further analysed in section 6.4.3. Against this background, a concurrent deployment of BEVs and FCEVs seems a viable option.

It was further investigated if the deployment of BEVs is affected by the consideration of a controlled vehicle charging. The results revealed that their deployment was increased even in the case when their purchase price was raised by 30 %, which corresponds to roughly 10,000 €/*vehicle*. According to the performed sensitivity analysis, especially the available discharge capacity for a possible power feedback into the grid plays a major role. By assuming a V2G factor of 0 %, 10 % and 25 %, the share of BEVs in 2050 was increased from 1 % to 19 % to 44 %, respectively. The flexible operation of vehicle batteries led to a gradual reduction of stationary batteries. In 2050, the installed capacity of stationary batteries was roughly cut by half once a CCSt share of 10 % and a V2G factor of 10 % was assumed. By increasing the V2G factor to 25 %, the deployment of stationary batteries was reduced by roughly two thirds. The analysis revealed that stationary batteries were replaced to a higher degree if a flexible charging and discharging of BEVs was considered. Even if there are no business cases for the flexible operation of BEVs yet [242, 243], it is likely to imagine that a certain share of users are willing to charge their vehicles when power surplus occurs and the electricity prices are lower.

Overall, the analysis showed that to achieve the set climate protection targets, a switch from conventional to alternative drive concepts is a cost-effective solution. For the motorised private road transport sector, which was studied in more detail, BEVs represent the dominant power train technology in 2050. This result is in line with other studies [16, 95], where the direct use of electricity is preferred over alternative fuels due to its higher primary efficiency. However, the analysis also revealed that the gap to FCEVs is rather small, as through the long-term storage capability of hydrogen, they indirectly increase the flexibility of the energy system. An alternative option to decouple the energy demand from the non-dispatchable generation of power is represented by the combination of heat generators with thermal energy storage systems. This concept is analysed in the next section.

6.3 Flexibility of Heat Generators and Thermal Energy Storage

As introduced in section 4.4, heat generators in REMod may either be operated according to a Heat-Controlled or Power-Controlled Strategy (HCSt, PCSt). How each operation mode affects the energy system is analysed through multiple model calculations. First, the deployment of heat generators with particular regard to electric heat pumps is investigated. After this, the operation of heating technologies is studied based on hourly resolved time series. The last section analyses the operation of thermal energy storage (TES) and shows how varying their capacity, may affect other load balancing options.

6.3.1 Role of Electric Heat Pumps for the Supply of Space Heat

Over the last years, multiple studies based on REMod analysed the cost-optimised deployment of heat generators for the supply of space heat and domestic hot water. For instance, [15] showed that especially electric air and brine heat pumps as well as heat grids represent the largest technology share in 2050. Their key role is also confirmed in [103, 106, 107, 113]. However, in each of these studies, a completely flexible operation of heat generators was assumed. As suggested by previous results in section 6.2.3, a grid supportive operation could favour the deployment of flexible technologies, such as electric heat pumps or heat grids. For this purpose, a calculation for which all heat generators are following a HCSt is performed. This means that heat generators are operated independently from the residual load and thus are not available as load balancing option. TES may still be deployed in combination with solar thermal systems (also within heat grids). Figure 6.17 shows the deployment of heat generators from 2015 to 2050 in case of a HCSt.

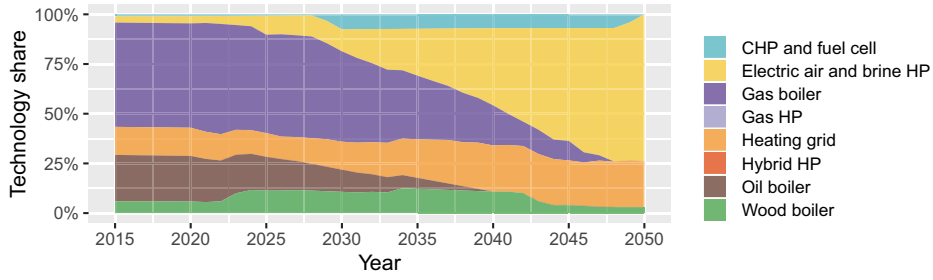

Figure 6.17: Development of the technology share for the supply of space heat and domestic hot water for a 85 % reduction of CO_2 emissions by 2050 compared to 1990 values. Heat generators are operated regardless of the residual load (Heat-Controlled Strategy). CHP: combined heat and power unit. HP: heat pump.

The illustrated development of heat generators in figure 6.17 appears similar to already known results, even though a HCSt is considered. Accordingly, today's dominant heat generators, oil and gas boilers, are both driven out as the CO_2 reduction targets become more ambitious. This is in part compensated by wood boilers, which slightly increase their share around 2022, when the first replacements of oil boilers take place. Their utilisation is again decreased around 2042, as biomass is more and more utilised for the production of process heat (cf. appendix D). Heat grids, which consist of a CCGT, a large scale electric heat pump, a methane-fired peak boiler, a TES and a solar thermal system, grow from 14 % in 2015 to 23 % in 2050. If a HCSt is assumed, their hourly heat demand share is primarily covered by the methane-fired CCGT units, meaning that electricity is produced concurrently. The same holds for micro-CHP units and fuel cells. Thus, there will be several hours during the year, when those technologies will generate electricity although power surplus already occurs. This unfavourable operation is why micro-CHP units and fuel cells are utilised from approximately 2030 to 2049. Similarly, electricity-based technologies will sometimes increase the electric load when the residual load is already positive. Nonetheless, the number of electric heat pumps increases substantially from 3 % in 2015 to 74 % in 2050. Their higher deployment, compared to heat generators with a CHP option, can be traced back to three factors. First, the performance factor of electric heat pumps is significantly higher than the thermal efficiency of other technologies with combined production of heat and power. This leads to a lower energy demand for a given amount of supplied heat. As a consequence, the load increase of electric heat pumps is - in relative terms - smaller than the power supply increase resulting from CHP units. Second, as the expansion of VRE continues, the carbon footprint of electricity-based heat generators gradually decreases and therefore electric heat pumps become more favourable. For CCGT power plants, CHP units or fuel cells, which are either run by methane gas or hydrogen, the carbon footprint could be reduced if synthetic fuels or biofuels were utilised. However, compared to the direct usage of renewable electricity, the generation of synthetic fuels or biofuels are technically more demanding. Third, especially towards the end of the observation period, the maximum value of power surplus (negative residual load) is higher than the maximum value of power deficiency (positive residual load). This is exemplarily shown in figure 6.18, where the minimum and maximum values of the residual load for a renewable energy share of 90 % amount to -233 GW_{el} and 114 GW_{el}, respectively. The illustrated development of the residual load is in a qualitative way confirmed by other studies, such as [17, 42, 59, 106]. From this, it could be concluded that a further increase of the negative residual load (due to combined production of heat and power) may on average lead to a higher demand for load balancing options, rather than vice versa.

In order to assess how robust the deployment of electric heat pumps is to a variation of their costs, two further calculations are performed. Similarly to the analysis performed

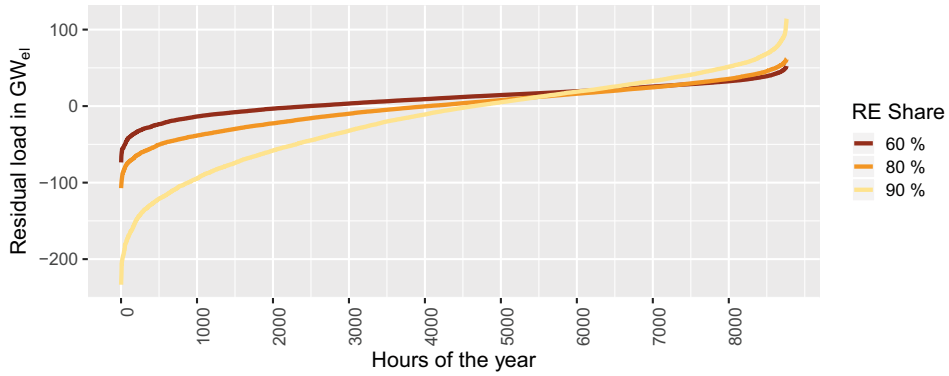

Figure 6.18: Sorted residual load curve in case of a Heat-Controlled Strategy for a renewable (RE) power generation share of 40 %, 60 %, 80 %, and 90 %. A negative value indicates a surplus of electricity and vice versa.

for the motorised private transport (cf. section 6.2.2), the purchase price of electric air and brine heat pumps is increased by 15 % and 30 % compared to the reference parameter setting. The obtained deployment of heat generators from 2015 to 2050 is presented in figure 6.19.

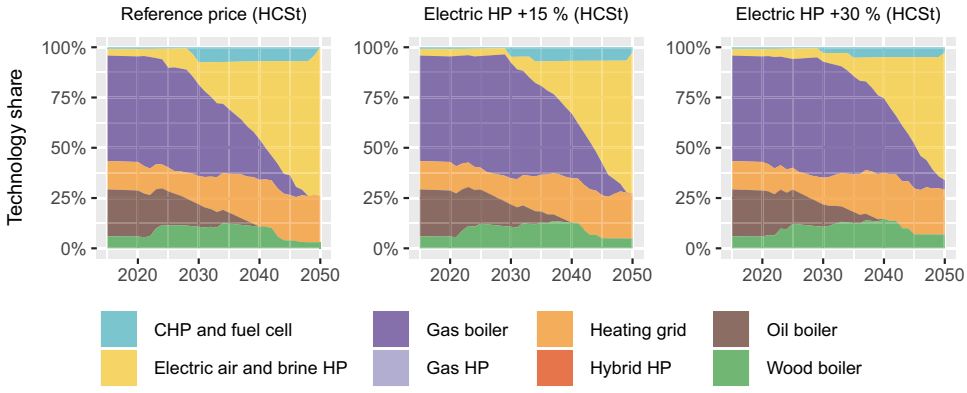

Figure 6.19: Cost sensitivity: Development of the technology share for the supply of space heat and domestic hot water for a 85 % reduction of CO_2 emissions by 2050 compared to 1990 values. Heat generators are operated regardless of the residual load (HCSt: Heat-Controlled Strategy). CHP: combined heat and power unit, HP: heat pump.

The illustrated results reveal that increasing the purchase price of electric heat pumps has a rather little influence on the deployment of heat generators. Although in 2050 their numbers are reduced by roughly one and two million units for a price increase of 15 % and 30 %, electric heat pumps still represent by far the dominant heating technology. At the same time, wood boilers, micro-CHP units and fuel cells are deployed to a slightly

higher degree. Further, the results show that if the purchase price of electric heat pumps is increased by 30 %, methane-fired boilers still persist in 2050, accounting for roughly 5 % of all heat generators (1.2 million units). These results are based on a HCSt which means that TES can only be used in combination with solar thermal systems. It is analysed if electric heat pumps are favoured once they follow a PCSt and thus have access to TES. For this purpose electric air and brine heat pumps are switched from a HCSt to a Power-Controlled Strategy (PCSt). Their purchase price is maintained at +30 % relative to the reference parametrisation. The resulting deployment of heat generators is shown in figure 6.20.

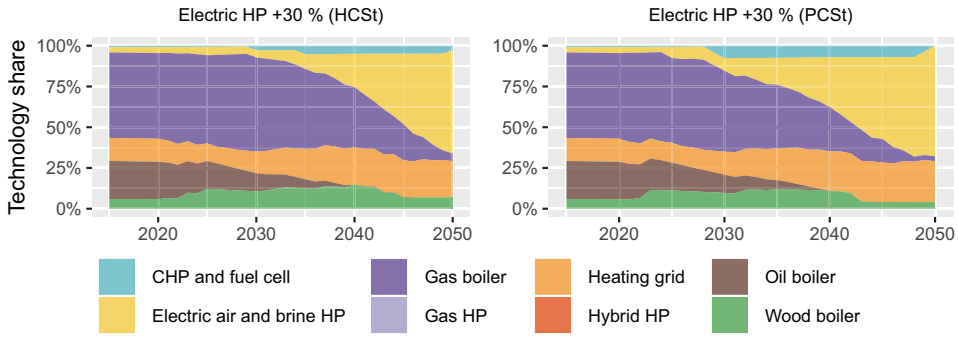

Figure 6.20: Development of the technology share for the supply of space heat and domestic hot water for a 85 % reduction of CO_2 emissions by 2050 compared to 1990 values. The purchase price of electric air and brine heat pumps is increased by 30 %. Left: all heat generators follow a Heat-Controlled Strategy (HCSt). Right: electric heat pumps are operated according to a Power-Controlled Strategy (PCSt). CHP: combined heat and power unit, HP: heat pump.

The illustrated development confirms that operating electric heat pumps according to a PCSt favours their deployment, even though only slightly. Compared to a HCSt, their numbers are increased by roughly one million (+ 4 %). As a consequence, micro-CHP units, fuel cells, wood boilers and methane gas fired boilers are decreased. Table 6.6 provides an overview of the technology shares in 2050 in the case that electric heat pumps are operated according to a HCSt or a PCSt and under variation of their purchase price.

Table 6.6: Summary of the technology share for the supply of space heat and hot water demand in 2050. HCSt/PCSt: Heat/Power-Controlled Strategy, HP: heat pump, CHP: combined heat and power.

Operative Strategy Purche price of electric HP		HCSt +0 %	HCSt +15 %	HCSt +30 %	PCSt +30 %
micro-CHP and fuel cell	%	0.0	2.5	2.6	0.1
gas and hybrid heat pump (HP)	%	0.0	0.0	0.0	0.0
heat grid	%	22.9	22.1	22.3	25.1
wood boiler	%	3.0	4.9	6.9	4.1
electric air and brine HP	%	74.1	70.4	63.5	67.7
gas boiler	%	0.0	0.2	4.7	3.0
oil boiler	%	0.0	0.0	0.0	0.0

The results obtained in this section show that electric heat pumps represent an important component of the energy system from different viewpoints. In 2050, their share varies between roughly 64 % and 74 % depending on the assumed purchase price and their operating mode. Heat grids represent the second largest technology share, ranging from 22 % to 25 %. If they are operated according to the residual load, heat grids can cope with power surplus by operating the electric heat pumps and with power deficiency by utilising the CCGT unit. Thus, it is expected that the number of buildings connected to heat grids will increase, once a PCSt is considered. This concept is analysed in more detail in the next section.

6.3.2 Assessment of a Power-Controlled Heat Generation

This section presents an analysis of the effects resulting from a HCSt and a PCSt on the energy system. The operation of heat generators and other technologies is assessed for both cases. For this purpose two calculations based on the reference parameter setting are performed. The resulting deployment of heat generators from 2015 to 2050 is shown in figure 6.21.

According to figure 6.21 the share of heat grids in 2050 is increased from 23 % to 31 % if a PCSt instead of a HCSt is considered. A PCSt allows them to contribute to balance the residual load regardless of whether it is positive or negative. Whenever power surplus occurs, heat grids may increase the overall electric load by operating large-scale electric heat pumps. In case of power deficiency they can produce heat and power via the CCGT unit. Moreover, if the heat demand of buildings connected to a heat grid is covered, but the residual load is not yet balanced, the operation of the electric heat pump or CCGT unit may be further increased. In this case, the occurring excess heat can be utilised to raise the temperature level of the TES. Besides heat grids, the only other implemented technology which can cope with power surplus and deficiency is the hybrid heat pumps. It is modelled as an electric air heat pump, which in case of power deficiency is switched

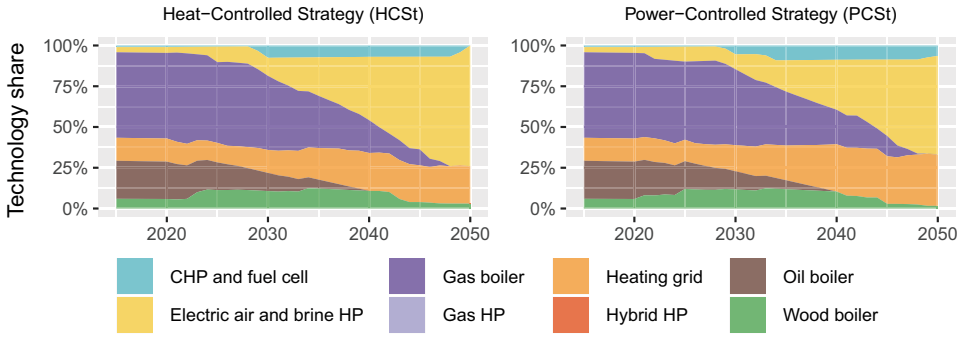

Figure 6.21: Development of the technology share for the supply of space heat and domestic hot water for a 85 % reduction of CO_2 emissions by 2050 compared to 1990 values. All heat generators either follow a Heat (HCSt) or a Power-Controlled Strategy (PCSt). CHP: combined heat and power unit.

to a fuel-based operation. This mechanism prevents a further increase of the electric load, which eventually would need to be covered by conventional thermal power plants. However, even though hybrid heat pumps are always operated according to a PCSt, they are not deployed. This is also the case if all other heat generators are operated in a heat controlled way (cf. figure 6.21). At the same time, electricity driven air heat pumps represent the dominant technology in 2050. While their unfavourable operation in times of power deficiency may lead to a higher electric load and thus increase the installed capacity of thermal power plants, their deployment overall results more cost-efficient.

To verify this, the heat production costs of two systems are compared to each other. The first system consists of a hybrid heat pump, while the second system is represented by a methane gas-fired thermal power plant, which is solely utilised to supply an electric air heat pump with power. The comparison is performed in times of power deficiency as in times of power surplus the hybrid heat pump would be operated like the electric air heat pump. This means that the hybrid heat pump utilises the gas unit and thus does not increase the electric load. It is further assumed that both systems may emit the exact same quantity of CO_2 m_{CO_2}. Thus, the available methane gas consumption of the hybrid heat pump or the thermal power plant E_{CH_4} is determined according to eq. 6.3. The heat supplied in either case $\dot{Q}_{th}$ depends on heat generator efficiency (η_{boiler} or COP) and, for the electric heat pump, also on power plant conversion efficiency η_{PP} (cf. eq. 6.4 and eq. 6.5). The electric load provided by the thermal power plant P_{PP} can be calculated as described by eq. 6.6, where P_{th} denotes the building and generator heat load (which is the same for both considered systems).

$$E_{CH_4} = {}^{m_{CO_2}}/_{f_{CH_4}} \tag{6.3}$$

$$\dot{Q}_{th,boiler} = E_{CH_4} \cdot \eta_{boiler} \tag{6.4}$$

$$\dot{Q}_{th,elHP} = E_{CH_4} \cdot \eta_{PP} \cdot COP \tag{6.5}$$

$$P_{PP} = \frac{\dot{Q}_{th,elHP}}{COP} \cdot \frac{P_{th}}{\dot{Q}_{th,elHP}} = \frac{P_{th}}{COP} \tag{6.6}$$

where:

E_{CH_4} = Methane gas consumption in $kWhCH_4$
$\dot{Q}_{th,boiler}$ = Generated heat from hybrid heat pump in kWh_{th}
$\dot{Q}_{th,elHP}$ = Generated heat from electric air heat pump in kWh_{th}
P_{th} = Building heat load in kW_{th}
P_{PP} = Electric load of thermal power plant in kW_{el}
m_{CO_2} = Total quantity of caused energy-related CO_2 emissions in t_{CO_2}
f_{CH_4} = Emission factor of methane gas in $^{kg_{CO_2}}/_{kWh_{CH_4}}$
η_{PP} = Electrical efficiency of thermal power plant in %
η_{boiler} = Thermal efficiency of gas unit (hybrid heat pump) in %
COP = Coefficient of performance in [−]

Based on this information, the costs for the hybrid heat pump C_{hybHP} and the for electric heat pump combined with a thermal power plant C_{elHP} can be calculated according to eq. 6.7 and 6.8, where p denotes the technology purchase price. Fuel costs are not accounted for as the comparison of both systems is performed for the same quantity of CO_2 emissions and thus methane gas consumption. As a result, the heat production costs $c_{HPC,hyb}$ and $c_{HPC,elHP}$ can be calculated as shown in eq. 6.9 and eq. 6.10. These costs can be subtracted from each other and the difference related to a the heat production costs resulting from the hybrid heat pump system. This is shown in eq. 6.11 where d_{HPC} denotes the relation of heat production costs between both systems.

$$C_{hybHP} = P_{th} \cdot p_{hybHP} \tag{6.7}$$

$$C_{elHP} = P_{th} \cdot p_{elHP} + \frac{P_{th}}{COP} \cdot p_{PP} \tag{6.8}$$

$$c_{HPC,hyb} = \frac{P_{th} \cdot p_{hybHP}}{\frac{m_{CO_2}}{f_{CH_4}} \cdot \eta_{boiler}} \tag{6.9}$$

$$c_{HPC,elHP} = \frac{P_{th} \cdot p_{elHP} + \frac{P_{th}}{COP} \cdot p_{PP}}{\frac{m_{CO_2}}{f_{CH_4}} \cdot \eta_{PP} \cdot COP} \tag{6.10}$$

$$d_{HPC} = \frac{c_{HPC,hbyHP} - c_{HPC,elHP}}{c_{HPC,hbyHP}} = 1 - \frac{p_{PP} + \frac{p_{PP}}{COP}}{\eta_{PP} \cdot \eta_{elHP}} \cdot \frac{\eta_{boiler}}{p_{hybHP}} \tag{6.11}$$

where:

P_{th}	= Building heat load in kW_{th}
P_{PP}	= Electric load of thermal power plant in kW_{el}
m_{CO_2}	= Total quantity of caused energy-related CO_2 emissions in t_{CO_2}
f_{CH_4}	= Emission factor of methane gas in $^{kg_{CO_2}}/_{kWh_{CH_4}}$
η_{PP}	= Electrical efficiency of thermal power plant in %
η_{boiler}	= Thermal efficiency of gas unit (hybrid heat pump) in %
COP	= Coefficient of performance in [−]
p_{hybHP}	= Specific purchase price of hybrid heat pump in $^{€}/_{kW_th}$
p_{elHP}	= Specific purchase price of electric heat pump in $^{€}/_{kW_th}$
p_{PP}	= Specific purchase price of thermal power plant in $^{€}/_{kW_{el}}$
C_{hybHP}	= Costs for the hybrid heat pump in €
C_{elHP}	= Costs for the electric air heat pump and the thermal power plant in €
$c_{HPC,hyb}$	= Heat production costs of the hybrid heat pump in $^{€}/_{kWh_th}$
$c_{HPC,elHP}$	= Heat production costs of electric heat pump and power plant in $^{€}/_{kWh_th}$
d_{HPC}	= Heat production costs related to hybrid heat pump in %

As shown in eq. 6.11, the relation in heat production costs only depends from the technology efficiencies and their purchase prices which in the model calculations represent exogenously set parameters[7]. Based on the current parametrisation the heat generation costs of an electric heat pump combined with gas turbine power plant are 16 % lower than those resulting from a hybrid heat pump. For CCGT plants this value amounts to 39 % in favour of the electric heat pump, explaining why under consideration of limited CO_2 emissions hybrid heat pumps are not part of the model results. It is further noted that the power demand of the electric heat pump could also be supplied by power storage systems, the conversion of biomass into electricity or other, more CO_2-neutral technology options. This would favour the deployment of electric air heat pumps even more.

[7] Assumptions: methane fired GT power plant: 385 $^{€}/_{kW_{el}}$ and $\eta_{el} = 40\,\%$, methane fired CCGT power plant: 700 $^{€}/_{kW_{el}}$ and $\eta_{el} = 63\,\%$, electric air heat pump: 640 $^{€}/_{kW_{th}}$ and performance factor = 3 (while the performance factor of electric heat pumps is calculated on an hourly basis, this value represents an approximation of the yearly average efficiency), hybrid heat pump: 737 $^{€}/_{kW_{th}}$ and $\eta_{th,gas-unit} = 97\,\%$, emission factor of methane gas: 0.202 $^{g_{CO_2}}/_{kWh_{CH_4}}$. Further information is listed in Appendix A.

Figure 6.21 also shows that if a PCSt is considered, micro-CHP units and fuel cells do no longer represent an interim technology. In this case, they still persist in 2050, with a relative share of 6.4 %. Technologies with a combined generation of heat and power can complement the production of electricity from thermal power plants in times when the residual load is positive. This is why in case of a PCSt, the cumulative installed capacity of the thermal power plant park is reduced by roughly 23 GW_{el} (13 %). The contribution of flexible power generation from heat grids, micro-CHP units and fuel cells is especially pronounced when the residual load exhibits its maximum value, i.e. when the maximum power deficiency occurs.

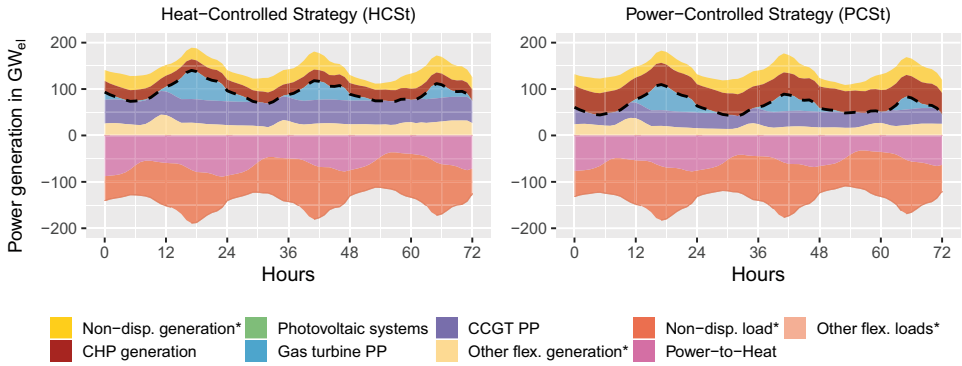

Figure 6.22: Power supply and demand for three days in December 2050. Maximum value of the residual load (dashed line) in hour 17. Non-dispatchable generation*: Excludes heat generators with combined supply of heat and power and photovoltaic systems. Non-dispatchable load*: Excludes electricity-based heat generators (Power-to-Heat). Other flexible loads*: includes stationary batteries, vehicles batteries, pumped-storage power plants (PP), Power-to-Gas and Power-to-Fuel, export of electricity and curtailment. Excluded are electric heat pumps and heating rods (Power-to-Heat). Other flexible generation*: includes stationary batteries, vehicles batteries, pumped-storage PP, biomass power generation, oil PP, lignite PP, hard coal PP and electricity imports. Excluded are heat generators with combined generation of heat and power, gas turbine (GT) PP and combined cycle gas turbine (CCGT) PP. Underlying weather data: 2014.

Figure 6.22 shows the power supply and demand for three days in December 2050, where the maximum value of the residual load occurs (hour 17). Due to a different system configuration and operation mode of heat generators, it amounts to 140 GW_{el} if a HCSt is considered and to 110 GW_{el} otherwise. The illustration shows that in the first case, the supply of power is mainly provided by CCGT (violet) and peak load GT power plants (blue). If a PCSt is assumed, the power generation from heat grids as well as micro-CHP units and fuel cells (red) substantially contributes to the overall generation of electricity. For a HCSt, the supply of power from CCGT, GT power plants and heat

generators with CHP option in hour 17 amounts to 61 GWh_{el}, 51 GWh_{el} and 24 GWh_{el}. If a PCSt is assumed, these numbers change to 55 GWh_{el}, 34 GWh_{el} and 47 GWh_{el}. The additional 23 GW_{el} produced by heat generators match the reduced installed capacity of thermal power plants, once more underlining their contribution as load balancing option. In case of power surplus, electricity-based heat generators may increase the electric load. The minimum residual load value in 2050 occurs at the end of March. The power supply and demand for three days during this period are illustrated in figure 6.23.

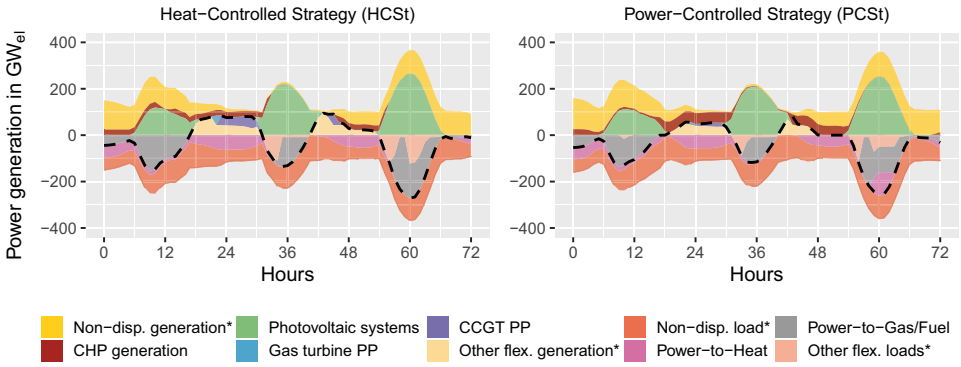

Figure 6.23: Power supply and demand for three days in March 2050. Minimum value of the residual load (dashed line) in hour 60. Non-dispatchable generation*: Excludes heat generators with combined supply of heat and power and photovoltaic systems. Non-dispatchable load*: Excludes electricity-based heat generators (Power-to-Heat). Other flexible loads*: includes stationary batteries, vehicles batteries, pumped-storage power plants (PP), export of electricity and curtailment. Excluded are electric heat pumps (HP), heating rods (Power-to-Heat), Power-to-Gas and Power-to-Fuel. Other flexible generation*: includes stationary batteries, vehicles batteries, pumped-storage PP, biomass power generation, oil PP, lignite PP, hard coal PP and electricity imports. Excluded are heat generators with combined generation of heat and power (CHP), gas turbine (GT) PP and combined cycle gas turbine (CCGT) PP. Underlying weather data: 2014.

The depicted three day period shown in figure 6.23 is characterised by frequent fluctuations of the residual load. It is negative especially during the midday hours, when the feed-in from photovoltaic stations is particularly pronounced. In this case, if a PCSt is assumed, electricity-based heat generators can contribute to the balancing of the residual load and increase the temperature of the TES. Once power deficiency occurs, the TES system is discharged and thus the electric load reduced. This is for example shown in figure 6.23 around hour 18. At this time, the electric load of Power-to-Heat technologies amounts to roughly 37 GW_{el} in case of a HCSt and to only 7 GW_{el} for a PCSt. This is also why the residual load is higher when a HCSt is considered and as a consequence, thermal power plants are operated on a larger scale. The minimum value of the residual

load occurs at the third day illustrated in figure 6.23, in hour 60. In case of a HCSt, approximately 150 GW_{el} out of 272 GW_{el} of surplus power are converted into synthetic gases and liquid fuels by PtG and PtL plants. Conversely, if a PCSt is assumed 102 GW_{el} of the total electricity surplus (258 GW_{el}) are converted into heat and stored in TES. In this case, the amount of power utilised for the production of synthetic fuels is reduced to 111 GW_{el}. Due to the utilisation of electricity for the conversion into heat at peak load times, the installed capacity of electrolysis plants in 2050 is reduced by roughly 26 % corresponding to 39 GW_{el} (cf. figure 6.24). Overall, this increases their full load hours by roughly 1,500 hours per year. From this it can be concluded that by exploiting the flexibility of heat generators and thus contributing to the balancing of the residual load, other system components can be operated more cost-efficiently. Moreover, the added flexibility for the supply of space heat and domestic hot water allows the deployment of additional inflexible, electricity-based technologies for the generation of process heat (cf. appendix D). This is a further example showing the sector coupling effects considered by the model.

A PCSt also influences the installed capacity of stationary batteries. As previously shown in section 6.2.3, their capacity heavily depends on whether other load balancing options are able to cope with only power surplus, power deficiency or both. In order to verify this trend, two more calculations are performed. In one case, only electricity-based technologies, i.e. electric heat pumps and heating rods, are switched to a PCSt. In the other case, a PCSt is applied only to heat generators with the possibility of combined heat and power generation (CCGT, micro-CHP units and fuel cells).

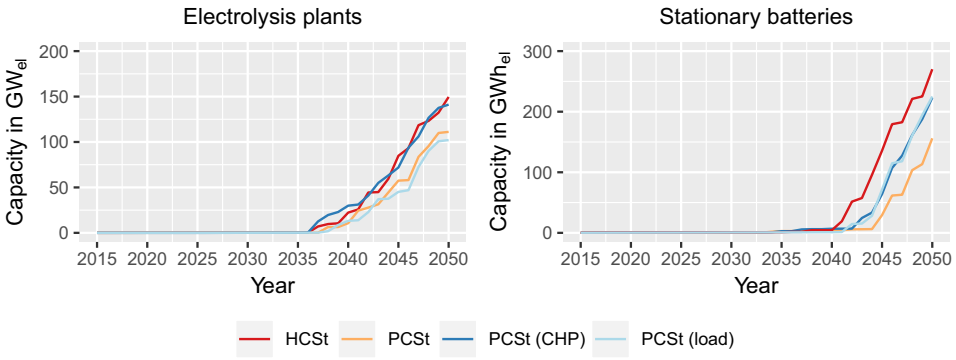

Figure 6.24: Development of the installed capacity of electrolysis plants and stationary batteries for a 85 % emission reduction by 2050 compared to 1990 values in case of a Heat-Controlled or Power-Controlled Strategy (HCSt or PCSt). PCSt (CHP): only CCGT units, micro-CHP units and fuel cells are set to a PCSt, PCSt (load): only electric heat pumps and heating rods are set to a PCSt.

Figure 6.24 shows the installed capacity of stationary batteries over the time period from 2015 to 2050. Compared to a HCSt, if heat generators serve as load balancing option either only in case of power surplus or deficiency, the installed capacity of stationary batteries starts a few years later and is roughly 46 GWh_{el} (17 %) lower in 2050. If all heat generators follow a PCSt, the installation of stationary batteries is further delayed by 10 years, reaching a value of 156 GW_{el} in 2050. This is 42 % lower compared to a HCSt. While the capacity of power storage systems is decreased if a PCSt is assumed, TES are deployed on a larger scale. The reason why is that, beside by solar thermal systems, they can also be charged by electricity-based technologies or heat generators with combined production of heat and power. Thus, a higher installed capacity of TES indirectly increases the load balancing potential of heat generators. A more detailed analysis of their operation is presented in the next section.

6.3.3 Operation of Thermal Energy Storages

Whether or not and to what extent a heat system in REMod is equipped with TES or a solar thermal system is endogenously determined, as it has been described in section 3.2.4. Figure 6.25 shows how their installed capacities are affected by the consideration of a HCSt and PCSt.

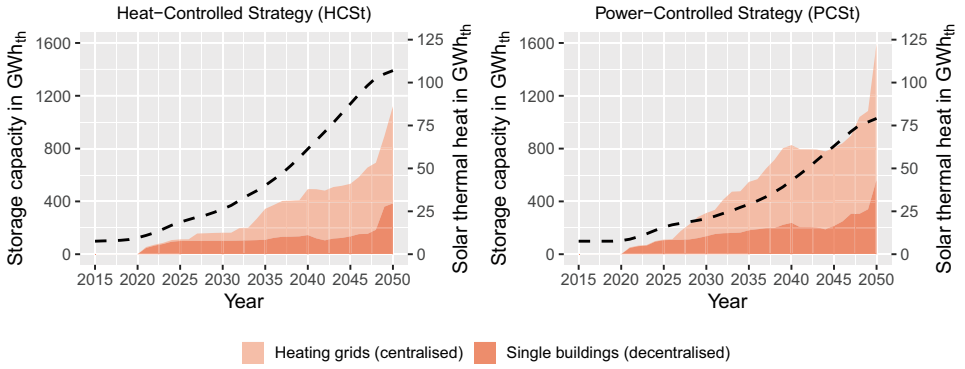

Figure 6.25: Development of the installed capacity of thermal energy storages for single buildings and heat grids. The dotted line represents the total installed capacity of solar thermal systems.

As shown, if a HCSt is considered, the TES system capacity reaches a value of 1121 GWh_{th} in 2050. Conversely, in case of a PCSt it is increased by 42 %, amounting to 1595 GWh_{th}. This is because not only solar thermal systems, but also other heat generators may provide a major contribution to the charging of TES. This, for instance, may occur when electricity-based heat generators increase their load to balance a surplus of electricity or when generators with a CHP option increase their power supply in case of power

deficiency. An exemplarily temperature profile for an electric air heat pump system in 2050 is represented in figure 6.26.

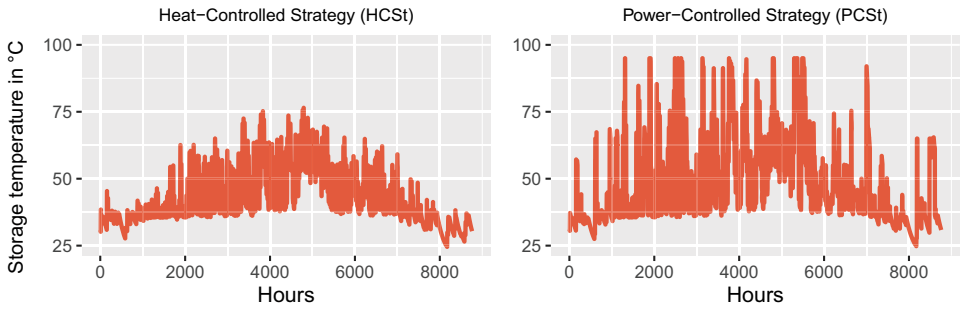

Figure 6.26: Exemplarily temperature profile in 2050 of an electric air heat pump system (panel heating) in case of a heat-controlled or power-controlled operation of heat generators.

While the temperature profiles shown in figure 6.26 exhibit high fluctuations in case of a PCSt, they are less pronounced when a HCSt is considered. The overall higher temperatures reached in case of a PCSt underline that TES is frequently charged not only by solar thermal systems and electric heat pumps but also by heating rods as they can raise the storage temperature up to 95 °C. Since TES temperature for a HCSt can only be increased by solar thermal systems, their installed capacity in 2050 (107 GWh_{th}) results 28 GWh_{th} higher than for a PCSt. This suggests that, to some extent, solar thermal systems counterbalance the lacking flexibility of heat generators. From this, it can be concluded that if a PCSt is considered, solar thermal systems should primarily be combined with gas boilers, as electricity-based heat generators exhibit greater synergies with photovoltaic systems. If a HCSt is considered instead, solar thermal systems could contribute to reduce the electric load of an air heat pump, which is beneficial if power deficiency occurs. This is for example shown in figure 6.27. Here, the supply and demand of power as well as the storage temperature of an electric air heat pump system is illustrated for a three day period in March 2050.

The depicted three day period exhibits regular fluctuations of the residual load, with its minimum value on the third day in hour 60. As previously mentioned, if a HCSt is considered, the storage temperature of electric air heat pump systems is only raised by solar thermal systems. This is shown in figure 6.27 (bottom, left), especially during the midday hours. In this case, the storage temperature is increased proportionally to the power supply from photovoltaic systems (green), which is also linked to the solar radiation. Once the residual load changes from a negative to a positive value, the TES is discharged and the remaining heat demand is provided by the electric air heat pump. In case of a PCSt, the storage temperature is visibly higher, especially at the beginning of the illustrated period (until hour 18). Accordingly, beginning in hour 18, the TES covers

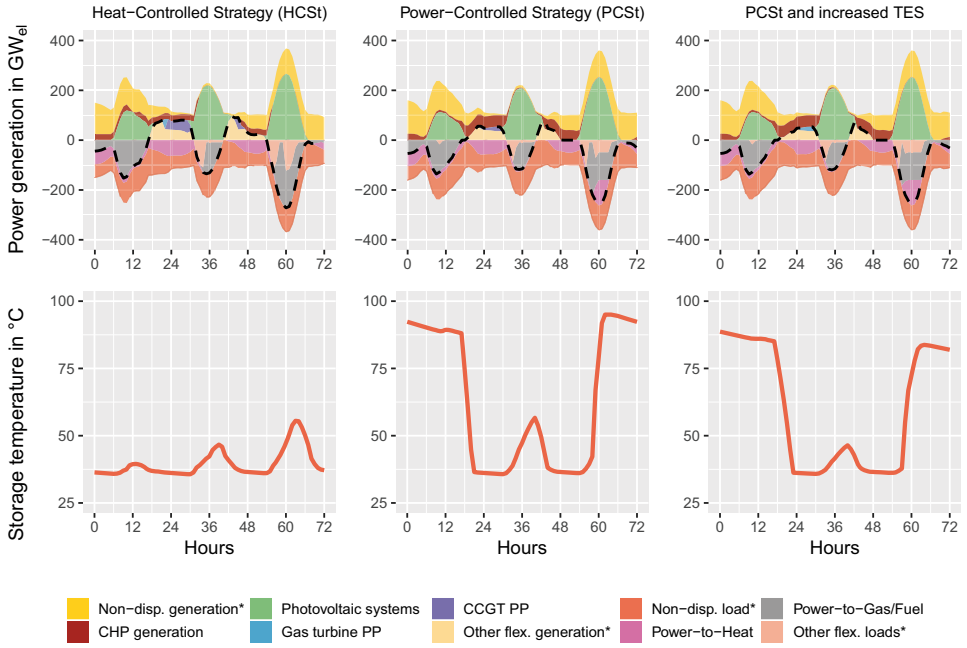

Figure 6.27: Power supply and demand and storage temperature of an electric air heat pump system for three days in March 2050. In the third figure (PCSt and increased TES), the endogenously determined TES capacity of the PCSt case is doubled. Non-dispatchable generation*: Excludes heat generators with combined supply of heat and power and photovoltaic systems. Non-dispatchable load*: Excludes electricity-based heat generators (Power-to-Heat), Power-to-Gas and Power-to-Fuel. Other flexible loads*: includes stationary batteries, vehicles batteries, pumped-storage power plants (PP), export of electricity and curtailment. Excluded are electric heat pumps and heating rods (Power-to-Heat). Other flexible generation*: includes stationary batteries, vehicles batteries, pumped-storage PP, biomass power generation, heat generators with combined generation of heat and power, oil PP, lignite PP, hard coal PP and electricity imports. Excluded are gas turbine (GT) PP and combined cycle gas turbine (CCGT) PP.

a higher share of the occurring heat demand. This leads to a more pronounced decrease of the electric load, otherwise arising from Power-to-Heat technologies. As a consequence, the electricity demand covered by GT and CCGT power plants results lower if a PCSt is considered (cf. figure 6.27, middle, hour 28). The storage temperature raises again around hour 56, when power surplus occurs. Here, electric heat pumps are operated first, while heating rods are utilised to increase the TES temperature until 95 °C. In the third calculation (figure 6.27, right) the endogenously determined storage capacity in case of a PCSt is doubled, while the remaining system configuration is kept identical. As a consequence, the TES temperature and its gradient are in general both slightly lower.

This is particularly visible once the TES is discharged for the first time. In the reference case (middle), the discharge process starts from 88 °C and lasts for roughly four hours. If the TES capacity is doubled (right) its temperature amounts to 85 °C, while the discharge time amounts to six hours. This means that the load increase provided by Power-to-Heat technologies is further delayed by two hours (cf. figure 6.27, middle and right, hours 18 to 24). The doubled TES size also affects the operation of thermal power plants. For instance, in hour 25, CCGT power plants are operated in case of a PCST (middle), while GT power plants for an increased TES (right). Another difference concerns the demand of electricity. During hour 60, when the highest electricity surplus over the year occurs, a larger part of power is converted into heat and stored in the TES. The higher storage capacity leads to a slower temperature increase, which is why electric heat pumps convert a higher amount of electricity into heat. The less efficient heating rods can be utilised at a later point to raise the temperature up to 95 °C. However, as depicted in figure 6.27 (right), due to the doubled TES capacity, its maximum temperature in hour 62 is not reached.

The illustrated example shows that by increasing the TES capacity, more power can be converted into heat, if a PCSt is considered. Figure 6.28 reveals that this affects the electricity exchange with neighbouring countries as well as the curtailed amount of power. The depicted quantities of electricity import, export and curtailment represent average values over the whole time period from 2015 to 2050. Further it is noted that the system configurations in case of a HCSt and PCSt are slightly different, as they are both endogenously determined. For instance, as previously shown, the installed capacity of stationary batteries is higher in case of a HCST. Thus, while the illustrated values provide insight about the effects resulting from a HCSt or a PCSt, there may be other factors which have to be accounted for.

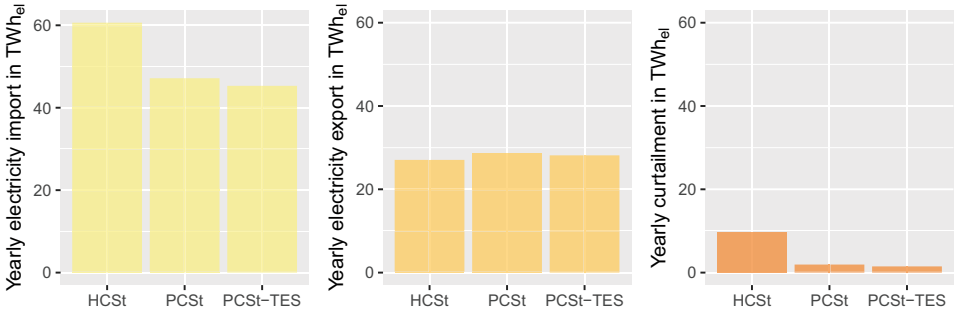

Figure 6.28: Cumulative import, export and curtailment of electricity from 2015 to 2050. HCSt/PCSt: Heat/Power-Controlled Strategy. In PCSt-TES the endogenously determined TES capacity of the PCSt case is doubled.

According to figure 6.28, the import of electricity is on average 13 TWh_{el} lower if a PCSt instead of a HCSt is assumed. This can in part be traced back to the flexible operation of CCGT units in heat grids as well as micro-CHP units and fuel cells. Whenever power deficiency occurs and the heat demand is met, they may still increase their operation and use excess heat to charge the TES. Therefore, if the storage capacity is doubled, the average electricity imports are further reduced by 2 TWh_{el}. The export of electricity results almost equal in all three cases, with values of 27 TWh_{el}, 29 TWh_{el} and 28 TWh_{el}. Conversely, the curtailed power amounts to 10 TWh_{el} for a HCSt, 2 TWh_{el} for a PCSt and 1 TWh_{el} if the TES capacity is doubled. According to the operational sequence in the case of electricity surplus, power is first converted into heat by electric heat pumps, then exported, then converted into heat by less efficient heating rods and only curtailed as last option. This result suggests that in case of power surplus heating rods allow for a higher increase of the electric load compared to heat pumps. One reason for this is that the conversion efficiency of electric heat pumps is higher, which means that their electricity demand for an equal supply of heat is lower. Another reason is that while the supply temperature of electric heat pumps is limited to 65 °C, heating rods may increase the TES temperature up to 95 °C and thus have access to a higher storage capacity. Overall, the results show that a PCSt leads to a higher utilisation of surplus power on the one hand and to a decrease of the electric load on the other hand.

6.3.4 Summary and Conclusions

This section presented an assessment of technologies for the supply of space heat and domestic hot water, with particular regard to their load balancing potential. For this purpose, multiple calculations under consideration of a heat- (HCSt) or power-controlled operation (PCSt) were assessed.

Previous studies performed with REMod showed that electric heat pumps represent the dominant heat generators by 2050 if a PCSt is assumed. This statement was confirmed also for a HCSt. In this case, the share of electric air and brine heat pumps in 2050 amounted to roughly 74 %. While in this analysis no inhibiting factors which could limit their installations were considered, this will be investigated in section 6.4.1. Instead, uncertainties concerning the costs of electric heat pumps were accounted for in form of a sensitivity analysis. The results revealed that even if the purchase price of electric air heat pumps was increased by 30 %, their share at the end of the observation period amounted to roughly 64 %. Such a price increase would mean that their costs in 2050 would almost have remained unchanged compared to 2020 values (900 €/kW_{th}). According to [244–247] this is rather unlikely as the authors expect improvements in the conversion efficiency of heat pumps as well as a reduction of their costs.

In another analysis the deployment of heat generators in case of a PCSt was investigated. It was shown that, compared to a HCSt, micro-CHP units and fuel cells as well as heat grids increased their shares in 2050 by roughly 7 % each. Especially heat grids played a larger role, as they could contribute to the balancing of the residual load for both cases, power surplus and deficiency. Another implemented heat generator able to cope with both positive and negative residual loads is the hybrid heat pump. Despite that, hybrid heat pumps were not deployed in any of the performed model calculations. A qualitative cost assessment revealed that for a fixed amount of CO_2 emissions, it is cheaper to operate electric air heat pumps, even if this may lead to a higher installed capacity of thermal power plants[8]. It is noted that this analysis was performed under consideration of the model objective, which is to determine a cost-optimised system configuration for a defined limit of CO_2 emissions. A cost-oriented evaluation of hybrid heat pumps, which accounts for the single operator point of view, could result in a different conclusion [248, 249].

Besides affecting the installations of heat generators, the consideration of a HCSt or PCSt revealed to influence the deployment of other load balancing options. For instance, the installed capacity of thermal power plants in 2050 was reduced by 23 GW_{el} if a PCSt was assumed. In this case, micro-CHP units, fuel cells as well as CCGT in heat grids provided a greater contribution to the supply of power in times of power deficiency. On the other hand, it was revealed that the conversion of surplus power into heat was primarily utilised for peak shaving purposes. This reduced the deployment of PtG and PtL plants by roughly 40 GW_{el}, as in case of power surplus they competed with electricity-based heat generators. As a consequence, their full load hours were increased by 1500 $^{hours}/_{year}$, leading to a more cost-efficient operation. Further, the analysis showed that a PCSt led to a more efficient usage of power, reducing the curtailed electricity as well as the power imports from neighbouring countries. While the installed capacity of stationary batteries was reduced by 42 %, TES systems followed the opposite trend. It was shown that for heat grids the cumulative TES capacity in 2050 was increased by 40 % if a PCSt was assumed. For single buildings it was raised by 46 %, amounting to 571 GWh_{th} in 2050. Assuming 27 million buildings in Germany by 2050, an average temperature difference within the TES of 45 K and a 30 % share of buildings supplied by heat grids, this led to an average TES size ranging between 390 $^{litres}/_{building}$ and 570 $^{litres}/_{building}$ for a HCSt and a PCSt, respectively.

[8] This hypothesis will be verifyied in section 6.4.1, where the market shares of electric heat pumps and BEVs are both restricted.

6.4 The Value of Demand-Side Management

This chapter presents an assessment of the residual load oriented operation of electricity-based vehicles and heat generators, hereinafter referred to as demand-side management (DSM). Based on previous results (cf. section 6.2.3 and 6.3), BEVs and electric heat pumps play a major role to achieve the set climate protection targets. Further, they represent the main DSM options within their respective sectors. In order to determine how valuable they are for the energy system, their market shares are restricted in the first analysis. In the following section, uncertainties resulting from a variation of meteorological data are assessed. For this purpose, multiple calculations based on different weather data are performed. It is also investigated how the system deals with extreme weather conditions, during which the power supply from VRE is set to zero for an entire month. The contribution of DSM and other load balancing options to overcome this period are analysed. Lastly, a cost assessment is performed and the value of DSM determined in a qualitative and quantitative way. For this purpose, five different CO_2 reduction targets are investigated, starting from 65% up to 95%. Moreover, the import of synthetic fuels from abroad is considered and effects on the utilisation of DSM are assessed. Unless otherwise stated, all system costs presented in this section are related to a business-as-usual case, which from 2015 to 2050 amounts to 2,900 billion euros. In this scenario, the current system configuration is kept the same over the entire observation period. However, the legally decided withdrawal from nuclear power by 2022 [250] as well as the planned phase out of coal power plants by 2035 [23] are still considered.

6.4.1 Restriction of Key Technologies

Based on the results obtained so far, in 2050, BEVs and electric heat pumps represent the key technologies in the motorised private transport and the supply of space heat and domestic hot water. The effects resulting from a limitation of their respective deployment are analysed in this section. For this purpose, the yearly market share of BEVs is set to 50 % according to [113], while for electric heat pumps it is restricted to 19 % as suggested in [251]. The calculations are performed with and without the consideration of DSM for an 85 % and a 95 % CO_2 reduction target. However, due to the introduced technology restrictions, the system is unable to meet the emission reduction target of 95 % compared to 1990 values. As a consequence, only the results for the 85 % reduction case are discussed. The system behaviour for a gradual increase of the considered CO_2 reduction target is analysed in section 6.4.3.

The obtained development of the motorised private road transport in the 85 % reduction scenario reflects the results presented in chapter 6.2.3. Accordingly, first liquid fuel-based internal combustion engines are replaced by CNG-vehicles, which are then substituted by

BEVs and FCEVs. This outcome is confirmed regardless of whether DSM is considered or not (cf. appendix E). Greater differences occur for the deployment of heat generators for the supply of space heat and domestic hot water. This is shown in figure 6.29.

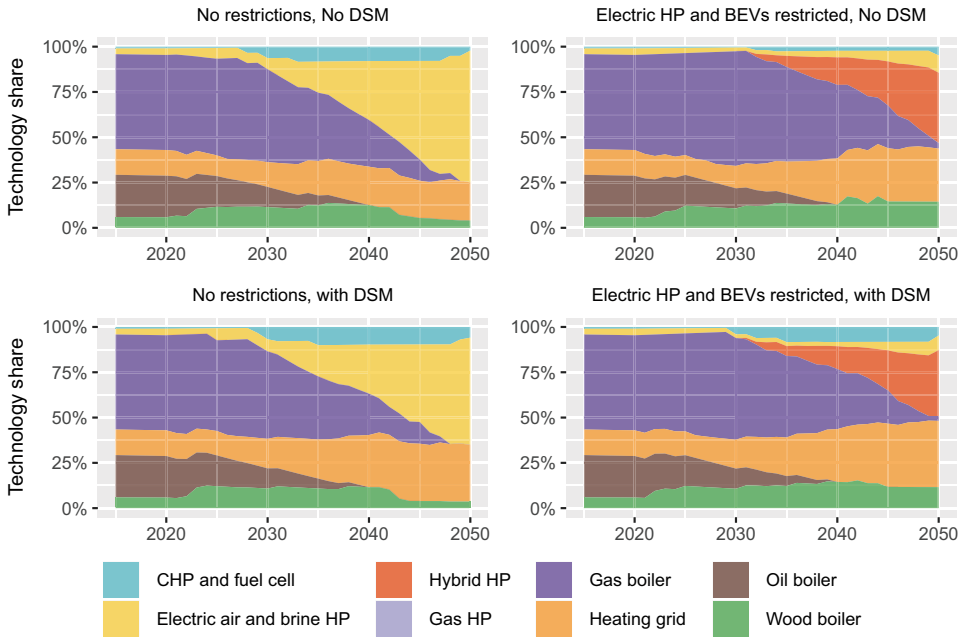

Figure 6.29: Development of the technology share for the supply of space heat and domestic hot water for a CO_2 emission reduction of 85 % by 2050 compared to 1990 values. The yearly technology market share of electric heat pumps (HP) and battery electric vehicles (BEVs) is limited to 19 % and 50 % on the right side. Demand-side management (DSM) describes a controlled charging behaviour of BEVs and a power-controlled operation of heat generators.

The illustrated results obtained without any restrictions in market share, for the most part show known developments to section 6.3. This, for instance, concerns the dominant share of electric heat pumps in 2050 and the increasing deployment of heat grids, CHP-units and fuel cells in the case dor which DSM is considered. Another example is the shift of biomass from the generation of space heat to the supply of process heat around 2042. If the deployment of electric heat pumps is limited (cf. figure 6.29, right), the number of wood boilers remains relatively constant after 2025, exhibiting a total share in 2050 of roughly 13 %. By utilising more biomass for the supply of space heat and domestic hot water, a part of the CO_2 emissions caused by other heat generators, such as CCGT units or hybrid heat pumps, are counterbalanced. According to previous results (cf. section 6.3.1), hybrid heat pumps were not deployed at all, even when the purchase price of purely electrically driven heat pumps was increased by 30 % . It was shown that the installation of electric air heat pumps overall reduces the CO_2 abatement costs, even

though the utilisation of hybrid heat pumps might decrease the installed capacity of the thermal power plant park. This is confirmed in figure 6.30, where it is shown that the introduction of hybrid heat pumps leads to a smaller installed capacity of thermal power plants[9].

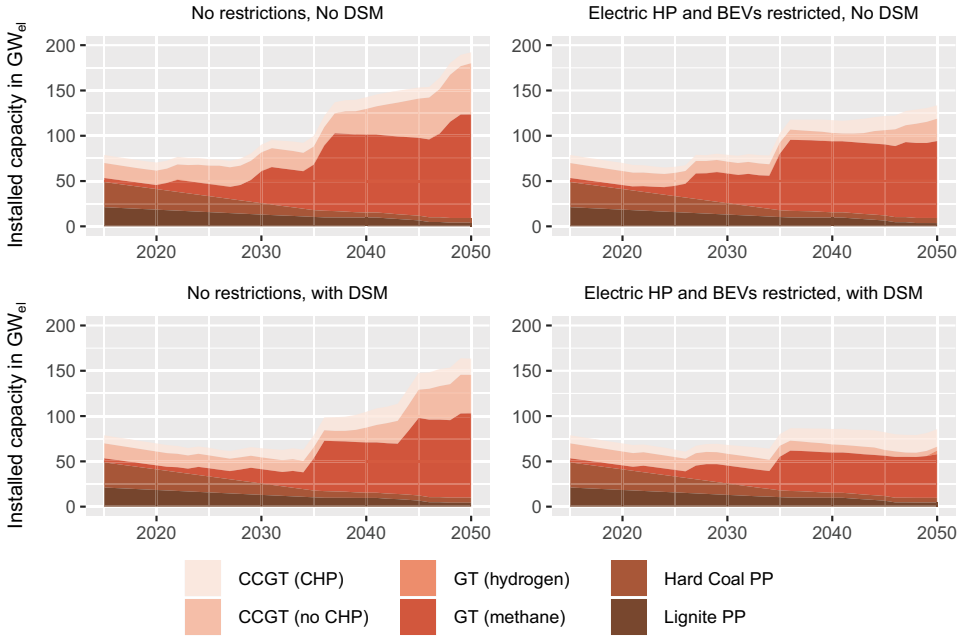

Figure 6.30: Development of the installed capacity of thermal power plants for a CO_2 emission reduction of 85 % by 2050 compared to 1990 values. The yearly technology market share of electric heat pumps (HP) and battery electric vehicles (BEVs) is limited to 19 % and 50 % on the right side. Demand-side management (DSM) describes a controlled charging behaviour of BEVs and a power-controlled operation of heat generators.

The installed capacity of thermal power plants reaches its maximum value of 190 GW_{el} in 2050 if neither market share restrictions nor DSM are considered. In this case, a substantial part of the heat demand and the vehicle drive power are based on electricity. This power demand can not be shifted in time by DSM, leading to high electric loads especially during the winter months and an accordingly high installed capacity of thermal power plants. By assuming DSM, BEVs and heat generators contribute to the balancing of the residual load curve. As a consequence, the cumulative installed capacity of thermal power plants in 2050 decreases by 20 GW_{el} to 170 GW_{el}. This value is even further reduced if hybrid heat pumps are installed instead of electric air heat pumps. This is because in times of power deficiency they can reduce the electrical load by switching

[9] The steep increase of GT in 2035 reults from the fact that, beginning in this year, coal power plants mainly function as reserve capacity systems, without providing a constant generation of electricity. This leads to a higher deployment of flexible thermal power plants (cf. section 6.1.1).

from an electricity-based to a methane gas-based operation. Compared to the sole consideration of DSM, the introduction of hybrid heat pumps reveals to have a greater impact on the decrease of the thermal power plant park. Accordingly, by combining both options, the lowest installed capacity of thermal power plants is achieved. In this case, it remains comparable to today's capacity levels (cf. figure 6.30, bottom right). The composition of thermal power plants still varies significantly over time, favouring plants with shorter start-up times.

The effect on power demand and supply resulting from the introduction of hybrid heat pumps is shown in figure 6.31, illustrating an exemplarily time series during winter 2050. On the left side, the market share of BEVs and electric heat pumps ranges from zero to 100 %, while being restricted to 50 % and 19 % respectively on the right side.

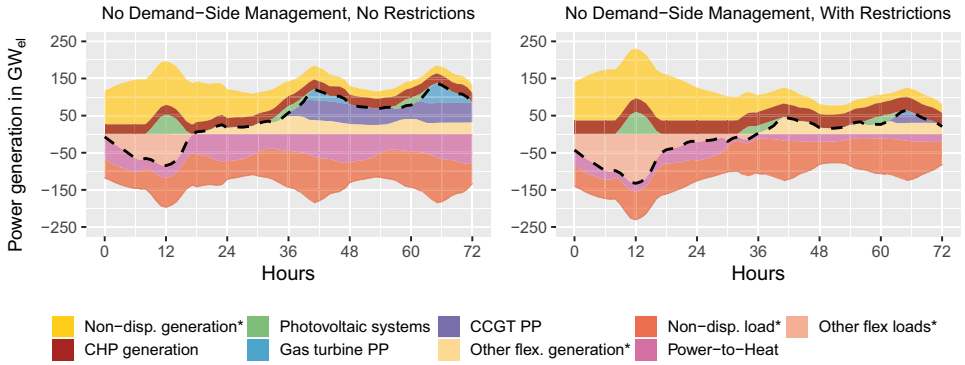

Figure 6.31: Exemplarily time series in January 2050 with and without technology restrictions. The dashed line represents the residual load. The yearly technology market share of electric heat pumps and battery electric vehicles is limited to 19 % and 50 % on the right side. Both calculations are performed without Demand-Side-Management for a CO_2 emission reduction of 85 % CO_2 by 2050 compared to 1990 values. Non-dispatchable generation*: Excludes heat generators with combined supply of heat and power and photovoltaic systems. Non-dispatchable load*: Excludes electricity-based heat generators (Power-to-Heat). Other flexible loads*: includes stationary batteries, vehicles batteries, pumped-storage power plants (PP), Power-to-Gas and Power-to-Fuel, export of electricity and curtailment. Excluded are electric heat pumps and heating rods (Power-to-Heat). Other flexible generation*: includes stationary batteries, vehicles batteries, pumped-storage PP, biomass power generation, heat generators with combined generation of heat and power, oil PP, lignite PP, hard coal PP and electricity imports. Excluded are gas turbine (GT) PP and combined cycle gas turbine (CCGT) PP.

By comparing the two depicted three day periods, it is observed that without considering market share restrictions or DSM, power surplus occurs until sunset of the first day (around hour 17). If market share restrictions are introduced power surplus lasts until midday of the following day (hour 36). Over the respective duration for which power surplus occurs, the maximum electric load resulting from heat pumps amounts to 60 GW_{el} in the case without restrictions and to 50 GW_{el} when market share restrictions are considered. However, once power deficiency occurs, the power demand of electric heat pumps is substantially lower in the case when hybrid heat pumps are deployed, i.e. in the case considering market share restrictions (cf. figure 6.31, Power-to-Heat, hours 18 and 36). Accordingly, in hour 66, CCGT and GT power plants provide an electricity supply of 34 GWh_{el}, while their power generation is increased to 102 GWh_{el} if no market shares a considered. This example underlines that particularly the deployment of hybrid heat pumps contributes to reducing the electric load in times of power deficiency and thus the necessary capacity of thermal power plants. While this decreases the methane gas consumption of the thermal power plant park on one hand, it substantially increases the methane gas consumption for the supply of space heat and domestic hot water on the other hand. The higher CO_2 emissions resulting from the gas-based operation of hybrid heat pumps are in part counterbalanced by a higher usage of biomass, which otherwise would be utilised for the supply of low temperature process heat. Instead, in this application field more electricity-based technologies are deployed. This means that the considered technology restrictions lead to a shift of electric heat pumps from the supply of space heat and domestic hot water to the supply of process heat. Further adjustments are undertaken in the motorised freight transport, where the number of FCEVs is increased up to 83 % in 2050. An overview of the main technological shifts caused by the restriction of BEVs and electric heat pumps as well as from the consideration of DSM are summarised in table 6.7.

Table 6.7: Technology share for the motorised freight traffic and for the low temperature supply of process heat in 2050 with and without demand-side management (DSM) as well as restrictions (res.) of electric heat pumps and battery electric vehicles. ICE: internal combustion engine, FCEV: fuel cell electric cehicle, HP: heat pump.

Sector	Technology	No res. No DSM	No res. With DSM	With res. No DSM	With res. With DSM
Freight traffic	ICE fuel	27%	42%	12%	21%
	FCEVs	73%	58%	83%	79%
Process heat <480°C	Wood boiler	7%	13%	0%	0%
	Electric HP	52%	48%	55%	55%
	Electrode boiler	34%	31%	36%	36%

As a consequence of the considered restrictions, roughly 50 % of private vehicles shift to FCEVs. Their share within the freight transport is higher as well, leading to an overall increase in hydrogen demand. Accordingly, the installed capacity of electrolysis plants over the four calculations varies between 100 GW_{el} to 180 GW_{el}. As for the deployment of stationary batteries, it heavily depends on whether DSM is considered or not. This is shown in figure 6.32.

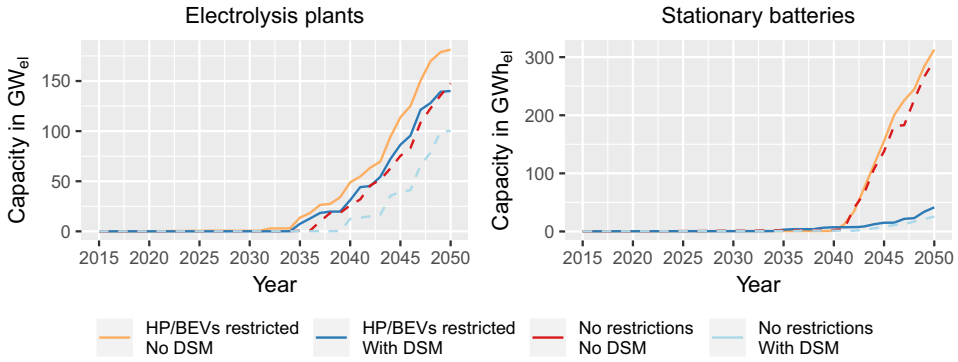

Figure 6.32: Development of the installed capacity of stationary batteries and electrolysis plants for a CO_2 emission reduction of 85 % by 2050 compared to 1990 values. The yearly technology market share of electric heat pumps (HP) and battery electric vehicles (BEVs) is limited to 19 % and 50 % on the right side. Demand-side management (DSM) describes a controlled charging behaviour of BEVs and a power-controlled operation of heat generators.

Overall, the presented analysis shows that by limiting the deployment of electric heat pumps and BEVs, the system is able to reach a CO_2 emission reduction of 85 % while a reduction of 95 % can not be achieved. Still, these restrictions require greater adjustments in other sectors, such as the freight transport or the supply of low temperature process heat. Compared to a BAU case, these adaptations lead to higher system costs, which amount to roughly 1,600 billion euros if DSM is not considered. By making use of DSM these costs can further be reduced by roughly 270 billion euros.

6.4.2 Influence of Weather Data

The weather data utilised to perform a model calculation may have a significant influence on the obtained results. Besides determining the full load hours of VRE, the underlying weather data indirectly affects other technologies and sectors of the energy system. For instance, the utilisation of thermal power plants and their conversion efficiencies varied according to the selected weather data (cf. section 6.1.3). The outside temperature is also an important factor, as it affects the resulting heat demand of buildings, the conversion efficiency of air heat pumps and overall, the electric load of electricity-based

heat generators. These examples show why considering differing weather data might be of great relevance. In order to assess uncertainties resulting from different weather data, four optimisation runs are performed. Each run assumes a CO_2 emission reduction of 90 % by 2050 compared to 1990 values as well as a consideration of DSM. Within all calculations, the technology parameters are maintained equal while the underlying weather data is changed as follows:

- **Fixed Sequence Parametrisation (FSP)**
  In this calculation, the weather data for all five implemented years (2011 to 2015) is distributed randomly over the observation period from 2015 to 2050, according to figure 6.33. The resulting sequence is kept unchanged and is utilised within each function call of the optimisation process.

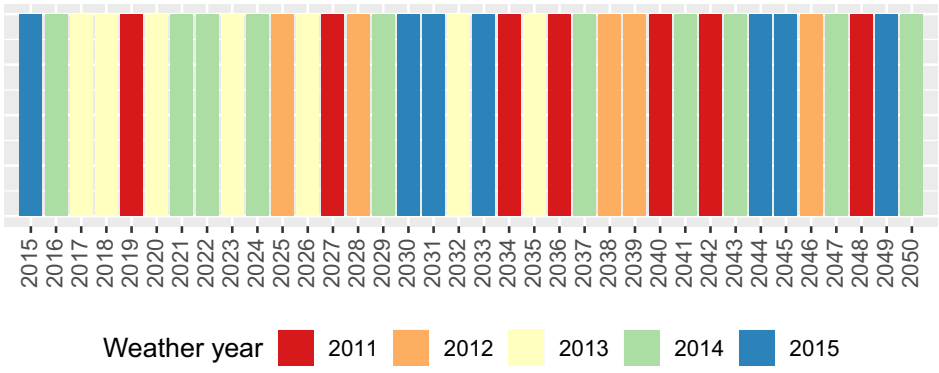

Figure 6.33: Randomly generated sequence of weather data utilised in the Fixed Sequence Parametrisation. The only exception is the starting year 2015, which is always calculated based on weather data of 2015.

- **Uniform Parametrisation: 2013 (UP-2013)**
  Over the entire observation period from 2015 to 2050, the underlying weather data is set to 2013. Relating to figure 6.33, this would translate to a uniformly yellow coloured plot. Meeting the set climate protection targets based on this configuration is expected to be rather challenging, as VRE on average exhibit the lowest amount of full load hours (section 3.5, table 3.6). Further, previous results suggest that the number of times when power deficiency occurs over a consecutive period of at least 12 hours is highest (section 6.1.3, table 6.3).

- **Uniform Parametrisation: 2015 (UP-2015)**
  Over the entire observation period from 2015 to 2050, the underlying weather data is set to 2015. Relating to figure 6.33, this would translate to a uniformly blue coloured plot. Meeting the set climate protection targets based on this configuration is expected to be less challenging, as VRE on average exhibit the highest

number of full load hours (section 3.5, table 3.6). Further, previous results suggest that the number of times when power deficiency occurs over a consecutive period of at least 12 hours is lowest (section 6.1.3, table 6.3).

- **Random Sequence Parametrisation (RSP)**
  In this calculation, the weather data for all five implemented years (2011 to 2015) is distributed randomly over the observation period from 2015 to 2050. This process is repeated within each function call. This leads to a stochastic optimisation, for which the combinations of the underlying weather data are continuously changed. Accordingly, it is expected that the resulting system configuration exhibits a higher resilience to weather influences.

The optimisation results for the four introduced calculations, i.e. FSP, UP-2013, UP-2015 and RSP, overall confirm the trends in technology deployment observed so far. This, for instance, concerns the shift from oil and gas boilers to electric air heat pumps and heat grids or from ICEs over CNG-vehicles to BEVs in the motorised private road transport. Instead of comparing all technologies within each sector, only the most relevant variations in 2050 are highlighted and discussed. Differences in the range of 1 % are not considered as relevant, as this most likely corresponds to the uncertainties resulting from the heuristic optimisation approach (cf. section 3.3.2). All variations are assessed in relation to the „Fixed Sequence Parametrisation“ (FSP), as, so far, most calculations in this work are based on this method. Figure 6.34 shows the resulting deviations regarding the cumulative installed capacity of VRE and of the thermal power plant park.

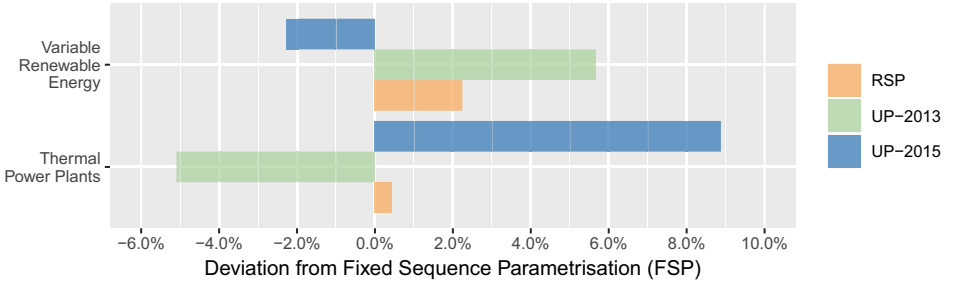

Figure 6.34: Variation of installed capacity of power generators for differing parametrisation of weather data related to the Fixed Sequence Parametrisation. UP-2013: Uniform Parametrisation 2013, UP-2015: Uniform Parametrisation 2015, RSP: Random Sequence Parametrisation.

Despite the total electricity demand within all runs in 2050 varies by less than 2 % from the FSP-results (1238 TWh_{el}), the installed capacities of VRE exhibit greater differences between each other. As shown in figure 6.34, if the weather data of 2013 is assumed (UP-2013), the deployment of VRE is increased by nearly 6 %. This mainly results from the

lower full load hours characterising this year[10]. Accordingly, since the weather data of 2015 exhibits the highest full load hours of VRE, their installed capacity is decreased by approximately 2 % in case of UP-2015. For RSP, their capacity is increased by 2 %, representing an intermediate result. One reason for this is the consideration of all five implemented years (2011 to 2015), instead of only 2013 or 2015. In the randomly generated sequence utilised in FSP (cf. figure 6.33) the weather data of 2013 is only used until 2035. Conversely, within RSP the distribution of the weather data is generated randomly within each function call. This increases the probability that within a part of all optimisation runs, the weather data of 2013 is utilised towards the end of the observation period.

An almost opposite trend to the deployment of VRE is observed with regard to thermal power plants, which is also illustrated in figure 6.34. Their installed capacity increases by roughly 9 % in case of UP-2015, while it decreases by approximately 5 % if UP-2013 is considered. On first glance this result might be counter-intuitive, however, it can be traced back to two main reasons: the outside temperature and the system configuration. The dimensioning of the thermal power plant park is mainly based on times when the electric load is particularly high and concurrently, the feed-in from VRE is relatively low. In the calculation based on UP-2013 this occurs during the third week of February around 6 pm, when the average outside temperature amounts to 1.2 °C[11]. The results obtained for UP-2015 show that the thermal power plant park is dimensioned based on the third week of January around 5 pm. At this time, the outside temperature amounts to -0.1 °C. This yields to a difference of 1.3 K, which under consideration of the whole building stock leads to a substantial increase of the resulting heat demand. In both scenarios this demand is mainly covered by electric heat pumps. Thus, at the cited time, the electric load of heat pumps is roughly 12 GW_{el} higher in the case of UP-2015. This example shows that beside the outside temperature, which is an exogenous parameter, also endogenous effects, such as the system configuration, need to be taken into account. This is especially the case in this example, where for UP-2013, more efficient brine heat pumps (mainly at the cost of air heat pumps) are deployed and more buildings are refurbished (cf. figure 6.35). As for RSP, the thermal power plant park is dimensioned based on the last week of November around 5 pm. At this time the average outside temperature amounts to -1 °C, suggesting a higher residual load value. However,

[10] For the year 2013 the full load hours of photovoltaic systems, onshore and offshore wind power stations on average amount to 949 hours, 1,636 hours and to 3,643 hours, respectively. If the weather data of the year 2015 is assumed, these numbers change to 1,086 hours (+14 %), 1,899 hours (+16 %) and 4074 hours (+12 %). More details are provided in section 3.5.

[11] The lowest average temperature for this year amounts to -8.1 °C and occurs at night. At this time the residual load does not present its maximum value for two reasons: fist, the feed-in from wind power stations is substantially higher compared to the third week of February. Further, while the charging load provided by BEVs over night time is neglectable, it exhibits its peak value around 5 pm to 6 pm, when most vehicle users return to a charging facility (in this example the maximum charging load of BEVs amounts to roughly 40 GW_{el}.)

the residual load is decreased by the power generation from VRE, which amounts to roughly 20 GWh_{el}. Further, a greater amount of electricity is imported to Germany from neighbouring countries as their feed-in from VRE is also higher (cf. section 4.5). Thus, despite the higher heat demand in case of RSP, the required installed capacity of thermal power plants lies in between the results obtained for UP-2013 and UP-2015.

Figure 6.35 shows the most relevant deviations concerning the supply of space heat and domestic hot water in 2050. This includes the deployment of brine heat pumps as well as the share of refurbished buildings.

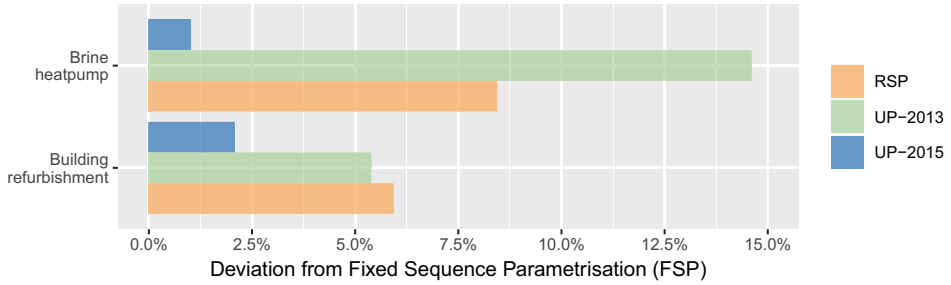

Figure 6.35: Variation in electric brine heat pump deployment and building refurbishment in 2050 for differing parametrisation of weather data related to the Fixed Sequence Parametrisation. UP-2013: Uniform Parametrisation 2013, UP-2015: Uniform Parametrisation 2015, RSP: Random Sequence Parametrisation.

The illustrated results show that the consideration of UP-2013 increases the deployment of brine heat pumps by roughly 15 % (four million units), mainly at the costs of air heat pumps. By installing more efficient brine heat pumps, the power generation and the fuel consumption of thermal power plants is indirectly decreased. This is in part also reflected by their lower capacity. Similarly, but to a lower degree, the higher deployment of brine heat pumps is also observed for RSP, which again represents an interim value compared to other results. The share of retrofitted buildings is increased by approximately 7 % for UP-2013 and by 9 % for RSP. Further, the number of highly efficient refurbishments (cf. section 3.2.4) is increased by 5 % and 6 %, respectively. The higher building refurbishment in case of RSP suggests that the system tries to dampen effects resulting from uncertainties related to different weather data. For UP-2015, the deviation concerning brine heat pumps and the number of refurbished buildings amounts to roughly 1 % which is almost equal to FSP and thus of neglectable impact.

The optimisation results reveal that the deployment of BEVs in the motorised private road transport is widely robust against the considered variations of weather data. In 2050 they still represent the dominant technology. This is also the case for FCEVs in

the motorised freight transport. Figure 6.36 illustrates the deviations of these two power train technologies.

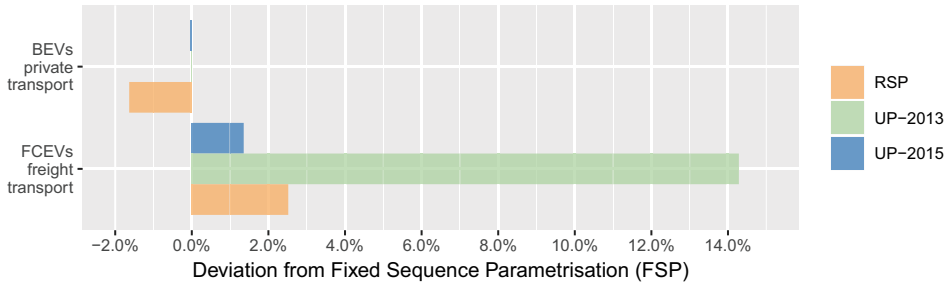

Figure 6.36: Variation in battery electric vehicle (BEV) and fuel cell electric vehicle (FCEV) deployment in 2050 for differing parametrisation of weather data related to the Fixed Sequence Parametrisation. UP-2013: Uniform Parametrisation 2013, UP-2015: Uniform Parametrisation 2015, RSP: Random Sequence Parametrisation.

As shown the share of BEVs in 2050 is decreased by less than 2 % at the cost of FCEVs only in case of RSP, while remaining steady at 100 % for UP-2013 and UP-2015. In the motorised freight transport 14 % of all vehicles are shifted from internal combustion engines to FCEVs, when the underlying weather data is set to 2013 (UP-2013). In this year, more emissions are caused by thermal power plants, which in part are compensated by a higher deployment of FCEVs. Compared to BEVs, which exhibit a direct electricity demand, FCEVs allow to decouple their energy demand from the assumed driving behaviour and further from the weather dependent feed-in of VRE to a certain extent. In case of RSP, their numbers are increased in the private and the freight transport, again suggesting that the system compensates for a higher uncertainty related to the randomly changing weather data. This hypothesis is supported by the total hydrogen production in 2050, which is increased by 21 % when RSP is considered. This conlcusion is supported by previous results (cf. figure 6.35), where the building refurbishment and the usage of brine heat pumps are increased by several percentage points. The illustrated differences in the system composition cause substantial variations concerning the total system costs: compared to the BAU case they amount to 1,333, 1,720, 1,185 and 1,697 billion euros for FSP, UP-2013, UP-2015 and RSP, respectively. The results show that the total system costs obtained with FSP are closer to UP-2015 (-3.5 %), as beginning in 2036 the weather data of 2013 is not utilised anymore. Accordingly, RSP leads to a total cost value closer to UP-2013 (roughly +9 % compared to FSP). Even though the trends in technology deployment are similar over all four calculations, it is helpful to keep in mind the outlined bandwidths concerning technology deployment and costs, especially when performing calculations based on only one of the mentioned methods for the consideration of weather data.

Consideration of Extreme Weather Influences

The analysis results presented so far account only for uncertainties within the weather data of one of the five implemented years, i.e. 2011-2015. Since they are based on real weather data, they do not include extreme weather events, which could have a major effect on an energy system based on VRE. Against this background, the weather data of 2012 is adjusted and the wind speed and the solar radiation are set to zero for the whole month of October. This does not only influence the generation of power, but also the solar gains of buildings or the heat generation from solar thermal systems. During the same period, the power generation of VRE in neighbouring countries is set to zero as well, limiting the available import capacity (cf. section 4.5). The occurrence of this modified year is highlighted in figure 6.37, affecting the years 2025, 2028, 2038, 2039 and 2046.

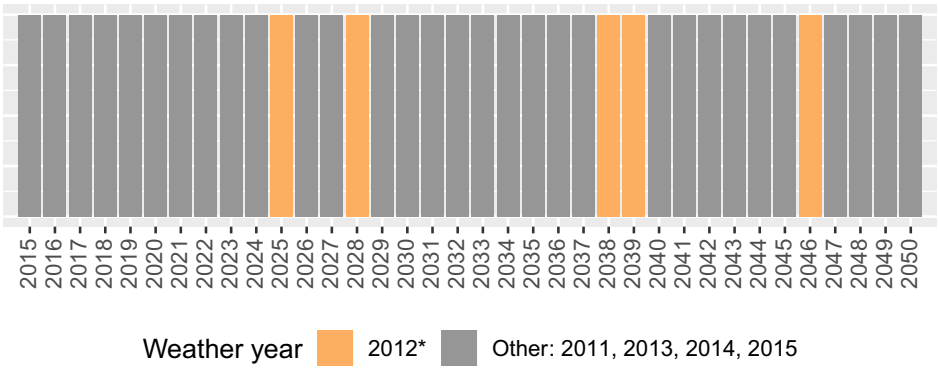

Figure 6.37: Randomly generated sequence of weather data utilised in the Fixed Sequence Parametrisation. The weather data of 2012* is highlighted, as during October of this month the wind speed and the solar radiation in Germany and neighbouring countries is set to zero.

The focus of this analysis is to investigate how the system deals with the prolonged period of low feed-in from VRE during October. For this purpose, first the operation of the three implemented power storage systems and then, of long-term storage systems is investigated. Figure 6.38 illustrates the charge levels of the three implemented power storages in 2038. This is the first year when not only pumped-storage power plants but also BEVs and stationary power storage units are present in the energy system configuration.

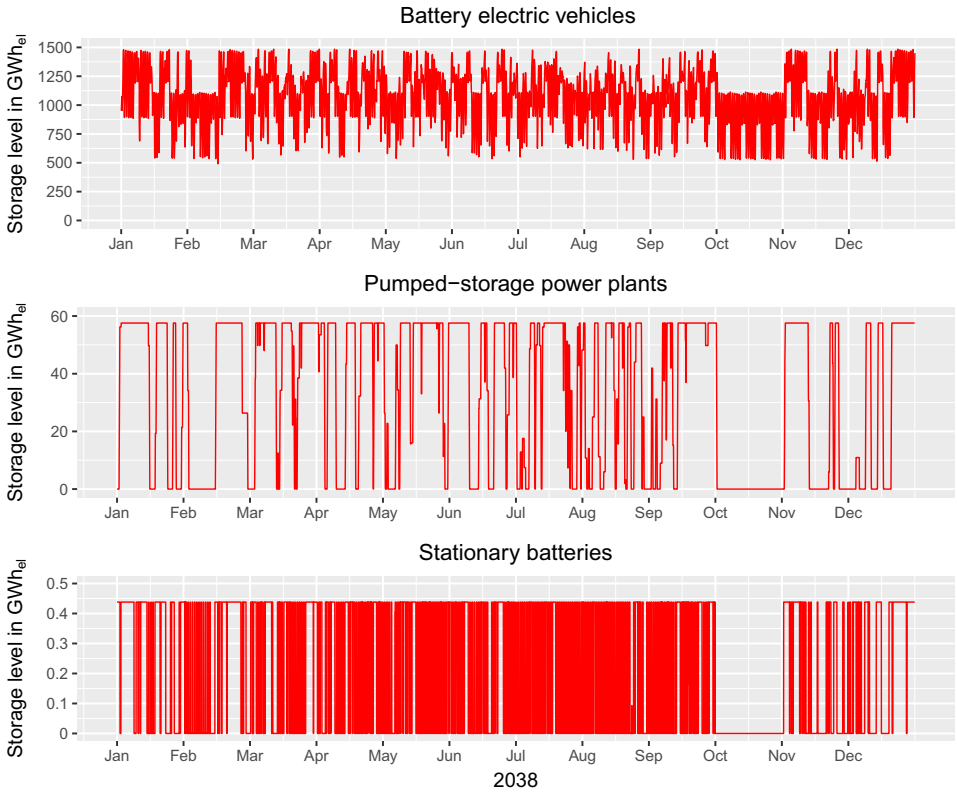

Figure 6.38: Charge levels of power storages in 2038. The wind speed and the solar radiation in October are set to zero for Germany and its neighbouring countries.

The top curve in figure 6.38 shows the charge level of BEVs in the motorised private transport. In 2038, their numbers amount to 23.7 million vehicles, which with an assumed average battery capacity of 66.6 kWh_{el} leads to a theoretically maximum capacity of roughly 1570 GWh_{el}. Assuming that 25 % of users follow a Controlled Charging Strategy, this means that of the maximum battery capacity 390 GWh_{el} can be utilised for Grid-to-Vehicle operation. As for a Vehicle-to-Grid operation, the accessible battery capacity amounts to 100 GWh_{el}, as it is further restricted by the maximum allowed depth of discharge (cf. section 4.3). The vehicle batteries are charged and discharged on a frequently basis, indicating an extensive usage of DSM throughout the year. During October, no surplus electricity is available and vehicles are charged as they reach a charging facility. As a consequence, the charge level of BEVs illustrated in figure 6.38 (top) is determined by the exogenously set driving behaviour and thus follows a predefined pattern during this period. Over the entire year of 2038, BEVs integrate 54 TWh_{el} of surplus electricity from VRE, while feeding back 46 TWh_{el} into the grid. In October, their feedback into the power grid amounts to 55 GWh_{el}, happening only at the very beginning of the month.

The second curve in figure 6.38 (middle) shows the charge level of pumped-storage power plants. Due to their ratio of storage capacity to filling and withdrawal rate of roughly 7:1 (cf. appendix A.4), they exhibit a lower number of charging cycles, which is especially visible during the winter months. In 2038, they are charged with 35 TWh_{el} of surplus electricity while their discharge amounts to 28 TWh_{el}. Similarly to BEVs, the contribution of pumped-storage power plants in October is restricted to the first few hours of the month. The third curve in figure 6.38 (bottom) describes the charge level of stationary batteries[12]. With an installed capacity of less than 0.5 GWh_{el} they play a minor role in 2038. This is also the case for all upcoming years, as due to the consideration of DSM their expansion is severely limited. Compared to BEVs and pumped-storage power plants, stationary batteries exhibit a higher number of charge cycles. In the considered year, they integrate 140 GWh_{el} of surplus electricity, while supplying 120 GWh_{el} back to the grid in times of power deficiency. Like other power storages, their contribution during the low feed-in period in October is neglectable.

According to the obtained results, the time in which power storages can provide a continuous supply of electricity to the grid usually accounts for less than half a day. The exact time range may vary, depending on various factors. One factor is the total storage capacity, which is endogenously determined. A second factor is represented by the respective storage charge level, which is mainly defined by its operation mode and the feed-in from VRE. Another aspect which has to be accounted for, is the extent of power deficiency affecting whether the storage is discharged at its maximum capacity or not. This again is connected to the power load which is influenced by the outside temperature and the endogenously determined system configuration, including the deployment of electricity-based heat generators or the number of refurbished buildings. Overall, the optimisation results show that the considered power storages are not designed to bridge such an extended period of power deficiency. However, by integrating higher shares of VRE during other months, they contribute to lower the resulting CO_2 emissions. For example, in 2038, roughly 15 % of the electricity generation from VRE is integrated alone by DSM in the motorised private transport (9 %) and the supply of space heat and domestic hot water (6 %). This allows other power generators, such as thermal power plants, to be operated during periods of low feed-in from VRE without violating the yearly CO_2 reduction target. During October, the electric load is mainly covered by CCGT power plants with and without heat extraction, GT power plants as well as CHP-units and fuel cells for the generation of space heat and domestic hot water. All of these technologies are based on methane gas or hydrogen. In order to contain the related CO_2 emissions, the system has two options. One option is to add CO_2-neutral gases to the methane gas mix. The other option is to shift part of the energy demand

[12] In this case, only stationary batteries operated to balance the residual load in case of power surplus or deficiency are considered. Batteries utilised exclusively to increase the operative hours of PtG plants are not included in this analysis.

towards CO_2-neutral technologies, which do not increase the electric load in this period any further. Both effects are represented in table 6.8, which compares the conversion of biomass into fuels as well as the production and usage of hydrogen in 2038 for the results obtained without the modification of the weather data of 2012.

Table 6.8: Comparison of biomass conversion into fuels as well as hydrogen production and demand in 2038 in TWh. Both calculations are obtained for the same parameter setting and a CO_2 emission reduction of 90 % by 2050 compared to 1990 values. In 2012* the wind speed and solar radiation in October are set to zero for Germany and its neighbouring countries. Hydrogen demand* includes the hydrogen demand of all energy-related sectors (transport, supply of space heat, domestic hot water and process heat).

Energy in TWh	Reference	2012*	Delta
Hydrogen demand*	2.2	17.0	750 %
Hydrogen added to gas grid	2.5	14.0	602 %
Hydrogen from electrolysis plants	0.7	20.3	2885 %
Hydrogen from storage	4.8	31.2	550 %
Biomass to methane gas	37.0	46.4	24 %
Biomass to hydrogen	4.2	7.4	75 %
Biomass to liquid fuels	15.5	22.6	44 %

Table 6.8 shows that the quantities of biomass converted into fuels in the calculation based on the reference parametrisation and on the modified weather data are of a similar magnitude. This is not the case for hydrogen, which exhibits a much higher demand once the feed-in from VRE is set to zero for an entire month. This indicates that hydrogen may provide a considerable contribution to overcome the implemented period of absent power generation from VRE. Figure 6.39 shows the charge level of the hydrogen storage, from 2035 to 2039.

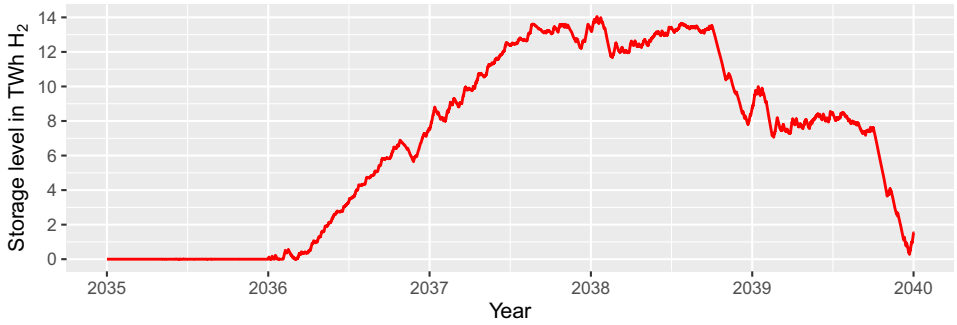

Figure 6.39: Charge level of hydrogen storages from 2035 to 2040. In 2038 and 2039 the wind speed and solar radiation in October are set to zero for Germany and its neighbouring countries.

As shown, the production of hydrogen starts in 2036 to prepare for the two consecutive years (2038 and 2039) when the wind speed and the solar radiation are set to zero for a whole month. Accordingly, the system is dimensioned in a way such that in 2036 and 2037 the hydrogen supply surpasses the demand. The difference is loaded into the hydrogen storage which gradually increases its charge level over the years. Once the critical period of 2038 and 2039 is reached, a large part of the hydrogen supply can be covered by the previously stored hydrogen without increasing the electric load. This behaviour is a consequence of the perfect foresight of the solver, implemented for the solution of the problem (cf. 3.3.2). As shown in figure 6.40, the effects resulting from the solver foresight become even more visible once the years following 2039 are considered.

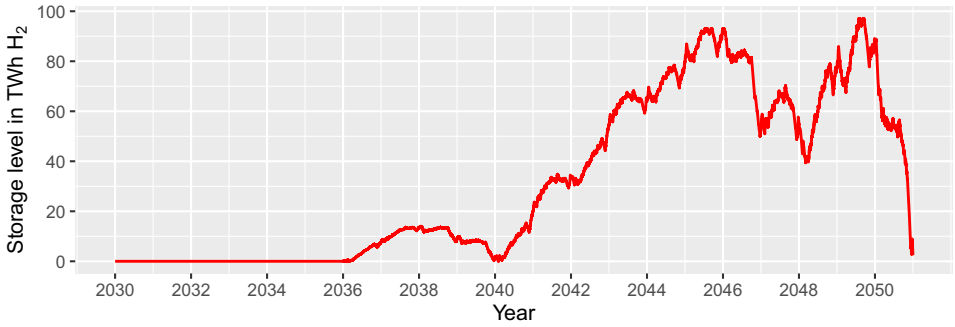

Figure 6.40: Charge level of hydrogen storages from 2020 to 2050. In 2025, 2028, 2038, 2039 and 2046 the wind speed and solar radiation in October are set to zero for Germany and its neighbouring countries.

Figure 6.40 shows the hydrogen charge level from 2030 to 2050. According to the results, the storage exhibits a maximum capacity of roughly 100 $\mathrm{TWh_{H_2}}$. Its charge level is not only increased over the years in order to cope with the critical time periods in 2938, 2039 and 2046, but also to be discharged towards the end of the observation period. While this behaviour is logical from a model perspective, it seems rather unrealistic that the storage charge level would be increased over the years to be discharged a few years later. Thus, an additional calculation is performed, for which the reservoir level of the hydrogen storage is not transferred from one year to the other. The hydrogen charge level for the year 2038 as well as for the time period from 2020 to 2050 is illustrated in figure 6.41.

The results show that disabling the transfer of the hydrogen charge level over the years leads to a substantially lower storage capacity of roughly 23 $\mathrm{TWh_{H_2}}$. The production and the demand of hydrogen are dimensioned in a way that at the end of each year the hydrogen storage is almost emptied. Accordingly, at the beginning of each year, the storage needs to be filled up before it can contribute to meeting the occurring hydrogen demand. This translates to a higher probability of a mandatory hydrogen generation

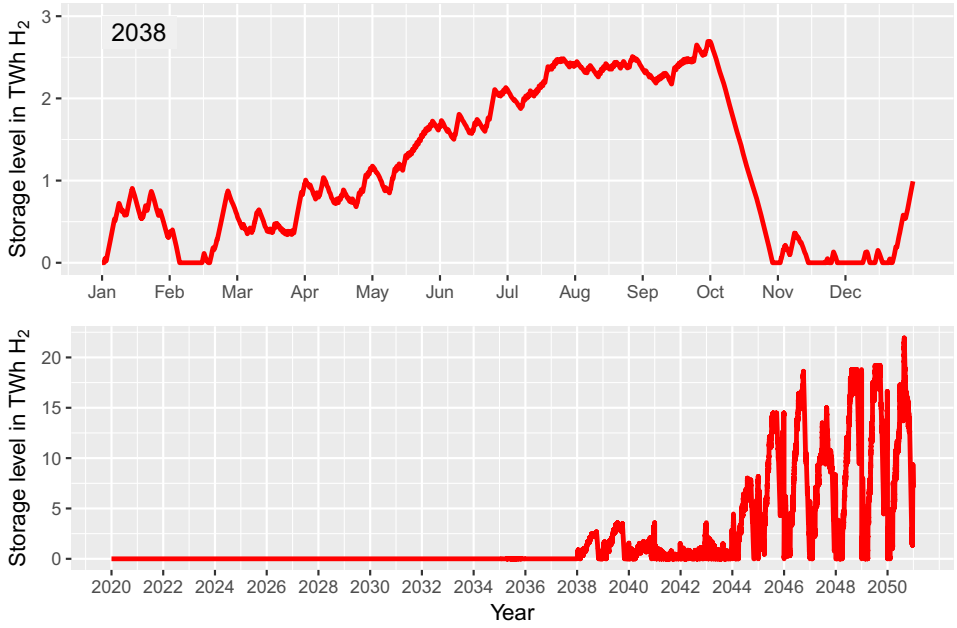

Figure 6.41: Charge level of hydrogen storages for 2038 and from 2015 to 2050 in case of modified weather data. In 2025, 2028, 2038, 2039 and 2046 the wind speed and solar radiation in October are set to zero for Germany and its neighbouring countries. The reservoir level of the hydrogen storage is not transferred to the next year.

by electrolysis plants in times of power deficiency. For the year 2038, this case accounts for roughly 5 % of the total hydrogen production from electrolysis plants. However, this means that 95 % of their hydrogen production occurs in times of power surplus, which is especially from photovoltaic systems during summer. The hydrogen storage is mostly discharged during winter, underlining its seasonal utilisation. Considering the entire observation period, it is shown that by disabling the transfer of the hydrogen storage level over the years, the hydrogen production begins in 2038 rather than in 2036. This delay results from the fact that the system can not prepare for the incoming period of absent power generation from VRE. Nevertheless, compared to the previous calculation (cf. figure 6.40), the hydrogen demand in 2038 is further increased by 7 $\mathrm{TWh_{H_2}}$. In order to meet this demand, a higher amount of biomass is converted into hydrogen (14.4 TWh instead of 7 TWh).

Overall, the analysis reveals that hydrogen-based technologies play a key role to bridge extended periods of low feed-in from VRE. For instance, figure 6.41 shows that the charge level of the hydrogen storage in 2038 is gradually increased over the year to be fully discharged in October. Even though, in this year electrolysis plants exhibit an

electricity demand in times of power deficiency of roughly 1.6 TWh_{el}, this is identified as a cost-efficient solution. It can be concluded that while power storages and DSM do not provide a direct contribution to overcome prolonged periods of low feed-in from VRE, they integrate higher shares of renewable energy. This suggests that DSM lowers the resulting CO_2 emissions and thus the CO_2 abatement costs. This aspect is verified in the next section, where a qualitative and quantitative cost assessment of DSM under consideration of different CO_2 reduction targets is presented.

6.4.3 Cost Assessment of Demand-Side Management

This section presents a cost assessment of DSM in the motorised road transport and the supply of space heat and domestic hot water. The analyisis is based on the evaluation of five different CO_2 reduction targets, namely 65 %, 75 %, 85 %, 90 % and 95 % by 2050 compared to 1990 values. Each calculation is performed with and without consideration of DSM, allowing a direct comparison within a set reduction target. According to the insights of previous results, the deployment of CNG-vehicles is restricted[13]. In the BAU case, DSM is not taken into account, as this better reflects the present day. Figure 6.42 shows the development of the annual system costs in billion euros for all performed calculations from 2015 to 2050.

Figure 6.42 shows that the system costs of the 65 % reduction target (red) are higher than those of the BAU case (black) only beginning in 2042, while being slightly lower before that. Similarly, also the 75 % reduction target (orange) exhibits higher costs only from 2038 on, showing that the intersection with the BAU case occurs the earlier, the more ambitious the set CO_2 reduction target in 2050. This is also confirmed by other results. According to figure 6.42, the relative intersection points with the BAU case lie around 2034, 2025 and 2021 for a 85 %, 90 % and 95 % target, respectively. There are two main reasons for this: first, a more ambitious CO_2 reduction target in 2050 translates to a steeper decrease of the yearly allowed CO_2 emissions over the considered time period. This means that for a specific year, different levels of emission reductions need to be achieved. The second reason is that the expansion potential of all technologies and components is distributed over the period from 2015 to 2050 (cf. 5). If the maximum expansion potential of key technologies (such as VRE) should be exploited, their deployment needs to start earlier in time, when they still exhibit higher costs. For example, the deployment of electric heat pumps for the supply of space heat and domestic hot water begins around 2037 in case of a 65 % reduction target. Conversely, if the CO_2 emissions are to be reduced by 95 %, electric heat pumps are installed right on from the

[13] The results in section 6.2.3 showed that CNG-vehicles are deployed for one life cycle from 2020 to 2035, serving as interim technology between gasoline and diesel based internal combustion engines and BEVs. According to current numbers of new admissions [240, 241], a complete shift to CNG-vehicles starting in 2020 at the costs of petrol vehicles is not foreseeable.

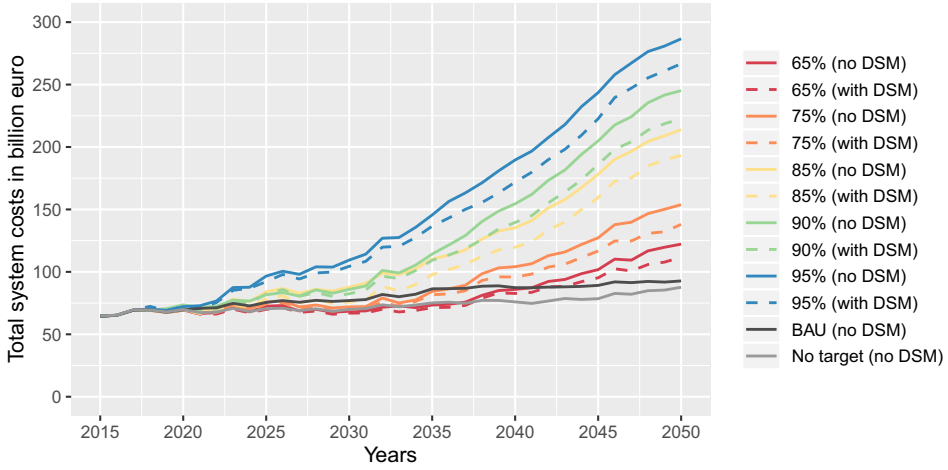

Figure 6.42: Development of the annual system costs for different CO_2 reduction targets from 2015 to 2050. The allowed quantity of CO_2 emissions per year is calculated by a linear interpolation between today's levels and the set reduction target. The dashed lines represent calculations, for which demand-side management (DSM) is considered. BAU indicates a business-as-usual case, in which the current system configuration is kept identical over the entire observation period. No CO_2 target: this configuration describes a pure cost-optimisation without regard of a yearly CO_2 limit.

start ($+250\,€/kW_{th}$), reaching substantially higher shares in 2050 (74 % instead of 14 %). The reason why the BAU case compared to the calculations with a set CO_2 emission reduction target exhibits higher costs during the earlier time periods, is because all other system configurations are endogenously determined according to a cost optimisation. Conversely, in the BAU case, the current state of the energy system is maintained unchanged over the entire observation period. This suggests that the BAU case becomes cheaper than other calculations only when the yearly allowed quantity of CO_2 emissions leads them towards technologies with higher costs and lower emissions. An example for this is the shift from gasoline or diesel based vehicles towards FCEVs in the freight transport.

In order to support this hypothesis, an additional calculation is performed. In this case, the yearly CO_2 limit is lifted and the system configuration (cf. appendix E) is endogenously determined. The results show that, compared to the BAU case, wind turbines are gradually decommissioned while photovoltaic systems are slightly increased. At the same time, the usage of methane gas for the supply of space heat and domestic hot water is increased, while for low and high temperature process heat, methane gas-fired CCGT power plants and coal boilers play a dominant role. The greater deployment of CCGT power plants represents a logical result from a model perspective as these

plants simultaneously provide heat and power in times when they are most needed. It is noted that the dimensioning of these plants is based on an average heat load. Especially for small-scale industry activities with a lower process heat demands, the utilisation of gas boilers could be more cost-efficient due to higher costs of CHP units. Further, while the model accounts for different supply temperatures (cf. section 3.2.3), other process requirements such as temperature accuracy or regulating speeds of heat generators (which might favour the usage of electric furnaces) are neglected. As for the usage of coal, the model assumes an ideal market without consideration of whether the facilities requiring process heat are located near a river for the transport of hard coal or next to a mining area in case of lignite. Keeping the mentioned simplifications in mind, the results confirm that this configuration (figure 6.42, grey) leads to the lowest costs not only in 2050 but also over the entire observation period. One exception is represented by the 65 % reduction target under consideration of DSM (red, dashed line). The results show that within a set CO_2 reduction target, the usage of DSM consistently leads to lower system costs. This becomes even more clear, when the total system costs from 2015 to 2050 are considered. In figure 6.43 they are depicted for all calculations, subdivided into ten different cost categories.

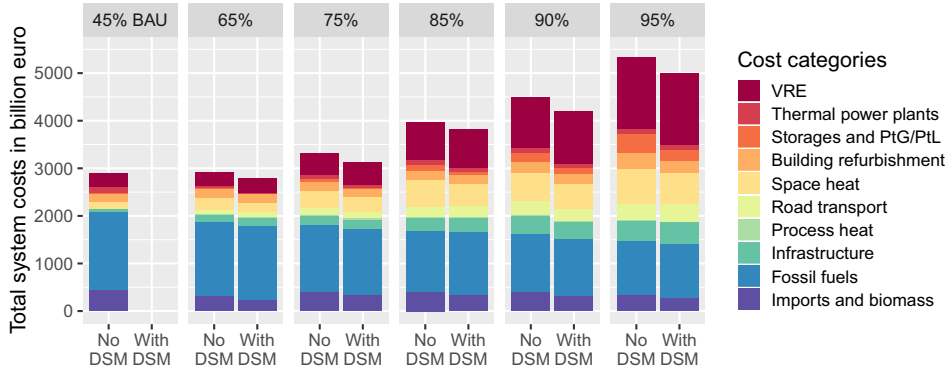

Figure 6.43: Total system costs summarised from 2015 to 2050 for different CO_2 reduction targets subdivided into ten different cost categories. BAU indicates a business-as-usual case, in which the current system configuration is kept identical over the entire observation period.

The illustrated results show that the total system costs become higher as more ambitious CO_2 reduction targets are considered. The main cost drivers are VRE, heat generators, energy storages and PtG plants as well as road transport and infrastructure expansion. At the same time, the expenses for energy imports, especially fossil fuels, are decreased. Within a set CO_2 reduction target, the total system costs are reduced in all cases once DSM is considered. For instance, the installed capacity of the thermal power plant park is decreased on average by 23 GW_{el} in 2050, leading to a cost-saving ranging from 20 to

30 billion euros, depending on the considered climate protection target. The savings in terms of electricity imports on average amount to 700 TWh_{el} over the entire observation period, corresponding to approximately 75 billion euros. This confirms the results of section 6.3.3, where it is shown that DSM contributes to the flattening of the residual load, lowering the power exchange with neighbouring countries. Another difference concerns the deployment of generators for the supply of space heat and domestic hot water, which in case of DSM leads to a cost-saving potential varying between 40 and 100 billion euros (for a 65 % to 95 % reduction of CO_2 emissions in 2050). The most evident reduction in costs is achieved by a reduced deployment of power storages and PtG or PtL technologies. As shown in previous results (cf. section 6.2.3 and 6.3.2), DSM can substitute a substantial part of these technologies. The related cost-savings amount to almost 20 billion euros for a 65 % reduction target. However, in this case stationary batteries and PtG plants play a minor role. As the CO_2 reduction target increases and these options become more and more meaningful from a cost-efficient point of view, the savings resulting from DSM rise up to 145 billion euros in case of a 95 % CO_2 reduction target. Further, by contributing to the integration of surplus electricity, DSM indirectly leads to a reduction of the total CO_2 emissions. This, in turn, allows the system to reduce the deployment of technologies with particularly high CO_2 abatement costs, which become necessary when more ambitious climate protection targets are considered. Thus, DSM also leads to indirect cost-savings in building refurbishment, freight transport or the supply of process heat. The cost-savings increase proportionally with the set CO_2 reduction target, amounting to 115 billion euros, 183 billion euros, 211 billion euros, 301 billion euros and 341 billion euros in case of a 65 %, 75 %, 85 %, 90 %, and 95 % reduction of the CO_2 emissions by 2050. In order to relate the total system costs to the achieved emission reduction, the CO_2 abatement costs are calculated according to eq. 6.12. It is noted that due to the planned withdrawal from coal power as well as technical improvements the BAU scenario reduces its emissions from 28 % in 2020 to 45 % by 2050 compared to 1990 values.

$$c_{CO_2,A,j} = \frac{m_{CO_2,BAU,j} - m_{CO_2,i,j}}{(C_{i,j} - C_{BAU,j})} \tag{6.12}$$

where:

$c_{CO_2,A}$ = CO_2 abatement costs in €/t_{CO_2}
m_{CO_2} = Total quantity of caused energy-related CO_2 emissions in t_{CO_2}
C = Total system costs in *euros*
BAU = Business-as-usual case (today's system configuration maintained)
i = Considered calculation with set CO_2 reduction target
j = Considered year for the calculation of the CO_2 abatement costs

According to previous findings, the consideration of more ambitious CO_2 targets in 2050 leads to an earlier system adaptation and thus to different CO_2 reduction levels for a particular year. Therefore, instead of comparing the CO_2 abatement costs over the years, they are assessed depending on the achieved emission reduction. This is exemplarily shown in figure 6.44 for a 65 %, 75 %, 85% and 95 % reduction target in 2050.

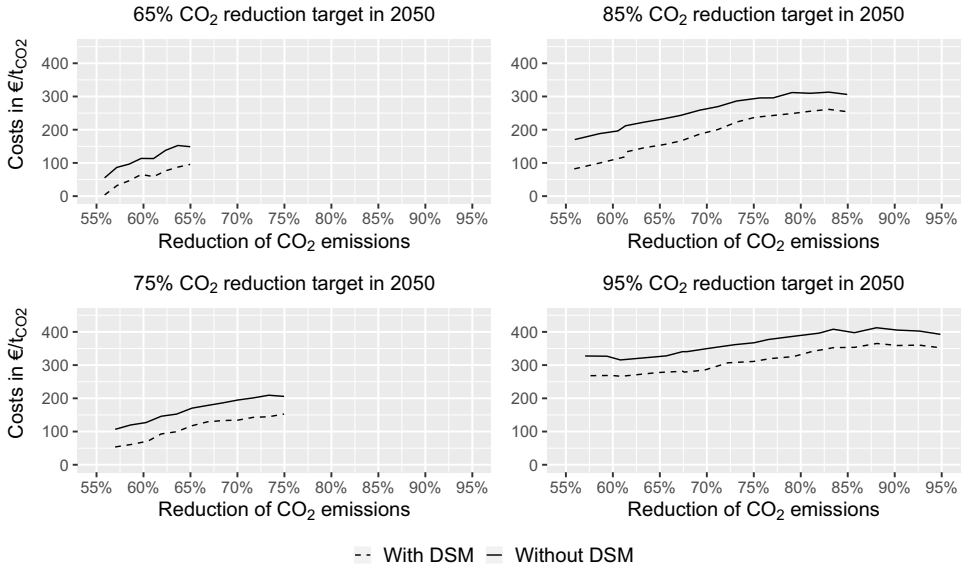

Figure 6.44: CO_2 abatement costs for different CO_2 reduction targets with and without consideration of demand-side management (DSM).

The illustrated CO_2 abatement costs for a specific reduction of CO_2 emissions vary substantially from each other, as they are achieved with different measures and at different times. Table 6.9 shows that among the investigated CO_2 reduction targets they exhibit a range of 180 €/t_{CO_2}.

Table 6.9: CO_2 abatement costs for different CO_2 reduction targets in 2050.

CO_2 emission reduction target in 2050	%	65	75	85	95
CO_2 abatement costs in 2050 (without DSM)	€/t_{CO_2}	150	206	297	393
CO_2 abatement costs in 2050 (with DSM)	€/t_{CO_2}	96	153	251	352

Figure 6.44 reveals that the depicted cost curves do not necessarily follow a monotonic increasing trend. While this may seem counterintuitive at first, it can be traced back to two factors. The first factor is the underlying weather data, as the shift from a year with less full load hours of VRE, a lower average outside temperature and extended periods of power deficiency may lead to higher CO_2 abatement costs and vice versa. This uncertainty mainly depends on exogenously set values and therefore could be avoided by relying on a uniform parametrisation of the weather data (cf. section 5.3). The

second factor is related to the charging and discharging of energy storages, which is mostly endogenously defined as it heavily depends on the system configuration, i.e. the dimensioning of all system components. For instance, if within one year more energy is discharged from a storage than charged, this would possibly lower the CO_2 abatement costs. Such a behaviour is shown in section 6.4.2, where the hydrogen storage is gradually filled up, in order to be emptied towards the end of the observation period. Accordingly, all illustrated curve progressions in figure 6.44 without consideration of DSM exhibit a slight decrease towards their end. Compared to the CO_2 abatement cost obtained assuming DSM, they suggest a parallel shift to each other, indicating a rather constant difference. From this it can be concluded that the exploitation of DSM in the motorised road transport and the supply of space heat and domestic hot water on average lowers the CO_2 abatement costs by roughly $50\,€/t_{CO_2}$. Overall, the results reveal that DSM represents a cost-efficient solution to integrate more VRE into the energy system and ultimately to reduce costs. Still, its exploitation is not absolutely necessary to achieve the set climate protection targets, as for instance the 95 % CO_2 reduction is nonetheless achieved. However, as shown throughout almost all results obtained so far, this requires higher efforts over all sectors of the energy system.

Import of Synthetic Fuels

An option which could facilitate the transition of the energy system while decreasing the dependency from weather influences in Germany is provided by the import of synthetic fuels. As described in section 5.3, their production could take place in regions with a substantially higher solar radiation, such as Northern Africa and then be transported to Germany by tankers[14]. In order to verify how their consideration affects the energy system two further calculations are performed, each assuming a 95 % reduction of the CO_2 emissions compared to 1990 values. The main differences observed in the system configuration in 2050, with and without consideration of DSM, are summarised in table 6.10.

Table 6.10 shows that to achieve a 95 % reduction of CO_2 emissions, the assumed expansion potential of VRE is almost fully exploited if the import of synthetic fuels from abroad is not considered. If their import is allowed, the installed capacity of VRE is decreased by 26 % without considering DSM and by 18 % if DSM is assumed. This suggests if DSM is utilised, a higher deployment of VRE is reasonable. As shown in section 6.3.3, DSM allows for a higher integration of VRE which otherwise would be used less efficiently or even curtailed. The results further reveal that the thermal power plant park is decreased if the import of synthetic fuels is considered, however, to a smaller extent compared to the deployment of VRE.

[14] All prices and further assumptions related to the import of synthetic fuels are listed in section 5.3.

Table 6.10: Main differences occurring in 2050 for a 95 % reduction of CO_2 emissions compared to 1990 values and under consideration of synthetic fuel imports and demand-side-management (DSM). VRE: Variable renewable energy, PP: Power plants, HP: Heat pumps, tr.: transport, PH*: Process heat supply, for supply temperatures >480 °C.

Technology	Unit	No DSM No Import	With DSM No Import	No DSM With Import	With DSM With Import
VRE	GW_{el}	834	833	613	683
Thermal PP	GW_{el}	214	194	186	186
Electrolysis plants	GW_{el}	204	146	94	49
Stationary batteries	GWh_{el}	648	300	324	20
Electric air HP	%	61	54	77	61
Electric brine HP	%	28	20	0	1
Heat grids	%	5	19	17	31
BEVs in private tr.	%	97	100	91	100
FCEVs in private tr.	%	3	0	9	0
Electricity PH*	%	54	77	12	43
Hydrogen PH*	%	46	23	70	41
Methane gas PH*	%	0	0	18	16

The installed capacity of electrolysis plants utilised for the generation of synthetic fuels in Germany, is gradually decreased from 200 GW_{el} to 49 GW_{el} in steps of roughly 50 GW_{el}, depending on whether the import of synthetic fuels from abroad and DSM are considered or not. From this it can be concluded that a local generation of hydrogen is still useful even if synthetic fuels can be imported from abroad. Especially towards the end of the observation period, when VRE exhibit a larger share of the total power generation, electricity, instead of being a scarce good, becomes abundantly available during generation peaks. In this case, the high ramping capability of electrolysis plants can provide a fast load increase and contribute to balancing the residual load while generating CO_2-neutral fuels. The import of synthetic fuels from abroad and DSM further replace roughly 300 GWh_{el} of stationary batteries at a time (cf. table 6.10). This reduction is connected to different factors, such as the lower installed capacities of VRE and PtG plants as well as the load shifting capability provided by DSM.

When DSM and the import of synthetic fuels are not considered, 28 % of all heat generators for the supply of space heat and domestic hot water are electric brine heat pumps. This underlines that in order to achieve the set CO_2 reduction target of 95 %, more efficient and more expensive technologies need to be deployed. Accordingly, the share of brine heat pumps is decreased to 20 % if DSM is considered, while being neglectable once that synthetic fuels can be imported. The connections to heat grids are increased by 12 % once a part of their methane gas consumption is provided by synthetic fuels, lowering their emissions. The share of heat grids is even more increased when DSM

is considered as in this case they can cope with power surplus and deficiency. This correlation confirms the findings of section 6.3.2.

In the motorised private transport BEVs remain the dominant power train technology for each of the four considered calculations. However, the import of synthetic fuels leads to an increase of FCEVs to roughly five million vehicles. If DSM is considered, the complete vehicle fleet is again composed by BEVs, confirming the results of section 6.2.3, showing that a Controlled Charging Strategy (CCSt) favours the deployment of BEVs. Similarly, the import of synthetic fuels affects the deployment of heat generators for the supply of process heat. Especially for supply temperatures above 480 °C, roughly 30 % of all heating technologies are shifted from an electricity-based to a hydrogen and methane gas-based operation.

The performed calculations considering the import of synthetic fuels assume an import capacity of 1,000 TWh per year of hydrogen, methane gas and liquid fuels each. As shown in figure 6.45, this capacity is exploited to 15 % and 17 % at most.

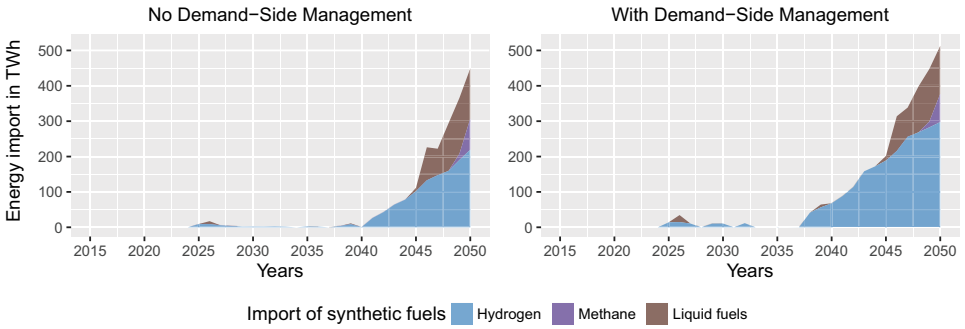

Figure 6.45: Imported quantities of synthetic hydrogen, synthetic methane gas and synthetic liquid fuels from abroad over the time period from 2015 to 2050 for a CO_2 emission reduction of 95 % compared to 1990 values.

The results reveal that if DSM is considered, the import of synthetic fuels from abroad begins roughly five years later, i.e. in 2040 instead of 2035. In this case, the imported fuels over the entire observation period from 2015 to 2050 are reduced from 3,000 TWh to less than 2,000 TWh. Regardless of whether DSM is considered or not, primarily hydrogen and liquid fuels are imported. This is because of the lower costs related to the production of hydrogen compared to other synthetic fuels: first, no air separation for the extraction of CO_2 is considered. Second, less conversion processes are necessary, leading to a higher efficiency. While within the considered synthetic fuels, liquid fuels exhibit the highest costs, figure 6.45 shows that their import is preferred over synthetic methane gas. This is because they are more valuable for the energy system, as they can be utilised to reduce the emissions of aviation, fuel-based railway traffic and shipping, which are per definition all based on liquid fuels.

Overall, the import of synthetic fuels substantially reduces the total system costs from 2,430 billion euros to 1,300 billion euros, compared to the BAU case. If DSM is considered, these costs are further decreased to 1,260 billion euros. This shows that the import of synthetic fuels represents an effective lever to reduce costs and to avoid otherwise necessary measures with relatively high CO_2 abatement costs. These measures become otherwise necessary, when particularly ambitious CO_2 reduction targets, such as pursuing an emission-neutral economy [2], are considered. On this regard, the results showed that the imported quantity of synthetic fuels is reduced once that DSM is considered. Thus, DSM does not only decrease the overall system costs, but also the energy dependency of Germany on its neighbouring countries.

6.4.4 Summary and Conclusions

In this section, the value of DSM was assessed under consideration of major uncertainties. First, the yearly market shares of key technologies using DSM, i.e. BEVs and electric heat pumps, were limited. Second, the underlying weather data was changed based on different parametrisation approaches and third, the level of pursued CO_2 emission reduction by 2050 was gradually increased from 65 % to 95 %. Finally, the import of synthetic fuels from abroad was considered and its effects on the overall system configuration assessed.

The restriction of BEVs and electric heat pumps showed that under this condition only an emission reduction of 85 % rather than 95 % could be achieved. This first result underlined the importance of these two technologies which in all calculations performed so far, based on the reference parameter setting, represented the dominant technology within their respective end-use sector. It was further shown that the introduced restrictions led to the introduction of hybrid heat pumps, which in times of power deficiency switched their operation to a gas based unit. This mechanism substantially contributed to lower the electric load and with it, the installed capacity of thermal power plants. However, the methane gas saved in this field was more than compensated by the the supply of space heat and domestic hot water. The emissions of hybrid heat pumps accordingly required adaptations throughout all sectors of the energy system. For instance, a higher number of electric heat pumps was deployed for the low temperature process heat supply. In the freight transport, more gasoline and diesel-based vehicles were replaced by FCEVs. The cost differences arising from this amounted to 280 billion euros. It was shown that these cost differences could be compensated by considering DSM.

The uncertainties related to different weather data were on a first step assessed through four calculations. It was shown that the consecutive hours of low feed-in from VRE or their full load hours are not sufficient to determine if the weather data of a specific year is more or less ambitious in every aspect. Other factors, such as the outside temperature

or the system configuration, might have a major influence on the results. Results based on the weather data of 2015 required the highest capacity of the thermal power plant park, despite this year exhibits the highest number of full load hours of VRE and the lowest periods of power deficiency. Calculations based on only one particular weather data set exhibited relative deviations amounting up to 15 % from each other. A lower difference of 6 % was determined for the share of refurbished buildings. This would translate to a necessary increase of the renovation rate by 0.2 %. In order to reduce uncertainties related to a specific weather data set, a stochastic approach was applied. In this case, the optimisation was performed based on a continuously and randomly changing sequence of weather data. Compared to the generally utilised method for the consideration of weather data, especially technologies which reduced the influence from intermittent generation of VRE were deployed to a higher extent. This, for instance, applied to electric brine heat pumps instead of electric air heat pumps, to the refurbishment of buildings or to the deployment of FCEVs in the motorised road transport. From this, it was concluded that the system tried to compensate the effects caused by constantly changing weather influences. Overall, the outlined range of outcomes should be kept in mind, especially when evaluating model results based on only one specific weather data (or even typical days).

It was further analysed how the system handles one entire month during which the wind speed and the solar radiation are set to zero for Germany as well as its bordering countries. It was shown that power storages or DSM can not provide any relevant contribution to the balancing of the residual load during such periods, as their discharge time normally amounts to at most half a day. Instead, thermal power plants were operated to meet the occurring electricity demand. In order to keep their CO_2 emissions low, a higher amount of biomass was converted into biofuels. Further, a part of the power demand was shifted towards hydrogen-based technologies. This led to a reduction of the residual load and thus reduced the necessary power generation from thermal power plants. The results revealed that, in such cases, hydrogen provided an effective seasonal storage option. Before facing a prolonged period of power deficiency, the hydrogen storage was filled up throughout the years and discharged once necessary. This behaviour was ensured by the implemented perfect foresight of the solver, which also influenced the deployment of electrolysis plants. This was confirmed by a calculation, for which the charge level of the hydrogen storage was not transferred throughout the years. As a result, the deployment of electrolysis plants was postponed in time. Power storages and DSM did not represent any direct contribution during extended periods of absent power generation from VRE. However, the results suggested that by integrating more electricity from VRE over the year, they indirectly permitted a higher emission level once necessary. This also allowed the coverage of the electricity demand by thermal power plants without violating the yearly set CO_2 emission limit.

A cost evaluation of DSM was performed based on the investigation of five different climate protection targets. It was shown that the cost-savings resulting from DSM were the higher the more ambitious the CO_2 reduction target were. For this, two main reasons were identified: first, the contribution of DSM became more important as the expansion of VRE continued, which in turn revealed to be proportional to the pursued emission reduction. Second, greater emission reductions required more investments in measures with relatively high CO_2 abatement costs, such as stationary batteries and PtG plants. It was shown that both technologies could in part be substituted by DSM in the private transport and the generation of heat. The cost-savings from 2015 to 2050 ranged from 115 to 340 billion euros. A distribution over the total number of BEVs (50 million) and heat generators (27 million), leads to roughly 1,500 € to 4,500 € per unit. Against the background that the costs for infrastructure (for example wallboxes) and their maintenance and operation were already considered, these values would represent the marginal costs for the profitable use of DSM. The cost-savings in case of DSM also arose from a reduced quantity of power imports from abroad (-33 %) over the entire observation period as well as from a reduction of the thermal power plant park, amounting on average to 16 % in 2050. Further, DSM revealed to be able to substitute up to 300 GWh_{el} of stationary battery capacity. A part of this capacity is provided by the motorised private transport. If the complete vehicle fleet in 2050 was to be shifted to BEVs, this would lead to a total battery capacity of roughly 3.4 TWh_{el}. By considering only users following a Controlled Charging Strategy as well as the maximum allowed depth of discharge equal to 25 % each, this capacity is reduced to 212 GWh_{el}. On top of that, it was shown that also the power-controlled operation of heat generators decreased the installed capacity of stationary batteries (cf. 6.3).

Based on a 95 % CO_2 reduction target by 2050, the import of synthetic fuels from abroad was considered. It was shown that, under the given assumptions, this option is highly effective to reduce costs, especially concerning the deployment of VRE, power storages, brine heat pumps or PtG plants. However, the results revealed that at most a rather small part of the available import capacity was utilised, suggesting that only measures with particularly high abatement costs were replaced. As a consequence, the system avoided technologies exhibiting relatively high CO_2 abatement costs, which might otherwise have been necessary to achieve ambitious climate protection targets. In this context, it was shown that DSM reduced the imported quantity of synthetic fuels by roughly 6%. The results confirmed that DSM besides representing an efficient measure to integrate VRE and to reduce the total system costs, further decreased the energy dependency on neighbouring countries.

7 Summary and Outlook

This work presented an assessment of technologies to balance intermittent power generation from variable renewable energy (VRE) in Germany. The focus was on thermal power plants, the controlled charging of electric vehicles, the heat-controlled or power-controlled operation of heat generators and the variation of key parameters, such as the set CO_2 reduction target or the underlying weather data. The analysis was performed based on the Renewable Energy Model (REMod). This model was designed to determine a cost-optimal configuration of the energy system under consideration of an exogenously set limit of energy-related CO_2 emissions. In an integrative approach it depicts interdependencies between all implemented technologies and sectors of the energy system.

The work begins by introducing the functioning principle of the model, the underlying data, the objective function and the main system components. After this, the model extensions required in order to address the research questions were presented. A general approach for the consideration of ramping behaviour was applied to thermal power plants and Power-to-Gas (PtG) plants. The transport sector was detailed in regard to electric vehicles, including hourly resolved driving profiles as well as two charging strategies. The generation of heat was divided into nine technology categories and each one could be set to a heat-controlled or a power-controlled operation. Further, a covariance matrix adaptation evolution strategy algorithm for the problem optimisation was implemented. This led to more reliable and higher quality results, compared to the previous particle swarm optimisation approach. In order to consider a greater variety of weather influences, the model was extended from three to five „weather years“. Lastly, it was calibrated for the year 2015, showing a good accordance to literature values and data provided by the Federal Government.

One aim of the analysis was to present the main model extensions and their sensitivity to different parameter settings. Another aim was to provide a qualitative and quantitative assessment of load balancing options, on the example of the German energy system. A summary of the key results, including suggestions for future research and model development, is subsequently presented.

The consideration of ramping behaviour showed little influence on the technology deployment within each end-use sector or on the total system costs. Based on two different

CO_2 reduction targets, the resulting variations amounted to less than 2 % at maximum. Conversely, the effect on the expansion of thermal power plants was significant, as with increasing share of VRE, highly flexible gas turbines were favoured over power plants with higher start-up times. At the same time, the consideration of ramping behaviour also influenced the operation mode of thermal power plants. Short periods of power deficiency, below four hours, were primarily met by gas turbine power plants. CCGT power plants were operated only in case of extended durations, leading to a more realistic plant utilisation from an economical point of view. As a consequence of the implemented priority dispatch of VRE determined in the EEG [38], the underlying weather data proved to have a major influence on the utilisation of thermal power plants. Especially years with greater full load hours of VRE increased the number of start-up proceedings of thermal power plants. This led to a more irregular plant operation and thus higher losses in the yearly conversion efficiency. While this impact proved to be neglectable for gas turbine plants, for CCGT and coal power plants it amounted to roughly 6 % of their nominal efficiency. For each TWh_{el} generated by methane gas-fired CCGT power plants and coal power plants this resulted in additional 26 kt_{CO_2} tons and 64 kt_{CO_2}, respectively. This analysis was performed as the renewable energy share to the gross electricity generation reached a value of 80 %, which corresponds to the 2050 target set by the Federal Government [3]. These effects will further increase as the expansion of VRE continues. Overall, the results showed that the implemented model extensions allowed for a more realistic description of power plant operation. For instance, it is was possible to resonate the suggestion of the coal committee [23]. In the model, coal power plants, beginning in 2035, were operated only as reserve capacity systems. Further, the endogenous deployment of thermal power plants, besides depending on their costs and carbon footprint, now also accounts for their flexibility characteristics.

The implemented operating principles and driving profiles of BEVs were analysed in chapter 6.2 with particular regard to the motorised private transport. Based on the consideration of three different CO_2 reduction targets it was shown that, despite the consideration of an uncontrolled vehicle charging[1], BEVs represented the dominant power train technology in 2050. However, their share proved to be rather sensitive to an increase in purchase price. Just 10 % increased the numbers of fuel cell electric vehicles (FCEVs) to almost one third of the vehicle fleet. Since the parametrisation of the vehicles considers average requirements, it could be assumed that in reality some vehicles would need to fulfil higher demands in terms of range coverage. This could translate to higher battery costs of BEVs and thus increase the attractiveness of FCEVs. In order to verify this, the model would need to be extended in regard of an additional vehicle class. The analysis

[1] This means that most vehicles are charged around 5 to 6 pm, as they return to a charging facility, without consideration of whether power surplus or deficiency occurs (cf. section 5.3).

further showed that another aspect favouring FCEVs was their ability to decouple a significant amount of their energy demand from the non-dispatchable generation of power. It was observed that the deployment of BEVs was increased once vehicle users charged them in a controlled way. This allowed BEVs to contribute to the balancing of the residual load in times of power surplus (Grid-to-Vehicle, G2V) and power deficiency (V2G). In this case, the considered discharge depth for a feed-back into the grid (V2G), rather than the share of users charging vehicles preferably in times of power surplus, demonstrated to be of greater value for BEVs. The presented analysis was performed under the assumption that users charge their vehicles exclusively at home, which might lead to a higher degree of simultaneous charging, thus possibly disadvantaging the deployment of BEVs. This was already confirmed in another study performed by the author, in which this charging behaviour was compared to a uniformly distributed charging profile [105]. In the upcoming years it is expected that charging facilities will be increasingly available at work, super markets, shopping centers or in car parks. This should be considered in future studies.

The effects resulting from a heat-controlled or power-controlled operation of heat generators were investigated under consideration of three different CO_2 reduction targets. Regardless of the considered operation mode, a shift from oil- and methane gas-fired boilers towards electric heat pumps and heat grids was observed. The analysis revealed that especially electric air heat pumps played a dominant role by 2050, even if their purchase price was increased by 30 %. It was shown that with the ongoing expansion of VRE, the residual load over time exhibited higher increases in power surplus rather than power deficiency. As a result, when a heat-controlled mode was considered, electric heat pumps proved to be more grid-supportive compared to cogeneration plants. Accordingly, a power-controlled operation increased the number of connections to heat grids and thus led a greater deployment of large-scale CHP units. Solar thermal systems presented a considerable increase in capacity compared to today's levels, although, lower than those resulting from a heat-controlled operation. This suggested that, to some extent, solar thermal systems compensated for the lacking flexibility of other heat generators. This led to the conclusion that, when considering a power-controlled mode, solar thermal systems should preferably be installed in combination with oil or gas boilers. Electric heat pumps and thermal energy storages (TES) presented better synergies with photovoltaic systems. It was further observed that to access the full potential of DSM, the TES capacity in Germany should be increased to 1600 GWh_{th} in 2050. On average, this corresponds to roughly 600 litres per building.

How the model results are affected by varying weather influences was analysed by performing multiple optimisation runs based on a changing parametrisation of the underlying weather data. Within the examined calculations, the results based only on the weather data of 2015 exhibited lower costs as well as less adaptations throughout all

sectors of the energy system. Despite that, the highest installed capacity of thermal power plants was reached. Besides considering the number of full load hours from VRE and the duration of power deficiency periods, the characterisation of a weather data set, should also account for additional factors. Included should be the outside temperature, the frequency and duration of low, medium or high feed-in from VRE periods, the implemented operation of energy storages and other conversion technologies or their assumed expansion limits. It was observed that calculations based on only one specific year exhibited a range of outcomes in technology deployment and total system costs of up to 15 %. To reduce this uncertainty, a stochastic approach was proposed, meaning that the underlying weather data was randomly determined within each function call[2]. In this case, a tendency towards system components, which reduced the effects of weather influences, for example the refurbishment of buildings or the deployment of more efficient brine heat pumps, was observed. The same also applied to hydrogen-based technologies, which in large parts allowed a decoupling of their energy demand from the non-dispatchable power generation. The hydrogen storage level proved to follow seasonal behaviour: the storage was charged especially during the summer, primarily by electrolysis plants mostly utilising surplus power from VRE. The storage was discharged during the winter months, when the hydrogen demand exceeded the occurring production.

The effect of weather influences on the results was investigated in another calculation, for which wind speed and solar radiation for Germany and its neighbouring countries were set to zero for the entire month of October. In this case, a greater part of the energy demand was shifted towards hydrogen-based technologies, decreasing the total electric load and thus contributing to overcoming this extreme weather condition. While the balancing of the residual load through DSM usually lasted for less than half a day, it was shown that DSM indirectly contributed to overcoming extended periods of absent power generation from VRE. On average, roughly 9 % and 4 % of VRE yearly electricity production were integrated by BEVs and heat generators combined with TES. This allowed thermal power plants to emit higher quantities of CO_2 once necessary, without violating the exogenously set CO_2 limit.

From an economic point of view the value of DSM was investigated based on the analysis of five different CO_2 reduction targets. On average, DSM proved to reduce the resulting CO_2 abatement costs by roughly 50 €/t_{CO_2}. This means that measures with particularly high CO_2 abatement costs could be avoided, which otherwise would be eventually necessary to meet the set climate protection target. It was shown that the reduction in total system costs achieved by utilising DSM, ranged from 115 billion euros to 341 billion euros, summed up from 2015 to 2050. By distributing these savings over all heat generators

[2] Each optimisation run performs approximately one million function calls. The exact number may however vary depending on the individual convergence pattern (cf. section 3.3.2).

and all private vehicles in Germany, marginal costs from 1,500 € to 4,500 € were determined. Since the expenses for investment, maintenance and operation of each technology (including infrastructure) were already considered, this suggested, that DSM provided a cost-efficient load balancing option. The achieved cost-savings increased when more ambitious climate protection targets were considered, mainly for two reasons: First, the contribution of DSM proved to correlate to the extent of intermittent power generation from VRE, which in turn was directly linked to the set CO_2 reduction target. Second, more ambitious climate protection targets led to higher capacities of thermal power plants, PtG plants, stationary batteries or energy imports. Since these load balancing options compete, to a certain extent, with DSM, their installations were reduced once it was considered. On average, the substituted capacity of thermal power plants in 2050 amounted to 23 GW_{el}. The capacity of electrolysis plants varied between 36 GW_{el} and 60 GW_{el}, while for stationary batteries it reached up to 300 GWh_{el}. Over the entire observation period, the imports of electricity and of synthetic fuels from abroad were decreased by one third. This revealed that besides lowering costs, DSM also contributed to reduce the energy dependency of Germany on other countries.

DSM may also reduce the necessary expansion of the electrical grid and improve its stability, for instance by distributing the charging of electric vehicles over time. While the grid expansion was considered from a cost point of view, technical restrictions, such as grid congestion, were not modelled. One possible option to close this gap is provided by coupling the results obtained from REMod to a grid expansion model. A combination with the simulation tool DIgSILENT PowerFactory [252] was presented in [253]. However, this approach neglects feedback effects on the energy system configuration, which is one of the key features of REMod. In order to preserve this characteristic, a more detailed depiction of the power grid needs to be directly implemented into the model. This requires the extension from a single-node to a multi-node approach. The implementation could be performed by applying the current model structure within each node and by modelling the transfer of energy between them. This extension would allow the allocation of technologies in Germany, or alternatively, to model the European energy system. Most likely this will require further enhancement of the utilised optimisation algorithm, especially in terms of computing time. One option could be to start the optimisation run based on known intermediary results, i.e. based on a „warm-start“, instead of starting from scratch. A second option would be to rely on more powerful computing servers, with higher processing power.

It is further suggested to include photovoltaic systems with an east-west orientation. Despite their lower peak generation capacity, a more regular electricity production could provide other benefits to the system. As for PtG and PtL plants, deriving the CO_2 for the production of synthetic fuels from biomass plants or coal power plants could be considered [254]. This could eventually lead to yet not depicted back-coupling effects,

increasing the value of plants that provide cheaper CO_2. Besides that, the addition of another hydrogen-fired gas turbine is suggested, which should be coupled to the developed forecast module. In this case, the reconversion of hydrogen into electricity should only be performed if prolonged periods of power deficiency occur. As a consequence, both hydrogen turbine plants could be individually dimensioned, thus providing more flexibility concerning the utilisation of hydrogen. Similarly, it is suggested to complement the already implemented stationary battery and to describe its charging or discharging rate as a function of the expected duration of the upcoming power surplus or power deficiency period. This would provide a more consistent contribution to the balancing of the residual load and possibly influence the dimensioning of other flexibility options.

Along with the suggested technological improvements it is also conceivable to emphasise social factors in future analyses. For instance, changes in traffic behaviour, market entry barriers or technology diffusion. Technology deployment could also be affected by the availability of specific materials. This includes BEVs and wind turbine plants, for which possible supply bottleneck for cobalt, lithium or copper could be taken into account [255].

A Model Input Parameters

A.1 Power Generators

Table A.1: Input parameters for power generators for 2015, 2020, 2030, 2040 an 2050. i_{int}: interest rate, f_{OM}: factor for maintenance and operation in % from purchase price, r_P: price change factor for the purchase of a technology or a building component, r_{OM}: price change rate for maintenance and operation, f_{VLH}: factor for adjustment of full load hours. CHP: combined heat and power, CCGT: combined cycle gas turbine.

Photovoltaic systems		2015	2020	2030	2040	2050	total	ref
Min. deployment	GW_{el}	1.3	0.0	0.0	0.0	0.0	5.1	[22]
Max. deployment	GW_{el}	1.3	10.0	15.8	15.8	15.8	530.0	[213]
Purchase price	€/kW_{el}	1166.0	976.0	718.0	597.0	571.0	/	[113, 256]
Service life	a	25.1	25.6	26.6	27.6	28.7	/	[113, 256]
i_{int}	%	7.0	7.0	7.0	7.0	7.0	/	[113]
$f_{OM,i}$	%	2.0	2.0	2.0	2.0	2.0	/	[113, 257]
r_P	%	1.7	1.7	1.7	1.7	1.7	/	[113]
r_{OM}	%	1.7	1.7	1.7	1.7	1.7	/	[113]
f_{VLH}	-	0.9	1.0	1.0	1.0	1.0	/	[22, 214]
Wind onshore		2015	2020	2030	2040	2050	total	ref
Min. deployment	GW_{el}	3.7	0.0	0.0	0.0	0.0	13.3	[22]
Max. deployment	GW_{el}	3.7	5.5	5.5	5.5	5.5	230.8	[258]
Purchase price	€/kW_{el}	1327.0	1193.0	1066.0	1037.0	1035.0	/	[113, 257]
Service life	a	23.1	23.6	24.5	25.4	26.4	/	[113, 257]
i_{int}	%	7.0	7.0	7.0	7.0	7.0	/	[113]
$f_{OM,i}$	%	3.0	3.0	3.0	3.0	3.0	/	[113, 257]
r_P	%	1.7	1.7	1.7	1.7	1.7	/	[113]
r_{OM}	%	1.7	1.7	1.7	1.7	1.7	/	[113]
f_{VLH}	-	0.9	1.0	1.0	1.0	1.0	/	[22, 214]

Continued on next page

Table A.1: Input parameters for power generators for 2015, 2020, 2030, 2040 an 2050. i_{int}: interest rate, f_{OM}: factor for maintenance and operation in % from purchase price, r_P: price change factor for the purchase of a technology or a building component, r_{OM}: price change rate for maintenance and operation, f_{VLH}: factor for adjustment of full load hours. CHP: combined heat and power, CCGT: combined cycle gas turbine.

Wind offshore		2015	2020	2030	2040	2050	total	ref
Min. deployment	GW_{el}	2.3	0.0	0.0	0.0	0.0	4.3	[22]
Max. deployment	GW_{el}	2.3	1.1	2.6	2.6	2.6	85.2	[22]
Purchase price	€/kW_{el}	3840.0	3512.0	2937.0	2493.0	2251.0	/	[113, 257]
Service life	a	20.0	20.0	20.0	20.0	20.0	/	[113, 257]
i_{int}	%	7.0	7.0	7.0	7.0	7.0	/	[113]
$f_{OM,i}$	%	3.0	3.0	3.0	3.0	3.0	/	[113, 257]
r_P	%	1.7	1.7	1.7	1.7	1.7	/	[113]
r_{OM}	%	1.7	1.7	1.7	1.7	1.7	/	[113]
f_{VLH}	-	0.6	1.0	1.0	1.0	1.0	/	[22, 214]
CCGT (without CHP)		2015	2020	2030	2040	2050	total	ref
Min. deployment	GW_{el}	0.0	0.0	0.0	0.0	0.0	0.0	/
Max. deployment	GW_{el}	0.5	0.5	2.0	3.0	3.0	100.5	[113]
Purchase price	€/kW_{el}	700.0	700.0	700.0	700.0	700.0	/	[259]
Service life	a	40.0	40.0	40.0	40.0	40.0	/	[260]
i_{int}	%	7.0	7.0	7.0	7.0	7.0	/	[113]
$f_{OM,i}$	%	3.0	3.0	3.0	3.0	3.0	/	[260]
r_P	%	1.7	1.7	1.7	1.7	1.7	/	[113]
r_{OM}	%	1.7	1.7	1.7	1.7	1.7	/	[113]
η	%	54.0	56.0	59.0	61.0	63.0	/	[261, 262]
Gasturbine (methane)		2015	2020	2030	2040	2050	total	ref
Min. deployment	GW_{el}	0.0	0.0	0.0	0.0	0.0	0.0	/
Max. deployment	GW_{el}	2.0	2.0	2.0	3.0	4.0	104.4	[113]
Purchase price	€/kW_{el}	385.0	385.0	385.0	385.0	385.0	/	[257]
Service life	a	40.0	40.0	40.0	40.0	40.0	/	[263]
i_{int}	%	7.0	7.0	7.0	7.0	7.0	/	[113]
$f_{OM,i}$	%	2.0	2.0	2.0	2.0	2.0	/	[257]
r_P	%	1.7	1.7	1.7	1.7	1.7	/	[113]
r_{OM}	%	1.7	1.7	1.7	1.7	1.7	/	[113]
η	%	35.0	35.0	35.0	35.0	35.0		[263]

Continued on next page

Table A.1: Input parameters for power generators for 2015, 2020, 2030, 2040 an 2050. i_{int}: interest rate, f_{OM}: factor for maintenance and operation in % from purchase price, r_P: price change factor for the purchase of a technology or a building component, r_{OM}: price change rate for maintenance and operation, f_{VLH}: factor for adjustment of full load hours. CHP: combined heat and power, CCGT: combined cycle gas turbine.

Gasturbine (hydrogen)		2015	2020	2030	2040	2050	total	ref
Min. deployment	GW_{el}	0.0	0.0	0.0	0.0	0.0	0.0	/
Max. deployment	GW_{el}	0.0	0.1	3.0	3.0	4.0	82.5	/
Purchase price	€/kW_{el}	567.0	500.0	419.0	389.0	385.0	/	[113]
Service life	a	40.0	40.0	40.0	40.0	40.0	/	[263]
i_{int}	%	7.0	7.0	7.0	7.0	7.0	/	[113]
$f_{OM,i}$	%	2.0	2.0	2.0	2.0	2.0	/	[257]
r_P	%	1.7	1.7	1.7	1.7	1.7	/	[113]
r_{OM}	%	1.7	1.7	1.7	1.7	1.7	/	[113]
η	%	40.0	40.0	40.0	40.0	40.0	/	[113]
Oil power plants		2015	2020	2030	2040	2050	total	ref
Installed capacity	GW_{el}	4.2	3.2	0.1	0.1	0.1	/	[22, 169]
Purchase price	€/kW_{el}	385.0	385.0	385.0	385.0	385.0	/	[257]
Service life	a	40.0	40.0	40.0	40.0	40.0	/	[173]
i_{int}	%	7.0	7.0	7.0	7.0	7.0	/	[113]
$f_{OM,i}$	%	2.0	2.0	2.0	2.0	2.0	/	[173]
r_P	%	1.7	1.7	1.7	1.7	1.7	/	[113]
r_{OM}	%	1.7	1.7	1.7	1.7	1.7	/	[113]
η	%	42.0	42.0	42.0	42.0	42.0	/	[173]
Lignite power plant		2015	2020	2030	2040	2050	total	ref
Min. deployment	GW_{el}	0.9	0.0	0.0	0.0	0.0	0.9	[22, 169]
Max. deployment	GW_{el}	0.9	1.0	3.0	3.0	3.0	107	[22, 169]
Purchase price	€/kW_{el}	1700.0	1700.0	1700.0	1700.0	1700.0	/	[263]
Service life	a	45.0	45.0	45.0	45.0	45.0	/	[263]
i_{int}	%	7.0	7.0	7.0	7.0	7.0	/	[113]
$f_{OM,i}$	%	1.6	1.6	1.6	1.6	1.6	/	[263]
r_P	%	1.7	1.7	1.7	1.7	1.7	/	[113]
r_{OM}	%	1.7	1.7	1.7	1.7	1.7	/	[113]
η	%	36.0	37.0	39.0	41.0	42.0	/	[60]
Must-run capacity	%	75.0	75.0	37.5	0.0	0.0	/	[22]

Continued on next page

Table A.1: Input parameters for power generators for 2015, 2020, 2030, 2040 an 2050. i_{int}: interest rate, f_{OM}: factor for maintenance and operation in % from purchase price, r_P: price change factor for the purchase of a technology or a building component, r_{OM}: price change rate for maintenance and operation, f_{VLH}: factor for adjustment of full load hours. CHP: combined heat and power, CCGT: combined cycle gas turbine.

Hard Coal power plant		2015	2020	2030	2040	2050	total	ref
Min. deployment	GW_{el}	0.9	0.0	0.0	0.0	0.0	0.9	[22, 169]
Max. deployment	GW_{el}	0.9	1.0	3.0	3.0	3.0	107	[22, 169]
Purchase price	€/kW_{el}	1500.0	1500.0	1500.0	1500.0	1500.0	/	[263]
Service life	a	45.0	45.0	45.0	45.0	45.0	/	[263]
i_{int}	%	7.0	7.0	7.0	7.0	7.0	/	[113]
$f_{OM,i}$	%	1.6	1.6	1.6	1.6	1.6	/	[263]
r_P	%	1.7	1.7	1.7	1.7	1.7	/	[113]
r_{OM}	%	1.7	1.7	1.7	1.7	1.7	/	[113]
η	%	40.0	41.0	42.0	42.0	42.0	/	[60]
Must-run capacity	%	43.5	43.5	21.8	0.0	0.0	/	[22]

A.2 Ramping Parameters

Table A.2: Ramping input parameters of thermal power plants and Power-to-Gas (PtG) or Power-to-Liquid (PtL) plants based on [60, 112, 173, 174, 227–232]. h_{CS}: cold start time, h_{HS}: hot start time, P_{Min}: minimum load capacity, S_{PL}: conversion efficiency in partial load related to maximum efficiency, E_S: energy demand for heat-up per installed plant capacity, R_{RR}: ramp rate.

	Year [-]	h_{CS} [h]	h_{HS} [h]	h_{PL} [h]	P_{Min} [[$\%_{P_{Nom}}$]]	S_{PL} [$\%_{\eta Nom}$]	E_S [kWh_{th}/kW]	R_{RR} [$\%/min$]
	2017	7.88	2.44	0.36	33.50	97	2.70	3.05
HardCoal PP	2030	7.13	2.18	0.32	30.75	97	2.70	3.58
	2050	6.38	1.92	0.29	28.00	97	2.70	4.10
	2017	9.00	5.00	0.50	55.00	97	2.70	1.50
Lignite PP	2030	7.81	3.75	0.32	47.60	97	2.70	2.70
	2050	6.88	3.00	0.30	42.20	97	2.70	3.20
	2017	0.18	0.18	0.09	45.00	83	0.10	10.00
Oil PP	2030	0.14	0.11	0.08	36.07	83	0.10	12.55
	2050	0.13	0.10	0.08	33.93	83	0.10	13.40
	2017	3.50	1.25	0.31	45.00	93	2.80	3.00
CCGT	2030	3.00	0.91	0.21	44.11	93	2.80	4.38
	2050	2.50	0.73	0.17	43.21	93	2.80	5.50
	2017	0.18	0.18	0.09	45.00	83	0.10	10.00
GT (CH4/H2)	2030	0.14	0.11	0.08	36.07	83	0.10	12.55
	2050	0.13	0.10	0.08	33.93	83	0.10	13.40
	2017	0.21	0.03	0.03	5.00	100	0.15	50.00
PEM electrolysis	2030	0.15	0.01	0.01	5.00	100	0.10	135.00
	2050	0.09	0.01	0.01	3.00	100	0.06	212.00
	2017	0.82	0.08	0.07	16.00	100	0.59	19.00
AEL electrolysis	2030	0.61	0.03	0.03	13.00	100	0.44	56.00
	2050	0.59	0.01	0.01	12.00	100	0.43	114.00
	2017	9.83	0.17	0.05	20.00	100	8.11	29.00
HTEL electrolysis	2030	2.92	0.08	0.09	3.00	100	2.54	19.00
	2050	0.48	0.02	0.02	3.00	100	0.42	97.00
	2017	0.76	0.08	0.06	15.00	100	0.54	22.00
Power-to-methane	2030	0.54	0.03	0.02	9.00	100	0.41	86.00
and/or liquid	2050	0.37	0.01	0.01	6.00	100	0.28	150.00

A.3 Synthetic Fuels and Steam Reforming

Table A.3: Input parameters of plants for the generation of synthetic fuels and steam reforming for 2015, 2020, 2030, 2040 an 2050. i_{int}: interest rate, f_{OM}: factor for maintenance and operation in % from purchase price, r_P: price change factor for the purchase of a technology or a building component, r_{OM}: price change rate for maintenance and operation.

Power-to-Gas (Electrolysis)		2015	2020	2030	2040	2050	total	ref
Min. deployment	GW	0.0	0.0	0.0	0.0	0.0	0.0	[113]
Max. deployment	GW	0.0	0.0	25.0	25.0	25.0	629.0	[113]
Purchase price	€/kW_{el}	776.0	738.4	613.0	554.0	495.0	/	[264]
Service life	a	26.8	26.5	25.3	27.7	30.0	/	[264]
i_{int}	%	7.0	7.0	7.0	7.0	7.0	/	[113]
f_{OM}	%	4.0	3.5	3.3	3.6	3.9	/	[264]
r_P	%	1.7	1.7	1.7	1.7	1.7	/	[113]
r_{OM}	%	1.7	1.7	1.7	1.7	1.7	/	[113]
η	%	64.3	64.5	65.1	67.6	70.2	/	[264]
Power-to-Gas (Methanation)		2015	2020	2030	2040	2050	total	ref
Min. deployment	GW	0.0	0.0	0.0	0.0	0.0	0.0	[113]
Max. deployment	GW	0.0	0.0	2.1	3.0	3.0	69.0	[113]
Purchase price	€/kW_{el}	2086.0	1914.0	1074.0	1006.0	995.0	/	[265]
Service life	a	20.0	21.4	24.3	27.1	30.0	/	[265]
i_{int}	%	7.0	7.0	7.0	7.0	7.0	/	[113]
f_{OM}	%	4.0	4.0	4.0	4.0	4.0	/	[265]
r_P	%	1.7	1.7	1.7	1.7	1.7	/	[113]
r_{OM}	%	1.7	1.7	1.7	1.7	1.7	/	[113]
$\eta_{electrolysis}$	%	74.3	74.3	74.3	74.3	74.3	/	[265]
$\eta_{sabatier}$	%	52.3	57.1	61.5	61.5	61.5	/	[265]
η_{th}	%	6.8	6.8	6.8	6.8	6.8	/	[265]
Power-to-Liquid		2015	2020	2030	2040	2050	total	ref
Min. deployment	GW	0.0	0.0	0.0	0.0	0.0	0.0	[113]
Max. deployment	GW	0.0	0.0	1.0	1.0	1.0	27.5	[113]
Purchase price	€/kW_{el}	2196.9	2041.5	1187.2	1125.7	1115.5	/	[266]
Service life	a	20.0	21.4	24.3	27.1	30.0	/	[266]
i_{int}	%	7.0	7.0	7.0	7.0	7.0	/	[113]
f_{OM}	%	4.0	4.0	4.0	4.0	4.0	/	[266]
r_P	%	1.7	1.7	1.7	1.7	1.7	/	[113]
r_{OM}	%	1.7	1.7	1.7	1.7	1.7	/	[113]
η	%	39.6	43.3	46.6	46.6	46.6	/	[266]

Continued on next page

Table A.3: Input parameters of plants for the generation of synthetic fuels and steam reforming for 2015, 2020, 2030, 2040 an 2050. i_{int}: interest rate, f_{OM}: factor for maintenance and operation in % from purchase price, r_P: price change factor for the purchase of a technology or a building component, r_{OM}: price change rate for maintenance and operation.

Steam methane reforming		2015	2020	2030	2040	2050	total	ref
Min. deployment	GW	0.0	0.0	0.0	0.0	0.0	0.0	[113]
Max. deployment	GW	0.0	0.0	1.0	1.0	1.0	30.0	[113]
Purchase price	€/kW_{CH_4}	995.0	995.0	995.0	995.0	995.0	/	[267]
Service life	a	15.0	15.0	15.0	15.0	15.0	/	[267]
i_{int}	%	7.0	7.0	7.0	7.0	7.0	/	[113]
f_{OM}	%	2.5	2.5	2.5	2.5	2.5	/	[267]
r_P	%	1.7	1.7	1.7	1.7	1.7	/	[113]
r_{OM}	%	1.7	1.7	1.7	1.7	1.7	/	[113]
η	%	52.3	57.1	61.5	61.5	61.5	/	[113]
Must-run capacity	%	10.0	10.0	10.0	10.0	10.0	/	[113]

A.4 Storage Technologies

Table A.4: Input parameters of storage technologies for 2015, 2020, 2030, 2040 an 2050. i_{int}: interest rate, f_{OM}: factor for maintenance and operation in % from purchase price, r_P: price change factor for the purchase of a technology or a building component, r_{OM}: price change rate for maintenance and operation.

Stationary batteries		2015	2020	2030	2040	2050	total	ref
Min. deployment	GWh_{el}	0.1	0.0	0.0	0.0	0.0	0.0	[113]
Max. deployment	GWh_{el}	0.1	1.0	40.5	40.5	40.5	1081.4	[113]
Purchase price	€/kWh_{el}	1146.7	752.0	333.5	211.8	200.0	/	[264]
Service life	a	10.0	10.0	15.0	15.0	15.0	/	[264]
i_{int}	%	7.0	7.0	7.0	7.0	7.0	/	[113]
f_{OM}	%	1.0	1.0	1.0	1.0	1.0	/	[264]
r_P	%	1.7	1.7	1.7	1.7	1.7	/	[113]
r_{OM}	%	1.7	1.7	1.7	1.7	1.7	/	[113]
η	%	85.1	85.8	87.2	88.5	90.0	/	[264]

Continued on next page

Table A.4: Input parameters of storage technologies for 2015, 2020, 2030, 2040 an 2050. i_{int}: interest rate, f_{OM}: factor for maintenance and operation in % from purchase price, r_P: price change factor for the purchase of a technology or a building component, r_{OM}: price change rate for maintenance and operation.

Pumped-storage power plants		2015	2020	2030	2040	2050	total	ref
Capacity	TWh_{el}	40.7	44.4	51.7	59.0	66.4	66.4	[19]
Charge rate	GW_{el}	6.4	6.7	7.3	7.9	8.5	8.5	[19]
purchase price	€/kWh_{el}	850.0	850.0	850.0	850.0	850.0	/	[19]
service life	a	80.0	80.0	80.0	80.0	80.0	/	[19]
i_{int}	%	7.0	7.0	7.0	7.0	7.0	/	[113]
f_{OM}	%	2.0	2.0	2.0	2.0	2.0	/	[19]
r_P	%	1.7	1.7	1.7	1.7	1.7	/	[113]
r_{OM}	%	1.7	1.7	1.7	1.7	1.7	/	[113]
η	%	80.0	80.0	80.0	80.0	80.0	/	[19]
Battery Power-to-Gas		2015	2020	2030	2040	2050	total	ref
Min. deployment	GWh_{el}	0.0	0.0	0.0	0.0	0.0	0.0	[113]
Max. deployment	GWh_{el}	0.0	0.0	5.5	8.0	8.0	175.4	[113]
Purchase price	€/kWh_{el}	1146.7	752.0	333.5	211.8	200.0	/	[264]
Service life	a	10.0	10.0	15.0	15.0	15.0	/	[264]
i_{int}	%	7.0	7.0	7.0	7.0	7.0	/	[113]
f_{OM}	%	1.0	1.0	1.0	1.0	1.0	/	[264]
r_P	%	1.7	1.7	1.7	1.7	1.7	/	[113]
r_{OM}	%	1.7	1.7	1.7	1.7	1.7	/	[113]
η	%	85.1	85.8	87.2	88.5	90.0	/	[264]
Hydrogen storage (capacity)		2015	2020	2030	2040	2050	total	ref
Min. deployment	TWh_{H_2}	0.0	0.0	0.0	0.0	0.0	0.0	[113]
Max. deployment	TWh_{H_2}	0.0	0.0	10.0	10.0	10.0	264.0	[113]
Purchase price	€/kWh_{H_2}	0.3	0.3	0.3	0.3	0.3	/	[113]
Service life	a	30.0	30.0	30.0	30.0	30.0	/	[113]
i_{int}	%	7.0	7.0	7.0	7.0	7.0	/	[113]
f_{OM}	%	13.8	13.8	13.8	13.8	13.8	/	[113]
r_P	%	1.7	1.7	1.7	1.7	1.7	/	[113]
r_{OM}	%	1.7	1.7	1.7	1.7	1.7	/	[113]

Continued on next page

Table A.4: Input parameters of storage technologies for 2015, 2020, 2030, 2040 an 2050. i_{int}: interest rate, f_{OM}: factor for maintenance and operation in % from purchase price, r_P: price change factor for the purchase of a technology or a building component, r_{OM}: price change rate for maintenance and operation.

Hydrogen storage (charge rate)		2015	2020	2030	2040	2050	total	ref
Min. deployment	GW_{H_2}	0.0	0.0	0.0	0.0	0.0	/	[113]
Max. deployment	GW_{H_2}	0.0	0.0	25.0	25.0	25.0	629.0	[113]
Purchase price	€/kW_{H_2}	162.9	162.9	162.9	162.9	162.9	/	[113]
Service life	a	30.0	30.0	30.0	30.0	30.0	/	[113]
i_{int}	%	7.0	7.0	7.0	7.0	7.0	/	[113]
f_{OM}	%	2.5	2.5	2.5	2.5	2.5	/	[113]
r_P	%	1.7	1.7	1.7	1.7	1.7	/	[113]
r_{OM}	%	1.7	1.7	1.7	1.7	1.7	/	[113]
η	%	95.0	95.0	95.0	95.0	95.0	/	[113]

A.5 Space Heat and Domestic Hot Water Supply

Table A.5: Input parameters of generators for the supply of space heat and domestic hot water for 2015, 2020, 2030, 2040 an 2050. i_{int}: interest rate, f_{OM}: factor for maintenance and operation in % from purchase price, r_P: price change factor for the purchase of a technology or a building component, r_{OM}: price change rate for maintenance and operation. COP: coefficient of performance, CCGT: combined cycle gas turbine, RH/PH: radiator/panel heating, CHP: combined heat and power.

Deep geothermics		2015	2020	2030	2040	2050	total	ref
Min. deployment	%	0.7	0.7	0.0	0.0	0.0	/	[113]
Max. deployment	%	0.7	0.7	2.6	0.7	0.7	/	[113]
Purchase price	€/kW_{th}	3837.0	3775.0	3392.0	3049.0	2740.0	/	[268]
Service life	a	30.0	30.0	35.0	40.0	50.0	/	[268]
i_{int}	%	7.0	7.0	7.0	7.0	7.0	/	[113]
f_{OM}	%	2.0	2.0	2.0	2.0	2.0	/	[268]
r_P	%	1.7	1.7	1.7	1.7	1.7	/	[113]
r_{OM}	%	1.7	1.7	1.7	1.7	1.7	/	[113]
COP	%	10.0	10.0	10.0	10.0	10.0	/	[268]

Continued on next page

Table A.5: Input parameters of generators for the supply of space heat and domestic hot water for 2015, 2020, 2030, 2040 an 2050. i_{int}: interest rate, f_{OM}: factor for maintenance and operation in % from purchase price, r_P: price change factor for the purchase of a technology or a building component, r_{OM}: price change rate for maintenance and operation. COP: coefficient of performance, CCGT: combined cycle gas turbine, RH/PH: radiator/panel heating, CHP: combined heat and power.

CCGT (heat grid)		2015	2020	2030	2040	2050	total	ref
Min. deployment	GW_{th}	0.0	0.0	0.0	0.0	0.0	0.0	[113]
Max. deployment	GW_{th}	0.5	0.5	0.5	0.5	0.5	22.0	[113]
Purchase price	€/kW_{el}	823.0	791.0	753.0	738.0	736.0	/	[269]
Service life	a	30.0	30.0	30.0	30.0	30.0	/	[269]
i_{int}	%	7.0	7.0	7.0	7.0	7.0	/	[113]
f_{OM}	%	3.0	3.0	3.0	3.0	3.0	/	[113]
r_P	%	1.7	1.7	1.7	1.7	1.7	/	[113]
r_{OM}	%	1.7	1.7	1.7	1.7	1.7	/	[113]
η_{el}	%	55.0	56.0	59.0	61.0	63.0	/	[113]
η_{th}	%	30.0	30.0	30.0	30.0	30.0	/	[113]
Heat pump (heat grid)		2015	2020	2030	2040	2050	total	ref
Min. deployment	GW_{th}	0.0	0.0	0.0	0.0	0.0	0.0	[113]
Max. deployment	GW_{th}	0.0	0.0	1.0	2.0	2.0	50.0	[113]
Purchase price	€/kW_{th}	250.0	250.0	250.0	250.0	250.0	/	[268]
Service life	a	25.0	25.0	25.0	25.0	25.0	/	[268]
i_{int}	%	7.0	7.0	7.0	7.0	7.0	/	[113]
f_{OM}	%	1.3	1.3	1.3	1.3	1.3	/	[113]
r_P	%	1.7	1.7	1.7	1.7	1.7	/	[113]
r_{OM}	%	1.7	1.7	1.7	1.7	1.7	/	[268]
Factor a	-	7.3	7.3	7.3	7.3	7.3	/	[103]
Factor b	10^{-2}	-1.2	-1.2	-1.2	-1.2	-1.2	/	[103]
Factor c	10^{-4}	9.0	9.0	9.0	9.0	9.0	/	[103]
Solar thermal (heat grid)		2015	2020	2030	2040	2050	total	ref
Min. deployment	GW_{th}	0.0	0.0	0.0	0.0	0.0	0.0	[113]
Max. deployment	GW_{th}	0.0	0.0	1.0	2.0	2.0	50.0	[113]
Purchase price	€/m^2	390.0	289.8	230.0	200.0	190.0	/	[270]
Service life	a	25.0	30.0	30.0	30.0	30.0	/	[270]
i_{int}	%	7.0	7.0	7.0	7.0	7.0	/	[113]
f_{OM}	%	1.2	1.2	1.2	1.2	1.2	/	[270]
r_P	%	1.7	1.7	1.7	1.7	1.7	/	[113]
r_{OM}	%	1.7	1.7	1.7	1.7	1.7	/	[113]

Continued on next page

Table A.5: Input parameters of generators for the supply of space heat and domestic hot water for 2015, 2020, 2030, 2040 an 2050. i_{int}: interest rate, f_{OM}: factor for maintenance and operation in % from purchase price, r_P: price change factor for the purchase of a technology or a building component, r_{OM}: price change rate for maintenance and operation. COP: coefficient of performance, CCGT: combined cycle gas turbine, RH/PH: radiator/panel heating, CHP: combined heat and power.

Thermal storage (heat grid)		2015	2020	2030	2040	2050	total	ref
Min. deployment	GWh_{th}	0.0	0.0	0.0	0.0	0.0	0.0	[113]
Max. deployment	GWh_{th}	0.0	0.0	100.0	100.0	300.0	4550.0	[113]
Purchase price	€/m^3	166.0	139.1	119.4	99.7	80.0	/	[113, 271]
Service life	a	40.0	40.0	40.0	40.0	40.0	/	[271]
i_{int}	%	7.0	7.0	7.0	7.0	7.0	/	[113]
f_{OM}	%	1.0	1.0	1.0	1.0	1.0	/	[271]
r_P	%	1.7	1.7	1.7	1.7	1.7	/	[113]
r_{OM}	%	1.7	1.7	1.7	1.7	1.7	/	[113]
η	%	85.0	85.0	85.0	85.0	85.0	/	[113]
Methane boiler (heat grid)		2015	2020	2030	2040	2050	total	ref
Min. deployment	%	0.0	0.0	0.0	0.0	0.0	/	[113]
Max. deployment	%	100.0	100.0	100.0	100.0	100.0	/	[113]
Purchase price	€/kW_{th}	55.8	51.8	47.9	47.1	47.0	/	[272]
Service life	a	20.0	20.0	20.0	20.0	20.0	/	[272]
i_{int}	%	7.0	7.0	7.0	7.0	7.0	/	[113]
f_{OM}	%	2.0	2.0	2.0	2.0	2.0	/	[272]
r_P	%	1.7	1.7	1.7	1.7	1.7	/	[113]
r_{OM}	%	1.7	1.7	1.7	1.7	1.7	/	[113]
η	%	92.0	92.0	92.0	92.0	92.0	/	[272]

Continued on next page

Table A.5: Input parameters of generators for the supply of space heat and domestic hot water for 2015, 2020, 2030, 2040 an 2050. i_{int}: interest rate, f_{OM}: factor for maintenance and operation in % from purchase price, r_P: price change factor for the purchase of a technology or a building component, r_{OM}: price change rate for maintenance and operation. COP: coefficient of performance, CCGT: combined cycle gas turbine, RH/PH: radiator/panel heating, CHP: combined heat and power.

Oil-fired boiler (RH)		2015	2020	2030	2040	2050	total	ref
Min. deployment	%	0.0	0.0	0.0	0.0	0.0	/	[113]
Max. deployment	%	100.0	100.0	100.0	100.0	100.0	/	[113]
Purchase price	€/kW_{th}	136.0	136.0	136.0	136.0	136.0	/	[273]
Service life	a	20.0	20.0	20.0	20.0	20.0	/	[273]
i_{int}	%	7.0	7.0	7.0	7.0	7.0	/	[113]
f_{OM}	%	2.0	2.0	2.0	2.0	2.0	/	[273]
r_P	%	1.7	1.7	1.7	1.7	1.7	/	[113]
r_{OM}	%	1.7	1.7	1.7	1.7	1.7	/	[113]
η	%	94.0	94.0	94.0	94.0	94.0	/	[273]
Biomass boiler (RH)		2015	2020	2030	2040	2050	total	ref
Min. deployment	%	0.0	0.0	0.0	0.0	0.0	/	[113]
Max. deployment	%	100.0	100.0	100.0	100.0	100.0	/	[113]
Purchase price	€/kW_{th}	258.0	251.0	236.0	221.0	206.0	/	[274]
Service life	a	20.0	20.0	20.0	20.0	20.0	/	[274]
i_{int}	%	7.0	7.0	7.0	7.0	7.0	/	[113]
f_{OM}	%	6.0	6.0	6.0	6.0	6.0	/	[274]
r_P	%	1.7	1.7	1.7	1.7	1.7	/	[113]
r_{OM}	%	1.7	1.7	1.7	1.7	1.7	/	[113]
η	%	93.0	93.0	93.0	93.0	93.0	/	[274]
Gas heat pump (RH)		2015	2020	2030	2040	2050	total	ref
Min. deployment	%	0.0	0.0	0.0	0.0	0.0	/	[113]
Max. deployment	%	100.0	100.0	100.0	100.0	100.0	/	[113]
Purchase price	€/kW_{th}	1800.0	1755.0	1530.0	1305.0	1080.0	/	[275, 276]
Service life	a	20.0	20.0	20.0	20.0	20.0	/	[275, 276]
i_{int}	%	7.0	7.0	7.0	7.0	7.0	/	[113]
f_{OM}	%	5.0	5.0	5.0	4.0	4.0	/	[275, 276]
r_P	%	1.7	1.7	1.7	1.7	1.7	/	[113]
r_{OM}	%	1.7	1.7	1.7	1.7	1.7	/	[113]
Factor a	-	1.7	1.7	1.7	1.7	1.7	/	[103]
Factor b	10^{-2}	-1.1	-1.1	-1.1	-1.1	-1.1	/	[103]
Factor c	10^{-5}	6.0	6.0	6.0	6.0	6.0	/	[103]

Continued on next page

Table A.5: Input parameters of generators for the supply of space heat and domestic hot water for 2015, 2020, 2030, 2040 an 2050. i_{int}: interest rate, f_{OM}: factor for maintenance and operation in % from purchase price, r_P: price change factor for the purchase of a technology or a building component, r_{OM}: price change rate for maintenance and operation. COP: coefficient of performance, CCGT: combined cycle gas turbine, RH/PH: radiator/panel heating, CHP: combined heat and power.

Brine heat pump (RH)		2015	2020	2030	2040	2050	total	ref
Min. deployment	%	0.0	0.0	0.0	0.0	0.0	/	[113]
Max. deployment	%	100.0	100.0	100.0	100.0	100.0	/	[113]
Purchase price	€/kW_{th}	1770.2	1656.2	1493.1	1325.0	1162.0	/	[277]
Service life	a	20.0	20.0	20.0	20.0	20.0	/	[277]
i_{int}	%	7.0	7.0	7.0	7.0	7.0	/	[113]
f_{OM}	%	1.5	1.3	1.0	1.0	1.0	/	[277]
r_P	%	1.7	1.7	1.7	1.7	1.7	/	[113]
r_{OM}	%	1.7	1.7	1.7	1.7	1.7	/	[113]
Factor a	-	6.1	6.1	6.1	6.1	6.1	/	[103]
Factor b	10^{-2}	-9.7	-9.7	-9.7	-9.7	-9.7	/	[103]
Factor c	10^{-4}	5.3	5.3	5.3	5.3	5.3	/	[103]
Air heat pump (RH)		2015	2020	2030	2040	2050	total	ref
Min. deployment	%	0.0	0.0	0.0	0.0	0.0	/	[113]
Max. deployment	%	100.0	100.0	100.0	100.0	100.0	/	[113]
Purchase price	€/kW_{th}	975.0	900.0	815.0	725.0	640.0	/	[278]
Service life	a	20.0	20.0	20.0	20.0	20.0	/	[135]
i_{int}	%	7.0	7.0	7.0	7.0	7.0	/	[113]
f_{OM}	%	1.0	1.0	1.0	1.0	1.0	/	[278]
r_P	%	1.7	1.7	1.7	1.7	1.7	/	[113]
r_{OM}	%	1.7	1.7	1.7	1.7	1.7	/	[113]
Factor a	-	6.1	6.1	6.1	6.1	6.1	/	[103]
Factor b	10^{-2}	-9.7	-9.7	-9.7	-9.7	-9.7	/	[103]
Factor c	10^{-4}	5.3	5.3	5.3	5.3	5.3	/	[103]

Continued on next page

Table A.5: Input parameters of generators for the supply of space heat and domestic hot water for 2015, 2020, 2030, 2040 an 2050. i_{int}: interest rate, f_{OM}: factor for maintenance and operation in % from purchase price, r_P: price change factor for the purchase of a technology or a building component, r_{OM}: price change rate for maintenance and operation. COP: coefficient of performance, CCGT: combined cycle gas turbine, RH/PH: radiator/panel heating, CHP: combined heat and power.

Hybrid heat pump (RH)		2015	2020	2030	2040	2050	total	ref
Min. deployment	%	0.0	0.0	0.0	0.0	0.0	/	[113]
Max. deployment	%	100.0	100.0	100.0	100.0	100.0	/	[113]
Purchase price	€/kW_{th}	1072.0	997.0	912.0	822.0	737.0	/	[278]
Service life	a	20.0	20.0	20.0	20.0	20.0	/	[278]
i_{int}	%	7.0	7.0	7.0	7.0	7.0	/	[113]
f_{OM}	%	3.0	3.0	3.0	3.0	3.0	/	[278]
r_P	%	1.7	1.7	1.7	1.7	1.7	/	[113]
r_{OM}	%	1.7	1.7	1.7	1.7	1.7	/	[113]
Factor a	-	6.1	6.1	6.1	6.1	6.1	/	[103]
Factor b	10^{-2}	-9.7	-9.7	-9.7	-9.7	-9.7	/	[103]
Factor c	10^{-4}	5.3	5.3	5.3	5.3	5.3	/	[103]
Micro-CHP unit (RH)		2015	2020	2030	2040	2050	total	ref
Min. deployment	%	0.0	0.0	0.0	0.0	0.0	/	[113]
Max. deployment	%	100.0	100.0	100.0	100.0	100.0	/	[113]
Purchase price	€/kW_{th}	1725.0	1614.0	1480.0	1431.0	1424.0	/	[279]
Service life	a	20.0	20.0	20.0	20.0	20.0	/	[279]
i_{int}	%	7.0	7.0	7.0	7.0	7.0	/	[113]
f_{OM}	%	3.0	3.0	3.0	3.0	3.0	/	[279]
r_P	%	1.7	1.7	1.7	1.7	1.7	/	[113]
r_{OM}	%	1.7	1.7	1.7	1.7	1.7	/	[113]
η_{el}	%	36.0	36.0	36.0	36.0	36.0	/	[113]
η_{th}	%	44.0	44.0	44.0	44.0	44.0	/	[113]
$\eta_{th,boiler}$	%	90.0	90.0	90.0	90.0	90.0	/	[113]

Continued on next page

Table A.5: Input parameters of generators for the supply of space heat and domestic hot water for 2015, 2020, 2030, 2040 an 2050. i_{int}: interest rate, f_{OM}: factor for maintenance and operation in % from purchase price, r_P: price change factor for the purchase of a technology or a building component, r_{OM}: price change rate for maintenance and operation. COP: coefficient of performance, CCGT: combined cycle gas turbine, RH/PH: radiator/panel heating, CHP: combined heat and power.

Hydrogen fuel cell (RH)		2015	2020	2030	2040	2050	total	ref
Min. deployment	%	0.0	0.0	0.0	0.0	0.0	/	[113]
Max. deployment	%	100.0	100.0	100.0	100.0	100.0	/	[113]
Purchase price	€/kW_{th}	17908.0	8285.0	2072.0	1308.0	1289.0	/	[273]
Service life	a	10.0	15.0	20.0	20.0	20.0	/	[273]
i_{int}	%	7.0	7.0	7.0	7.0	7.0	/	[113]
f_{OM}	%	3.7	3.6	3.3	3.3	3.3	/	[273]
r_P	%	1.7	1.7	1.7	1.7	1.7	/	[113]
r_{OM}	%	1.7	1.7	1.7	1.7	1.7	/	[113]
η_{el}	%	53.0	57.0	65.0	65.0	65.0	/	[273]
η_{th}	%	32.0	32.7	34.0	34.0	34.0	/	[273]
$\eta_{th,boiler}$	%	90.0	90.0	90.0	90.0	90.0	/	[113]
Methane fuel cell (PH)		2015	2020	2030	2040	2050	total	ref
Min. deployment	%	0.0	0.0	0.0	0.0	0.0	/	[113]
Max. deployment	%	100.0	100.0	100.0	100.0	100.0	/	[113]
Purchase price	€/kW_{th}	19699.0	9113.0	2280.0	1438.0	1418.0	/	[273]
Service life	a	10.0	15.0	20.0	20.0	20.0	/	[273]
i_{int}	%	7.0	7.0	7.0	7.0	7.0	/	[113]
f_{OM}	%	3.7	3.6	3.3	3.3	3.3	/	[273]
r_P	%	1.7	1.7	1.7	1.7	1.7	/	[113]
r_{OM}	%	1.7	1.7	1.7	1.7	1.7	/	[113]
η_{el}	%	53.0	57.0	65.0	65.0	65.0	/	[273]
η_{th}	%	32.0	33.0	34.0	34.0	34.0	/	[273]
$\eta_{th,boiler}$	%	90.0	90.0	90.0	90.0	90.0	/	[113]

Continued on next page

Table A.5: Input parameters of generators for the supply of space heat and domestic hot water for 2015, 2020, 2030, 2040 an 2050. i_{int}: interest rate, f_{OM}: factor for maintenance and operation in % from purchase price, r_P: price change factor for the purchase of a technology or a building component, r_{OM}: price change rate for maintenance and operation. COP: coefficient of performance, CCGT: combined cycle gas turbine, RH/PH: radiator/panel heating, CHP: combined heat and power.

Methane boiler (PH)		2015	2020	2030	2040	2050	total	ref
Min. deployment	%	0.0	0.0	0.0	0.0	0.0	/	[113]
Max. deployment	%	100.0	100.0	100.0	100.0	100.0	/	[113]
Purchase price	€/kW_{th}	97.0	97.0	97.0	97.0	97.0	/	[272]
Service life	a	20.0	20.0	20.0	20.0	20.0	/	[272]
i_{int}	%	7.0	7.0	7.0	7.0	7.0	/	[113]
f_{OM}	%	2.0	2.0	2.0	2.0	2.0	/	[272]
r_P	%	1.7	1.7	1.7	1.7	1.7	/	[113]
r_{OM}	%	1.7	1.7	1.7	1.7	1.7	/	[113]
η	%	93.0	93.0	93.0	93.0	93.0	/	[272]
Oil-fired boiler (PH)		2015	2020	2030	2040	2050	total	ref
Min. deployment	%	0.0	0.0	0.0	0.0	0.0	/	[113]
Max. deployment	%	100.0	100.0	100.0	100.0	100.0	/	[113]
Purchase price	€/kW_{th}	136.0	136.0	136.0	136.0	136.0	/	[273]
Service life	a	20.0	20.0	20.0	20.0	20.0	/	[273]
i_{int}	%	7.0	7.0	7.0	7.0	7.0	/	[113]
f_{OM}	%	2.0	2.0	2.0	2.0	2.0	/	[273]
r_P	%	1.7	1.7	1.7	1.7	1.7	/	[113]
r_{OM}	%	1.7	1.7	1.7	1.7	1.7	/	[113]
η	%	89.0	89.0	89.0	89.0	89.0	/	[273]
Biomass-fired boiler (PH)		2015	2020	2030	2040	2050	total	ref
Min. deployment	%	0.0	0.0	0.0	0.0	0.0	/	[113]
Max. deployment	%	100.0	100.0	100.0	100.0	100.0	/	[113]
Purchase price	€/kW_{th}	258.0	251.0	236.0	221.0	206.0	/	[274]
Service life	a	20.0	20.0	20.0	20.0	20.0	/	[274]
i_{int}	%	7.0	7.0	7.0	7.0	7.0	/	[113]
f_{OM}	%	6.0	6.0	6.0	6.0	6.0	/	[274]
r_P	%	1.7	1.7	1.7	1.7	1.7	/	[113]
r_{OM}	%	1.7	1.7	1.7	1.7	1.7	/	[113]
η	%	88.0	88.0	88.0	88.0	93.0	/	[274]

Continued on next page

Table A.5: Input parameters of generators for the supply of space heat and domestic hot water for 2015, 2020, 2030, 2040 an 2050. i_{int}: interest rate, f_{OM}: factor for maintenance and operation in % from purchase price, r_P: price change factor for the purchase of a technology or a building component, r_{OM}: price change rate for maintenance and operation. COP: coefficient of performance, CCGT: combined cycle gas turbine, RH/PH: radiator/panel heating, CHP: combined heat and power.

Gas heat pump (PH)		2015	2020	2030	2040	2050	total	ref
Min. deployment	%	0.0	0.0	0.0	0.0	0.0	/	[113]
Max. deployment	%	100.0	100.0	100.0	100.0	100.0	/	[113]
Purchase price	€/kW_{th}	1800.0	1755.0	1530.0	1305.0	1080.0	/	[275, 276]
Service life	a	20.0	20.0	20.0	20.0	20.0	/	[275, 276]
i_{int}	%	7.0	7.0	7.0	7.0	7.0	/	[113]
f_{OM}	%	5.0	5.0	5.0	4.0	4.0	/	[275, 276]
r_P	%	1.7	1.7	1.7	1.7	1.7	/	[113]
r_{OM}	%	1.7	1.7	1.7	1.7	1.7	/	[113]
Factor a	-	1.7	1.7	1.7	1.7	1.7	/	[103]
Factor b	10^{-2}	-1.1	-1.1	-1.1	-1.1	-1.1	/	[103]
Factor c	10^{-5}	6.0	6.0	6.0	6.0	6.0	/	[103]
Brine heat pump (PH)		2015	2020	2030	2040	2050	total	ref
Min. deployment	%	0.0	0.0	0.0	0.0	0.0	/	[113]
Max. deployment	%	100.0	100.0	100.0	100.0	100.0	/	[113]
Purchase price	€/kW_{th}	1947.2	1821.8	1642.4	1457.5	1278.1	/	[277]
Service life	a	20.0	20.0	20.0	20.0	20.0	/	[277]
i_{int}	%	7.0	7.0	7.0	7.0	7.0	/	[113]
f_{OM}	%	1.5	1.3	1.0	1.0	1.0	/	[277]
r_P	%	1.7	1.7	1.7	1.7	1.7	/	[113]
r_{OM}	%	1.7	1.7	1.7	1.7	1.7	/	[113]
Factor a	-	6.1	6.1	6.1	6.1	6.1	/	[103]
Factor b	10^{-2}	-9.7	-9.7	-9.7	-9.7	-9.7	/	[103]
Factor c	10^{-4}	5.3	5.3	5.3	5.3	5.3	/	[103]

Continued on next page

Table A.5: Input parameters of generators for the supply of space heat and domestic hot water for 2015, 2020, 2030, 2040 an 2050. i_{int}: interest rate, f_{OM}: factor for maintenance and operation in % from purchase price, r_P: price change factor for the purchase of a technology or a building component, r_{OM}: price change rate for maintenance and operation. COP: coefficient of performance, CCGT: combined cycle gas turbine, RH/PH: radiator/panel heating, CHP: combined heat and power.

Air heat pump (PH)		2015	2020	2030	2040	2050	total	ref
Min. deployment	%	0.0	0.0	0.0	0.0	0.0	/	[113]
Max. deployment	%	100.0	100.0	100.0	100.0	100.0	/	[113]
Purchase price	€/kW_{th}	1073.0	990.0	897.0	798.0	704.0	/	[278]
Service life	a	20.0	20.0	20.0	20.0	20.0	/	[135]
i_{int}	%	7.0	7.0	7.0	7.0	7.0	/	[113]
f_{OM}	%	1.0	1.0	1.0	1.0	1.0	/	[278]
r_P	%	1.7	1.7	1.7	1.7	1.7	/	[113]
r_{OM}	%	1.7	1.7	1.7	1.7	1.7	/	[113]
Factor a	-	6.1	6.1	6.1	6.1	6.1	/	[103]
Factor b	10^{-2}	-9.7	-9.7	-9.7	-9.7	-9.7	/	[103]
Factor c	10^{-4}	5.3	5.3	5.3	5.3	5.3	/	[103]
Hybrid heat pump (PH)		2015	2020	2030	2040	2050	total	ref
Min. deployment	%	0.0	0.0	0.0	0.0	0.0	/	[113]
Max. deployment	%	100.0	100.0	100.0	100.0	100.0	/	[113]
Purchase price	€/kW_{th}	1179.0	1097.0	1003.0	904.0	811.0	/	[278]
Service life	a	20.0	20.0	20.0	20.0	20.0	/	[278]
i_{int}	%	7.0	7.0	7.0	7.0	7.0	/	[113]
f_{OM}	%	3.0	3.0	3.0	3.0	3.0	/	[278]
r_P	%	1.7	1.7	1.7	1.7	1.7	/	[113]
r_{OM}	%	1.7	1.7	1.7	1.7	1.7	/	[113]
Factor a	-	6.1	6.1	6.1	6.1	6.1	/	[103]
Factor b	10^{-2}	-9.7	-9.7	-9.7	-9.7	-9.7	/	[103]
Factor c	10^{-4}	5.3	5.3	5.3	5.3	5.3	/	[103]

Continued on next page

Table A.5: Input parameters of generators for the supply of space heat and domestic hot water for 2015, 2020, 2030, 2040 an 2050. i_{int}: interest rate, f_{OM}: factor for maintenance and operation in % from purchase price, r_P: price change factor for the purchase of a technology or a building component, r_{OM}: price change rate for maintenance and operation. COP: coefficient of performance, CCGT: combined cycle gas turbine, RH/PH: radiator/panel heating, CHP: combined heat and power.

Micro-CHP unit (PH)		2015	2020	2030	2040	2050	total	ref
Min. deployment	%	0.0	0.0	0.0	0.0	0.0	/	[113]
Max. deployment	%	100.0	100.0	100.0	100.0	100.0	/	[113]
Purchase price	€/kW_{th}	1725.0	1614.0	1480.0	1431.0	1424.0	/	[279]
Service life	a	20.0	20.0	20.0	20.0	20.0	/	[279]
i_{int}	%	7.0	7.0	7.0	7.0	7.0	/	[113]
f_{OM}	%	3.0	3.0	3.0	3.0	3.0	/	[279]
r_P	%	1.7	1.7	1.7	1.7	1.7	/	[113]
r_{OM}	%	1.7	1.7	1.7	1.7	1.7	/	[113]
η_{el}	%	36.0	36.0	36.0	36.0	36.0	/	[113]
η_{th}	%	44.0	44.0	44.0	44.0	44.0	/	[113]
$\eta_{th,boiler}$	%	90.0	90.0	90.0	90.0	90.0	/	[113]
Hydrogen fuel cell (PH)		**2015**	**2020**	**2030**	**2040**	**2050**	**total**	**ref**
Min. deployment	%	0.0	0.0	0.0	0.0	0.0	/	[113]
Max. deployment	%	100.0	100.0	100.0	100.0	100.0	/	[113]
Purchase price	€/kW_{th}	17500.0	12500.0	9500.0	6500.0	6500.0	/	[273]
Service life	a	10.0	10.0	10.0	10.0	10.0	/	[273]
i_{int}	%	7.0	7.0	7.0	7.0	7.0	/	[113]
f_{OM}	%	3.0	3.0	3.0	3.0	3.0	/	[273]
r_P	%	1.7	1.7	1.7	1.7	1.7	/	[113]
r_{OM}	%	1.7	1.7	1.7	1.7	1.7	/	[113]
η_{el}	%	53.0	57.0	65.0	65.0	65.0	/	[273]
η_{th}	%	32.0	32.7	34.0	34.0	34.0	/	[273]
$\eta_{th,boiler}$	%	90.0	90.0	90.0	90.0	90.0	/	[113]

Continued on next page

Table A.5: Input parameters of generators for the supply of space heat and domestic hot water for 2015, 2020, 2030, 2040 an 2050. i_{int}: interest rate, f_{OM}: factor for maintenance and operation in % from purchase price, r_P: price change factor for the purchase of a technology or a building component, r_{OM}: price change rate for maintenance and operation. COP: coefficient of performance, CCGT: combined cycle gas turbine, RH/PH: radiator/panel heating, CHP: combined heat and power.

Methane fuel cell (PH)		2015	2020	2030	2040	2050	total	ref
Min. deployment	%	0.0	0.0	0.0	0.0	0.0	/	[113]
Max. deployment	%	100.0	100.0	100.0	100.0	100.0	/	[113]
Purchase price	€/kW_{th}	16545.0	7826.0	2071.0	1429.0	7150.0	/	[273]
Service life	a	11.0	17.0	20.0	20.0	10.0	/	[273]
i_{int}	%	7.0	7.0	7.0	7.0	7.0	/	[113]
f_{OM}	%	3.7	3.5	3.3	3.3	3.0	/	[273]
r_P	%	1.7	1.7	1.7	1.7	1.7	/	[113]
r_{OM}	%	1.7	1.7	1.7	1.7	1.7	/	[113]
η_{el}	%	53.0	57.0	65.0	65.0	65.0	/	[273]
η_{th}	%	32.0	33.0	34.0	34.0	34.0	/	[273]
$\eta_{th,boiler}$	%	90.0	90.0	90.0	90.0	90.0	/	[113]
Solar thermal (RH)		2015	2020	2030	2040	2050	total	ref
Min. deployment	kW_{th}/#	0.0	0.0	0.0	0.0	0.0	0.0	[113]
Max. deployment	kW_{th}/#	2.0	2.0	2.0	2.0	2.0	75.9	[113]
Purchase price	€/m^2	692.0	550.0	400.0	350.0	310.0	/	[273]
Service life	a	25.0	25.0	25.0	25.0	25.0	/	[273]
i_{int}	%	7.0	7.0	7.0	7.0	7.0	/	[113]
f_{OM}	%	1.2	1.2	1.2	1.2	1.2	/	[273]
r_P	%	1.7	1.7	1.7	1.7	1.7	/	[113]
r_{OM}	%	1.7	1.7	1.7	1.7	1.7	/	[113]
η_{opt}	%	80.0	80.0	80.0	80.0	80.0	/	[113]
U-factor	W/m^2K	3.0	3.0	3.0	3.0	3.0	/	[113]

Continued on next page

Table A.5: Input parameters of generators for the supply of space heat and domestic hot water for 2015, 2020, 2030, 2040 an 2050. i_{int}: interest rate, f_{OM}: factor for maintenance and operation in % from purchase price, r_P: price change factor for the purchase of a technology or a building component, r_{OM}: price change rate for maintenance and operation. COP: coefficient of performance, CCGT: combined cycle gas turbine, RH/PH: radiator/panel heating, CHP: combined heat and power.

Solar thermal (PH)		2015	2020	2030	2040	2050	total	ref
Min. deployment	$kW_{th}/\#$	0.0	0.0	0.0	0.0	0.0	0.0	[113]
Max. deployment	$kW_{th}/\#$	2.0	2.0	2.0	2.0	2.0	79.9	[113]
Purchase price	$€/m^2$	692.0	550.0	400.0	350.0	310.0	/	[273]
Service life	a	25.0	25.0	25.0	25.0	25.0	/	[273]
i_{int}	%	7.0	7.0	7.0	7.0	7.0	/	[113]
f_{OM}	%	1.2	1.2	1.2	1.2	1.2	/	[273]
r_P	%	1.7	1.7	1.7	1.7	1.7	/	[113]
r_{OM}	%	1.7	1.7	1.7	1.7	1.7	/	[113]
η_{opt}	%	80.0	80.0	80.0	80.0	80.0	/	[113]
U-factor	W/m^2K	3.0	3.0	3.0	3.0	3.0	/	[113]
Thermal storage (heat pump)		2015	2020	2030	2040	2050	total	ref
Min. deployment	10^9 l	0.0	0.0	0.0	0.0	0.0	0.0	[113]
Max. deployment	10^9 l	0.0	0.0	3.0	3.0	3.0	90.0	[113]
Purchase price	$€/l$	1.4	1.4	1.1	1.0	1.0	/	[280]
Service life	a	20.0	20.0	20.0	20.0	20.0	/	[280]
i_{int}	%	7.0	7.0	7.0	7.0	7.0	/	[113]
f_{OM}	%	1.3	1.3	1.3	1.3	1.3	/	[280]
r_P	%	1.7	1.7	1.7	1.7	1.7	/	[113]
r_{OM}	%	1.7	1.7	1.7	1.7	1.7	/	[113]
η_{PH}	%	95.0	95.0	95.0	95.0	95.0	/	[280]
η_{RH}	%	90.0	90.0	90.0	90.0	90.0	/	[280]

Continued on next page

Table A.5: Input parameters of generators for the supply of space heat and domestic hot water for 2015, 2020, 2030, 2040 an 2050. i_{int}: interest rate, f_{OM}: factor for maintenance and operation in % from purchase price, r_P: price change factor for the purchase of a technology or a building component, r_{OM}: price change rate for maintenance and operation. COP: coefficient of performance, CCGT: combined cycle gas turbine, RH/PH: radiator/panel heating, CHP: combined heat and power.

Thermal storage (liquid fuels)		2015	2020	2030	2040	2050	total	ref
Min. deployment	10^9 l	0.0	0.0	0.0	0.0	0.0	0.0	[113]
Max. deployment	10^9 l	0.0	0.0	3.0	3.0	3.0	90.0	[113]
Purchase price	€/l	1.4	1.4	1.1	1.0	1.0	/	[280]
Service life	a	20.0	20.0	20.0	20.0	20.0	/	[280]
i_{int}	%	7.0	7.0	7.0	7.0	7.0	/	[113]
f_{OM}	%	1.3	1.3	1.3	1.3	1.3	/	[280]
r_P	%	1.7	1.7	1.7	1.7	1.7	/	[113]
r_{OM}	%	1.7	1.7	1.7	1.7	1.7	/	[113]
η_{PH}	%	95.0	95.0	95.0	95.0	95.0	/	[280]
η_{RH}	%	90.0	90.0	90.0	90.0	90.0	/	[280]
Thermal storage (fuel cell)		2015	2020	2030	2040	2050	total	ref
Min. deployment	10^9 l	0.0	0.0	0.0	0.0	0.0	0.0	[113]
Max. deployment	10^9 l	0.0	0.0	3.0	3.0	3.0	90.0	[113]
Purchase price	€/l	1.4	1.4	1.1	1.0	1.0	/	[280]
Service life	a	20.0	20.0	20.0	20.0	20.0	/	[280]
i_{int}	%	7.0	7.0	7.0	7.0	7.0	/	[113]
f_{OM}	%	1.3	1.3	1.3	1.3	1.3	/	[280]
r_P	%	1.7	1.7	1.7	1.7	1.7	/	[113]
r_{OM}	%	1.7	1.7	1.7	1.7	1.7	/	[113]
η_{PH}	%	95.0	95.0	95.0	95.0	95.0	/	[280]
η_{RH}	%	90.0	90.0	90.0	90.0	90.0	/	[280]

Table A.6: Input parameters of building refurbishment and heat transfer system for 2015, 2020, 2030, 2040 an 2050. i_{int}: interest rate, f_{OM}: factor for maintenance and operation in % from purchase price, r_P: price change factor for the purchase of a technology or a building component, r_{OM}: price change rate for maintenance and operation.

Fully refurbished		2015	2020	2030	2040	2050	total	ref
Min. deployment	*Millions*	0.0	0.0	0.0	0.0	0.0	0.0	[113]
Max. deployment	*Millions*	0.5	0.5	0.5	0.5	0.5	27.0	[113]
Purchase price	€/m^2	102.0	102.0	102.0	102.0	102.0	/	[281]
Service life	a	50.0	50.0	50.0	50.0	50.0	/	[113]
i_{int}	%	7.0	7.0	7.0	7.0	7.0	/	[113]
f_{OM}	%	1.0	1.0	1.0	1.0	1.0	/	[113]
r_P	%	1.7	1.7	1.7	1.7	1.7	/	[113]
r_{OM}	%	1.7	1.7	1.7	1.7	1.7	/	[113]
Heat demand to	%	50.2	50.2	50.2	50.2	50.2	/	[113]
Highly efficient		2015	2020	2030	2040	2050	total	ref
Min. deployment	*Millions*	0.0	0.0	0.0	0.0	0.0	0.0	[113]
Max. deployment	*Millions*	0.5	0.5	0.5	0.5	0.5	27.0	[113]
Purchase price	€/m^2	180.0	180.0	180.0	180.0	180.0	/	[281]
Service life	a	50.0	50.0	50.0	50.0	50.0	/	[113]
i_{int}	%	7.0	7.0	7.0	7.0	7.0	/	[113]
f_{OM}	%	1.0	1.0	1.0	1.0	1.0	/	[113]
r_P	%	1.7	1.7	1.7	1.7	1.7	/	[113]
r_{OM}	%	1.7	1.7	1.7	1.7	1.7	/	[113]
Heat demand to	%	35.7	35.7	35.7	35.7	35.7	/	[113]
Panel heating system		2015	2020	2030	2040	2050	total	ref
Purchase price	€/m^2	60.0	60.0	60.0	60.0	60.0	/	[281]
Service life	a	50.0	50.0	50.0	50.0	50.0	/	[281]
i_{int}	%	7.0	7.0	7.0	7.0	7.0	/	[113]
f_{OM}	%	1.5	1.5	1.5	1.5	1.5	/	[281]
r_P	%	1.7	1.7	1.7	1.7	1.7	/	[113]
r_{OM}	%	1.7	1.7	1.7	1.7	1.7	/	[113]

A.6 Biomass

Table A.7: Input parameters of biomass conversion for 2015, 2020, 2030, 2040 an 2050. i_{int}: interest rate, f_{OM}: factor for maintenance and operation in % from purchase price, r_P: price change factor for the purchase of a technology or a building component, r_{OM}: price change rate for maintenance and operation.

Biomass-to-CH4		2015	2020	2030	2040	2050	total	ref
Min. deployment	GW	0.0	0.0	0.0	0.0	0.0	0.0	[113]
Max. deployment	GW	0.0	0.0	0.5	0.5	1.0	19.5	[113]
Purchase price	€/kW	3067.0	2560.9	1955.1	1731.9	1700.0	/	[282]
Service life	a	20.0	20.0	20.0	20.0	20.0	/	[282]
i_{int}	%	7.0	7.0	7.0	7.0	7.0	/	[113]
f_{OM}	%	5.0	5.0	5.0	5.0	5.0	/	[282]
r_P	%	1.7	1.7	1.7	1.7	1.7	/	[113]
r_{OM}	%	1.7	1.7	1.7	1.7	1.7	/	[113]
η	%	55.0	55.0	55.0	55.0	55.0	/	[282]
Full load hours	h	8000.0	8000.0	8000.0	8000.0	8000.0	/	[282]
Biomass-to-H2		2015	2020	2030	2040	2050	total	ref
Min. deployment	GW	0.0	0.0	0.0	0.0	0.0	0.0	[113]
Max. deployment	GW	0.0	0.0	0.5	0.5	1.0	19.5	[113]
Purchase price	€/kW	2244.5	1874.1	1430.7	1267.3	1244.0	/	[282]
Service life	a	20.0	20.0	20.0	20.0	20.0	/	[282]
i_{int}	%	7.0	7.0	7.0	7.0	7.0	/	[113]
f_{OM}	%	5.0	5.0	5.0	5.0	5.0	/	[282]
r_P	%	1.7	1.7	1.7	1.7	1.7	/	[113]
r_{OM}	%	1.7	1.7	1.7	1.7	1.7	/	[113]
η	%	61.0	61.0	61.0	61.0	61.0	/	[282]
Full load hours	h	8000.0	8000.0	8000.0	8000.0	8000.0	/	[282]
Biomass-to-liquid fuels		2015	2020	2030	2040	2050	total	ref
Min. deployment	GW	0.0	0.0	0.0	0.0	0.0	0.0	[113]
Max. deployment	GW	0.0	0.0	0.5	0.5	1.0	19.5	[113]
Purchase price	€/kW	3395.4	2835.1	2164.4	1917.3	1882.0	/	[282]
Service life	a	20.0	20.0	20.0	20.0	20.0	/	[282]
i_{int}	%	7.0	7.0	7.0	7.0	7.0	/	[113]
f_{OM}	%	5.0	5.0	5.0	5.0	5.0	/	[282]
r_P	%	1.7	1.7	1.7	1.7	1.7	/	[113]
r_{OM}	%	1.7	1.7	1.7	1.7	1.7	/	[113]
η	%	46.0	46.0	46.0	46.0	46.0	/	[282]
Full load hours	h	8000.0	8000.0	8000.0	8000.0	8000.0	/	[282]

Continued on next page

Table A.7: Input parameters of biomass conversion for 2015, 2020, 2030, 2040 an 2050. i_{int}: interest rate, f_{OM}: factor for maintenance and operation in % from purchase price, r_P: price change factor for the purchase of a technology or a building component, r_{OM}: price change rate for maintenance and operation.

Bio-diesel plant (rape)		2015	2020	2030	2040	2050	total	ref
Min. deployment	GW	0.0	0.0	0.0	0.0	0.0	0.0	[113]
Max. deployment	GW	0.0	0.0	0.5	0.5	1.0	19.5	[113]
Purchase price	€/kW	150.0	150.0	150.0	150.0	150.0	/	[283]
Service life	a	20.0	20.0	20.0	20.0	20.0	/	[283]
i_{int}	%	7.0	7.0	7.0	7.0	7.0	/	[113]
f_{OM}	%	5.0	5.0	5.0	5.0	5.0	/	[283]
r_P	%	1.7	1.7	1.7	1.7	1.7	/	[113]
r_{OM}	%	1.7	1.7	1.7	1.7	1.7	/	[113]
η	%	60.0	60.0	60.0	60.0	60.0	/	[283]
Full load hours	h	4000.0	4000.0	4000.0	4000.0	4000.0		[113]
Bio-diesel plant (methane)		2015.0	2020.0	2030.0	2040.0	2050.0	total	ref
Min. deployment	GW	0.0	0.0	0.0	0.0	0.0	0.0	[113]
Max. deployment	GW	1.0	1.0	1.0	1.0	1.0	37.0	[113]
Purchase price	€/kW	1122.8	965.1	776.4	706.9	697.0	/	[284]
Service life	a	20.0	20.0	20.0	20.0	20.0	/	[284]
i_{int}	%	7.0	7.0	7.0	7.0	7.0	/	[113]
f_{OM}	%	5.0	5.0	5.0	5.0	5.0	/	[284]
r_P	%	1.7	1.7	1.7	1.7	1.7	/	[113]
r_{OM}	%	1.7	1.7	1.7	1.7	1.7	/	[113]
Full load hours	-	8400.0	8400.0	8400.0	8400.0	8400.0	/	[284]
Biogas treatment		2015	2020	2030	2040	2050	total	ref
Min. deployment	TWh	0.0	0.0	0.0	0.0	0.0	0.0	[113]
Max. deployment	TWh	0.1	0.4	1.0	1.5	2.0	46.4	[113]
Purchase price	€/kWh	714.0	538.5	328.4	251.1	240.0	/	[284]
Service life	a	25.0	25.0	25.0	25.0	25.0	/	[284]
i_{int}	%	7.0	7.0	7.0	7.0	7.0	/	[113]
f_{OM}	%	3.0	3.0	3.0	3.0	3.0	/	[284]
r_P	%	1.7	1.7	1.7	1.7	1.7	/	[113]
r_{OM}	%	1.7	1.7	1.7	1.7	1.7	/	[113]
η	%	88.0	88.0	88.0	88.0	88.0	/	[285]

Continued on next page

Table A.7: Input parameters of biomass conversion for 2015, 2020, 2030, 2040 an 2050. i_{int}: interest rate, f_{OM}: factor for maintenance and operation in % from purchase price, r_P: price change factor for the purchase of a technology or a building component, r_{OM}: price change rate for maintenance and operation.

Cogeneration plant		2015	2020	2030	2040	2050	total	ref
Min. deployment	GW	0.2	0.0	0.0	0.0	0.0	0.7	[22]
Max. deployment	GW	0.2	0.1	1.0	2.0	2.0	57.7	[22, 113]
Purchase price	€/kW	572.8	556.0	528.1	508.7	500.0	/	[279]
Service life	a	20.0	20.0	20.0	20.0	20.0	/	[279]
i_{int}	%	7.0	7.0	7.0	7.0	7.0	/	[113]
f_{OM}	%	2.5	2.5	2.5	2.5	2.5	/	[279]
r_P	%	1.7	1.7	1.7	1.7	1.7	/	[113]
r_{OM}	%	1.7	1.7	1.7	1.7	1.7	/	[113]
η_{el}	%	28.0	28.0	28.0	28.0	28.0	/	[113]
η_{th}	%	40.0	40.0	40.0	40.0	40.0	/	[113]

Table A.8: Input parameters of infrastructure for 2015, 2020, 2030, 2040 an 2050. i_{int}: interest rate, f_{OM}: factor for maintenance and operation in % from purchase price, r_P: price change factor for the purchase of a technology or a building component, r_{OM}: price change rate for maintenance and operation.

Distribution grid		2015	2020	2030	2040	2050	total	ref
Purchase price	€/kW_{el}	140.0	140.0	140.0	140.0	140.0	/	[113]
Service life	a	40.0	40.0	40.0	40.0	40.0	/	[113]
i_{int}	%	7.0	7.0	7.0	7.0	7.0	/	[113]
f_{OM}	%	3.0	3.0	3.0	3.0	3.0	/	[113]
r_P	%	1.7	1.7	1.7	1.7	1.7	/	[113]
r_{OM}	%	1.7	1.7	1.7	1.7	1.7	/	[113]
kW_{grid}/kW_{PV}	-	1.0	1.0	1.0	1.0	1.0	/	[113]
Medium voltage grid		**2015**	**2020**	**2030**	**2040**	**2050**	**total**	**ref**
Purchase price	€/kW_{el}	180.0	180.0	180.0	180.0	180.0	/	[113]
Service life	a	40.0	40.0	40.0	40.0	40.0	/	[113]
i_{int}	%	7.0	7.0	7.0	7.0	7.0	/	[113]
f_{OM}	%	3.0	3.0	3.0	3.0	3.0	/	[113]
r_P	%	1.7	1.7	1.7	1.7	1.7	/	[113]
r_{OM}	%	1.7	1.7	1.7	1.7	1.7	/	[113]
kW_{grid}/kW_{WindOn}	-	1.0	1.0	1.0	1.0	1.0	/	[113]

Continued on next page

Table A.8: Input parameters of infrastructure for 2015, 2020, 2030, 2040 an 2050. i_{int}: interest rate, f_{OM}: factor for maintenance and operation in % from purchase price, r_P: price change factor for the purchase of a technology or a building component, r_{OM}: price change rate for maintenance and operation.

High voltage grid		2015	2020	2030	2040	2050	total	ref
Purchase price	€/kW_{el}	200.0	200.0	200.0	200.0	200.0	/	[113]
Service life	a	40.0	40.0	40.0	40.0	40.0	/	[113]
i_{int}	%	7.0	7.0	7.0	7.0	7.0	/	[113]
f_{OM}	%	3.0	3.0	3.0	3.0	3.0	/	[113]
r_P	%	1.7	1.7	1.7	1.7	1.7	/	[113]
r_{OM}	%	1.7	1.7	1.7	1.7	1.7	/	[113]
Submarine cable		2015	2020	2030	2040	2050	total	ref
Purchase price	€/kW_{el}	430.0	430.0	430.0	430.0	430.0	/	[113]
Service life	a	40.0	40.0	40.0	40.0	40.0	/	[113]
i_{int}	%	7.0	7.0	7.0	7.0	7.0	/	[113]
f_{OM}	%	3.0	3.0	3.0	3.0	3.0	/	[113]
r_P	%	1.7	1.7	1.7	1.7	1.7	/	[113]
r_{OM}	%	1.7	1.7	1.7	1.7	1.7	/	[113]
$kW_{grid}/kW_{WindOff}$	-	1.0	1.0	1.0	1.0	1.0	/	[113]
Loading station BEV (private)		2015	2020	2030	2040	2050	total	ref
Purchase price	€/$vehicle$	1485.0	1282.5	1004.6	1004.6	1004.6	/	[113]
Service life	a	30.0	30.0	30.0	30.0	30.0	/	[113]
i_{int}	%	7.0	7.0	7.0	7.0	7.0	/	[113]
f_{OM}	%	1.6	1.6	1.6	1.6	1.6	/	[113]
r_P	%	1.7	1.7	1.7	1.7	1.7	/	[113]
r_{OM}	%	1.7	1.7	1.7	1.7	1.7	/	[113]
Loading stations	#/$vehicle$	1.0	1.0	1.0	1.0	1.0	/	[113]
η	%	95.0	95.0	95.0	95.0	95.0	/	[113]
Fast-loading station BEV (private)		2015	2020	2030	2040	2050	total	ref
Purchase price	k€/$vehicle$	760.4	629.1	448.9	448.9	448.9	/	[113]
Service life	a	30.0	30.0	30.0	30.0	30.0	/	[113]
i_{int}	%	7.0	7.0	7.0	7.0	7.0	/	[113]
f_{OM}	%	1.6	1.6	1.6	1.6	1.6	/	[113]
r_P	%	1.7	1.7	1.7	1.7	1.7	/	[113]
r_{OM}	%	1.7	1.7	1.7	1.7	1.7	/	[113]
Loading stations	10^{-3}/$vehicle$	8.9	1.5	1.1	1.1	1.1	/	[113]

Continued on next page

Table A.8: Input parameters of infrastructure for 2015, 2020, 2030, 2040 an 2050. i_{int}: interest rate, f_{OM}: factor for maintenance and operation in % from purchase price, r_P: price change factor for the purchase of a technology or a building component, r_{OM}: price change rate for maintenance and operation.

Loading station FCEV (private)		2015	2020	2030	2040	2050	total	ref
Purchase price	k€/*vehicle*	2518.6	2243.1	1787.9	1788.4	1788.4	/	[113]
Service life	a	30.0	30.0	30.0	30.0	30.0	/	[113]
i_{int}	%	7.0	7.0	7.0	7.0	7.0	/	[113]
f_{OM}	%	2.2	2.2	2.2	2.2	2.2	/	[113]
r_P	%	1.7	1.7	1.7	1.7	1.7	/	[113]
r_{OM}	%	1.7	1.7	1.7	1.7	1.7	/	[113]
Loading stations	10^{-3}/*vehicle*	33.6	3.7	0.5	0.5	0.5	/	[113]
Loading station CNG (private)		**2015**	**2020**	**2030**	**2040**	**2050**	**total**	**ref**
Purchase price	k€/*vehicle*	429.4	429.4	429.4	429.4	429.4	/	[113]
Service life	a	30.0	30.0	30.0	30.0	30.0	/	[113]
i_{int}	%	7.0	7.0	7.0	7.0	7.0	/	[113]
f_{OM}	%	91.0	91.0	91.0	91.0	91.0	/	[113]
r_P	%	1.7	1.7	1.7	1.7	1.7	/	[113]
r_{OM}	%	1.7	1.7	1.7	1.7	1.7	/	[113]
Loading stations	10^{-3}/*vehicle*	3.5	1.1	1.1	1.1	1.1	/	[113]
Loading station BEV (freight)		**2015**	**2020**	**2030**	**2040**	**2050**	**total**	**ref**
Purchase price	k€/*vehicle*	31.0	31.0	31.0	31.0	31.0	/	[113]
Service life	a	30.0	30.0	30.0	30.0	30.0	/	[113]
i_{int}	%	7.0	7.0	7.0	7.0	7.0	/	[113]
f_{OM}	%	1.6	1.6	1.6	1.6	1.6	/	[113]
r_P	%	1.7	1.7	1.7	1.7	1.7	/	[113]
r_{OM}	%	1.7	1.7	1.7	1.7	1.7	/	[113]
Loading stations	#/*vehicle*	1.0	1.0	1.0	1.0	1.0	/	[113]
Fast-loading station BEV (freight)		**2015**	**2020**	**2030**	**2040**	**2050**	**total**	**ref**
Purchase price	k€/*vehicle*	760.4	629.1	448.9	448.9	448.9	/	[113]
Service life	a	30.0	30.0	30.0	30.0	30.0	/	[113]
i_{int}	%	7.0	7.0	7.0	7.0	7.0	/	[113]
f_{OM}	%	1.6	1.6	1.6	1.6	1.6	/	[113]
r_P	%	1.7	1.7	1.7	1.7	1.7	/	[113]
r_{OM}	%	1.7	1.7	1.7	1.7	1.7	/	[113]
Loading stations	10^{-3}/*vehicle*	175.2	29.5	21.9	21.9	21.9	/	[113]

Continued on next page

Table A.8: Input parameters of infrastructure for 2015, 2020, 2030, 2040 an 2050. i_{int}: interest rate, f_{OM}: factor for maintenance and operation in % from purchase price, r_P: price change factor for the purchase of a technology or a building component, r_{OM}: price change rate for maintenance and operation.

Loading station FCEV (freight)		2015	2020	2030	2040	2050	total ref
Purchase price	k€/$vehicle$	2518.6	2243.1	1787.9	1787.9	1787.9	/ [113]
Service life	a	30.0	30.0	30.0	30.0	30.0	/ [113]
i_{int}	%	7.0	7.0	7.0	7.0	7.0	/ [113]
f_{OM}	%	2.2	2.2	2.2	2.2	2.2	/ [113]
r_P	%	1.7	1.7	1.7	1.7	1.7	/ [113]
r_{OM}	%	1.7	1.7	1.7	1.7	1.7	/ [113]
Loading stations	10^{-3}/$vehicle$	66.0	14.8	13.2	13.2	13.2	/ [113]
Loading station CNG (freight)		2015	2020	2030	2040	2050	total ref
Purchase price	k€/$vehicle$	1843.0	1708.9	1469.2	1469.2	1469.2	/ [113]
Service life	a	30.0	30.0	30.0	30.0	30.0	/ [113]
i_{int}	%	7.0	7.0	7.0	7.0	7.0	/ [113]
f_{OM}	%	50.0	50.0	50.0	50.0	50.0	/ [113]
r_P	%	1.7	1.7	1.7	1.7	1.7	/ [113]
r_{OM}	%	1.7	1.7	1.7	1.7	1.7	/ [113]
Loading stations	10^{-3}/$vehicle$	13.7	13.7	13.7	13.7	13.7	/ [113]
Heat grid		2015	2020	2030	2040	2050	total ref
Purchase price	€/kW_{th}	400.0	400.0	400.0	400.0	400.0	/ [113]
Service life	a	40.0	40.0	40.0	40.0	40.0	/ [113]
i_{int}	%	7.0	7.0	7.0	7.0	7.0	/ [113]
f_{OM}	%	1.0	1.0	1.0	1.0	1.0	/ [113]
r_P	%	1.7	1.7	1.7	1.7	1.7	/ [113]
r_{OM}	%	1.7	1.7	1.7	1.7	1.7	/ [113]
kW_{grid}/$kW_{griddemand}$	-	1.0	1.0	1.0	1.0	1.0	/ [113]
Gas distribution system		2015	2020	2030	2040	2050	total ref
Purchase price	€/kW	28.0	28.0	28.0	28.0	28.0	/ [113]
Service life	a	30.0	30.0	30.0	30.0	30.0	/ [113]
i_{int}	%	7.0	7.0	7.0	7.0	7.0	/ [113]
f_{OM}	%	2.5	2.5	2.5	2.5	2.5	/ [113]
r_P	%	1.7	1.7	1.7	1.7	1.7	/ [113]
r_{OM}	%	1.7	1.7	1.7	1.7	1.7	/ [113]
$frackW_{grid}kW_{griddemand}$	-	1.0	1.0	1.0	1.0	1.0	/ [113]

A.7 Process Heat Supply

Table A.9: Input parameters of generators for the supply of process heat for 2015, 2020, 2030, 2040 an 2050. i_{int}: interest rate, f_{OM}: factor for maintenance and operation in % from purchase price, r_P: price change factor for the purchase of a technology or a building component, r_{OM}: price change rate for maintenance and operation.

Biomass boiler (LMT)		2015	2020	2030	2040	2050	total	ref
Min. deployment	%	0.0	0.0	0.0	0.0	0.0	/	[113]
Max. deployment	%	100.0	100.0	100.0	100.0	100.0	/	[113]
Purchase price	€/kW_{th}	258.1	250.7	235.8	221.0	206.5	/	[113]
Service life	a	20.0	20.0	20.0	20.0	20.0	/	[113]
i_{int}	%	7.0	7.0	7.0	7.0	7.0	/	[113]
f_{OM}	%	3.0	3.0	3.0	3.0	3.0	/	[113]
r_P	%	1.7	1.7	1.7	1.7	1.7	/	[113]
r_{OM}	%	1.7	1.7	1.7	1.7	1.7	/	[113]
η	%	85.0	85.0	85.0	85.0	85.0	/	[113]
Solar thermal (LMT)		2015	2020	2030	2040	2050	total	ref
Min. deployment	%	0.0	0.0	0.0	0.0	0.0	/	[113]
Max. deployment	%	100.0	100.0	100.0	100.0	100.0	/	[113]
Purchase price	€/kWh_{th}	96.7	88.9	75.1	63.4	53.6	/	[113]
Service life	a	30.0	30.0	30.0	30.0	30.0	/	[113]
i_{int}	%	7.0	7.0	7.0	7.0	7.0	/	[113]
f_{OM}	%	1.3	1.3	1.3	1.3	1.3	/	[113]
r_P	%	1.7	1.7	1.7	1.7	1.7	/	[113]
r_{OM}	%	1.7	1.7	1.7	1.7	1.7	/	[113]
Heat pump (LMT)		2015	2020	2030	2040	2050	total	ref
Min. deployment	Mio #	0.0	0.0	0.0	0.0	0.0	/	[113]
Max. deployment	Mio #	100.0	100.0	100.0	100.0	100.0	/	[113]
Purchase price	€/kW_{th}	250.0	250.0	250.0	250.0	250.0	/	[113]
Service life	a	20.0	20.0	20.0	20.0	20.0	/	[113]
i_{int}	%	7.0	7.0	7.0	7.0	7.0	/	[113]
f_{OM}	%	3.5	3.5	3.5	3.5	3.5	/	[113]
r_P	%	1.7	1.7	1.7	1.7	1.7	/	[113]
r_{OM}	%	1.7	1.7	1.7	1.7	1.7	/	[113]
COP	-	2.5	2.5	2.5	2.5	2.5	/	[113]

Continued on next page

Table A.9: Input parameters of generators for the supply of process heat for 2015, 2020, 2030, 2040 an 2050. i_{int}: interest rate, f_{OM}: factor for maintenance and operation in % from purchase price, r_P: price change factor for the purchase of a technology or a building component, r_{OM}: price change rate for maintenance and operation.

Oil-fired boiler (LMT)		2015	2020	2030	2040	2050	total	ref
Min. deployment	%	0.0	0.0	0.0	0.0	0.0	/	[113]
Max. deployment	%	100.0	100.0	100.0	100.0	100.0	/	[113]
Purchase price	€/kW_{th}	136.0	136.0	136.0	136.0	136.0	/	[113]
Service life	a	20.0	20.0	20.0	20.0	20.0	/	[113]
i_{int}	%	7.0	7.0	7.0	7.0	7.0	/	[113]
f_{OM}	%	2.0	2.0	2.0	2.0	2.0	/	[113]
r_P	%	1.7	1.7	1.7	1.7	1.7	/	[113]
r_{OM}	%	1.7	1.7	1.7	1.7	1.7	/	[113]
η	%	88.0	88.0	88.0	88.0	88.0	/	[113]
Methane boiler (LMT)		2015	2020	2030	2040	2050	total	ref
Min. deployment	%	0.0	0.0	0.0	0.0	0.0	/	[113]
Max. deployment	%	100.0	100.0	100.0	100.0	100.0	/	[113]
Purchase price	€/kW_{th}	97.0	97.0	97.0	97.0	97.0	/	[113]
Service life	a	20.0	20.0	20.0	20.0	20.0	/	[113]
i_{int}	%	7.0	7.0	7.0	7.0	7.0	/	[113]
f_{OM}	%	2.0	2.0	2.0	2.0	2.0	/	[113]
r_P	%	1.7	1.7	1.7	1.7	1.7	/	[113]
r_{OM}	%	1.7	1.7	1.7	1.7	1.7	/	[113]
η	%	92.0	92.0	92.0	92.0	92.0	/	[113]
Electrode boiler (LMT)		2015	2020	2030	2040	2050	total	ref
Min. deployment	%	0.0	0.0	0.0	0.0	0.0	/	[113]
Max. deployment	%	100.0	100.0	100.0	100.0	100.0	/	[113]
Purchase price	€/kW_{th}	136.0	136.0	136.0	136.0	136.0	/	[113]
Service life	a	20.0	20.0	20.0	20.0	20.0	/	[113]
i_{int}	%	7.0	7.0	7.0	7.0	7.0	/	[113]
f_{OM}	%	2.0	2.0	2.0	2.0	2.0	/	[113]
r_P	%	1.7	1.7	1.7	1.7	1.7	/	[113]
r_{OM}	%	1.7	1.7	1.7	1.7	1.7	/	[113]
η	%	98.0	98.0	98.0	98.0	98.0	/	[113]

Continued on next page

Table A.9: Input parameters of generators for the supply of process heat for 2015, 2020, 2030, 2040 an 2050. i_{int}: interest rate, f_{OM}: factor for maintenance and operation in % from purchase price, r_P: price change factor for the purchase of a technology or a building component, r_{OM}: price change rate for maintenance and operation.

CCGT (LMT)		2015	2020	2030	2040	2050	total	ref
Min. deployment	%	0.0	0.0	0.0	0.0	0.0	/	[113]
Max. deployment	%	100.0	100.0	100.0	100.0	100.0	/	[113]
Purchase price	€/kW_{th}	650.0	650.0	650.0	650.0	650.0	/	[113]
Service life	a	20.0	20.0	20.0	20.0	20.0	/	[113]
i_{int}	%	7.0	7.0	7.0	7.0	7.0	/	[113]
f_{OM}	%	3.0	3.0	3.0	3.0	3.0	/	[113]
r_P	%	1.7	1.7	1.7	1.7	1.7	/	[113]
r_{OM}	%	1.7	1.7	1.7	1.7	1.7	/	[113]
η_{el}	%	45.0	45.0	45.0	45.0	45.0	/	[113]
η_{th}	%	45.0	45.0	45.0	45.0	45.0	/	[113]
Hydrogen boiler (LMT)		2015	2020	2030	2040	2050	total	ref
Min. deployment	%	0.0	0.0	0.0	0.0	0.0	/	[113]
Max. deployment	%	100.0	100.0	100.0	100.0	100.0	/	[113]
Purchase price	€/kW_{th}	136.0	136.0	136.0	136.0	136.0	/	[113]
Service life	a	20.0	20.0	20.0	20.0	20.0	/	[113]
i_{int}	%	7.0	7.0	7.0	7.0	7.0	/	[113]
f_{OM}	%	2.0	2.0	2.0	2.0	2.0	/	[113]
r_P	%	1.7	1.7	1.7	1.7	1.7	/	[113]
r_{OM}	%	1.7	1.7	1.7	1.7	1.7	/	[113]
η	%	92.0	92.0	92.0	92.0	92.0	/	[113]
Coal boiler (LMT)		2015	2020	2030	2040	2050	total	ref
Min. deployment	%	0.0	0.0	0.0	0.0	0.0	/	[113]
Max. deployment	%	100.0	100.0	100.0	100.0	100.0	/	[113]
Purchase price	€/kW_{th}	258.1	250.7	235.8	221.0	206.5	/	[113]
Service life	a	20.0	20.0	20.0	20.0	20.0	/	[113]
i_{int}	%	7.0	7.0	7.0	7.0	7.0	/	[113]
f_{OM}	%	2.0	2.0	2.0	2.0	2.0	/	[113]
r_P	%	1.7	1.7	1.7	1.7	1.7	/	[113]
r_{OM}	%	1.7	1.7	1.7	1.7	1.7	/	[113]
η	%	85.0	85.0	85.0	85.0	85.0	/	[113]

Continued on next page

Table A.9: Input parameters of generators for the supply of process heat for 2015, 2020, 2030, 2040 an 2050. i_{int}: interest rate, f_{OM}: factor for maintenance and operation in % from purchase price, r_P: price change factor for the purchase of a technology or a building component, r_{OM}: price change rate for maintenance and operation.

Oil-fired boiler (HT)		2015	2020	2030	2040	2050	total	ref
Min. deployment	%	0.0	0.0	0.0	0.0	0.0	/	[113]
Max. deployment	%	100.0	100.0	100.0	100.0	100.0	/	[113]
Purchase price	€/kW_{th}	136.0	136.0	136.0	136.0	136.0	/	[113]
Service life	a	20.0	20.0	20.0	20.0	20.0	/	[113]
i_{int}	%	7.0	7.0	7.0	7.0	7.0	/	[113]
f_{OM}	%	2.0	2.0	2.0	2.0	2.0	/	[113]
r_P	%	1.7	1.7	1.7	1.7	1.7	/	[113]
r_{OM}	%	1.7	1.7	1.7	1.7	1.7	/	[113]
η	%	88.0	88.0	88.0	88.0	88.0	/	[113]
Methane boiler (HT)		2015	2020	2030	2040	2050	total	ref
Min. deployment	%	0.0	0.0	0.0	0.0	0.0	/	[113]
Max. deployment	%	100.0	100.0	100.0	100.0	100.0	/	[113]
Purchase price	€/kW_{th}	97.0	97.0	97.0	97.0	97.0	/	[113]
Service life	a	20.0	20.0	20.0	20.0	20.0	/	[113]
i_{int}	%	7.0	7.0	7.0	7.0	7.0	/	[113]
f_{OM}	%	2.0	2.0	2.0	2.0	2.0	/	[113]
r_P	%	1.7	1.7	1.7	1.7	1.7	/	[113]
r_{OM}	%	1.7	1.7	1.7	1.7	1.7	/	[113]
η	%	92.0	92.0	92.0	92.0	92.0	/	[113]
Electrode boiler (HT)		2015	2020	2030	2040	2050	total	ref
Min. deployment	%	0.0	0.0	0.0	0.0	0.0	/	[113]
Max. deployment	%	100.0	100.0	100.0	100.0	100.0	/	[113]
Purchase price	€/kW_{th}	136.0	136.0	136.0	136.0	136.0	/	[113]
Service life	a	20.0	20.0	20.0	20.0	20.0	/	[113]
i_{int}	%	7.0	7.0	7.0	7.0	7.0	/	[113]
f_{OM}	%	2.0	2.0	2.0	2.0	2.0	/	[113]
r_P	%	1.7	1.7	1.7	1.7	1.7	/	[113]
r_{OM}	%	1.7	1.7	1.7	1.7	1.7	/	[113]
η	%	98.0	98.0	98.0	98.0	98.0	/	[113]

Continued on next page

Table A.9: Input parameters of generators for the supply of process heat for 2015, 2020, 2030, 2040 an 2050. i_{int}: interest rate, f_{OM}: factor for maintenance and operation in % from purchase price, r_P: price change factor for the purchase of a technology or a building component, r_{OM}: price change rate for maintenance and operation.

Hydrogen boiler (HT)		2015	2020	2030	2040	2050	total	ref
Min. deployment	%	0.0	0.0	0.0	0.0	0.0	/	[113]
Max. deployment	%	100.0	100.0	100.0	100.0	100.0	/	[113]
Purchase price	€/kW_{th}	136.0	136.0	136.0	136.0	136.0	/	[113]
Service life	a	20.0	20.0	20.0	20.0	20.0	/	[113]
i_{int}	%	7.0	7.0	7.0	7.0	7.0	/	[113]
f_{OM}	%	2.0	2.0	2.0	2.0	2.0	/	[113]
r_P	%	1.7	1.7	1.7	1.7	1.7	/	[113]
r_{OM}	%	1.7	1.7	1.7	1.7	1.7	/	[113]
η	%	92.0	92.0	92.0	92.0	92.0	/	[113]
Coal boiler (HT)		2015	2020	2030	2040	2050	total	ref
Min. deployment	%	0.0	0.0	0.0	0.0	0.0	/	[113]
Max. deployment	%	100.0	100.0	100.0	100.0	100.0	/	[113]
Purchase price	€/kW_{th}	258.1	250.7	235.8	221.0	206.5	/	[113]
Service life	a	20.0	20.0	20.0	20.0	20.0	/	[113]
i_{int}	%	7.0	7.0	7.0	7.0	7.0	/	[113]
f_{OM}	%	2.0	2.0	2.0	2.0	2.0	/	[113]
r_P	%	1.7	1.7	1.7	1.7	1.7	/	[113]
r_{OM}	%	1.7	1.7	1.7	1.7	1.7	/	[113]
η	%	85.0	85.0	85.0	85.0	85.0	/	[113]

A.8 Motorised Road Transport

Table A.10: Input parameters of motorised road transport for 2015, 2020, 2030, 2040 an 2050. i_{int}: interest rate, f_{OM}: factor for maintenance and operation in % from purchase price, r_P: price change factor for the purchase of a technology or a building component, r_{OM}: price change rate for maintenance and operation.

Liquid fuels ICE (private)		2015	2020	2030	2040	2050	total	ref
Min. deployment	%	0.0	0.0	0.0	0.0	0.0	/	[113]
Max. deployment	%	100.0	100.0	100.0	100.0	100.0	/	[113]
Purchase price	k€	22.8	23.6	25.0	26.2	26.9	/	[113]
Service life	a	15.0	15.0	15.0	15.0	15.0	/	[113]
i_{int}	%	7.0	7.0	7.0	7.0	7.0	/	[113]
f_{OM}	%	1.6	1.6	1.6	1.6	1.6	/	[113]
r_P	%	1.7	1.7	1.7	1.7	1.7	/	[113]
r_{OM}	%	1.7	1.7	1.7	1.7	1.7	/	[113]
η	%	21.5	21.5	21.5	21.5	21.5	/	[113]
Gas ICE (private)		2015	2020	2030	2040	2050	total	ref
Min. deployment	%	0.0	0.0	0.0	0.0	0.0	/	[113]
Max. deployment	%	100.0	100.0	100.0	100.0	100.0	/	[113]
Purchase price	k€	24.6	25.0	25.9	26.9	28.0	/	[113]
Service life	a	15.0	15.0	15.0	15.0	15.0	/	[113]
i_{int}	%	7.0	7.0	7.0	7.0	7.0	/	[113]
f_{OM}	%	1.4	1.4	1.4	1.4	1.4	/	[113]
r_P	%	1.7	1.7	1.7	1.7	1.7	/	[113]
r_{OM}	%	1.7	1.7	1.7	1.7	1.7	/	[113]
η	%	20.0	21.5	21.5	21.5	21.5	/	[113]
Methane slip	mg_{CH_4}/m^3	500	500	500	500	500	/	[122]

Continued on next page

Table A.10: Input parameters of motorised road transport for 2015, 2020, 2030, 2040 an 2050. i_{int}: interest rate, f_{OM}: factor for maintenance and operation in % from purchase price, r_P: price change factor for the purchase of a technology or a building component, r_{OM}: price change rate for maintenance and operation.

FCEV (private)		2015	2020	2030	2040	2050	total	ref
Min. deployment	%	0.0	0.0	0.0	0.0	0.0	/	[113]
Max. deployment	%	100.0	100.0	100.0	100.0	100.0	/	[113]
Purchase price	k€	65.0	45.0	32.0	29.0	27.7	/	[113]
Service life	a	15.0	15.0	15.0	15.0	15.0	/	[113]
i_{int}	%	7.0	7.0	7.0	7.0	7.0	/	[113]
f_{OM}	%	0.5	1.1	1.1	1.2	1.2	/	[113]
r_P	%	1.7	1.7	1.7	1.7	1.7	/	[113]
r_{OM}	%	1.7	1.7	1.7	1.7	1.7	/	[113]
η	%	48.0	48.0	48.0	48.0	48.0	/	[113]
PHEV (FCEV) (private)		2015	2020	2030	2040	2050	total	ref
Min. deployment	%	0.0	0.0	0.0	0.0	0.0	/	[113]
Max. deployment	%	100.0	100.0	100.0	100.0	100.0	/	[113]
Purchase price	k€	68.4	49.4	35.0	31.3	29.7	/	[113]
Service life	a	15.0	15.0	15.0	15.0	15.0	/	[113]
i_{int}	%	7.0	7.0	7.0	7.0	7.0	/	[113]
f_{OM}	%	0.5	1.1	1.1	1.2	1.2	/	[113]
r_P	%	1.7	1.7	1.7	1.7	1.7	/	[113]
r_{OM}	%	1.7	1.7	1.7	1.7	1.7	/	[113]
η_{bat}	%	74.1	74.1	74.1	74.1	74.1	/	[113]
η_{FC}	%	56.0	56.0	56.0	56.0	56.0	/	[113]
Cap. battery	kWh_{el}	5.0	12.5	20.0	20.0	20.0	/	[113]
Share of battery	%	40.0	40.0	40.0	40.0	40.0	/	[113]

Continued on next page

Table A.10: Input parameters of motorised road transport for 2015, 2020, 2030, 2040 an 2050. i_{int}: interest rate, f_{OM}: factor for maintenance and operation in % from purchase price, r_P: price change factor for the purchase of a technology or a building component, r_{OM}: price change rate for maintenance and operation.

PHEV (ICE fuel) (private)		2015	2020	2030	2040	2050	total	ref
Min. deployment	%	0.0	0.0	0.0	0.0	0.0	/	[113]
Max. deployment	%	100.0	100.0	100.0	100.0	100.0	/	[113]
Purchase price	k€	30.4	31.8	30.4	30.0	31.0	/	[113]
Service life	a	15.0	15.0	15.0	15.0	15.0	/	[113]
i_{int}	%	7.0	7.0	7.0	7.0	7.0	/	[113]
f_{OM}	%	1.3	1.3	1.3	1.3	1.3	/	[113]
r_P	%	1.7	1.7	1.7	1.7	1.7	/	[113]
r_{OM}	%	1.7	1.7	1.7	1.7	1.7	/	[113]
η_{bat}	%	74.1	74.1	74.1	74.1	74.1	/	[113]
η_{ICE}	%	25.3	27.4	27.8	27.8	27.8	/	[113]
Cap. battery	kWh_{el}	5.0	12.5	20.0	20.0	20.0	/	[113]
Share of battery	%	40.0	40.0	40.0	40.0	40.0	/	[113]
Methane hybrid ICE (private)		2015	2020	2030	2040	2050	total	ref
Min. deployment	%	0.0	0.0	0.0	0.0	0.0	/	[113]
Max. deployment	%	100.0	100.0	100.0	100.0	100.0	/	[113]
Purchase price	k€	32.6	34.1	32.7	32.4	33.3	/	[113]
Service life	a	15.0	15.0	15.0	15.0	15.0	/	[113]
i_{int}	%	7.0	7.0	7.0	7.0	7.0	/	[113]
f_{OM}	%	1.0	1.3	1.3	1.3	1.3	/	[113]
r_P	%	1.7	1.7	1.7	1.7	1.7	/	[113]
r_{OM}	%	1.7	1.7	1.7	1.7	1.7	/	[113]
η_{bat}	%	74.1	74.1	74.1	74.1	74.1	/	[113]
η_{ICE}	%	22.2	24.3	25.6	25.6	25.6	/	[113]
Cap. battery	kWh	6.5	14.0	20.0	20.0	5.0	/	[113]
Share of battery	%	40.0	40.0	40.0	40.0	40.0	/	[113]
Methane slip	mg_{CH_4}/m^3	500	500	500	500	500	/	[122]

Continued on next page

Table A.10: Input parameters of motorised road transport for 2015, 2020, 2030, 2040 an 2050. i_{int}: interest rate, f_{OM}: factor for maintenance and operation in % from purchase price, r_P: price change factor for the purchase of a technology or a building component, r_{OM}: price change rate for maintenance and operation.

BEV (private)		2015	2020	2030	2040	2050	total	ref
Min. deployment	%	0.0	0.0	0.0	0.0	0.0	/	[113]
Max. deployment	%	100.0	100.0	100.0	100.0	100.0	/	[113]
Purchase price	k€	37.8	38.5	31.0	28.5	27.7	/	[113]
Service life	a	15.0	15.0	15.0	15.0	15.0	/	[113]
i_{int}	%	7.0	7.0	7.0	7.0	7.0	/	[113]
f_{OM}	%	0.9	0.9	0.9	0.9	0.9	/	[113]
r_P	%	1.7	1.7	1.7	1.7	1.7	/	[113]
r_{OM}	%	1.7	1.7	1.7	1.7	1.7	/	[113]
η_{bat}	%	74.1	74.1	74.1	74.1	74.1	/	[113]
η_{bat}	%	68.0	68.0	68.0	68.0	68.0	/	[113]
Cap. battery	kWh_{el}	25.0	50.0	66.7	66.7	66.7	/	[113]
Liquid fuels ICE (freight)		2015	2020	2030	2040	2050	total	ref
Min. deployment	%	0.0	0.0	0.0	0.0	0.0	/	[113]
Max. deployment	%	100.0	100.0	100.0	100.0	100.0	/	[113]
Purchase price	k€	97.0	99.8	105.3	110.9	116.4	/	[113]
Service life	a	15.0	15.0	15.0	15.0	15.0	/	[113]
i_{int}	%	7.0	7.0	7.0	7.0	7.0	/	[113]
f_{OM}	%	18.5	18.0	17.1	16.2	15.5	/	[113]
r_P	%	1.7	1.7	1.7	1.7	1.7	/	[113]
r_{OM}	%	1.7	1.7	1.7	1.7	1.7	/	[113]
η	%	37.3	37.3	37.3	37.3	37.3	/	[113]
Methane ICE (freight)		2015	2020	2030	2040	2050	total	ref
Min. deployment	%	0.0	0.0	0.0	0.0	0.0	/	[113]
Max. deployment	%	100.0	100.0	100.0	100.0	100.0	/	[113]
Purchase price	k€	106.2	107.8	111.3	115.4	120.2	/	[113]
Service life	a	15.0	15.0	15.0	15.0	15.0	/	[113]
i_{int}	%	7.0	7.0	7.0	7.0	7.0	/	[113]
f_{OM}	%	16.9	16.7	16.2	15.6	15.0	/	[113]
r_P	%	1.7	1.7	1.7	1.7	1.7	/	[113]
r_{OM}	%	1.7	1.7	1.7	1.7	1.7	/	[113]
η	%	30.1	30.1	30.1	30.1	30.1	/	[113]
Methane slip	mg_{CH_4}/m^3	500	500	500	500	500	/	[122]

Continued on next page

Table A.10: Input parameters of motorised road transport for 2015, 2020, 2030, 2040 an 2050. i_{int}: interest rate, f_{OM}: factor for maintenance and operation in % from purchase price, r_P: price change factor for the purchase of a technology or a building component, r_{OM}: price change rate for maintenance and operation.

FCEV (freight)		2015	2020	2030	2040	2050	total	ref
Min. deployment	%	0.0	0.0	0.0	0.0	0.0	/	[113]
Max. deployment	%	100.0	100.0	100.0	100.0	100.0	/	[113]
Purchase price	k€	245.6	151.6	116.5	120.2	125.7	/	[113]
Service life	a	15.0	15.0	15.0	15.0	15.0	/	[113]
i_{int}	%	7.0	7.0	7.0	7.0	7.0	/	[113]
f_{OM}	%	6.2	10.1	13.1	12.7	12.2	/	[113]
r_P	%	1.7	1.7	1.7	1.7	1.7	/	[113]
r_{OM}	%	1.7	1.7	1.7	1.7	1.7	/	[113]
η	%	56.0	56.0	56.0	56.0	56.0	/	[113]
Hybrid hydrogen FCEV (freight)		2015	2020	2030	2040	2050	total	ref
Min. deployment	%	0.0	0.0	0.0	0.0	0.0	/	[113]
Max. deployment	%	100.0	100.0	100.0	100.0	100.0	/	[113]
Purchase price	k€	265.7	165.7	124.8	127.7	132.3	/	[113]
Service life	a	15.0	15.0	15.0	15.0	15.0	/	[113]
i_{int}	%	7.0	7.0	7.0	7.0	7.0	/	[113]
f_{OM}	%	5.7	9.2	12.2	12.0	11.5	/	[113]
r_P	%	1.7	1.7	1.7	1.7	1.7	/	[113]
r_{OM}	%	1.7	1.7	1.7	1.7	1.7	/	[113]
η_{bat}	%	74.1	74.1	74.1	74.1	74.1	/	[113]
η_{FC}	%	56.0	56.0	56.0	56.0	56.0	/	[113]
Cap. battery	kWh	50.0	50.0	50.0	50.0	50.0	/	[113]
Share of battery	%	5.0	5.0	5.0	5.0	5.0	/	[113]

Continued on next page

Table A.10: Input parameters of motorised road transport for 2015, 2020, 2030, 2040 an 2050. i_{int}: interest rate, f_{OM}: factor for maintenance and operation in % from purchase price, r_P: price change factor for the purchase of a technology or a building component, r_{OM}: price change rate for maintenance and operation.

PHEV (ICE fuel) (freight)		2015	2020	2030	2040	2050	total	ref
Min. deployment	%	0.0	0.0	0.0	0.0	0.0	/	[113]
Max. deployment	%	100.0	100.0	100.0	100.0	100.0	/	[113]
Purchase price	k€	130.1	124.7	119.6	120.5	125.1	/	[113]
Service life	a	15.0	15.0	15.0	15.0	15.0	/	[113]
i_{int}	%	7.0	7.0	7.0	7.0	7.0	/	[113]
f_{OM}	%	13.8	14.4	15.0	14.9	14.4	/	[113]
r_P	%	1.7	1.7	1.7	1.7	1.7	/	[113]
r_{OM}	%	1.7	1.7	1.7	1.7	1.7	/	[113]
η_{bat}	%	74.1	74.1	74.1	74.1	74.1	/	[113]
η_{ICE}	%	37.3	37.3	37.3	37.3	37.3	/	[113]
Cap. battery	kWh_{el}	50.0	50.0	50.0	50.0	50.0	/	[113]
Share of battery	%	5.0	5.0	5.0	5.0	5.0	/	[113]
Methane hybrid ICE (freight)		2015	2020	2030	2040	2050	total	ref
Min. deployment	%	0.0	0.0	0.0	0.0	0.0	/	[113]
Max. deployment	%	100.0	100.0	100.0	100.0	100.0	/	[113]
Purchase price	k€	139.0	133.8	128.8	129.7	134.3	/	[113]
Service life	a	15.0	15.0	15.0	15.0	15.0	/	[113]
i_{int}	%	7.0	7.0	7.0	7.0	7.0	/	[113]
f_{OM}	%	12.9	13.4	14.0	13.9	13.4	/	[113]
r_P	%	1.7	1.7	1.7	1.7	1.7	/	[113]
r_{OM}	%	1.7	1.7	1.7	1.7	1.7	/	[113]
η_{bat}	%	74.1	74.1	74.1	74.1	74.1	/	[113]
η_{ICE}	%	30.1	30.1	30.1	30.1	30.1	/	[113]
Cap. battery	kWh_{el}	50.0	50.0	50.0	50.0	50.0	/	[113]
Share of battery	%	5.0	5.0	5.0	5.0	5.0	/	[113]
Methane slip	mg_{CH_4}/m^3	500	500	500	500	500	/	[122]

Continued on next page

Table A.10: Input parameters of motorised road transport for 2015, 2020, 2030, 2040 an 2050. i_{int}: interest rate, f_{OM}: factor for maintenance and operation in % from purchase price, r_P: price change factor for the purchase of a technology or a building component, r_{OM}: price change rate for maintenance and operation.

BEV (freight)		2015	2020	2030	2040	2050	total	ref
Min. deployment	%	0.0	0.0	0.0	0.0	0.0	/	[113]
Max. deployment	%	100.0	100.0	100.0	100.0	100.0	/	[113]
Purchase price	k€	195.9	135.2	116.1	120.7	126.2	/	[113]
Service life	a	15.0	15.0	15.0	15.0	15.0	/	[113]
i_{int}	%	7.0	7.0	7.0	7.0	7.0	/	[113]
f_{OM}	%	7.8	11.3	13.2	12.7	12.1	/	[113]
r_P	%	1.7	1.7	1.7	1.7	1.7	/	[113]
r_{OM}	%	1.7	1.7	1.7	1.7	1.7	/	[113]
η_{bat}	%	74.1	74.1	74.1	74.1	74.1	/	[113]
η_{bat}	%	68.0	68.0	68.0	68.0	68.0	/	[113]
Cap. battery	kWh_{el}	100.0	100.0	100.0	100.0	100.0	/	[113]

B Results: Thermal Power Plants

System Configuration: 85 % CO_2 Reduction Target

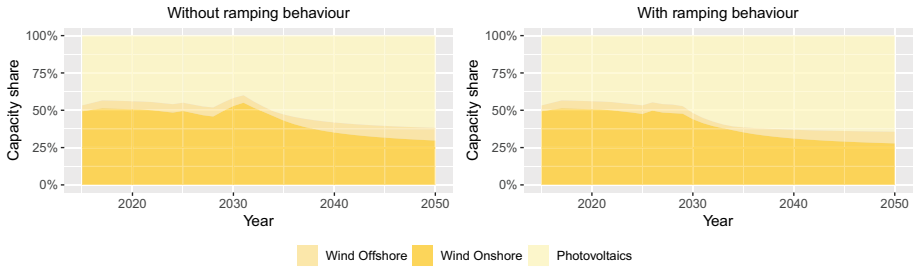

Figure B.1: Share of installed VRE capacity from 2015 to 2050 for a 85 % CO_2 emission reduction compared to 1990 values, obtained with and without the consideration of ramping behaviour.

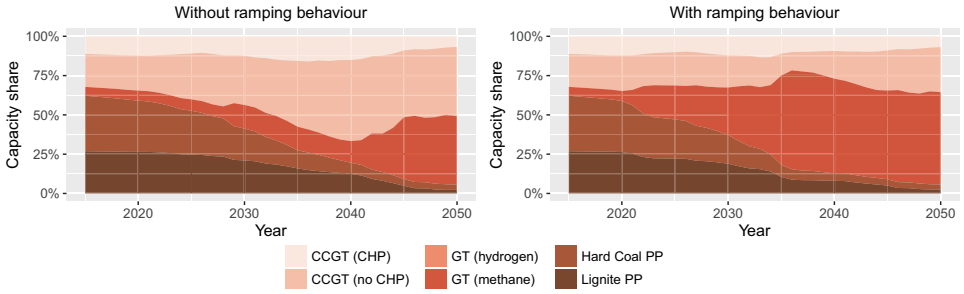

Figure B.2: Share of installed thermal power plant capacity from 2015 to 2050 for a 85 % CO_2 emission reduction compared to 1990 values, obtained with and without the consideration of ramping behaviour. Hydrogen-based gas turbine (GT) power plants (PP) are not installed. CCGT: combined cycle gas turbine.

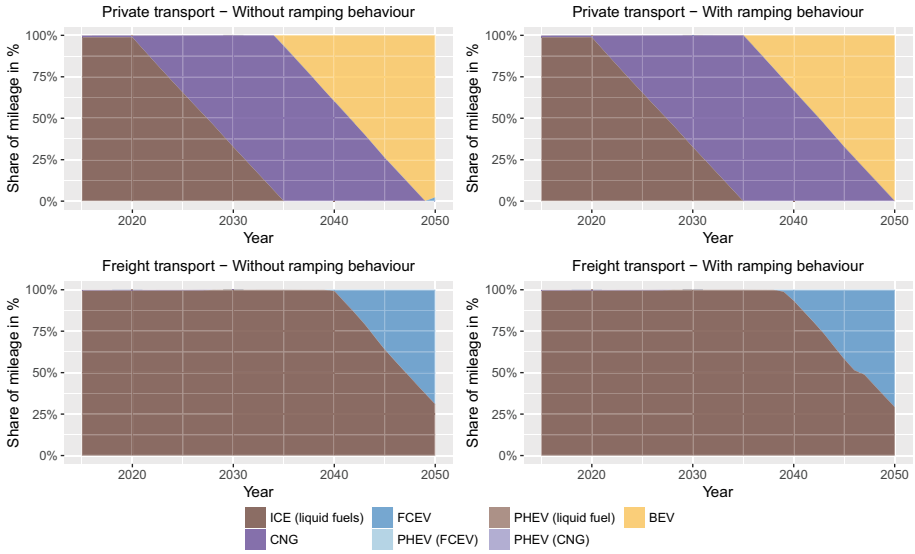

Figure B.3: Development of milage share per power train technology for a 85 % CO_2 emission reduction in 2050 compared to 1990 values, with and without the consideration of ramping behaviour. BEV: battery electric vehicle, CNG: compressed natural gas vehicle, PHEV: plug-in hybrid electric vehicle, FCEV: fuel cell electric vehicle, ICE: internal combustion engine.

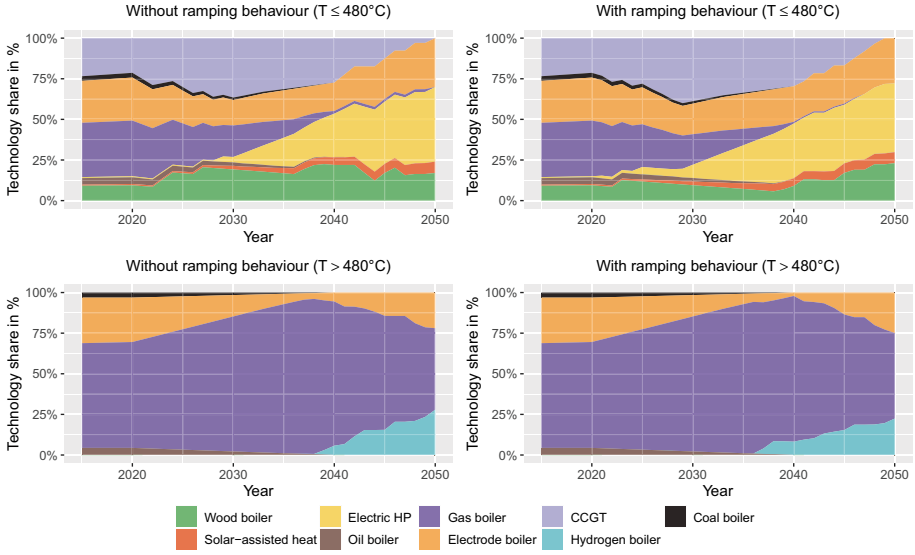

Figure B.4: Share of heat generators for the supply of process heat from 2015 to 2050 for a 85 % CO_2 emission reduction compared to 1990 values, with and without the consideration of ramping behaviour. CHP: combined heat and power unit, HP: heat pump, CCGT: combined cycle gas turbine.

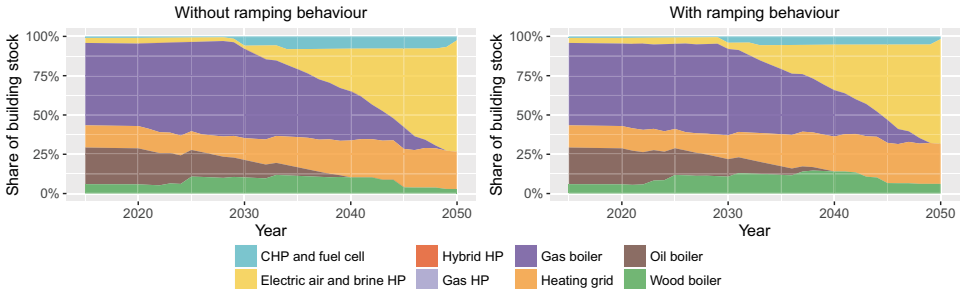

Figure B.5: Share of heat generators for the supply of space heat and domestic hot water from 2015 to 2050 for a 85 % CO_2 emission reduction compared to 1990 values, with and without the consideration of ramping behaviour. CHP: combined heat and power unit, HP: heat pump.

System Configuration: 90 % CO_2 Reduction Target

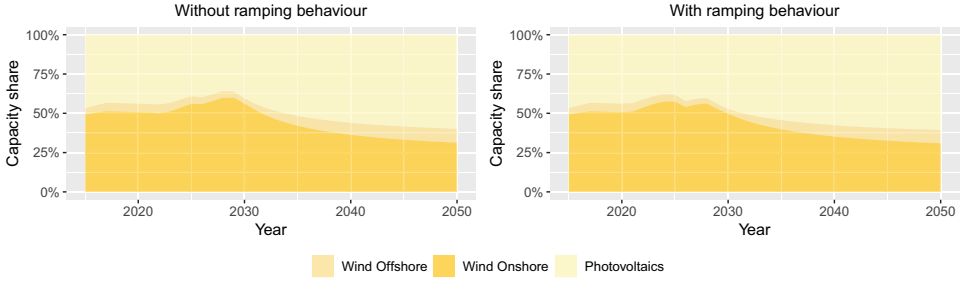

Figure B.6: Share of installed VRE capacity from 2015 to 2050 for a 90 % CO_2 emission reduction compared to 1990 values, obtained with and without the consideration of ramping behaviour.

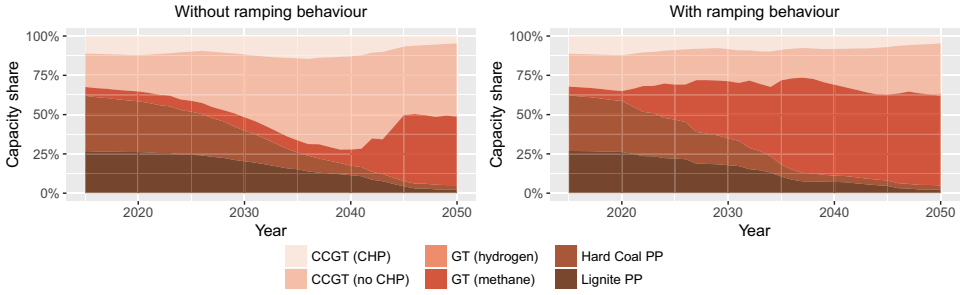

Figure B.7: Share of installed thermal power plant capacity from 2015 to 2050 for a 90 % CO_2 emission reduction compared to 1990 values, obtained with and without the consideration of ramping behaviour. Hydrogen-based gas turbine (GT) power plants (PP) are not installed. CCGT: combined cycle gas turbine.

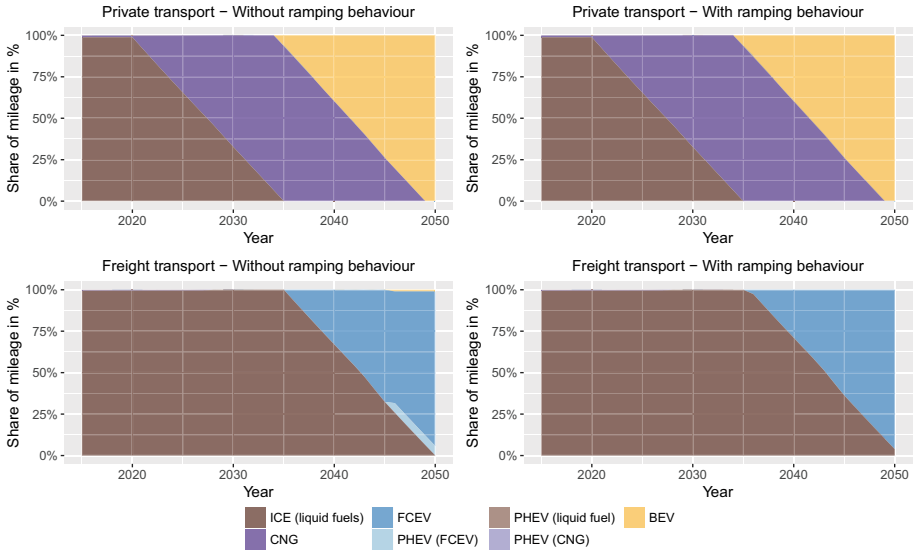

Figure B.8: Development of milage share per power train technology for a 90 % CO_2 emission reduction in 2050 compared to 1990 values, with and without the consideration of ramping behaviour. BEV: battery electric vehicle, CNG: compressed natural gas vehicle, PHEV: plug-in hybrid electric vehicle, FCEV: fuel cell electric vehicle, ICE: internal combustion engine.

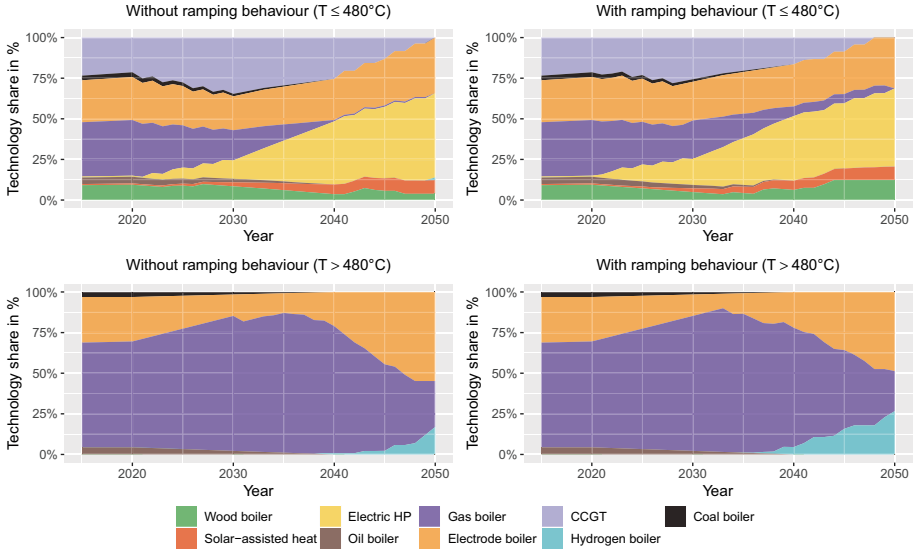

Figure B.9: Share of heat generators for the supply of process heat from 2015 to 2050 for a 90 % CO_2 emission reduction compared to 1990 values, with and without the consideration of ramping behaviour. CHP: combined heat and power unit, HP: heat pump, CCGT: combined cycle gas turbine.

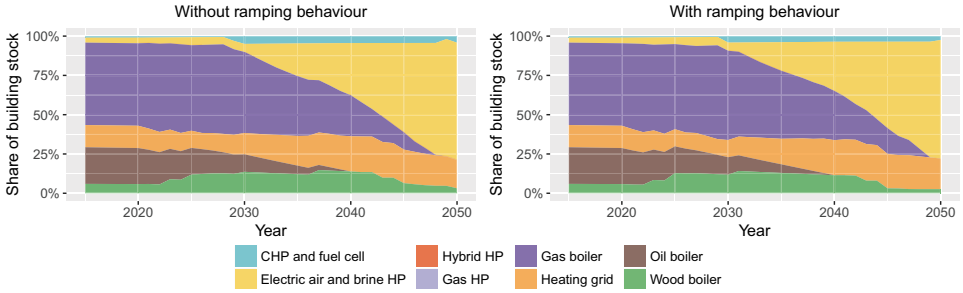

Figure B.10: Share of heat generators for the supply of space heat and domestic hot water from 2015 to 2050 for a 85 % CO_2 emission reduction compared to 1990 values, with and without the consideration of ramping behaviour. CHP: combined heat and power unit, HP: heat pump.

C Results: Alternative Drive Concepts

Figure C.1: Development of the degree of electrification for the sectors of the energy system for three CO_2 reduction targets compared to 1990 values. The indirect electrification accounts for synthetic fuels, generated by Power-to-Gas or Power-to-Liquid plants. DHW: domestic hot water.

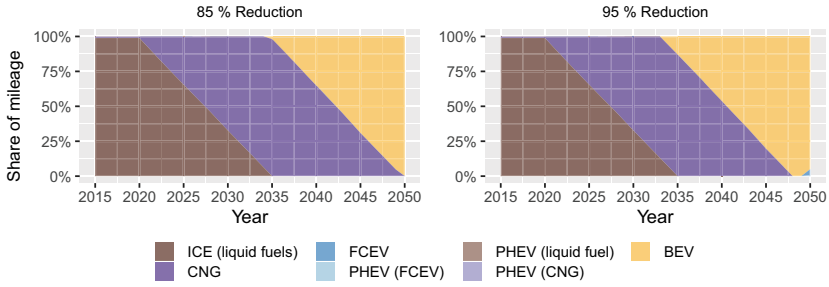

Figure C.2: Development of the milage share per power train technology for a 90 % and 95 % CO_2 emission reduction in 2050 compared to 1990 values. BEV: battery electric vehicle, CNG: compressed natural gas vehicle, PHEV: plug-in hybrid electric vehicle, FCEV: fuel cell electric vehicle, ICE: internal combustion engine.

D Results: Heat Generators and Thermal Energy Storage

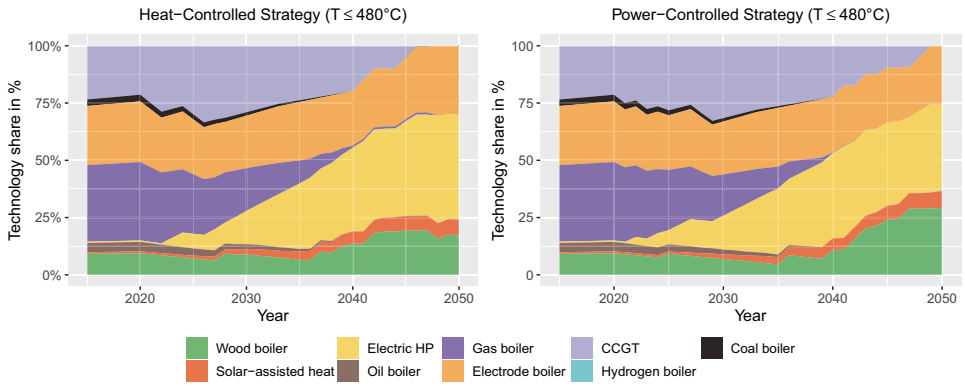

Figure D.1: Share of heat generators for the supply of process heat from 2015 to 2050 for a 85 % CO_2 emission reduction compared to 1990 values. Heat generators for the supply of space heat and domestic hot water are operated in a heat-controlled (left) or power-controlled (right) way. CHP: combined heat and power unit, HP: heat pump, CCGT: combined cycle gas turbine.

E Results: The Value of Demand-Side Management

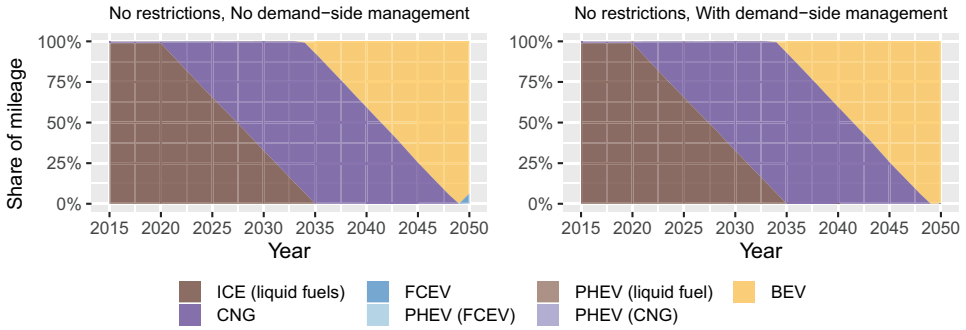

Figure E.1: Development of the milage share per power train technology for a 85 % CO_2 emission reduction in 2050 compared to 1990 values. The yearly technology market share of electric heat pumps (HP) and battery electric vehicles (BEVs) is limited to 19 % and 50 % on the left side. BEV: battery electric vehicle, CNG: compressed natural gas vehicle, PHEV: plug-in hybrid electric vehicle, FCEV: fuel cell electric vehicle, ICE: internal combustion engine.

Optimised System Configuration without CO_2 Reduction Target

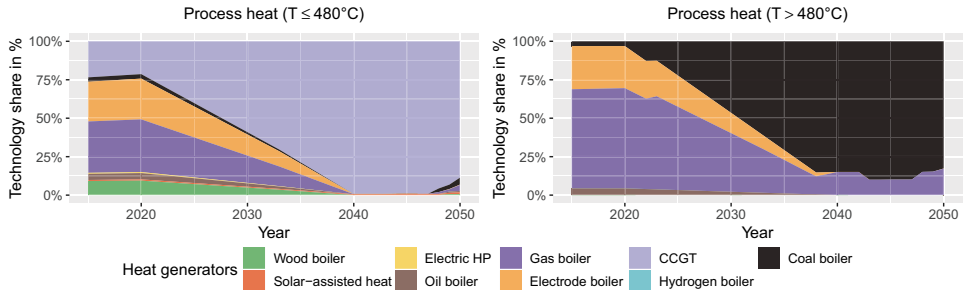

Figure E.2: Share of heat generators for the supply of process heat from 2015 to 2050 without consideration of a CO_2 emission reduction target. The deployment of CNG-vehicles is restricted. CHP: combined heat and power unit, HP: heat pump, CCGT: combined cycle gas turbine.

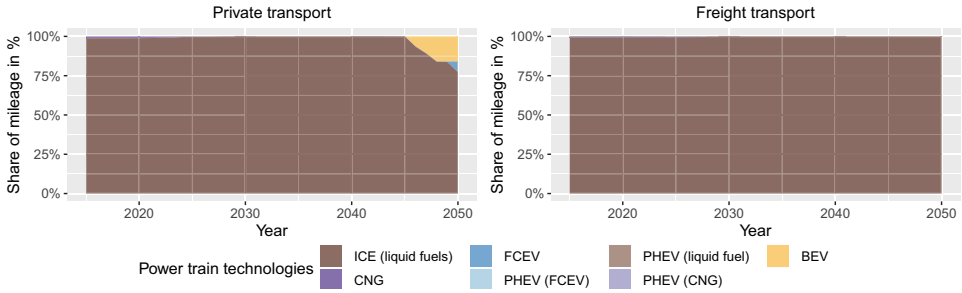

Figure E.3: Development of the milage share per power train technology without consideration of a CO_2 emission reduction target. The deployment of CNG-vehicles is restricted. BEV: battery electric vehicle, CNG: compressed natural gas vehicle, PHEV: plug-in hybrid electric vehicle, FCEV: fuel cell electric vehicle, ICE: internal combustion engine.

Table E.1: Configuration of variable renewable energy, thermal power plants, generators for the supply of space heat and domestic hot water and building refurbishment without consideration of a CO_2 emission reduction target. The deployment of CNG-vehicles is restricted. CHP: combined heat and power unit, HP: heat pump, CCGT: combined cycle gas turbine.

Variable renewable energy	Unit	2015	2020	2030	2040	2050
Offshore Wind	Gwel	3.3	5.3	5.2	0.0	0.0
Onshore Wind	Gwel	41.3	49.5	30.4	0.0	0.0
Photovoltaic systems	Gwel	39.2	43.0	40.1	44.9	67.1
Thermal Power plants	Unit	2015	2020	2030	2040	2050
Gas turbine (methane gas)	Gwel	4.4	4.4	12.6	26.1	34.0
Gas turbine (hydrogen)	Gwel	0.0	0.0	0.0	0.0	0.0
CCGT (no CHP)	Gwel	16.5	15.3	12.8	8.7	4.3
Lignite PP	Gwel	21.9	21.6	16.8	13.3	7.3
Hard coal PP	Gwel	27.8	22.7	12.6	5.3	4.9
CCGT (with CHP)	Gwel	8.9	8.9	11.0	11.1	14.4
Synthetic fuel production	Unit	2015	2020	2030	2040	2050
Power-to-H2	Gwel	0	0	0.0	0.0	0.0
Power-to-CH4	Gwel	0	0	0.0	0.0	0.0
Power-to-Fuel	Gwel	0	0	0.0	0.0	1.2

Continued on next page

Table E.1: Configuration of variable renewable energy, thermal power plants, generators for the supply of space heat and domestic hot water and building refurbishment without consideration of a CO_2 emission reduction target. The deployment of CNG-vehicles is restricted. CHP: combined heat and power unit, HP: heat pump, CCGT: combined cycle gas turbine.

Heat generators	Unit	2015	2020	2030	2040	2050
Heat grid	%	14.0	14.0	14.0	14.1	14.1
Oil boiler	%	23.3	23.2	23.2	23.1	23.0
Gas boiler	%	52.4	52.5	52.5	52.5	52.5
Wood boiler	%	6.0	5.9	5.9	5.9	5.9
Gas heat pump	%	0.0	0.0	0.0	0.0	0.0
Electric brine heat pump	%	1.6	1.6	1.7	1.7	1.8
Electric air heat pump	%	1.6	1.6	1.7	1.7	1.8
Hybrid heat pump	%	0.0	0.0	0.0	0.0	0.0
Micro-CHP	%	1.0	1.0	1.0	1.0	1.0
Hydrogen fuel cell	%	0.0	0.0	0.0	0.0	0.0
Methane fuel cell	%	0.0	0.0	0.0	0.0	0.0
Building refurbishment	Unit	2015	2020	2030	2040	2050
Fully refurbished	%	33.9	34.0	34.1	34.3	34.4
Highly efficient	%	0.0	0.0	0.0	0.0	0.0
Unrenovated	%	66.1	66.0	65.9	65.7	65.6

Bibliography

[1] United Nations Climate Change: *UNFCCC Process: Paris Agreement - Status of Ratification*. https://unfccc.int/process#:a0659cbd-3b30-4c05-a4f9-268f16e5dd6b. Version: 2019

[2] BMU (Hrsg.): *Klimaschutz in Zahlen: Klimaschutzziele Deutschland und EU*. https://www.bmu.de/fileadmin/Daten_BMU/Download_PDF/Klimaschutz/klimaschutz_in_zahlen_klimaziele_bf.pdf

[3] BMWi (Hrsg.): *Energiekonzept für eine umweltschonende, zuverlässige und bezahlbare Energieversorgung*

[4] BMU (Hrsg.): *Klimaschutzplan 2050: Klimaschutzpolitische Grundsätze und Ziele der Bundesregierung*. https://www.bmu.de/fileadmin/Daten_BMU/Download_PDF/Klimaschutz/klimaschutzplan_2050_bf.pdf

[5] BMUB (Hrsg.): *Aktionsprogramm Klimaschutz 2020: Kabinettsbeschluss von 3. Dezember 2014*. https://www.bmu.de/fileadmin/Daten_BMU/Download_PDF/Aktionsprogramm_Klimaschutz/aktionsprogramm_klimaschutz_2020_broschuere_bf.pdf

[6] BMWi (Hrsg.): *Mehr aus Energie machen: Nationaler Aktionsplan Energieeffizienz*. https://www.bmwi.de/Redaktion/DE/Publikationen/Energie/nationaler-aktionsplan-energieeffizienz-nape.pdf?__blob=publicationFile&v=6

[7] Helgenberger, Sebastian: Klimaschutzgesetz: Klare Ansage für die Wirtschaft. In: *DIE ZEIT* (2019). https://www.zeit.de/wirtschaft/2019-02/klimaschutzgesetz-svenja-schulze-kritik-klimaziele-vorreiter

[8] Christian Reimer, Sören: Klimaschutzgesetz für 2019 geplant: Schulze will sozialverträglichen Kohleausstieg. In: *Das Parlament* (2019). https://www.das-parlament.de/2018/13_14/wirtschaft_und_finanzen/548756-548756

[9] BMU (Hrsg.): *Referentenentwurf des Bundesministerium für Umwelt, Naturschutz und nukleare Sicherheit Artikel 1: Bundest-Klimaschutzgesetzt (KSG)*. https://www.klimareporter.de/images/dokumente/2019/02/ksg.pdf. Version: 2019

[10] BMWi (Hrsg.): *Klimaschutzbericht 2018: zum AKtionsprogramm Klimaschutz 2020 der Bundesregierung*. https://www.bmu.de/fileadmin/Daten_BMU/Download_PDF/Klimaschutz/klimaschutzbericht_2018_bf.pdf

[11] BMWi (Hrsg.): *Energieeffizienz in Zahlen 2018*. https://www.bmwi.de/Redaktion/DE/Publikationen/Energie/energieeffizienz-in-zahlen-2018.pdf?__blob=publicationFile&v=8

[12] BMWi (Hrsg.): *Gesamtausgabe der Energiedaten - Datensammlung des BMWi.* https://www.bmwi.de/Redaktion/DE/Binaer/Energiedaten/energiedaten-gesamt-xls.html. Version: 2019

[13] Umweltbundesamt (Hrsg.): *Nationale Trendtabellen für die deutsche Berichterstattung atmosphärischer Emissionen 1990 - 2017.* 2018

[14] BAFA (Hrsg.): *Merkblatt zu den CO2-Faktoren: Energieeffizienz in der Wirtschaft – Zuschuss und Kredit.* https://www.bafa.de/SharedDocs/Downloads/DE/Energie/eew_merkblatt_co2.pdf?__blob=publicationFile&v=2

[15] Henning, H.-M. ; Palzer, Andreas ; Fraunhofer ISE (Hrsg.): *What will the energy transformation cost? Pathways for transforming the German energy system by 2050.* https://www.ise.fraunhofer.de/content/dam/ise/en/documents/publications/studies/What-will-the-energy-transformation-cost.pdf

[16] Gerhardt, Norman: *INTERAKTION EE-STROM, WÄRME UND VERKEHR: Analyse der Interaktion zwischen den Sektoren Strom, Wärme/Kälte und Verkehr in Deutschland in Hinblick auf steigende Anteile fluktuierender Erneuerbarer Energien im Strombereich unter Berücksichtigung der europäischen Entwicklung Ableitung von optimalen strukturellen Entwicklungspfaden für den Verkehrs- und Wärmesektor.* https://www.iee.fraunhofer.de/content/dam/iwes-neu/energiesystemtechnik/de/Dokumente/Veroeffentlichungen/2015/Interaktion_EEStrom_Waerme_Verkehr_Endbericht.pdf. Version: 2015

[17] Öko-Institut ; Fraunhofer ISI: *Klimaschutzszenario 2050 – 2. Endbericht: Studie im Auftrag des Bundesministeriums für Umwelt, Naturschutz, Bau und Reaktorsicherheit.* https://www.oeko.de/oekodoc/2451/2015-608-de.pdf

[18] Lechtenböhmer, Stefan ; Palzer, Andreas ; Pregger, Thomas ; Gils, Hans C. ; Sterchele, Philip ; Kost, Christoph ; Brucker, Lucas ; Tomke, Jansen ; Krüger, Christine ; Luhmann, Dietmar ; Mathis, Buddeke: *RegMex - Modellexperimente und -vergleiche zur Simulation von Wegen zu einer vollständig regenerativen Energieversorgung : Schlussbericht.* https://epub.wupperinst.org/frontdoor/index/index/docId/7096

[19] UBA (Hrsg.): *Treibhausgasneutrales Deutschland im Jahr 2050.* https://www.umweltbundesamt.de/sites/default/files/medien/378/publikationen/climate-change_07_2014_treibhausgasneutrales_deutschland_2050_0.pdf

[20] Schlesinger, Michael ; Lindenberger, Dietmar ; Lutz, Christian ; Hofer, Peter ; Kemmler, Andreas ; Kirchner, Almut ; Koziel, Sylvie ; Ley, Andrea ; Piégsa, Alexander ; Seefeldt, Friedrich ; Strassburg, Samuel ; Weinert, Karsten ; Knaut, Andreas ; Malischek, Raimund ; Nick, Sebastian ; Panke, Timo ; Paulus, Simon ; Tode, Christian ; Wagner, Johannes ; Lehr, Ulrike ; Ulrich, Philip ; Bundesministerium für Wirtschaft und Energie (Hrsg.): *Entwicklung der Energiemärkte - Energiereferenzprognose: Projekt Nr. 57/12 des Bundesministeriums für Wirtschaft und Technologie, Berlin.* http://www.bmwi.de/BMWi/Redaktion/PDF/Publikationen/entwicklung-der-energiemaerkte-energiereferenzprognose-endbericht,property%3Dpdf,bereich%3Dbmwi2012,sprache%3Dde,rwb%3Dtrue.pdf

[21] UBA (Hrsg.): *Erneuerbare Energien in Zahlen*. https://www.umweltbundesamt.de/themen/klima-energie/erneuerbare-energien/erneuerbare-energien-in-zahlen#textpart-1. Version: 2019

[22] Fraunhofer ISE (Hrsg.): *Energy Charts*. https://www.energy-charts.de/power_inst_de.htm

[23] Kohlekommission: *Kommission „Wachstum, Strukturwandel und Beschäftigung“: Beschluss vom 26.01.2019*. http://docs.dpaq.de/14440-190126_abschlussbericht_kommission_wachstum_strukturwandel_und_besch_ftigung_beschluss.pdf

[24] IRENA (Hrsg.): *Renewable Power Generation Costs in 2017*. https://www.irena.org/-/media/Files/IRENA/Agency/Publication/2018/Jan/IRENA_2017_Power_Costs_2018.pdf

[25] BMWi (Hrsg.): *Marktanalyse Photovoltaik-Dachanlagen*. https://www.bmwi.de/Redaktion/DE/Downloads/M-O/marktanalyse-photovoltaik-dachanlagen.pdf?__blob=publicationFile&v=1

[26] IRENA (Hrsg.): *THE POWER TO CHANGE: SOLAR AND WIND COST REDUCTION POTENTIAL*. https://www.irena.org/-/media/Files/IRENA/Agency/Publication/2016/IRENA_Power_to_Change_2016.pdf

[27] Williams, Eric ; Hittinger, Eric ; Carvalho, Rexon ; Williams, Ryan: Wind power costs expected to decrease due to technological progress. In: *Energy Policy* 106 (2017), S. 427–435. http://dx.doi.org/10.1016/j.enpol.2017.03.032. – DOI 10.1016/j.enpol.2017.03.032. – ISSN 03014215

[28] Fraunhofer IWES, Fraunhofer I.: *Interaktion EE-Strom, Wärme und Verkehr: Analyse der Interaktion zwischen den Sektoren Strom, Wärme/Kälte und Verkehr in Deutschland in Hinblick auf steigende Anteile fluktuierender Erneuerbarer Energien im Strombereich unter Berücksichtigung der europäischen Entwicklung: Endbericht*. https://www.energiesystemtechnik.iwes.fraunhofer.de/content/dam/iwes-neu/energiesystemtechnik/de/Dokumente/Veroeffentlichungen/2015/Interaktion_EEStrom_Waerme_Verkehr_Endbericht.pdf

[29] Ausfelder, Florian ; Fischedick, Manfred ; Münch, Wolfram ; Sauer, Jörg ; Themann, Michael ; Wagner, Hermann-Josef ; Deutsche Akademie der Technikwissenschaften e. V., Deutsche Akademie der Naturforscher Leopoldina e. V., Union der deutschen Akademien der Wissenschaften e. V. (Hrsg.): *»Sektorkopplung« – Untersuchungen und Überlegungen zur Entwicklung eines integrierten Energiesystems* (Schriftenreihe Energiesysteme der Zukunft)

[30] Elsland, Rainer ; Pfluger, Benjamin ; Tersteegen, Bernd ; Franke, Bernd ; Bossmann, Tobias ; Fleiter, Tobias ; Ragwitz, Mario ; Sensfuss, Frank ; Steinbach, Jan ; Maurer, Christoph ; Pehnt, Martin ; Rettenmaier, Nils ; Hartner, Michael ; Kranzl, Lukas ; Schade, Wolfgang ; Catenazzi, Giacomo ; Jakob, Martin ; Reiter, Ulrich: *Langfristszenarien für die Transformation des Energiesystems in Deutschland*. 2017

[31] Sijm, Jos ; Gockel, Pieter ; Van der Welle, Adrian ; Van Westering, Werner: *Demand and supply of flexibility in the power system of the Netherlands, 2015-2050: Summary report of the FLEXNET project*

[32] Dr. Rüdiger Paschotta: *RP-Energie-Lexikon: fachlich fundiert, unabhängig von Lobby-Interessen: Residuallast.* https://www.energie-lexikon.info/residuallast.html

[33] Agora Energiewende: *Glossar.* https://www.agora-energiewende.de/service/glossar/?tx_dpnglossary_glossarylist%5B%40widget_0%5D%5Bcharacter%5D=R&cHash=f5016027728dd1e3aefc4e74456c564f. Version: 2018

[34] Papaefthymiou, G. ; Dragoon, Ken: Towards 100% renewable energy systems: Uncapping power system flexibility. In: *Energy Policy* 92 (2016), S. 69–82. http://dx.doi.org/10.1016/j.enpol.2016.01.025. – DOI 10.1016/j.enpol.2016.01.025. – ISSN 03014215

[35] Wissenschaftliche Dienste Deutscher Bundestag (Hrsg.): *Entwicklung der Stromspeicherkapazitäten in Deutschland von 2010 bis 2016.* https://www.bundestag.de/resource/blob/496062/759f6162c9fb845aa0ba7d51ce1264f1/wd-8-083-16-pdf-data.pdf

[36] Die Bundesregierung: *Strom speichern.* https://www.bundesregierung.de/breg-de/themen/energiewende/fragen-und-antworten/netzausbau-und-stromspeicher/strom-speichern-455734. Version: 2019

[37] Jansen, Malte ; Richts, Christoph ; Gerhardt, Norman ; Lenck, Thorsten ; Heddrich ; Marie-Louise: *Strommarkt-Flexibilisierung: Hemmnisse und Lösungskonzepte ; eine Studie im Auftrag des BEE e.V.* Bochum : Ponte Press, 2015. – ISBN 978–3–920328–72–0

[38] BMWi: *Erneuerbare-Energien-Gesetz - EEG 2000: EEG 2014.* http://bundesrecht.juris.de/bundesrecht/eeg_2014/gesamt.pdf. Version: 22.7.2014

[39] Cochran, Jaquelin ; et al.: *Flexibility in 21st Century Power Systems.* https://www.nrel.gov/docs/fy14osti/61721.pdf. Version: 2014

[40] Kondziella, Hendrik ; Bruckner, Thomas: Flexibility requirements of renewable energy based electricity systems – a review of research results and methodologies. In: *Renewable and Sustainable Energy Reviews* 53 (2016), S. 10–22. http://dx.doi.org/10.1016/j.rser.2015.07.199. – DOI 10.1016/j.rser.2015.07.199. – ISSN 13640321

[41] Alizadeh, M. I. ; Parsa Moghaddam, M. ; Amjady, N. ; Siano, P. ; Sheikh-El-Eslami, M. K.: Flexibility in future power systems with high renewable penetration: A review. In: *Renewable and Sustainable Energy Reviews* 57 (2016), S. 1186–1193. http://dx.doi.org/10.1016/j.rser.2015.12.200. – DOI 10.1016/j.rser.2015.12.200. – ISSN 13640321

[42] Agentur für Erneuerbare Energien (Hrsg.): *METAANALYSE - Flexibilität durch Kopplung von Strom, Wärme & Verkehr.* http://www.forschungsradar.de/fileadmin/content/bilder/Vergleichsgrafiken/meta_sektorkopplung_

042016/AEE_Metaanalyse_Flexibilitaet_Sektorkopplung_apr16_fixed.pdf. Version: 2016

[43] Yasuda, Yoh ; Rygg, Atle ; Huertas, Daniel ; Carlini, Enrico ; Estanqueiro, Ana ; Flynn, Damian ; Gomez-Lazaro, Emilio ; Holttinen, Hannele ; Kiviluoma, Juha ; Hulle, Frans ; Kondoh, Junji ; Lange, Bernhard ; Menemenlis, Nickie ; Milligan, Michael ; Orths, Antje ; Smith, Charles ; Soder, Lennart: Flexibility Chart – Evaluation on diversity of flexibility in various areas, 2013

[44] Ma, Juan ; Silva, Vera ; Belhomme, Régine ; Kirschen, Daniel S. ; Ochoa, Luis F.: Evaluating and Planning Flexibility in Sustainable Power Systems. In: *IEEE Transactions on Sustainable Energy* 4 (2013), Nr. 1, S. 200–209. http://dx.doi.org/10.1109/TSTE.2012.2212471. – DOI 10.1109/TSTE.2012.2212471. – ISSN 1949–3029

[45] Ulbig, Andreas ; Göran, Andersson: *Analyzing Operational Flexibility of Power Systems*. https://arxiv.org/abs/1312.7618

[46] Schill, Wolf-Peter ; Pahle, Michael ; Gambardella, Christian: Start-up costs of thermal power plants in markets with increasing shares of variable renewable generation. In: *Nature Energy* 2 (2017), Nr. 6, S. 17050. http://dx.doi.org/10.1038/nenergy.2017.50. – DOI 10.1038/nenergy.2017.50. – ISSN 2058–7546

[47] Weidlich, Anke ; Künzel, Thomas ; Klumpp, Florian: Bidding Strategies for Flexible and Inflexible Generation in a Power Market Simulation Model: Model Description and Findings, 2018, S. 532–537

[48] Künzel, Thomas ; Klumpp, Florian ; Weidlich, Anke: Methodische Quantifizierung der Bereitstellungskosten flexibler Systemkomponenten im deutschen Stromsystem. In: *Zeitschrift für Energiewirtschaft* 41 (2017), Nr. 1, S. 33–55. http://dx.doi.org/10.1007/s12398-016-0192-5. – DOI 10.1007/s12398–016–0192–5. – ISSN 0343–5377

[49] Agentur für Erneuerbare Energien (Hrsg.): *Studienvergleich: Bedarf an steuerbaren Kapazitäten im Stromsystem*. http://www.forschungsradar.de/fileadmin/content/news_import/AEE_Dossier_Studienvergleich_Versorgungssicherheit_dez13.pdf

[50] Klaus, Thomas ; Vollmer, Carla ; Werner, Kathrin ; Lehmann, Harry ; Müschen, Klaus: *Energieziel 2050: 100% Strom aus erneuerbaren Quellen*. http://www.umweltbundesamt.de/sites/default/files/medien/378/publikationen/energieziel_2050.pdf

[51] Schlesinger, Lindenberger, Lutz: *Energieszenarien für eine Energiekonzept der Bundesregierung: Projekt Nr. 12/10 des Bundesministeriums für Wirtschaft und Technologie*. Berlin, 2010

[52] DENA (Hrsg.): *Roadmap Demand Side Management. Industrielles Lastmanagement für ein zukunftsfähiges Energiesystem. Schlussfolgerungen aus dem Pilotprojekt DSM Bayern*. https://www.dena.de/themen-projekte/energiesysteme/flexibilitaet-und-speicher/demand-side-management/

[53] Universität Stuttgart (Hrsg.): *ENERGIEFLEXIBILITÄT IN DER INDUSTRIE*. https://www.eep.uni-stuttgart.de/dokumente/20180502_Metastudie_Energieflexibilitaet-in-der-Industrie.pdf

[54] Klobasa, Marian: *Dynamische Simulation eines Lastmanagements und Integration von Windenergie in ein Elektrizitätsnetz*. Stuttgart : Fraunhofer-IRB-Verl., 2009 (ISI-Schriftenreihe Innovationspotenziale). – ISBN 978–3–8167–7991–9

[55] Gils, Hans C.: *Balancing of Intermittent Renewable Power Generation by Demand Response and Thermal Energy Storage*. https://elib.uni-stuttgart.de/handle/11682/6905

[56] Lund, Peter D. ; Lindgren, Juuso ; Mikkola, Jani ; Salpakari, Jyri: Review of energy system flexibility measures to enable high levels of variable renewable electricity. In: *Renewable and Sustainable Energy Reviews* 45 (2015), S. 785–807. http://dx.doi.org/10.1016/j.rser.2015.01.057. – DOI 10.1016/j.rser.2015.01.057. – ISSN 13640321

[57] Dufter, Christa ; et al.: *Lastflexibilisierung in der Industrie – Metastudienanalyse zur Identifikation relevanter Aspekte bei der Potenzialermittlung*. https://www.ffegmbh.de/attachments/article/673/Kurzfassung%20Tagungsbeitrag.pdf. Version: 2017

[58] Eisenhauer, S. ; Zimmermann, F. ; Reichart, M. ; Accordi, P. ; Sauer, A.: *Metastudie industrieller Energieflexibilität*: Ein Ansatz zur optimierten Identifikation energetischer Flexibilitätspotenziale*

[59] Elsner, Peter (Hrsg.) ; Fischedick, Manfred (Hrsg.) ; Sauer, Marc U. (Hrsg.): *Flexibilitätskonzepte für die Stromversorgung 2050: Technologien - Szenarien - Systemzusammenhänge*. München : Deutsche Akademie der Technikwissenschaften, 2015 (Energiesysteme der Zukunft). – ISBN 978–3–9817048–5–3

[60] Agora Energiewende: *Flexibility in thermal power plants: With a focus on existing coal-fired power plants*. https://www.agora-energiewende.de/fileadmin/Projekte/2017/Flexibility_in_thermal_plants/115_flexibility-report-WEB.pdf

[61] Klein, Konstantin ; Kalz, Doreen ; Herkel, Sebastian: Netzdienlicher Betrieb von Gebäuden: Analyse und Vergleich netzbasierter Referenzgrößen und Definition einer Bewertungskennzahl. In: *Bauphysik* 36 (2014), Nr. 2, S. 49–58. http://dx.doi.org/10.1002/bapi.201410019. – DOI 10.1002/bapi.201410019

[62] Ellerbrok, Charlotte: Potentials of Demand Side Management Using Heat Pumps with Building Mass as a Thermal Storage. In: *Energy Procedia* 46 (2014), S. 214–219. http://dx.doi.org/10.1016/j.egypro.2014.01.175. – DOI 10.1016/j.egypro.2014.01.175. – ISSN 18766102

[63] Zhang, Yang ; Campana, Pietro E. ; Yang, Ying ; Lundblad, Anders ; Yan, Jinyue: Energy Flexibility through the Integrated Energy Supply System in Buildings: A Case Study in Sweden. In: *Energy Procedia* 145 (2018), S. 564–569. http://dx.doi.org/10.1016/j.egypro.2018.04.082. – DOI 10.1016/j.egypro.2018.04.082. – ISSN 18766102

[64] Yilmaz, Murat ; Krein, Philip T.: Review of the Impact of Vehicle-to-Grid Technologies on Distribution Systems and Utility Interfaces. In: *IEEE Transactions on Power Electronics* 28 (2013), Nr. 12, S. 5673–5689. http://dx.doi.org/10.1109/TPEL.2012.2227500. – DOI 10.1109/TPEL.2012.2227500. – ISSN 0885–8993

[65] Mesarić, Petra ; Krajcar, Slavko: Home demand side management integrated with electric vehicles and renewable energy sources. In: *Energy and Buildings* 108 (2015), S. 1–9. http://dx.doi.org/10.1016/j.enbuild.2015.09.001. – DOI 10.1016/j.enbuild.2015.09.001. – ISSN 03787788

[66] López, M. A. ; La Torre, S. de ; Martín, S. ; Aguado, J. A.: Demand-side management in smart grid operation considering electric vehicles load shifting and vehicle-to-grid support. In: *International Journal of Electrical Power & Energy Systems* 64 (2015), S. 689–698. http://dx.doi.org/10.1016/j.ijepes.2014.07.065. – DOI 10.1016/j.ijepes.2014.07.065. – ISSN 01420615

[67] Finn, P. ; Fitzpatrick, C. ; Connolly, D.: Demand side management of electric car charging: Benefits for consumer and grid. In: *Energy* 42 (2012), Nr. 1, S. 358–363. http://dx.doi.org/10.1016/j.energy.2012.03.042. – DOI 10.1016/j.energy.2012.03.042. – ISSN 03605442

[68] Gils, Hans C.: *Balancing of intermittent renewable power generation by demand response and thermal energy storage*

[69] Scholz, Yvonne: *Renewable energy based electricity supply at low costs: Development of the REMix model and application for Europe*

[70] Luca de Tena, Diego: *Large scale renewable power integration with electric vehicles: Long term analysis for Germany with a renewable based power supply*

[71] Stetter, Daniel: *Enhancement of the REMix energy system model: Global renewable energy potentials, optimized power plant siting and scenario validation*

[72] Tomaschek, Jan: *Long-term optimization of the transport sector to address greenhouse gas reduction targets under rapid growth: Application of an energy system model for Gauteng province, South Africa*

[73] Bruchof, David: *Energiewirtschaftliche Verkehrsstrategie - Möglichkeiten und Grenzen alternativer Kraftstoffe und Antriebe in Deutschland und der EU-27*

[74] Özdemir, Enver D.: *The future role of alternative powertrains and fuels in the German transport sector: A model based scenario analysis with respect to technical, economic and environmental aspects with a focus on road transport*

[75] Trost, Tobias: *Erneuerbare Mobilität im motorisierten Individualverkehr: Modellgestützte Szenarioanalyse der Marktdiffusion alternativer Fahrzeugantriebe und deren Auswirkungen auf das Energieversorgungssystem.* Stuttgart : Fraunhofer Verlag, 2017. – ISBN 978–3–8396–1129–6

[76] Härtel, Philipp ; Korpås, Magnus: Aggregation Methods for Modelling Hydropower and Its Implications for a Highly Decarbonised Energy System in Europe. In: *Energies* 10 (2017), Nr. 11, S. 1841. http://dx.doi.org/10.3390/en10111841. – DOI 10.3390/en10111841. – ISSN 1996–1073

[77] Scholz, Angela ; Sandau, Fabian ; Pape, Carsten: A European Investment and Dispatch Model for Determining Cost Minimal Power Systems with High Shares of Renewable Energy. Version: 2016. http://dx.doi.org/10.1007/978-3-319-28697-6{_}72. In: Lübbecke, Marco (Hrsg.) ; Koster, Arie (Hrsg.) ; Letmathe, Peter (Hrsg.) ; Madlener, Reinhard (Hrsg.) ; Peis, Britta (Hrsg.) ; Walther, Grit (Hrsg.): *Operations Research Proceedings 2014*. Cham : Springer International Publishing, 2016 (Operations Research Proceedings). – DOI 10.1007/978–3–319–28697–6_72. – ISBN 978–3–319–28695–2, S. 515–521

[78] Jentsch, Mareike: *Potenziale von Power-to-Gas Energiespeichern: Modellbasierte Analyse des markt- und netzseitigen Einsatzes im zukünftigen Stromversorgungssystem*. Stuttgart : Fraunhofer-Verl., 2015. – ISBN 3–8396–0865–1

[79] Gül, Timur: *An energy-economic scenario analysis of alternative fuels for transport*

[80] Bolívar Jaramillo, Lucas ; Weidlich, Anke: Optimal microgrid scheduling with peak load reduction involving an electrolyzer and flexible loads. In: *Applied Energy* 169 (2016), S. 857–865. http://dx.doi.org/10.1016/j.apenergy.2016.02.096. – DOI 10.1016/j.apenergy.2016.02.096. – ISSN 0306–2619

[81] CEDEC, Eurogas, GEODE (Hrsg.): *Flexibilität in der Energiewende: Werkzeugkasten für Gas-VNB*. https://www.vku.de/fileadmin/user_upload/Verbandsseite/Sparten/Energiewirtschaft/Gasthemen/Deutsch-gas_DSOs_2018-converted.pdf

[82] Agora (Hrsg.): *The Future Cost of Electricity-Based Synthetic Fuels*. https://www.agora-energiewende.de/fileadmin2/Projekte/2017/SynKost_2050/Agora_SynKost_Study_EN_WEB.pdf

[83] Julia Welsch, Ulrich Fahl, Markus Blesl, Kai Hufendiek: *Modellierung von Energiespeichern und Power-to-X-Technologien mit dem europäischen Energiesystemmodell TIMES PanEU*. 10.-12.02.2016

[84] Welsch, Julia: *Modellierung von Energiespeichern und Power-to-X im europäischen Energiesystem*. http://www.strise.de/fileadmin/user_upload/Aktuelles/2017_Stgt_Dialog/09_Poster_Welsch_TIMES_PanEU.pdf. Version: 2018

[85] Blesl, Markus ; Kober, Tom ; Bruchof, David ; Kuder, Ralf: Effects of climate and energy policy related measures and targets on the future structure of the European energy system in 2020 and beyond. In: *Energy Policy* 38 (2010), Nr. 10, S. 6278–6292. http://dx.doi.org/10.1016/j.enpol.2010.06.018. – DOI 10.1016/j.enpol.2010.06.018. – ISSN 03014215

[86] IEA: *etsap*. https://iea-etsap.org/. Version: 2019

[87] Loulou, Richard ; Remme, Uwe ; Kanudia, Amit ; Lehtila, Antti ; Goldstein, Gary: *Documentation for the TIMES Model: PART I*. http://www.etsap.org/tools.htm

[88] BMWi (Hrsg.): *Langfrist- und Klimaszenarien*. https://www.bmwi.de/Redaktion/DE/Artikel/Energie/langfrist-und-klimaszenarien.html. Version: 2019

[89] Dr. Dierk Bauknecht et. al: *Systematischer Vergleich von Flexibilitäts- und Speicheroptionen im deutschen Stromsystem zur Integration von erneuerbaren Energien und Analyse entsprechender Rahmenbedingungen*

[90] Bauknecht, Dierk ; Heinemann, Christoph ; Koch, Matthias ; Ritter, David ; Ralph, Harthan ; Tröster, Eckehard ; Langanke, Stefan: Entwicklung des Flexibilitätsbedarfs im Stromsystem und der Beitrag verschiedener Flexibilitätsoptionen. In: *Energiewirtschaftliche Tagesfragen* (2014), Nr. 11

[91] Babrowski, Sonja: *Bedarf und Verteilung elektrischer Tagesspeicher im zukünftigen deutschen Energiesystem*

[92] Heinrichs, Heidi U.: *Produktion und Energie / Karlsruher Institut für Technologie, Institut für Industriebetriebslehre und industrielle Produktion u. Deutsch-Französisches Institut für Umweltforschung*. Bd. 5: *Analyse der langfristigen Auswirkungen von Elektromobilität auf das deutsche Energiesystem im europäischen Energieverbund*. Print on demand. Karlsruhe : KIT Scientific Publishing, 2013. – ISBN 978–3–7315–0131–2

[93] Koch, Matthias ; Flachsbarth, Franziska ; Bauknecht, Dierk ; Heinemann, Christoph ; Ritter, David ; Winger, Christian ; Timpe, Christof ; Gandor, Malin ; Klingenberg, Thole ; Tröschel, Martin: Dispatch of Flexibility Options, Grid Infrastructure and Integration of Renewable Energies Within a Decentralized Electricity System. Version: 2017. http://dx.doi.org/10.1007/978-3-319-51795-7{_}5. 2017. – DOI 10.1007/978–3–319–51795–7_5. – ISBN 978–3–319–51794–0, S. 67–86

[94] Steurer, Martin: *Analyse von Demand Side Integration im Hinblick auf eine effiziente und umweltfreundliche Energieversorgung*. https://elib.uni-stuttgart.de/bitstream/11682/9198/3/Dissertation_Martin_Steurer.pdf

[95] Zimmer, Wiebke ; et al.: *ENDBERICHT RENEWBILITY III: OPTIONEN EINER DEKARBONISIERUNG DES VERKEHRSSEKTORS*. http://www.renewbility.de/wp-content/uploads/Renewbility_III_Endbericht.pdf

[96] Breyer, Christian ; Müller, Berit: *VERGLEICH UND OPTIMIERUNG VON ZENTRAL UND DEZENTRAL ORIENTIERTEN AUSBAUPFADEN ZU EINER STROMVERSORGUNG AUS ERNEUERBAREN ENERGIEN IN DEUTSCHLAND*. https://reiner-lemoine-institut.de/wp-content/publications/0_Vergleich_und_Optimierung_zentral_und_dezentral_071_100EE/Breyer2013.pdf

[97] Müller, Berit ; Möller, Caroline ; Gaudchau, Elisa: Ausbaupfade der Energiewende – Stromversorgung aus Erneuerbaren Energien. In: *uwf UmweltWirtschaftsForum* 22 (2014), Nr. 1, 29–35. http://dx.doi.org/10.1007/s00550-014-0306-7. – DOI 10.1007/s00550–014–0306–7. – ISSN 1432–2293

[98] Haasz, Thomas: *Entwicklung von Methoden zur Abbildung von Demand Side Management in einem optimierenden Energiesystemmodell: Fallbeispiele für Deutschland in den Sektoren Industrie, Gewerbe, Handel, Dienstleistungen und Haushalte*

[99] Pina, André ; Silva, Carlos ; Ferrão, Paulo: The impact of demand side management strategies in the penetration of renewable electricity. In: *Energy* 41 (2012), Nr. 1, S. 128–137. http://dx.doi.org/10.1016/j.energy.2011.06.013. – DOI 10.1016/j.energy.2011.06.013. – ISSN 03605442

[100] Fehrenbach, Daniel ; Merkel, Erik ; McKenna, Russell ; Karl, Ute ; Fichtner, Wolf: On the economic potential for electric load management in the German residential heating sector – An optimising energy system model approach. In: *Energy* 71 (2014), S. 263–276. http://dx.doi.org/10.1016/j.energy.2014.04.061. – DOI 10.1016/j.energy.2014.04.061. – ISSN 03605442

[101] Palzer, Andreas ; Henning, H.-M.: A future German energy system with a dominating contribution from renewable energies: A holistic model based on hourly simulation. In: *Energy Technology* 2 (2014), S. 13–28

[102] Henning, Hans-Martin ; Palzer, Andreas: *ENERGIESYSTEM DEUTSCHLAND 2050: Sektor- und Energieträgerübergreifende, modellbasierte, ganzheitliche Untersuchung zur langfristigen Reduktion energiebedingter CO2-Emissionen durch Energieeffizienz und den Einsatz Erneuerbarer Energien*. Freiburg,

[103] Palzer, Andreas: *Sektorübergreifende Modellierung und Optimierung eines zukünftigen deutschen Energiesystems unter Berücksichtigung von Energieeffizienzmaßnahmen im Gebäudesektor*. Karlsruhe, Karlsruher Institut für Technologie, (genehmigte) Dissertation, 28.04.2016. http://publica.fraunhofer.de/documents/N-408742.html

[104] Sterchele, Philip ; Kalz, Doreen ; Palzer, Andreas: Technisch-ökonomische Analyse von energetischen Sanierungsmaßnahmen und –potenzialen im Wohngebäudesektor heute und für das Jahr 2050. In: *Bauphysik* 38 (2016), Nr. 4, S. 192–211. http://dx.doi.org/10.1002/bapi.201610022. – DOI 10.1002/bapi.201610022

[105] Sterchele, Philip ; Kersten, Konstantin ; Palzer, Andreas ; Hentschel, Jan ; Henning, Hans-Martin: Assessment of flexible electric vehicle charging in a sector coupling energy system model: Modelling approach and Case study. In: *Submitted to Applied Energy. Not yet published* (2019)

[106] Sterchele, Philip ; Palzer, Andreas ; Henning, Hans-Martin: The role of heat pumps in the transformation of national energy systems - Example Germany. In: *IEA Heat Pump Conference* (2017). https://hpc2017.org/wp-content/uploads/2017/05/P0.01-The-role-of-heat-pumps-in-the-transformation-of-national-energy\-systems-Example-Germany.pdf

[107] Sterchele, Philip ; Palzer, Andreas ; Henning, Hans-Martin: Electrify Everything? Exploring the Role of the Electric Sector in a Nearly CO2 Neutral National Energy System. In: *IEEE Power and Energy Magazine* 16 (2018), Nr. 4, S. 24–33. http://dx.doi.org/10.1109/MPE.2018.2824100. – DOI 10.1109/MPE.2018.2824100. – ISSN 1540–7977

[108] Energieinstitut Vorarlberg (Hrsg.): *Economicum: Alles Strom!? Hocheffiziente Gebäude und PV im Energiesystem der Zukunft*. https://www.energieinstitut.at/pdfviewer/economicum_themenband-6/

[109] Kost, Christoph ; Palzer, Andreas ; Sterchele, Philip ; Stephanos, Cyril ; Hartmann, Niklas ; Henning, Hans-Martin: Coal phase out, energy efficiency, and electricity imports: Key elements to realize the energy transformation. In: *Applied Physics Reviews* 6 (2019), Nr. 1, S. 011308. http://dx.doi.org/10.1063/1.5055269. – DOI 10.1063/1.5055269

[110] Brandes, Julian ; Palzer, Andreas ; Sterchele, Philip ; Roscher, Björn ; Henning, Hans-Martin: *Analyzing the transformation of the German energy system by 2050 with restricted potential of renewable energies. 7th Eur. Conf. Ren. Energy Sys. 10-10 June 2019, Madrid, Spain.* 2019

[111] Bundesministerium für Bildung und Forschung (Hrsg.): *Systemintegration: Kopernikus-Projekt ENavi.* https://www.kopernikus-projekte.de/projekte/systemintegration. Version: 2019

[112] Smolinka, Tom ; Wiebe, Nikolai ; Palzer, Andreas ; Sterchele, Philip ; Lehner, Franz ; Jansen, Malte ; Kiemel, Steffen ; Miehe, Robert ; Wahren, Sylvia ; Bundesministerium für Verkehr und digitale Infrastruktur (Hrsg.): *Studie IndWEDe: Industrialisierung der Wasserelektrolyse in Deutschland: Chancen und Herausforderungen für nachhaltigen Wasserstoff für Verkehr, Strom und Wärme.* Berlin,

[113] BBH ; LBST, Fraunhofer I. ; IKEM: *Integriertes Energiekonzept 2050: Strom Wärme Verkehr Industrie (geplante Veröffentlichung Q2 2019)*

[114] Brucker, Lucas: *Analyse von Energiewandlungstechnologien im Industriessektor und deren Einbindung im zukünftigen Energiesystem*, Master thesis, 2017

[115] Al-Dabbas, Khaled: *Analysis of GHG emissions reduction from road transport: a case study of the German passenger vehicles*, Master thesis, 2018. http://www.diva-portal.org/smash/record.jsf?pid=diva2%3A1238567&dswid=-2853

[116] Möllers, Reinhild: *Analyse von Energiewandlungstechnologien im Wärmesektor und deren systematische Einbindung im zukünftigen deutschen Energiesystem*, Master thesis, 2018

[117] Brandes, Julian: *Analyse der Transformation des deutschen Energiesystems bis zum Jahr 2050 unter der Annahme eingeschränkter Potenziale regenerativer Stromerzeuger*, Master thesis, 2018

[118] Heilig, Judith: *Einfluss von Wetterdaten auf die Simulation nationaler Energiesysteme*, Master thesis, 2018

[119] Henning, Hans-Martin ; Palzer, Andreas: *100 % ERNEUERBARE ENERGIEN FÜR STROM UND WÄRME IN DEUTSCHLAND.* Freiburg,

[120] Henning, Hans-Martin ; Palzer, Andreas: A comprehensive model for the German electricity and heat sector in a future energy system with a dominant contribution from renewable energy technologies—Part I: Methodology. In: *Renewable and Sustainable Energy Reviews* 30 (2014), 1003–1018. http://dx.doi.org/10.1016/j.rser.2013.09.012. – DOI 10.1016/j.rser.2013.09.012. – ISSN 13640321

[121] Palzer, Andreas ; Henning, H.-M.: A future German energy system with a dominating contribution from renewable energies: a holistic model based on hourly simulation. In: *Energy Technology* 2 (2014), S. 13–28

[122] UBA (Hrsg.): *Motoranlagen und Blockheizkraftwerke*. https://www.umweltbundesamt.de/themen/wirtschaft-konsum/industriebranchen/feuerungsanlagen/motoranlagen-blockheizkraftwerke#textpart-2. Version: 2013

[123] BMWi: *Zahlen und Fakten Energiedaten: Nationale und Internationale Entwicklung*. https://www.bmwi.de/Redaktion/DE/Binaer/Energiedaten/energiedaten-gesamt-xls.xls?__blob=publicationFile&v=73. Version: 2018

[124] ifeu, DLR, ZSW: *Prozesswärme im Marktanreizprogramm*. https://www.ifeu.de/wp-content/uploads/Prozesswaerme-im-MAP.pdf

[125] Bastian Schmitt: *Integration thermischer Solaranlagen zur Bereitstellung von Prozesswärme in Industriebetrieben*

[126] Blesl, Markus ; Kessler, Alois: *Energieeffizienz in der Industrie*. Berlin : Springer Verlag, 2013. – ISBN 978–3–642–36513–3

[127] Bundesverband Kraft-Wärme-Kopplung e.V.: *Kraft-Wärme-Kopplung in der Industrie: effizient produzieren - nachhaltig wirtschaften*. https://www.bkwk.de/fileadmin/users/bkwk/industrie/Broschuere_KWK_in_der_Industrie.pdf

[128] Arpagaus, Cordin: *Review on High Temperature Heat Pumps: Market Overview and Research Status*. https://www.ntb.ch/fileadmin/NTB_Institute/IES/bilder/Projekte_TES/91__SCCER-EIP/2017-10-24_11-45Uhr_Review_on_High_Temperature_Heat_Pumps_Arpagaus.pdf. Version: 2017

[129] Wolf, Stefan and Lambauer, Jochen and Blesl, Markus and Fahl, Ulrich and Voss, Alfred: *Industrial heat pumps in Germany: Potentials, technological development and market barriers*. 2012

[130] IEA: *Application of Industrial Heat Pumps: IEA Industrial Energy-related Systems and Technologies Annex 13 IEA Heat Pump Programme Annex 35*. https://iea-industry.org/app/uploads/annex-xiii-part-a.pdf

[131] Verein der Kohleimporteure: *Jahresbericht 2018 Fakten und Trends 2017/18*. www.kohlenimporteure.de/publikationen/jahresbericht-2018.html?file=files/user_upload/jahresberichte/vdki_jahresbericht_2018.pdf

[132] Bäck, Eduard ; Schenk, Johannes ; Badr, Karim ; Sormann, Axel ; Plaul, Jan F.: Wasserstoff als Reduktionsmittel für die Eisen- und Rohstahlerzeugung – Ist-Situation, Potentiale und Herausforderungen. In: *BHM Berg- und Hüttenmännische Monatshefte* 160 (2015), Nr. 3, S. 96–102. http://dx.doi.org/10.1007/s00501-015-0346-5. – DOI 10.1007/s00501–015–0346–5. – ISSN 0005–8912

[133] Jakobs, Stephanus: *Wasserstoff in der Stahlindustrie: Erzeugungs- und Einsatzmöglichkeiten in der Zukunft*. 2016

[134] Bundesministerium für Justiz und Verbraucherschutz: *Verordnung über energiesparenden Wärmeschutz und energiesparende Anlagentechnik bei Gebäuden (Energieeinsparverordnung - EnEV): EnEV*. 2015

[135] Verein Deutscher Ingenieure e.V: *Wirtschaftlichkeit gebäudetechnischer Anlagen Grundlagen und Kostenberechnung*. Berlin, 2012

[136] tools.de finanz: *Inflationsraten in Deutschland*. https://www.finanz-tools.de/inflation/inflationsraten-deutschland. Version: 2018

[137] Yeniay, Özgür: PENALTY FUNCTION METHODS FOR CONSTRAINED OPTIMIZATION WITH GENETIC ALGORITHMS. In: *Mathematical and Computational Applications* (2005), Nr. 10

[138] Parsopoulos, Konstantinos E. ; Vrahatis, Michael N.: *Particle Swarm Optimization Method for Constrained Optimization Problems*. 2002

[139] Gils, Hans C. ; Scholz, Yvonne ; Pregger, Thomas ; Luca de Tena, Diego ; Heide, Dominik: Integrated modelling of variable renewable energy-based power supply in Europe. In: *Energy* 123 (2017), S. 173–188. http://dx.doi.org/10.1016/j.energy.2017.01.115. – DOI 10.1016/j.energy.2017.01.115. – ISSN 03605442

[140] Lübbecke, Marco (Hrsg.) ; Koster, Arie (Hrsg.) ; Letmathe, Peter (Hrsg.) ; Madlener, Reinhard (Hrsg.) ; Peis, Britta (Hrsg.) ; Walther, Grit (Hrsg.): *Operations Research Proceedings 2014*. Cham : Springer International Publishing, 2016 (Operations Research Proceedings). http://dx.doi.org/10.1007/978-3-319-28697-6. http://dx.doi.org/10.1007/978-3-319-28697-6. – ISBN 978–3–319–28695–2

[141] Babrowski, Sonja ; Heffels, Tobias ; Jochem, Patrick ; Fichtner, Wolf: Reducing computing time of energy system models by a myopic approach. In: *Energy Systems* 5 (2014), Nr. 1, 65–83. http://dx.doi.org/10.1007/s12667-013-0085-1. – DOI 10.1007/s12667–013–0085–1. – ISSN 1868–3967

[142] Fishbone, Leslie G. ; Abilock, Harold: MARKAL, a linear-programming model for energy systems analysis: Technical description of the BNL version. In: *Energy Research* 5 (1981), S. 353–375

[143] Noha Saad Hussein: *Effects of building refurbishment on a districts energy system: Optimization of the deployment and operation of heat, power and sector coupling technologies*, Albert-Ludwigs-Universität Freiburg, Diss., 2018

[144] Rothlauf, Franz: *Design of modern heuristics: Principles and application*. Berlin : Springer, 2011 (Natural computing series). – ISBN 978–3–540–72962–4

[145] Saber M. Elsayed, Ruhul A. Sarker and Efrén Mezura-Montes: *Particle Swarm Optimizer for Constrained Optimization*. 2013

[146] Konstantinos E. Parsopoulos and Michael N. Vrahatis: *Particle Swarm Optimization Method for Constrained Optimization Problems*. http://citeseerx.ist.psu.edu/viewdoc/similar?doi=10.1.1.18.7873&type=ab. Version: 2002

[147] Helwig, Sabine: *Particle Swarms for Constrained Optimization*. Erlangen, Universität Erlangen-Nuernberg, Dissertation, 2010

[148] Lozano, José A.: *Studies in fuzziness and soft computing*. Bd. 192: *Towards a new evolutionary computation: Advances in the estimation of distribution algorithms*. Berlin and New York : Springer, 2006. – ISBN 978–3–540–29006–3

[149] Kachitvichyanukul, Voratas: Comparison of Three Evolutionary Algorithms: GA, PSO, and DE. In: *Industrial Engineering and Management Systems* 11 (2012), Nr. 3, S. 215–223. http://dx.doi.org/10.7232/iems.2012.11.3.215. – DOI 10.7232/iems.2012.11.3.215. – ISSN 1598–7248

[150] Bussar, Christian ; Moos, Melchior ; Alvarez, Ricardo ; Wolf, Philipp ; Thien, Tjark ; Chen, Hengsi ; Cai, Zhuang ; Leuthold, Matthias ; Sauer, Dirk U. ; Moser, Albert: Optimal Allocation and Capacity of Energy Storage Systems in a Future European Power System with 100% Renewable Energy Generation. In: *Energy Procedia* 46 (2014), S. 40–47. http://dx.doi.org/10.1016/j.egypro.2014.01.156. – DOI 10.1016/j.egypro.2014.01.156. – ISSN 18766102

[151] Nikolaus Hansen: *The CMA Evolution Strategy: A Tutorial*. http://www.cmap.polytechnique.fr/~nikolaus.hansen/cmatutorial110628.pdf

[152] Volker Krey: *Vergleich kurz- und langfristig ausgerichteter Optimierungsansätze mit einem multi-regionalen Energiesystemmodell unter Berücksichtigung stochastischer*, Ruhr-Universität Bochum, Diss., 2006

[153] Dag Martinsen, Volker Krey, Peter Markewitz, Stefan Vögele: A Time Step Energy Process Model A Time Step Energy Process Model for Germany - Model Structure and Results. In: *Energy Studies Review* (2006), Nr. Vol. 14 No. I, pp. 35-57. file:///D:/Users/psterche/Downloads/480-Article%20Text-622-1-10-20140820.pdf

[154] Keppo, Ilkka ; Strubegger, Manfred: Short term decisions for long term problems – The effect of foresight on model based energy systems analysis. In: *Energy* 35 (2010), Nr. 5, S. 2033–2042. http://dx.doi.org/10.1016/j.energy.2010.01.019. – DOI 10.1016/j.energy.2010.01.019. – ISSN 03605442

[155] Sterner, Michael ; Stadler, Ingo: *Energiespeicher - Bedarf, Technologien, Integration*. Berlin : Springer Vieweg, 2014. – ISBN 978–3–642–37380–0

[156] Serafin von Roon, Matthias Huber: *Modeling Spot Market Pricing with the Residual Load*. https://www.ffe.de/download/wissen/297_Enerday/20100416_FfE_von_Roon-Huber_paper.pdf. Version: 2010

[157] Kreutz, S. ; Belitz, H.-J. ; Rehtanz, C.: The impact of Demand Side Management on the residual load. In: *2010 IEEE PES Innovative Smart Grid Technologies Conference Europe (ISGT Europe)*, IEEE, 2010. – ISBN 978–1–4244–8508–6, S. 1–5

[158] Plattform Erneuerbare Energien ; Plattform Erneuerbare Energien (Hrsg.): *Bericht der AG 3 Interaktion: an den Steuerungskreis der Plattform Erneuerbare Energien, die Bundeskanzlerin und die Ministerpräsidentinnen und Ministerpräsidenten der Länder*. https://www.bmwi.de/Redaktion/DE/

Downloads/A/abschlussbericht-ag-3-plattform-erneuerbare-energien.pdf?__blob=publicationFile&v=1

[159] Krzikalla, Norbert ; Achner, Siggi ; Brühl, Stefan: *Möglichkeiten zum Ausgleich fluktuierender Einspeisungen aus erneuerbaren Energien: Studie im Auftrag des Bundesverbandes Erneuerbare Energie*. Bochum : Ponte Press, 2013. – ISBN 978–3–920328–64–5

[160] Schellong, Wolfgang: *Analyse und Optimierung von Energieverbundsystemen*. [Place of publication not identified] : Springer Science and Business Media, 2016. – ISBN 978–3–662–49463–9

[161] NEXT Kraftwerke: *Was ist die Residuallast?* https://www.next-kraftwerke.de/wissen/strommarkt/residuallast

[162] Hentschel, Jan: *AutoUni-Schriftenreihe*. Bd. 61: *Potenziale nachhaltiger Power-to-Gas Kraftstoffe aus Elektrizitätsüberschüssen im Jahr 2030*. Berlin : Logos-Verl., 2014. – ISBN 3832537023

[163] *Renewables.ninja*. https://www.renewables.ninja/

[164] Pfenninger, Stefan ; Staffell, Iain: Long-term patterns of European PV output using 30 years of validated hourly reanalysis and satellite data. In: *Energy* 114 (2016), S. 1251–1265. http://dx.doi.org/10.1016/j.energy.2016.08.060. – DOI 10.1016/j.energy.2016.08.060. – ISSN 03605442

[165] BDEW Bundesverband der Energie- und Wasserwirtschaft e.V: *Erneuerbare Energien und das EEG: Zahlen, Fakten, Grafiken (2013): Anlagen, installierte Leistung, Stromerzeugung, EEG-Auszahlungen, Marktintegration der Erneuerbaren Energien und regionale Verteilung der EEG-induzierten Zahlungsströme*. https://www.iee.uni-rostock.de/fileadmin/uni-rostock/Alle_IEF/IEE/Energieinfo_EE-und-das-EEG-Januar-2013.pdf

[166] BDEW Bundesverband der Energie- und Wasserwirtschaft e.V: *Erneuerbare Energien und das EEG: Zahlen, Fakten, Grafiken (2014): Anlagen, installierte Leistung, Stromerzeugung, EEG-Auszahlungen, Marktintegration der Erneuerbaren Energien und regionale Verteilung der EEG-induzierten Zahlungsströme*. https://www.bdew.de/media/documents/20140224_Energie-Info-Erneuerbare-Energien-und-das-EEG-2014.pdf

[167] BDEW Bundesverband der Energie- und Wasserwirtschaft e.V: *Erneuerbare Energien und das EEG: Zahlen, Fakten, Grafiken (2016): Anlagen, installierte Leistung, Stromerzeugung, EEG-Auszahlungen, Marktintegration der Erneuerbaren Energien und regionale Verteilung der EEG-Anlagen*. https://www.bdew.de/media/documents/20160218_Energie-Info-Erneuerbare-Energien-und-das-EEG-2016.pdf

[168] BDEW Bundesverband der Energie- und Wasserwirtschaft e.V: *Erneuerbare Energien und das EEG: Zahlen, Fakten, Grafiken (2017): Grafik- und Tabellenband*. https://www.bdew.de/media/documents/Awh_20170710_Erneuerbare-Energien-EEG_2017.pdf

[169] *Kraftwerksliste.* http://www.bundesnetzagentur.de/DE/Sachgebiete/ElektrizitaetundGas/Unternehmen_Institutionen/Versorgungssicherheit/Erzeugungskapazitaeten/Kraftwerksliste/kraftwerksliste-node.html. Version: 2018

[170] Günther, Danny ; Miara, Marek ; Langner, Robert ; Helmling, Sebastian ; Wapler, Jeanette ; ISE (Hrsg.): *„WP Monitor“ Feldmessung von Wärmepumpenanlagen*

[171] WWF Deutschland: *KOHLEKRAFTWERKE IN DEUTSCHLAND.* https://www.wwf.de/fileadmin/fm-wwf/Publikationen-PDF/WWF-Flyer-Kohlekraftwerke_in_Deutschland.pdf

[172] BMWi: *Gesetz für den Ausbau erneuerbarer Energien (Erneuerbare-Energien-Gesetz - EEG 2017).* BundesministeriumsderJustizundf\unhbox\voidb@x\bgroup\accent127u\penalty\@M\hskip\z@skip\egrouprVerbraucherschutz. Version: 2017

[173] VDMA: *Fähigkeiten von Stromerzeugungsanlagen im Energiemix: Ein Expertenausblick des VDMA Power Systems*

[174] Angerer, Michael ; Kahlert, Steffen ; Spliethoff, Hartmut: Transient simulation and fatigue evaluation of fast gas turbine startups and shutdowns in a combined cycle plant with an innovative thermal buffer storage. In: *Energy* 130 (2017), S. 246–257. http://dx.doi.org/10.1016/j.energy.2017.04.104. – DOI 10.1016/j.energy.2017.04.104. – ISSN 03605442

[175] FDBR: *Anpassung thermischer Kraftwerke Anpassung thermischer Kraftwerke an künftige Herausforderungen im Strommarkt: Maßnahmenkatalog*

[176] IEA: *Global EV Outlook 2018: Towards cross-modal electrification.* https://www.connaissancedesenergies.org/sites/default/files/pdf-actualites/globalevoutlook2018.pdf

[177] Statista: *Anzahl der Elektroautos in Deutschland von 2006 bis 2018.* https://de.statista.com/statistik/daten/studie/265995/umfrage/anzahl-der-elektroautos-in-deutschland/. Version: 2019

[178] Bundesministerium für Wirtschaft und Energie: *Elektromobilität in Deutschland.* https://www.bmwi.de/Redaktion/DE/Dossier/elektromobilitaet.html. Version: 2019

[179] Opel: *DER AMPERA-E.* https://www.opel.de/fahrzeuge/ampera-e/uebersicht.html#_trim-ultimate. Version: 2019

[180] Kraftfahrt-Bundesamt: *Jahresbilanz des Fahrzeugbestandes am 1. Januar 2018.* https://www.kba.de/DE/Statistik/Fahrzeuge/Bestand/bestand_node.html. Version: 2018

[181] Deutsches Institut für Wirtschaftsforschung: *Verkehr in Zahlen 2017/18.* 45. aktualisierte Neuauflage, revidierte Ausgabe. Hamburg : DVV Media Group, 2017. – ISBN 978–3–87154–617–4

[182] BMWi: *7. Energieforschungsprogramm: Innovationen für die Energiewende*. https://www.bmwi.de/Redaktion/DE/Publikationen/Energie/7-energieforschungsprogramm-der-bundesregierung.pdf?__blob=publicationFile&v=10

[183] Die Bundesregierung: *Intelligente Messsysteme für die Energiewende: Gesetz in Kraft getreten*. https://www.bundesregierung.de/breg-de/aktuelles/intelligente-messsysteme-fuer-die-energiewende-336380. Version: 2016

[184] Weidlich, Anke ; Renelt, Sven ; Schmidt, Peter ; Sobotka, Michal ; Storace, Stefan: Gesellschaftliche Akzeptanz von Smart Metering: Nicht ohne meine Kunden! In: *Energiewirtschaftliche Tagesfragen* (2013), Nr. 6. https://www.stiftung-nv.de/sites/default/files/201306_beitrag_gesellschaftliche_akzeptanz_von_smart_metering.pdf

[185] IEA: *TRENDS 2013 IN PHOTOVOLTAIC APPLICATIONS: Survey Report of Selected IEA Countries between 1992 and 2012*. http://www.iea-pvps.org/fileadmin/dam/public/report/statistics/FINAL_TRENDS_v1.02.pdf

[186] vreg: *Geïnstalleerd vermogen en aantal groenestroominstallaties*. https://www.vreg.be/sites/default/files/uploads/statistieken/00-20101231-gsc_-_vermogen_en_aantal_installaties_per_provincie_6.pdf. Version: 2012

[187] IEA: *Snapshot of Global PV Markets*

[188] EurObserv'ER (Hrsg.): *PHOTOVOLTAIC BAROMETER*. http://www.energies-renouvelables.org/observ-er/stat_baro/observ/EurObservER-barojdpv13-Photovoltaic-Barometer-2015-EN.pdf

[189] EurObserv'ER (Hrsg.): *PHOTOVOLTAIC BAROMETER*. http://www.energies-renouvelables.org/observ-er/stat_baro/observ/baro-jdp9.pdf

[190] Masson, Gaëtan ; Orlandi, Sinead ; Rekinger, Manoël: *GLOBAL MARKET OUTLOOK: For Photovoltaics 2014-2018*

[191] Statista: *Solar photovoltaic capacity installed and connected in Luxembourg from 2013 to 2017 (in megawatts)*. https://www.statista.com/statistics/497405/installed-photovoltaic-capacity-luxembourg/. Version: 2019

[192] EPIA (Hrsg.): *GLOBAL MARKET OUTLOOK FOR PHOTOVOLTAICS UNTIL 2015*

[193] the wind power (Hrsg.): *Production capacities*. https://www.thewindpower.net/country-datasheet-13-austria.php. Version: 2018

[194] IEA: *IEA WIND: 2015 Annual Report*. https://www.seai.ie/resources/publications/IEA_Wind_Annual_Report_2015.pdf

[195] Wind EUROPE (Hrsg.): *Wind in power 2017: Annual combined onshore and offshore wind energy statistics*. https://windeurope.org/wp-content/uploads/files/about-wind/statistics/WindEurope-Annual-Statistics-2017.pdf

[196] EurObserv'ER (Hrsg.): *WIND ENERGY BAROMETER*. https://www.eurobserv-er.org/pdf/wind-energy-barometer-2017-en/

[197] EWEA: *Wind in power: 2014 European statistics*

[198] Northern Ireland Assembly (Hrsg.): *Onshore Wind Power in Denmark: Research and Information Service Briefing Paper*. http://www.niassembly.gov.uk/globalassets/Documents/RaISe/Publications/2014/environment/12714.pdf

[199] ADEME: *ANALYSIS OF THE FRENCH WIND POWER SECTOR: OVERVIEW, PROSPECTIVE ANALYSIS AND STRATEGY*. https://www.ademe.fr/sites/default/files/assets/documents/filiere_eolienne_francaise_2017-syntheseeng.pdf

[200] GWEC: *GLOBAL WIND REPORT: ANNUAL MARKET UPDATE*. https://www.gwec.net/wp-content/uploads/vip/GWEC-Global-Wind-2015-Report_April-2016_22_04.pdf

[201] Staffell, Iain ; Pfenninger, Stefan: Using bias-corrected reanalysis to simulate current and future wind power output. In: *Energy* 114 (2016), S. 1224–1239. http://dx.doi.org/10.1016/j.energy.2016.08.068. – DOI 10.1016/j.energy.2016.08.068. – ISSN 03605442

[202] Bundesnetzagentur: *Monitoringbericht 2016*. https://www.bundesnetzagentur.de/SharedDocs/Downloads/DE/Sachgebiete/Energie/Unternehmen_Institutionen/DatenaustauschUndMonitoring/Monitoring/Monitoringbericht2016.pdf?__blob=publicationFile&v=2

[203] Forschungsstelle für Energiewirtschaft e.V.: *Gutachten zur Rentabilität von Pumpspeicherkraftwerken*. https://www.stmwi.bayern.de/fileadmin/user_upload/stmwi/Themen/Energie_und_Rohstoffe/Dokumente_und_Cover/2014-Pumpspeicher-Rentabilitaetsanalyse.pdf

[204] BVES: *Pumpspeicherwerk (PSW) Goldisthal*. https://www.bves.de/wp-content/uploads/2017/04/Pumpspeicherwek.pdf. Version: 2016

[205] DENA: *Systemlösung Power to Gas. Chancen, Herausforderungen und Stellschrauben auf dem Weg zur Marktreife.*

[206] ENCON.Europe GmbH (Hrsg.): *Potentialatlas für Wasserstoff: Analyse des Marktpotentials für Wasserstoff, der mit erneuerbaren Strom hergestellt wird, im Raffineriesektor und im zukünftigen Mobilitätssektor*

[207] Linde Gas GmbH (Hrsg.): *Rechnen Sie mit Wasserstoff. Die Datentabelle*

[208] Deutscher Bundestag (Hrsg.): *Energieverbrauch bei der Produktion von mineralischem Stickstoffdünger*. https://www.bundestag.de/blob/567976/bb4895f14291074b0a342d4c714b47f8/wd-8-088-18-pdf-data.pdf

[209] Rogers, Everett M.: *Diffusion of innovation*. 3. ed. London : The Free Press, 1982. – ISBN 0–02–926650–5

[210] Kaltschmitt, Martin ; Wiese, Andreas ; Streicher, Wolfgang: *Erneuerbare Energien: Systemtechnik, Wirtschaftlichkeit, Umweltaspekte*. 3., vollständig neu bearbeitete und erw. Aufl. Berlin and Hong Kong : Springer, 2003. – ISBN 3–540–43600–6

[211] Reich, Gerhard ; Reppich, Marcus: *Regenerative Energietechnik: Überblick über ausgewählte Technologien zur nachhaltigen Energieversorgung*. Wiesbaden and s.l. : Springer Fachmedien Wiesbaden, 2013. http://dx.doi.org/10.1007/978-3-8348-8614-9. http://dx.doi.org/10.1007/978-3-8348-8614-9. – ISBN 978–3–8348–0981–0

[212] UBA: *Potenzial der Windenergie an Land: Studie zur Ermittlung des bundesweiten Flächen- und Windenergienutzung an Land*. Dessau-Roßlau, 2013

[213] Schuler, Johannes ; Krämer, Christine ; Hildebrandt, Silvio ; Steinhäusser, Reimund ; Starick, Anja ; Reutter, Michaela: *BfN-Skripten*. Bd. 463: *Kumulative Wirkungen des Ausbaus erneuerbarer Energien auf Natur und Landschaft*. Bonn : Bundesamt für Naturschutz, 2017. – ISBN 978–3–89624–200–6

[214] AG Energiebilanzen e.V.: *Bruttostromerzeugung in Deutschland ab 1990 nach Energieträgern*. https://ag-energiebilanzen.de/index.php?article_id=29&fileName=20171221_brd_stromerzeugung1990-2017.pdf

[215] Diefenbach, Nikolaus ; Cischinsky, Holger ; Rodenfels, Markus ; Clausnitzer, Klaus-Dieter ; IWU (Hrsg.): *Datenbasis Gebäudebestand: Datenerhebung zur energetischen Qualität und zu den Modernisierungstrends im deutschen Wohngebäudebestand*. Darmstadt,

[216] Destatis (Hrsg.): *Ergebnisse der Gebäudezählung des Zensus 2011 auf Gemeindeebene*. Wiesbaden,

[217] Schlomann, Barbara ; Kleeberger, Heinrich ; Geiger, Bernd ; Linhardt, Antje ; Gruber, Edelgard ; Mai, Michael ; Gerspacher, Andreas ; Schiller, Werner ; Institut für Ressourceneffizienz und Energiestrategien (Hrsg.) ; Lehrstuhl für Energiewirtschaft und Anwendungstechnik (Hrsg.) ; GfK Retail and Technology GmbH (Hrsg.) ; Fraunhofer ISI (Hrsg.) ; BASE-ING. GmbH (Hrsg.): *Energieverbrauch des Sektors Gewerbe, Handel, Dienstleistungen (GHD) in Deutschland für die Jahre 2007 bis 2010*. Karlsruhe and München and Nürnberg,

[218] Kasten, Peter ; Mottschall, Moritz ; Köppel, Wolfgang ; Degünther, Charlotte ; Schmied, Martin ; Wüthrich, Phillipp ; Umweltbundesamt (Hrsg.): *Erarbeitung einer fachlichen Strategie zur Energieversorgung des Verkehrs bis zum Jahr 2050*

[219] Hacker, Florian ; Blanck, Ruth ; Hülsmann, Frederike ; Kassten, Peter ; Loreck, Charlotte ; Ludwig, Sylvie ; Mottschall, Moritz ; Zimmer, Wiebke ; Öko Institut e.V. (Hrsg.): *eMobil 2050: Szenarien zum möglichen Beitrag des elektrischen Verkehrs zum langfristigen Klimaschutz*. Berlin,

[220] Schubert, Markus, Kluth, Tobias ; Nebauer, Gregor ; Ratzenberger, Ralf ; Kotzagiorgis, Stefanos ; Butz, Bernd ; Schneider, Walter ; Leible, Markus ; Bundesministerium für Verkehr und digitale Infrastruktur (Hrsg.): *Verkehrsverflechtungsprognose 2030*

[221] Miara, Marek ; Günther, Danny ; Kramer, Thomas ; Oltersdorf, Thore ; Wapler, Jeanette: *Wärmepumpen Effizienz, Messtechnische Untersuchung von*

Wärmepumpenanlagen zur Analyse und Bewertung der Effizienz im realen Betrieb, Abschlussbericht. Freiburg,

[222] Miara, M. ; Russ, C. ; Günther, D. ; Kramer, T. ; Henning, H.-M.: Efficiency of heat pump systems under real operatating conditions. In: Centre, Heat P. (Hrsg.): *10th IEA Heat Pump Conference*, 2011

[223] Miara, M. ; Platt, M. ; Günther, D. ; Kramer, T. ; Dittmer, H. ; Lechner, T. ; Kurz, C.: *Feldmessung Wärmepumpen im Gebäudebestand*. Freiburg,

[224] Lenz, Barbara ; et al.: *Mobilität in Deutschland 2008: Struktur – Aufkommen – Emissionen – Trends*. http://www.mobilitaet-in-deutschland.de/pdf/MiD2008_Abschlussbericht_I.pdf

[225] https://www.bast.de/BASt_2017/DE/Home/home_node.html

[226] Kersten, Konstantin: *Der Einfluss des automatisierten Fahrens auf den Mobilitäts- und Energiebedarf in Deutschland*

[227] Buttler, A. ; Buttler, A. and Hentschel, J. and Kahlert, S. and Angerer, M.: *Statusbericht Flexibilitätsbedarf im Stromsektor: Eine Analyse der aktuellen marktwirtschaftlichen und technischen Herausforderungen an Speicher und Kraftwerke im Zuge der Energiewende.*

[228] Görner, Klaus ; Uwe Sauer, Dirk: *Konventionelle Kraftwerke: Technologiesteckbrief zur Analyse „Flexibilitätskonzepte für die Stromversorgung 2050“*. https://energiesysteme-zukunft.de/fileadmin/user_upload/Publikationen/pdf/ESYS_Technologiesteckbrief_Konventionelle_Kraftwerke.pdf

[229] Schill, Wolf-Peter ; Pahle, Michael ; Gambardella, Christian: *On Start-up Costs of Thermal Power Plants in Markets with Increasing Shares of Fluctuating Renewables*. https://www.diw.de/documents/publikationen/73/diw_01.c.524200.de/dp1540.pdf

[230] van den Bergh, Kenneth ; Delarue, Erik: Cycling of conventional power plants: Technical limits and actual costs. In: *Energy Conversion and Management* 97 (2015), S. 70–77. http://dx.doi.org/10.1016/j.enconman.2015.03.026. – DOI 10.1016/j.enconman.2015.03.026. – ISSN 01968904

[231] Hencke, Ernst-Günter ; Manske, Dirk: *Fossil befeuerte Großkraftwerke in Deutschland: Stand, Tendenzen, Schlussfolgerungen*

[232] Wietschel, Martin: *Energietechnologien der Zukunft: Erzeugung, Speicherung, Effizienz und Netze*. Wiesbaden : Springer Vieweg, 2015. – ISBN 978–3–658–07128–8

[233] Hundt, Matthias ; Barth, Rüdiger ; Sun, Ninghong ; Wissel, Steffen ; Voss, Alfred: *Verträglichkeit von erneuerbaren Energien und Kernenergie im Erzeugungsportfolio: Technische und ökonomische Aspekte*. https://www.ier.uni-stuttgart.de/publikationen/pb_pdf/Hundt_EEKE_Langfassung.pdf

[234] Umweltbundesamt: *Daten zur Umwelt: Aktuelle Daten, Trends und Bewertungen zur Umweltsituation in Deutschland*. https://www.umweltbundesamt.de/daten. Version: 2018

[235] Gores, S. and Jörss, W. and Zell-Ziegler, C. ; Öko Institut e.V. (Hrsg.): *Aktueller Stand der KWK-Erzeugung (Dezember 2015).* https://www.oeko.de//oekodoc/2450/2015-607-de.pdf

[236] Agora Energiewende: *Die Energiewende im Stromsektor: Stand der Dinge 2015. Rückblick auf die wesentlichen Entwicklungen sowie Ausblick auf 2016.* https://www.agora-energiewende.de/fileadmin/Projekte/2016/Jahresauswertung_2016/Agora_Jahresauswertung_2015_web.pdf

[237] Statista: *Biogas - Stromerzeugung in Deutschland bis 2017.* https://de.statista.com/statistik/daten/studie/622560/umfrage/stromerzeugung-aus-biogas-in-deutschland/. Version: 2018

[238] Umweltbundesamt: *Entwicklung der spezifischen Kohlendioxid-Emissionen des deutschen Strommix in den Jahren 1990 – 2016.* https://www.umweltbundesamt.de/sites/default/files/medien/1410/publikationen/2017-05-22_climate-change_15-2017_strommix.pdf

[239] Die Bundesregierung (Hrsg.): *Neue Kraftstoffe und Antriebe.* https://www.bundesregierung.de/breg-de/themen/neue-kraftstoffe-und-antriebe-994216. Version: 2019

[240] Kraftfahrt-Bundesamt (Hrsg.): *Neuzulassungen von Pkw in den Jahren 2008 bis 2017 nach ausgewählten Kraftstoffarten.* https://www.kba.de/DE/Statistik/Fahrzeuge/Neuzulassungen/Umwelt/n_umwelt_z.html. Version: 2019

[241] Kraftfahrt-Bundesamt (Hrsg.): *Pressemitteilung Nr. 01/2019- Fahrzeugzulassungen im Dezember 2018 - Jahresbilanz.* https://www.kba.de/DE/Presse/Pressemitteilungen/2019/Fahrzeugzulassungen/pm01_2019_n_12_18_pm_komplett.html. Version: 2019

[242] Madina, Carlos ; Zamora, Inmaculada ; Zabala, Eduardo: Methodology for assessing electric vehicle charging infrastructure business models. In: *Energy Policy* 89 (2016), S. 284–293. http://dx.doi.org/10.1016/j.enpol.2015.12.007. – DOI 10.1016/j.enpol.2015.12.007. – ISSN 03014215

[243] Brandt, Tobias ; Wagner, Sebastian ; Neumann, Dirk: Evaluating a business model for vehicle-grid integration: Evidence from Germany. In: *Transportation Research Part D: Transport and Environment* 50 (2017), S. 488–504. http://dx.doi.org/10.1016/j.trd.2016.11.017. – DOI 10.1016/j.trd.2016.11.017. – ISSN 13619209

[244] BDH ; bwp: *Branchenstudie 2018: Marktanalyse – Szenarien – Handlungsempfehlungen*

[245] Köhler, Benjamin et a.: *Guideline II: nZEB Technologies: COST REDUCTION AND MARKET ACCELERATION FOR VIABLE NEARLY ZEROENERGY BUILDINGS.* https://www.researchgate.net/publication/328610763_D41_Guideline_II_nZEB_Technologies_Report_on_cost_reduction_potentials_for_technical_nZEB_solution_sets

[246] Bürger, Veit ; Hesse, Tilmann ; Palzer, Andreas ; Herkel, Sebastian ; Engelmann, Peter: *Klimaneutraler Gebäudebestand 2050: aktuell in Bearbeitung*. Dessau - Roßlau,

[247] IEA (Hrsg.): *Energy technology perspectives 2010. Scenarios & stragegies to 2050*

[248] DAIKIN: *Hybrid heating system*

[249] VIESSMANN: *Hybrid solutions: Heating with hybrid appliances – future safety included*. https://www.viessmann.com/com/content/dam/vi-corporate/COM/Download/Hybrid-solutions.pdf/_jcr_content/renditions/original.media_file.download_attachment.file/Hybrid-solutions.pdf. Version: 2017

[250] Deutscher Bundestag: *Entwurf eines Deizehnten Gesetzes zur Änderurung des Atomgesetzes*. http://dip21.bundestag.de/dip21/btd/17/060/1706070.pdf

[251] Zukunft ERDGAS e. V (Hrsg.): *WÄRMEMARKT 2050: SO ERREICHT DEUTSCHLAND KOSTENEFFIZIENT DAS KLIMAZIEL*

[252] DIgSILENT (Hrsg.): *DIgSILENT — PowerFactory: PowerFactory Anwendungen*. https://www.digsilent.de/de/powerfactory.html. Version: 2019

[253] Wittwer, Christof: *Eurosolar-Symposium: Die Praxis der Energiewende: Die Rolle von Energiespeichern und ihre Implikationen für die Netzstrukturen im künftigen Energiesystem*. 2015

[254] Götz, Manuel et a.: Renewable Power-to-Gas: A technological and economic review. In: *Renewable Energy* 85 (2016), S. 1371–1390. http://dx.doi.org/10.1016/j.renene.2015.07.066. – DOI 10.1016/j.renene.2015.07.066. – ISSN 09601481

[255] Shammugam, Shivenes et a.: Raw metal needs and supply risks for the development of wind energy in Germany until 2050. In: *Journal of Cleaner Production* 221 (2019), S. 738–752. http://dx.doi.org/10.1016/j.jclepro.2019.02.223. – DOI 10.1016/j.jclepro.2019.02.223. – ISSN 09596526

[256] Agora ; Agora (Hrsg.): *Current and Future Cost of Photovoltaics: Long-term Scenarios for Market Development, System Prices and LCOE of Utility-Scale PV Systems*. https://www.ise.fraunhofer.de/content/dam/ise/de/documents/publications/studies/AgoraEnergiewende_Current_and_Future_Cost_of_PV_Feb2015_web.pdf

[257] IEA (Hrsg.): *Energy technology perspectives 2012. Pathways to a Clean Energy System*. https://www.iea.org/publications/freepublications/publication/ETP2012_free.pdf

[258] Masurowski, Frank ; Drechsler, Martin ; Frank, Karin: *A spatially explicit assessment of the wind energy potential in response to an increased distance between wind turbines and settlements in Germany*. Bd. 97. 2016. http://dx.doi.org/10.1016/j.enpol.2016.07.021. http://dx.doi.org/10.1016/j.enpol.2016.07.021

[259] Nitsch, Joachim ; Pregger, Yvonne ; Naegler, Tobias ; Sterner, Michael ; Gerhardt, Norman ; Oehsen, Amany ; Pape, Carsten ; Saint-Drenan, Yves-Marie ; DLR (Hrsg.): *Langfristszenarien und Strategien für den Ausbau der erneuerbaren Energien in Deutschland bei Berücksichtigung der Entwicklung in Europa und global „Leitstudie 2010“*

[260] DENA (Hrsg.): *dena-Netzstudie I – Energiewirtschaftliche Planung für die Netzintegration von Windenergie in Deutschland an Land und Offshore bis zum Jahr 2020.* https://shop.dena.de/fileadmin/denashop/media/Downloads_Dateien/esd/9113_dena-Netzstudie_I.pdf

[261] VGB (Hrsg.): *Kraftwerke (KW) 2020+: Kraftwerksoptionen für die Zukunft und der damit verbundene Forschungsbedarf.* https://www.vgb.org/vgbmultimedia/News/Kraftwerke2020plus_D.pdf

[262] Wietschel, Martin et a.: *Energietechnologien 2050 - Schwerpunkte für Forschung und Entwicklung.* Fraunhofer Verlag, 2010 https://www.dbu.de/OPAC/fp/Energietechnologien2050.pdf. – ISBN 978–3–8396–0084–9

[263] Prognos AG (Hrsg.): *Entwicklung von Stromproduktionskosten: Die Rolle von Freiflächen-Solarkraftwerken in der Energiewende.* https://www.prognos.com/fileadmin/pdf/aktuelles/131010_Studie_Belectric_Freiflaechen_Solarkraftwerke_Final.pdf

[264] DLR (Hrsg.) ; LBSt (Hrsg.) ; Fraunhofer ISE (Hrsg.) ; KBB (Hrsg.): *Studie über die Planung einer Demonstrationsanlage zur Wasserstoff-Kraftstoffgewinnung durch Elektrolyse mit Zwischenspeicherung in Slazkavernen unter Druck.* http://www.lbst.de/ressources/docs2015/BMBF_0325501_PlanDelyKaD-Studie.pdf

[265] Luschtinetz, Thomas: *Nutzung regenerativer Energiequellen und Wasserstofftechnik 2008: [15. Symposium Nutzung Regenerativer Energiequellen und Wasserstofftechnik, Stralsund, 6. - 8. November 2008.* Stralsund : Fachhochsch, 2008 (Praxis verstehen, Chancen erkennen, Zukunft gestalten). https://www.hochschule-stralsund.de/fileadmin/hs-stralsund/FAK_ETI/Dateien/REGWA/TagungsBaende/Tagungsband_2008.pdf. – ISBN 3980995380

[266] Foster Wheeler Energy Limited (Hrsg.): *Decarbonisation of fossil fuels.* https://www.worldcat.org/title/decarbonisation-of-fossil-fuels/oclc/48069255. Version: 1996

[267] Bolle, Friedrich-Wilhelm et a.: *WaStraK NRW Einsatz der Wasserstofftechnologie in der Abwasserbeseitigung - Phase I.* https://www.lanuv.nrw.de/fileadmin/forschung/wasser/klaeranlage_abwasser/WaStraK_Abschlussbericht_Teil%201.pdf

[268] Heumann, Arnd ; Huenges, Ernst: *Technologiebericht 1.2 Tiefengeothermie innerhalb des Forschungsprojekts TF_Energiewende.* https://epub.wupperinst.org/files/7042/7042_Tiefengeothermie.pdf

[269] IER (Hrsg.) ; RWI (Hrsg.) ; ZEW (Hrsg.): *Die Entwicklung der Energiemärkte bis 2030: Energieprognose 2009.* http://www.rwi-essen.de/media/content/pages/publikationen/rwi-projektberichte/PB_Energieprognose-2009.pdf

[270] Giovannetti, Federico ; Kastner, Oliver ; Lampe, Carsten ; Reineke-Koch, Rold ; Park, Sunah ; Steinweg, Jan: *Technologiebericht 1.4 Solare Wärme und Kälte innerhalb des Forschungsprojekts TF_Energiewende*. https://epub.wupperinst.org/files/7044/7044_Solare_Waerme_Kaelte.pdf

[271] QUASCHNING: *ENERGIESYSTEME 9.A.* [Place of publication not identified] : CARL HANSER Verlag GMBH &, 2015. – ISBN 978–3–446–44267–2

[272] BKI (Hrsg.): *BKI Positionen 6 - Neubau 2018 / 2019*. https://www.bki.de/positionen/bki-positionen-6-neubau-2018-2019.html. Version: 2018

[273] Ammermann, Heiko et a.: *Advancing Europe's energy systems: Stationary fuel cells in distributed generation : a study for the Fuel Cells and Hydrogen Joint Undertaking*. Luxembourg : EUR-OP, 2015 https://www.rolandberger.com/publications/publication_pdf/roland_berger_fuel_cells_study_20150330.pdf. – ISBN 978–92–9246–134–8

[274] FNR (Hrsg.): *PELLETHEIZUNGEN: Marktübersicht*. http://www.fnr.de/fileadmin/allgemein/pdf/broschueren/mu_pellet_web.pdf

[275] BKI (Hrsg.): *BKI Positionen 6 - Neu- und Altbau 2018 / 2019*. https://www.bki.de/positionen/bki-positionen-6-neu-und-altbau-2018-2019.html. Version: 2018

[276] ASUE (Hrsg.): *Marktübersicht Gaswärmepumpen 2012: Gasklimageräte, Gasmotorwärmepumpen, Gasabsorptionswärmepumpen, Gasabsorptionskälteanlagen, Gasadsorptionswärmepumpen: Angebot und Anbieter*

[277] GZB (Hrsg.): *Analyse des deutschen Wärmepumpenmarktes: Bestandsaufnahme und Trends*. http://www.geothermie-zentrum.de/fileadmin/media/geothermiezentrum/GeothermieCampus_Bochum/Forschung_und_Projekte/Analyse_des_deutschen_Waermepumpenmarktes/WP-StudieII_GZB_2014.pdf

[278] Nitsch, Joachim ; Pregger, Thomas ; Naegler, Tobias ; Heide, Dominik ; Luca de Tena, Diego ; Trieb, Franz ; Scholz, Yvonne: *Langfristszenarien und Strategien für den Ausbau der erneuerbaren Energien in Deutschland bei Berücksichtigung der Entwicklung in Europa und global*. https://www.dlr.de/dlr/Portaldata/1/Resources/documents/leitstudie2010.pdf

[279] ASUE (Hrsg.): *BHKW - Kenndaten 2011: Module Anbieter Kosten*. asue.de/cms/upload/broschueren/2011/bhkw-kenndaten/asue-bhkw-kenndaten-0311.pdf

[280] Lucas, K. ; Gebhardt, M. ; Kohl, H. ; Steinrötter, Th.: *PREISATLAS: Ableitung von Kostenfunktionen für Komponenten der rationellen Energienutzung*. http://docplayer.org/33002259-Preisatlas-ableitung-von-kostenfunktionen-fuer-komponenten\-der-rationellen-energienutzung.html. Version: 2002

[281] Kah, Oliver ; Feist, Wolfgang: *Wirtschaftlichkeit von Wärmedämm - Maßnahmen im Gebäudebestand 2005*. http://www.passipedia.org/_media/picopen/wirtschaftlichkeit_waermedaemmung.pdf

[282] DBFZ (Hrsg.): *Monitoring Biokraftstoffsektor (2. Auflage).* https://www.google.com/url?sa=t&rct=j&q=&esrc=s&source=web&cd=3&ved=2ahUKEwi_sJGMgbHhAhXPZlAKHQiaAy8QFjACegQIBBAC&url=http%3A%2F%2Fwww.qucosa.de%2Ffileadmin%2Fdata%2Fqucosa%2Fdocuments%2F13786%2FDBFZ_Report11A.pdf&usg=AOvVaw1bWd7Grai3fbeMrxo7wClN

[283] DBFZ (Hrsg.): *Bioenergie heute und morgen - 11 Bereitstellungskonzepte: Sonderheft zum DBFZ Report.* https://www.dbfz.de/fileadmin/user_upload/Presseinformationen/pm_bereitstellungskonzepte.pdf

[284] Eckhard Weidner (Hrsg.): *Bioenergie: Technologiesteckbrief zur Analyse Flexibilitätskonzepte für die Stromversorgung 2050.* https://energiesysteme-zukunft.de/fileadmin/user_upload/Publikationen/pdf/ESYS_Technologiesteckbrief_Bioenergie.pdf

[285] DBFZ (Hrsg.): *Evaluierung der Verfahren und Technologien für die Bereitstellung von Wasserstoff auf Basis von Biomasse.* https://www.dbfz.de/fileadmin/user_upload/Referenzen/DBFZ_Reports/DBFZ_Report_19.pdf